Compact Dual and Broadband Planar Antennas for Modern Communication Systems

Ph.D Thesis

Submitted by

Sanyog Rawat
(ID-2009REC103)

Under the Supervision of

Dr. Kamalesh K. Sharma
Professor and Head, Dept. of ECE, MNIT Jaipur

This thesis is submitted in partial fulfillment of the Ph.D. Programme in Engineering

November, 2015

Department of Electronics and Communication Engineering
MALAVIYA NATIONAL INSTITUTE OF TECHNOLOGY
JAIPUR-302017

Certificate

This is to certify that the thesis entitled "**Compact Dual and Broadband Planar Antennas for Modern Communication Systems**" being submitted by **Sanyog Rawat** to the Department of Electronics and Communication Engineering, Malaviya National Institute of Technology Jaipur for the award of the degree of **Doctor of Philosophy,** is a bonafide research work carried out by him under my supervision and guidance. The results obtained in this thesis have not been submitted to any other University or Institute for the award of any other degree.

(Dr. K. K. Sharma)
(Professor and Head)
Department of Electronics and Communication Engineering
Malaviya National Institute of Technology, Jaipur
Jaipur-302017, Rajasthan (India)

Declaration

I, **Sanyog Rawat** declare that this thesis entitled " "**Compact Dual and Broadband Planar Antennas for Modern Communication Systems**" is an original piece of research work carried out under the supervision of Prof. (Dr.) Kamalesh K. Sharma. I confirm that:

1. This work was done wholly or mainly while in candidature for a Ph.D. degree at M.N.I.T. Jaipur.
2. Where any part of this thesis has previously been submitted for a degree or any other qualification at M.N.I.T. Jaipur or any other institution, this has been clearly stated.
3. Where I have consulted the published work of others, this is clearly attributed.
4. Where I have quoted from the works of others, this source is always given. With the exception of such quotations, this thesis is entirely my own work.
5. I have acknowledged all main source of help.
6. Where the thesis is based on work done by myself, jointly with others, I have made clear exactly what was done by others and what I have contributed myself.

(Sanyog Rawat)

(ID-2009REC103)

Acknowledgements

Any research endeavour of meaningful worth cannot be possible without the collective assistance and support of persons connected with the knowledge of men, matters and events. As such, I feel obliged to acknowledge with gratitude in whatever way they have helped my study to emerge out.

My heartfelt and sincere gratitude to my supervisor Prof. K. K. Sharma for his guidance, insightful comments, high standards, enthusiasm, kindness and willingness always to make time for another lengthy scientific discussion, without which, this thesis would not exist. I express my sincere gratitude to family members of my supervisor for their affection and co-operation throughout my research work.

I wish to express sincere gratitude to Mr. V.V Srinivasan, Prof. D. Bhatnagar and Dr. K. P Ray for providing me an opportunity to use the measurement facilities. I am also thankful to my DPGC and DREC members for their valuable suggestions and guidance.

I would also like to thank my friend's Dr. Brajraj Sharma, Dr. Pushpendra Singh and Mr. Ajay Tiwari for their whole-hearted support, good wishes and continuous encouragement that helped me in overcoming many hardships during the period of my research work.

I would also like to thank my sisters and brother, Mrs. Sakshi Sharma, Mrs. Ritu Mishra and Mr. Shailabh Sharma for enormous encouragement, inspiration and moral support. I am also thankful to my sister in law Mrs. Rajani Sharma for her helpful attitude and moral support during my entire research work. Indubitably, it is inexcusable if I forget to write a few words for my wife Mrs. Parul Rawat for her everlasting and ineffable affection and cooperation which helped me during the course of this work. Words are inadequate to express my indebtedness to my father Mr. B.S Rawat who always encouraged me, my mother, Mrs. Asha Rawat who has always supported me in every decision and for being source of tremendous strength and energy to me throughout this work.

Finally I must say thanks to the Almighty, who seems to be supporting me at the critical phases of my life.

Sanyog Rawat
(2009REC103)

Abstract

Microstrip patch antennas have established extensive application in wireless communication systems owing to their advantages such as compact size, low profile, conformability, low cost fabrication and ease of integration with other circuit components. However, the main limitations associated with these patch antennas are their narrow bandwidth, low gain and capability to operate at a single frequency corresponding to their dominant mode. Looking at the inherent properties of microstrip patch antennas, it is realized that in their conventional form microstrip antennas are not suitable for modern communication systems. However their compact size and easy integration with other circuit components attracted scientists to modify these antennas to find their possible applications in modern communication systems. Thus size reduction, bandwidth enhancement, multi frequency/multi band operation and circular polarization are becoming major design considerations for practical applications of microstrip antennas. For this reason, studies to achieve compactness, circularly polarized radiations and broadband operations of patch antenna have greatly increased. Significant progress in the design of compact microstrip antennas with broadband, dual-frequency/dual band operation and gain-enhanced have been reported in the recent past.

The objective of this thesis is to design compact dual and broadband microstrip patch antennas which can be used in the modern wireless communication systems for the applications in Wireless Local Area Network (WLAN) Computer Communication, Bluetooth, Worldwide Interoperability for Microwave Access (Wi-Max) Communication Systems, Deep Space Satellite Communication Systems, and Hiper LAN applications. In this thesis five different antenna geometries with detailed analysis have been proposed. The first geometry is slotted modified pentagonal patch antenna and second geometry is modified square patch antenna, both the geometries operate in different dual band with improved radiation performance.

The third and fourth geometries consist of triangular patch antenna with asymmetric slots in the ground plane to achieve broadband operation and modified circular patch

antenna with ground truncation and etching slots in the patch to obtain broad bandwidth.

In the fifth geometry the circularly polarized broadband antenna is proposed. Parasitic patch and shorting pins have been applied to achieve wide bandwidth and circular polarization.

Table of Contents

List of Figures **viii**

List of Tables **xviii**

List of Abbreviations **xix**

List of Symbols **xx**

Chapter 1– Introduction **1**

1.1 Introduction 1

1.2 Shapes of patches 4

1.3 Advantages and disadvantages of microstrip antennas 11

1.4 Motivation 13

1.5 Applications of microstrip antennas 13

1.6 Scope and outline of thesis 14

Chapter 2 - Literature review and preliminaries **18**

2.1 Challenges in the research area 18

2.1.1 The techniques commonly used for reducing size of an antenna 18

(a) Using substrate with high dielectric constant 18

(b) Using meandered patch 19

(c) Punching vias and shorting pin through the substrate 20

(d) Use of diodes 21

2.1.2 The commonly used techniques for obtaining broad bandwidth in antennas 23

(a) Implanting slots at appropriate location in the radiating patch 23

(b) Use of multiple closely spaced patches 24

(c) Use of stacked patches 25

2.2 Literature review 26

2.2.1 Dual Band Microstrip Antennas 26

2.2.2 Broadband Microstrip Antennas 33

2.2.3 Stacked Microstrip Antennas 38

2.3 Preliminaries 41
2.3.1 Antenna Characteristics 41
(a) Reflection Coefficient or Return Loss 42
(b) Voltage Standing Wave Ratio 43
(c) Input Impedance 43
(d) Bandwidth 44
(e) Radiation Pattern 45
(f) Directivity 46
(g) Gain 47
(h) Radiation Efficiency 47
(i) Axial Ratio (AR) 47
(j) Polarization in antennas 48
2.3.2 Feeding Techniques 48
(a) Microstrip line feed or edge-feed 49
(b) Coaxial or Probe feed technique 49
(c) Aperture coupled feed technique 51
(d) Proximity coupled feed technique 52
2.3.3 Numerical Techniques of analysis for microstrip patch antennas 52
(a) Transmission line model 54
(b) Cavity model technique 55
(c) Spectral domain full wave analysis 57
(d) Mixed potential integral equation analysis 57
(e) Finite difference time domain analysis 57
(f) Method of moments (MOM) 59
(g) Finite element method (FEM) 59
2.3.4 Electromagnetic simulation software for microstrip antennas 60
(a) IE3D simulation software 61
(b) CST Microwave Studio 62
(c) Ansoft HFSS 62
(d) FEKO 62
(e) Advanced Design System (ADS) 63
2.3.5 Fabrication process 64

2.3.6 Antenna measurement methods 64

Chapter 3 - Compact microstrip patch antennas with defected ground for Wi-Max and WLAN applications 66

3.1 Introduction 66

3.2 Work done in past on compact dualband microstrip antennas for wireless applications 67

3.3 Analysis of conventional rectangular microstrip patch antenna 69

3.3.1 Performance of pentagonal patch antenna 72

3.3.2 Pentagonal patch antenna geometry with rectangular slot in ground plane 73

3.3.3 Pentagonal patch antenna with defected ground 77

3.3.4 Modified pentagonal patch antenna with defected ground 81

3.3.5 Performance of modified pentagonal patch antenna with defected ground 82

(a) Reflection coefficient, VSWR and input impedance of proposed geometry 82

(b) Gain and Radiation efficiency of proposed antenna 84

(c) Radiation patterns of proposed antenna 86

(d) Current distribution of proposed antenna 88

3.4 Analysis of conventional square patch antenna 89

3.4.1 Square patch antenna with reduced ground 91

3.4.2 Square patch antenna with circular slot and reduced ground 94

3.4.3 Modified square patch antenna with defected ground 96

3.4.4 Performance of modified square patch antenna with defected ground plane 97

3.5 Summary 105

Chapter 4 - Compact microstrip patch antennas with finite ground plane for broadband performance 106

4.1 Introduction 106

4.2 Work done in past on broadband microstrip patch antenna 107

4.3 Analysis of conventional triangular patch antenna 109

4.3.1 Triangular patch antenna with slots in ground plane 111
4.3.2 Triangular patch antenna with slots in ground plane 113
4.4 Analysis of conventional circular patch antenna 119
4.4.1 Circular patch antenna with reduced ground plane 121
4.4.2 Modified circular patch antenna with elliptical slot and reduced ground plane 125
4.4.3 Modified circular patch antenna with reduced ground plane 128
4.5 Summary 136

Chapter 5 - Stacked arrangement of microstrip antennas for improved performance 137
5.1 Introduction 137
5.2 Performance of conventional hexagonal patch antenna 141
5.3 Stacked antenna structure 143
5.4 Preliminary study 144
5.4.1 Dimension of parasitic patch 144
5.4.2 Optimization of thickness of air gap 148
5.4.3 Using pin short 150
5.5 Stacked arrangement of hexagonal and rectangular microstrip patches for circularly polarized broadband performance 152
5.5.1 Experimental performance of fabricated arrangement of antennas 153
(a) Reflection coefficient 153
(b) Input impedance and polarization 156
(c) Gain, Radiation efficiency and radiation patterns of antenna 159
5.6 Summary 162

Chapter 6 – Conclusions and Future Work 163
6.1 Conclusions 163
6.2 Scope for future work 165
References 167
Publication details 184
Author Biography 185

List of Figures

Fig. No.	Description	Page No.
1.1	Basic features of a patch antenna	4
1.2	Geometries of common microstrip patch antennas	5
1.3	Radiation Pattern for (a) Square (b) Elliptical (c) Annular Ring (d) Triangular shaped Microstrip Patch Antennas	11
2.1	Square microstrip antennas with Corner-truncated (a) Design with a microwave substrate (ε_r = 3.0, h= 1.524 mm); (b) Design with a ceramic substrate (ε_r = 28.2, h= 4.75 mm)	19
2.2	Geometry of meandered rectangular microstrip antenna with slots	20
2.3	Measured return loss of shorted and conventional triangular microstrip antennas	21
2.4	Measured and calculated reflection coefficient of the antenna	22
2.5	Geometry of broadband microstrip antenna with directly coupled and parasitic patches	24
2.6	Radiation pattern	46
2.7	Microsripline feed and its equivalent circuit	49
2.8	Coaxial feed and its equivalent circuit	50
2.9	Aperture coupled feed arrangement and equivalent circuit	51
2.10	Proximity coupled feeding mechanism and equivalent circuit	52
3.1	Radiation mechanism of patch antenna	69
3.2	Top view of simple rectangular geometry	70
3.3	Variation of reflection coefficient (S_{11}) with frequency for rectangular geometry	70
3.4	Variation of VSWR with frequency for rectangular geometry	71
3.5	E and H plane radiation pattern at 7.48 GHz	71
3.6	E and H plane radiation pattern at 8.04 GHz	71
3.7	Top view of pentagonal patch geometry	72
3.8	Variation of reflection coefficient (S_{11}) with frequency for pentagonal geometry	73
3.9	Variation of VSWR with frequency for pentagonal geometry	73

Fig. No.	Description	Page No.
3.10	(a) Top view of pentagonal geometry (b) Ground plane geometry with rectangular slot	74
3.11	Variation of reflection coefficient (S_{11}) with frequency for different ground slot dimensions	74
3.12	Variation of reflection coefficient (S_{11}) with frequency for pentagonal geometry with ground slot	75
3.13	Variation of VSWR with frequency for pentagonal geometry with ground slot	75
3.14	Variation of gain as a function of frequency for lower band (2.69 GHz)	76
3.15	Variation of gain as a function of frequency for upper band (6.11 GHz)	76
3.16	E and H plane radiation pattern at 2.69 GHz	77
3.17	E and H plane radiation pattern at 6.11 GHz	77
3.18	(a) Top view of pentagonal geometry (b) Modified ground plane	78
3.19	Variation of reflection coefficient(S_{11}) with frequency for different ground strip dimensions	78
3.20	Variation of reflection coefficient (S_{11}) with frequency for pentagonal geometry with modified ground	79
3.21	Variation of VSWR with frequency for pentagonal geometry with modified ground	79
3.22	Variation of gain as a function of frequency for lower band (2.57 GHz)	79
3.23	Variation of gain as a function of frequency for upper band (5.64 GHz)	80
3.24	E and H plane radiation pattern at 2.57 GHz	80
3.25	E and H plane radiation pattern at 5.64 GHz	80
3.26	(a) Top view of the proposed geometry (b) Back view of the proposed geometry (c) Top view designed geometry (d) Back view of designed geometry	81
3.27	Variation of reflection coefficient(S_{11}) with frequency for modified pentagonal patch with defected ground	82

Fig. No.	Description	Page No.
3.28	Measured reflection coefficient (S_{11}) with frequency for modified pentagonal patch with defected ground	83
3.29	Variation of VSWR with frequency for modified pentagonal patch with defected ground	83
3.30	Measured VSWR with frequency for modified pentagonal patch with defected ground	83
3.31	Measured input impedance for modified pentagonal patch with defected ground	84
3.32	Variation of gain as a function of frequency for lower band	84
3.33	Variation of gain as a function of frequency for upper band	85
3.34	Variation of radiation efficiency as a function of frequency for lower band	85
3.35	Variation of radiation efficiency as a function of frequency for upper band	85
3.36	Simulated E and H plane radiation pattern at 2.72 GHz	86
3.37	Simulated E and H plane radiation pattern at 5.75 GHz	86
3.38	Measured E and H plane radiation pattern of proposed geometry at 2.72 GHz	87
3.39	Measured E and H plane radiation pattern of proposed geometry at 5.75 GHz	87
3.40	Current distributions of the proposed antenna at patch and ground plane for 2.72 GHz	88
3.41	Current distributions of the proposed antenna at patch and ground plane for 5.75 GHz	89
3.42	Top view of square geometry	89
3.43	Variation of reflection coefficient (S_{11}) with frequency for square geometry	90
3.44	Variation of VSWR with frequency for square geometry	90
3.45	E and H plane radiation pattern at 6.88 GHz	90
3.46	E and H plane radiation pattern at 7.74 GHz	91
3.47	Top and Bottom view of ground truncated geometry	92
3.48	Effect of varying ground dimensions on reflection coefficient as a function of frequency	92

Fig. No.	Description	Page No.
3.49	Variation of reflection coefficient (S_{11}) with frequency for square geometry with ground truncation	92
3.50	Variation of VSWR with frequency for square geometry with ground truncation	93
3.51	Variation of gain as a function of frequency for square geometry with ground truncation	93
3.52	E and H plane radiation pattern at 3.984 GHz	93
3.53	Effect of varying circular slot radius in patch on reflection coefficient as a function of frequency	94
3.54	Variation of reflection coefficient (S_{11}) with frequency for square patch with circular slot and reduced ground	94
3.55	Variation of VSWR with frequency for square patch with circular slot and reduced ground	95
3.56	Variation of gain as a function of frequency for square patch with circular slot and reduced ground	95
3.57	E and H plane radiation pattern at 3.70 GHz	95
3.58	Top and back view of the modified square patch with defected ground	96
3.59	Effect of varying strip length at ground on reflection coefficient as a function of frequency	96
3.60	Effect of varying strip position on reflection coefficient as a function of frequency	96
3.61	(a) Top view designed geometry (b) Back view of designed geometry	97
3.62	Variation of simulated reflection coefficient (S_{11}) as a function of frequency for modified square patch antenna with defected ground	97
3.63	Measured reflection coefficient with frequency for modified square patch antenna with defected ground	98
3.64	Variation of VSWR with frequency for modified square patch antenna with defected ground	98
3.65	Variation of measured VSWR with frequency for modified square patch antenna with defected ground	99
3.66	Measured input impedance modified for square patch antenna with defected ground	99

Fig. No.	Description	Page No.
3.67	Variation of gain as a function of frequency for lower band of modified square patch antenna with defected ground	100
3.68	Variation of gain as a function of frequency for upper band of modified square patch antenna with defected ground	100
3.69	Variation of radiation efficiency as a function of frequency for lower band of modified square patch antenna with defected ground	101
3.70	Variation of radiation efficiency as a function of frequency for upper band of modified square patch antenna with defected ground	101
3.71	Simulated E and H plane radiation pattern at 3.56 GHz	102
3.72	Simulated E and H plane radiation pattern at 3.56 GHz	102
3.73	Measured E and H plane radiation pattern at 5.40 GHz	103
3.74	Measured E and H plane radiation pattern at 5.40 GHz	103
3.75	Surface current distributions in patch and ground at resonant frequencies (a) 3.56 GHz and (b) 5.40 GHz.	104
4.1	Top view of triangular geometry	109
4.2	Variation of reflection coefficient (S_{11}) as a function of frequency for triangular geometry	109
4.3	Variation of VSWR as a function of frequency for triangular geometry	110
4.4	E and H plane radiation pattern at 8.77 GHz	110
4.5	Variation of shape and dimensions of the slot in the ground plane	111
4.6	Effect of varying slot dimensions on reflection coefficient as a function of frequency	111
4.7	Variation of reflection coefficient (S_{11}) as a function of frequency for triangular patch with slots in ground	111
4.8	Variation of VSWR as a function of frequency for triangular patch with slots in ground	112
4.9	E and H plane radiation pattern at 8.16 GHz	112
4.10	Effect of varying ground slot dimensions on reflection coefficient as a function of frequency for four considered cases	113

Fig. No.	Description	Page No.
4.11	Top and back view of the triangular patch with asymmetric slots in ground	113
4.12	Top and back view of the fabricated triangular patch with asymmetric slots in ground	114
4.13	Simulated reflection coefficient (S_{11}) as a function of frequency for triangular patch with asymmetric slots in ground	114
4.14	Measured reflection coefficient (S_{11}) as a function of frequency for triangular patch with asymmetric slots in ground	114
4.15	Simulated VSWR as a function of frequency for triangular patch with asymmetric slots in ground	115
4.16	Measured VSWR as a function of frequency for triangular patch with asymmetric slots in ground	115
4.17	Measured input impedance for triangular patch with asymmetric slots in ground	116
4.18	Variation of gain with frequency for triangular patch with asymmetric slots in ground	116
4.19	Variation of radiation efficiency with frequency for triangular patch with asymmetric slots in ground	117
4.20	Simulated E and H plane radiation pattern at 2.90 GHz	117
4.21	Measured E and H plane radiation pattern at 2.90 GHz	118
4.22	The current distributions of the proposed antenna at patch and ground plane	118
4.23	Top view of circular geometry	119
4.24	Variation of reflection coefficient (S_{11}) as a function of frequency for circular geometry	120
4.25	Variation of VSWR as a function of frequency for circular geometry	120
4.26	E and H plane radiation pattern at 7.81 GHz	121
4.27	E and H plane radiation pattern at 9.43 GHz	121
4.28	Effect of varying ground dimensions on reflection coefficient as a function of frequency	122
4.29	The bottom view of the truncated ground plane	122

Fig. No.	Description	Page No.
4.30	Variation of reflection coefficient (S_{11}) as a function of frequency for circular patch with reduced ground	123
4.31	Variation of VSWR as a function of frequency for circular patch with reduced ground	123
4.32	Variation of gain as a function of frequency for circular patch with reduced ground	124
4.33	E and H plane radiation pattern at 7.19 GHz	124
4.34	E and H plane radiation pattern at 7.98 GHz	124
4.35	Top view of modified circular patch with elliptical slot	125
4.36	Effect of varying elliptical slot minor axis and major axis radius in patch on reflection coefficient as a function of frequency	125
4.37	Variation of reflection coefficient (S_{11}) as a function of frequency for circular patch antenna with elliptical slot	126
4.38	Variation of VSWR as a function of frequency for circular patch antenna with elliptical slot	126
4.39	Variation of gain as a function of frequency for circular patch antenna with elliptical slot	127
4.40	E and H plane radiation pattern at 6.953 GHz	127
4.41	E and H plane radiation pattern at 8.53 GHz	127
4.42	(a) Top view of the proposed geometry (b) Back view of the proposed geometry (c) Top view designed geometry (d) Back view of designed geometry	128
4.43	Simulated reflection coefficient (S_{11}) as a function of frequency for modified circular patch with reduced ground	129
4.44	Measured reflection coefficient with frequency for modified circular patch with reduced ground	129
4.45	Simulated VSWR as a function of frequency for modified circular patch with reduced ground	130
4.46	Variation of measured VSWR with frequency for modified circular patch with reduced ground	130
4.47	Measured input impedance for modified circular patch with reduced ground	131
4.48	Variation of gain as a function of frequency for modified circular patch with reduced ground	131

Fig. No.	Description	Page No.
4.49	Variation of radiation efficiency as a function of frequency for modified circular patch with reduced ground	132
4.50	Simulated E and H plane radiation pattern at 4.75 GHz	132
4.51	Measured E and H plane radiation pattern at 4.75 GHz	133
4.52	Simulated E and H plane radiation pattern at 5.98 GHz	133
4.53	Measured E and H plane radiation pattern at 5.98 GHz	134
4.54	Surface current distributions on the patch and the system ground plane at (a) 4.75 GHz (b) 5.98 GHz	135
5.1	Top view of simple hexagonal geometry	141
5.2	(a) Simulated return loss of simple hexagonal geometry as a function of frequency	141
5.2	(b) Simulated VSWR of simple hexagonal geometry as a function of frequency	142
5.3	Variation of input impedance with frequency for hexagonal geometry	142
5.4	Variation of gain (dBi) with frequency for hexagonal geometry	143
5.5	Simulated co and cross polar radiation pattern of simple hexagonal at 3.61GHz a) E-plane b) H-plane	143
5.6	Top and side views of stacked antenna geometry without airgap	144
5.7	Variations of reflection coefficient with frequency for seven considered configuration	145
5.8	Variations of broadside directive gain with frequency for six considered configurations	146
5.9	Variation of reflection coefficient (S_{11}) of stacked geometry without air gap with respect to frequency	147
5.10	VSWR of stacked geometry without air gap as a function of frequency	147
5.11	Input impedance of geometry stacked geometry without air gap	148

Fig. No.	Description	Page No.
5.12	Reflection coefficient versus frequency for different values of air gap in between driven and parasitic patches of stacked microstrip antenna configurations	149
5.13	Directive gain versus frequency for different values of air gap in between driven and parasitic patches of stacked microstrip antenna configurations	150
5.14	Reflection coefficient versus frequency for different location of shorting pin in driven patch of stacked microstrip antenna configurations	151
5.15	Axial ratio versus frequency for different location of shorting pin in driven patch of stacked microstrip antenna configurations	152
5.16	(a) Side view of stacked antenna structure with shorting pin. (b) Top view of designed rectangular patch. (c) Top view of designed hexagonal patch with feed and shorting pin.	153
5.17	Simulated reflection coefficient (S_{11}) of stacked geometry with air gap and shorting pin	154
5.18	Measured reflection coefficient (S_{11}) of stacked geometry with air gap and shorting pin	154
5.19	Measured Voltage Standing Wave Ratio (VSWR) of stacked geometry with air gap h_a = 1.59 mm and shorting pin	155
5.20	Measured Voltage Standing Wave Ratio (VSWR) of stacked geometry with air gap h_a = 1.59 mm and shorting pin	155
5.21	Simulated input impedance of stacked antenna geometry with air gap and shorting pin	156
5.22	Measured input impedance of stacked antenna geometry with air gap and shorting pin	157
5.23	Variation of axial ratio of stacked antenna geometry with air gap and shorting pin	158
5.24	E-plane left and right circular polarization patterns at 4.352 GHz	158
5.25	E-plane left and right circular polarization patterns at 4.352 GHz	158
5.26	Variation of gain with frequency of stacked antenna geometry with air gap and shorting pin	159

Fig. No.	Description	Page No.
5.27	Variation of Radiation Efficiency with frequency for proposed antenna	159
5.28	Elevation gain pattern of antenna as a function of elevation angle and frequencies (a) Phi=0^0 and (b) Phi=90^0	160
5.29	Measured E and H radiation pattern at 3.41 GHz	160
5.30	Measured E and H radiation pattern at 4.40 GHz	161

List of Tables

Table No.	Description	Page No.
1.1	Comparisons of Various Regularly Shaped Microstrip Antennas	10
1.2	Applications using printed circuit antennas	14
2.1	Variation of Bandwidth with no. of slits	20
2.2	Comparison of recently reported Dual Band Antennas	33
2.3	Comparison of recently reported Broadband Antennas	37
2.4	Comparison of recently reported Stacked Antennas	41
3.1	Comparison of proposed antennas with other reported antennas	105
4.1	Comparison of proposed antennas with other reported antennas	135
5.1	Dimensions of upper radiating patch	145
5.2	Variation of airgap thickness	149
5.3	Variation of shorting pin location	151
5.4	Comparison of radiation properties of different antenna geometries	161
5.5	Comparison of proposed antenna with other reported antennas	162

List of Abbreviations

ADS	Advanced Design System
AUT	Antenna-Under-Test
AR	Axial Ratio
CAD	Computer Added Drawing/Design
dB	Decibels
DBS	Direct Broadcasting Systems
DTH	Direct to Home
RFID	Radio Frequency Identification
PCS	Personal Communication Systems
EMC	Electromagnetically coupled
FDTD	Finite Difference Time Domain
FEM	Finite Element Method
FR	Frequency Ratio
GPS	Global Positioning Systems
HPBW	Half Power Beamwidth
ISM	Industrial Scientific Medical Band
IEEE	Institute of Electrical and Electronics Engineers
MOM	Method of Moments
MPIE	Mixed Potential Integral Equation
MIC	Microwave Integrated Circuit
MMIC	Monolithic Microwave Integrated Circuit
PCB	Printed Circuit Board
DGS	Defective Ground Structure
RF	Radio Frequency
TEM	Transverse Electric Magnetic Mode
TE	Transverse Electric Mode
TM	Transverse Magnetic Mode
UHF	Ultra High Frequency
UV	Ultra Violet
UWB	Ultra Wideband
UMTS	Universal Mobile Telecommunication System
VNA	Vector Network Analyzer
VSWR	Voltage Standing Wave Ratio
WLAN	Wireless Local Area Network
Wi-MAX	Worldwide Interoperability for Microwave Access
DCS	Digital Communication System
CP	Circular Polarization
WLAN	Wireless Local Area Network
RL	Return Loss

List of Symbols

Symbol	Description
$\vec{\mathbf{A}}$	Magnetic vector potential
$\vec{\mathbf{E}}$	Electric field vector
$\vec{\mathbf{H}}$	Magnetic field vector
$\vec{\mathbf{J}}$	Electric source current density
$\vec{\mathbf{M}}$	Magnetic surface current density
η_0	Free space impedance (120π)
ε_0	Permittivity of free space
ω_0	Precession angular frequency
η_d	Wave impedance in the dielectric medium $\eta_d = (\eta_0/\sqrt{\varepsilon_r})$
a	Size of patch (length or radius)
a_e	Effective size of patch antenna
BW	Bandwidth
c	Velocity of light in free space
d	Feed point location on the patch
D	Directivity of an antenna
f	Antenna design frequency
f_r	Resonant frequency of the antenna
h	Thickness of dielectric substrate
k_0	Propagation constant in free space
Q_t	Total quality factor of an antenna
RL	Return loss
$tan\delta$	Dielectric loss factor
U_T	Total energy stored
Z_{in}	Input impedance of an antenna
ε_e	Effective permittivity of substrate material
ϕ	Azimuth angle
η	Efficiency of an antenna
λ_0	Free-space wavelength
λ_d	Wavelength inside dielectric
μ	Permeability of free space
θ	Elevation angle
ψ	Phase angle between incident and reflected waves

Chapter 1
Introduction

1.1 Introduction

Antennas have been in use for more than a century. The design and applications of antenna have also seen many changes and it is not very old that the electromagnetic band, has been utilized for communication using radio [1]. Electromagnetic spectrum has been one of the greatest resources provided by nature to us and the antenna has been instrumental in exploiting this resource [2].

Presently wireless communication, by measure is the fastest growing segment of the communication field. There are many commercial and government applications including cellular, radar and satellite systems and wireless communication where heaviness, dimension, cost, performance, trouble-free installation, aerodynamics profile are major restrictions. The vision of the wireless communication helping information swap between people and machines is the communication frontier for the future years. This vision will permit communication between multimedia across the world. In the last few years, the development of WLAN, Wi-Fi, Bluetooth and Wi-MAX symbolize one of the significant interests in the communication and information area. Also, in the today's environment, technology demands antenna which can operate on different wireless bands and should have different features like economical in price, lighter in weight, low profile antennas that are proficient of maintaining good radiation performance over a large band of frequencies [3]. The swift growth of wireless communication systems has prompted industry to bring new wireless devices and systems to fulfill the need of multimedia system applications. Devices such as mobile phones and WPANs (Wireless Personal Area Network) have increased the requirement of antennas [4].

Antennas are base line components in electronic systems that use free space electromagnetic wave transmission for various applications. In general an antenna has collection of metallic conductors, which are linked to the receiver or transmitter through a transmission line. A fluctuating current pushed through the antenna by a

transmitter will generate a fluctuating magnetic field in the region of the antenna, whereas the charge of the electrons also produces an oscillating electric field along the antenna. These time-varying fields will spread out away from the antenna into space as an electromagnetic field radiation. On the contrary, when antenna is linked with receiver, the oscillating fields of an arriving electromagnetic wave apply force on the electrons in the antenna and cause them to move, thus oscillating currents are produced in the antenna. Antennas can have different configurations and characteristics, depending upon the purpose for which they are used, the environment in which they have to operate and frequency band for which they are designed [5-6].

Miniaturization is an important concept in the field of science and engineering. As antenna is one of the most critical component in a communication system, the need for a new generation of antenna systems having smaller size, lightweight and compatibility to integrated electronic circuits has been felt. Such demand gave rise to the concept of "Microstrip Antennas". Although the concept of microstrip antenna came into existence in 1953 by Deschamps but not much work was done in this area for next twenty years. In 1970s, when requirement for antennas with low profile characteristics was felt for various applications, the scientists and researchers understood the importance of microstrip antennas and research in this field started worldwide [7]. Patch antennas are preferred over other antenna configurations due to its characteristics suitable mainly for applications operating in higher frequency range including RF and microwave region. A conventional microstrip antenna is a three layer structure having patch on the top, dielectric substrate layer in the middle and metallic ground plane at the bottom. In size a patch is larger than a strip and its size and shape is an important deciding factor in the radiation characteristics of the antenna. A microstrip patch antenna in its conventional form generally resonates at a single frequency and its performance can be considerably enhanced when its dimensions are optimized in such a way that cavity underneath the patch is resonating in its dominant mode at the desired frequency [8-9]. There are various types of microstrip antennas which may be categorized as per appearance, shapes

and dimensions. In general, these microstrip antennas can be classified into four main categories namely:

(a) Microstrip dipoles (b) Microstrip traveling wave antennas

(c) Printed slot antennas (d) Microstrip Patch Antennas

A brief description on each type of microstrip antennas listed above is given below, which provides a direction that how each type of antenna works:

The microstrip dipole antennas are similar to microstrip patch antennas in terms of radiation pattern but they have different length to width ratio. These antennas are normally linearly polarized and have small size. The microstrip dipole antennas can yield good bandwidth at high frequency due to thickness of dielectric substrate and the feeding technique plays a very crucial role in deciding its performance.

Microstrip traveling wave antennas are generally circularly polarized in nature and due to their long microstrip line having good width it operates in TE mode. The one end of the antenna is connected to the resistive load for impedance matching in such a way that standing wave may be reduced to minimum.

The printed slot antennas are made by etching a slot in the ground plane of a grounded substrate. Due to slot in the ground plane radiations occurs on the both sides of the antenna, they can be designed in any shape and in these antennas edge feed technique is used for feeding.

Microstrip patch antenna in its simple form has patch placed on the top with negligible thickness as compared to dielectric substrate placed in the middle, followed by ground plane at the bottom. Generally same conductor is used for patch and the ground like gold or copper and a low tangent loss dielectric is used for substrate. The radiations occur in a microstrip patch antenna due to fringing fields present at the edges. The typical geometry of a simple microstrip patch antenna is shown in figure 1.1. Although microstrip antennas are considered to be low profile but their ability to radiate efficiently is a very important characteristic. The radiation performance of microstrip antenna depends on several parameters such as thickness

of the substrate, size and shape of the patch, type of feeding and dielectric constant of the substrate. [10].

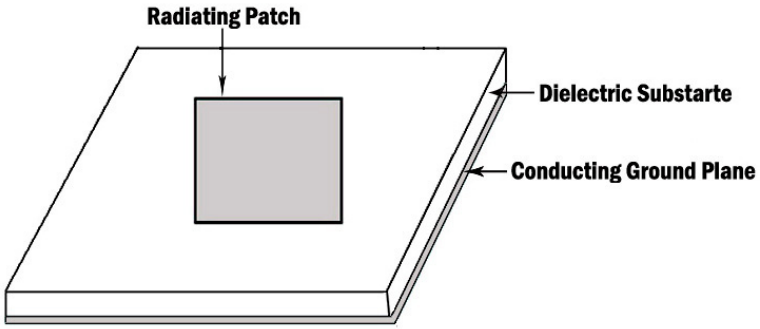

Fig. 1.1 Basic features of a patch antenna

1.2 Shapes of patches

Different shapes of the conductors have been reported and investigated over the years for a microstrip patch antenna. The shape of the patch is the main parameter which affects the bandwidth of the antenna. It also affects its electrical characteristics such as polarization and gain. If the patch is like the square or the circle, the bandwidth is same and proportional to size. The deviation starts when the shape changes significantly and becomes narrow or wide at the edges. If the radiation edge becomes narrow, the radiation loss decreases and the antenna Q increases, and the opposite are true for a patch with a wide radiating edge. The patch geometries are generally rectangular but square, circular and triangular patches are also possible. The radiating element may be square, rectangular, triangular, annular ring or circular in shape are decided by the characteristics of the transmitted wave and must be separated by a finite distance from the ground plane [11-12]. Thin sheet of dielectric substrate is introduced between these two conducting layers. Schematic diagrams of few common patch geometries are shown in Fig.1.2.

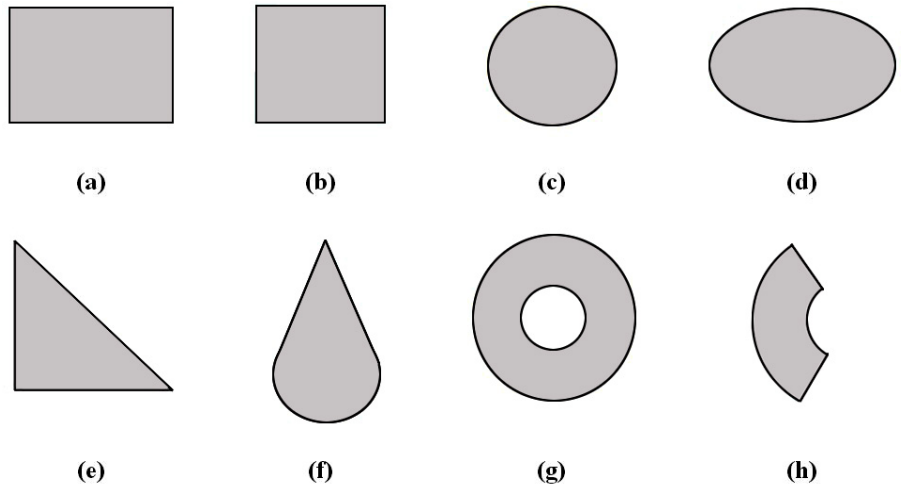

Fig. 1.2 Geometries of common microstrip patch antennas

Among the geometries mentioned below, rectangular and square shapes of the patch [Figs. 1.2(a) and 1.2(b)] are most common geometries. Due to larger in shape, rectangular patches provide broadest bandwidth. A rectangular patch is defined by its length L and width W. For a simple microstrip line, the width is much smaller than the wavelength. However, for the rectangular patch, the width is comparable to the wavelength to enhance the radiation from the edges. Since the substrate thickness is much smaller than the wavelength, the rectangular patch antenna is considered to be a two-dimensional planar configuration for analysis.

For rectangular patch antenna, generally W >> h, so for quick analysis or design, the extension in length due to fringing field may be approximately calculated by the following simple formula:

$$\Delta L = \frac{h}{\sqrt{\varepsilon_e}} \tag{1.1}$$

$$\text{Where } \varepsilon_e = \frac{(\varepsilon_r + 1)}{2} + \frac{(\varepsilon_r - 1)}{2}\left[1 + \frac{10h}{W}\right]^{-\frac{1}{2}} \tag{1.2}$$

Since the effective length of the patch is nearly equal to λ/2, it can be calculated for a given resonance frequency f_0 as:

$$L_e = L + 2\Delta L = \frac{\lambda_0}{2\sqrt{\varepsilon_e}} = \frac{c}{2f_0\sqrt{\varepsilon_e}} \tag{1.3}$$

where c= velocity of light in free space = 3×10^8 m/sec. This expression simplifies to

$$L_e = \frac{15}{f_0\sqrt{\varepsilon_e}} \tag{1.4}$$

where L_e is in cm and f_0 is in gigahertz. For a given length L, f_0 is calculated from

$$f_0 = \frac{c}{2L_l\sqrt{\varepsilon_l}} = \frac{15}{L_e\sqrt{\varepsilon_l}} \tag{1.5}$$

In general, the resonance frequency of the rectangular patch excited at any TM_{mn} mode is obtained using the following expression [13]:

$$f_0 = \frac{c}{2\sqrt{\varepsilon_e}}\left[\left(\frac{m}{L}\right)^2 + \left(\frac{n}{W}\right)^2\right]^{1/2} \tag{1.6}$$

where *m* and *n* are the modes along the L and W, respectively.

To calculate ε_e, the value of W should be known. For a rectangular patch to be an efficient radiator, W should be approximated to a half wavelength corresponding to the average of the two dielectric mediums (i.e., substrate and air) [12].

$$W = \frac{c}{2f_0\sqrt{\frac{(\varepsilon_e + 1)}{2}}} \tag{1.7}$$

The width W of the patch can be taken smaller or larger than the value obtained using (eq. 1.7). If W is smaller, then the BW and gain will decrease. If W is larger, then the BW increases due to the increase in the radiated fields. However, if W is too large, then the higher order modes could get excited.

The normalized radiation patterns for rectangular patch in the E-plane (E_θ in $\phi = 0°$ plane) and the H-plane (E_ϕ in $\phi = 90°$ plane) are given by

$$E_\theta = \frac{\sin\left(\frac{(k_0\Delta L\sin\theta)}{2}\right)}{\frac{k_0\Delta L\sin\theta}{2}}\cos\left(\frac{k_0(L+\Delta L)}{2}\sin\theta\right) \tag{1.8}$$

$$E_\phi = \frac{\sin\left(\frac{k_0 W_e}{2}\sin\theta\right)}{\frac{k_0 W_e}{2}\sin\theta}\cos\theta \tag{1.9}$$

where θ is the angle measured from the broadside.

A circular patch is another widely used configuration [Figs. 1.2(c)]. In the case of the rectangular patch, the field variation underneath the patch is defined in terms of sine or cosine functions. On the other hand, the fields for a circular patch are defined in terms of the Bessel function.

The resonance frequency of a circular patch is obtained using the formula [13-14]:

$$f_0 = \frac{K_{nm} c}{2\pi a_e \sqrt{\varepsilon_e}} \tag{1.10}$$

where K_{nm} is the m^{th} root of the derivative of the Bessel function of order n [12-13].

For the fundamental TM_{11} mode, the value of K_{nm} is 1.84118. The a_e and ε_e are the effective radius and the effective dielectric constant of the circular patch, respectively. The fringing fields along the circumference of the circular patch are taken into account by replacing the patch radius a by the effective radius a_e [13, 14–20]

$$a_e = a\left[1 + \frac{2h}{\pi a \varepsilon_r}\left\{In\left(\frac{a}{2h}\right) + 1.41\varepsilon_r + 1.77 + \frac{h}{a}(0.268\varepsilon_r + 1.65)\right\}\right]^{1/2} \tag{1.11}$$

The normalized radiation pattern of the circular patch may also be calculated using the following equations [1]:

$$E_\phi = \left[J_{n+1}(k_0 a \sin\theta) + J_{n-1}(k_0 a \sin\theta)\right]\cos\theta \sin n\phi \tag{1.12}$$

$$E_\theta = \left[J_{n+1}(k_0 a \sin\theta) - J_{n-1}(k_0 a \sin\theta)\right]\cos n\phi \tag{1.13}$$

where Jn +1 and Jn -1 are the Bessel functions of order n + 1 and n - 1,respectively.

Among various geometries elliptical shapes has less popularity due to involvement of elliptical coordinate system and Mathieu function in association with applicable boundary conditions [21]. The elliptical shape patch geometries are becoming popular recently as they easily provides better bandwidth, allows better control of the polarization characteristics and facilitates the design by changing both eccentricity and focal length to tune the parameters of interest. For an ellipse of semi-major axis 'a' and semi-minor axis b, the foci of ellipse are at x = ± c where $'c' = \left[a^2 - b^2\right]^{1/2}$ [Figs. 1.2(d)]. The theoretical resonant frequency of elliptical

waveguide following Kretzschmar (1970), can be modified and simplified for the elliptical microstrip antenna as

$$f_{c11} = \frac{15}{\pi e a}\sqrt{\frac{q_{c11}}{\varepsilon_r}} \quad GHz \tag{1.14}$$

Where f_{c11} is the dual-resonant frequency of TMc_{11}, and TMs_{11} mode and a is the physical semi-major axis (cm). Generally, the measured results of the f_{c11} are lower than calculated values due to effective (electrical) semi-major axis a_{ef}, ($a_{ef} > a$). Therefore closed-form formula for resonance frequency f_{c11} can be determined accurately by replacing the physical semi-major axis a with the effective semi-major axis a_{ef} as:

$$f_{c11} = \frac{15}{\pi e a_{ef}}\sqrt{\frac{q_{c11}}{\varepsilon_r}} \quad GHz \tag{1.15}$$

Here f_{c11} is the resonance frequency of elliptical patch antenna with eccentricities $\left(e = \sqrt{1-\left(b/a\right)^2}\right)$ corresponding aspect ratios b / a of the physical semi-minor axis / the physical semi-major axis. The suggested approach of Suzuki and Chiba [1984] is applicable to the elliptical microstrip antennas. The f_{c11} for elliptical patch antenna considering fringing field effects may be calculated using relation for a_{ef} proposed by modifying the relation of a_{ef} for a circular patch antenna for the TM_{11} mode of excitation [22].

$$a_{ef} = \left[a^2 + \frac{ha}{0.3525\pi\varepsilon_r}\left\{\ell n\left(\frac{a}{2h}\right) + \left(1.41\varepsilon_r + 1.77\right) + \frac{h}{a}\left(0.268\varepsilon_r + 1.65\right)\right\}\right]^{\frac{1}{2}} \tag{1.16}$$

The determination of the exact value of the parameter q for a given mode and eccentricity is rather complicated. To avoid this complexity, Kretzschmar [1970] derived an approximate analytic relation between e and q for the eight lowest order modes.

A semicircular patch with half the area of a circular patch has nearly same resonance frequency and radiation pattern (for TM_{11}) as that of a circular patch antenna [14, 23]. The disc sector patch geometry [Figs. 1.2(f)] is also smaller in size and can be used to achieve dual polarization but at the expense of small bandwidth and low gain.

Triangular patch as shown in [Figs. 1.2(e)] is further smaller in size. The resonance frequency of the equilateral triangular patch antenna is given by [14]:

$$f_{mnl} = f_{mn} = \frac{2c\left(m^2 + mn + n^2\right)^{1/2}}{3S_e\sqrt{\varepsilon_e}} \tag{1.17}$$

where S_e is the effective side length, and $m + n + l = 0$. Instead of using m, n, and l, only m, n has been used for simplicity, it is implied that $l = -(m + n)$.
Alternatively, the following approximate formula can be used for quick estimate of S_e

$$S_e = S + \frac{4h}{\sqrt{\varepsilon_e}} \tag{1.18}$$

An annular patch can be considered as a removal of a smaller inner concentric circle from the outer circle. The resonance frequency of the annular patch is always smaller than that of the circular because of its larger resonant length. The resonance frequency of the annular patch antenna is given by [13]:

$$f_{nm} = \frac{X_{nm}c}{2\pi b\sqrt{\varepsilon_e}} \tag{1.19}$$

where c is the velocity of light and Xnm represents the roots of the equation

$$J_n'(CX_{nm})Y_n'(X_{nm}) - J_n'(X_{nm})Y_n'(CX_{nm}) = 0 \tag{1.20}$$

Jn (x) and Yn (x) are the Bessel functions of the first and second kind, and $C = a/b$.

Annular ring [Fig. 1.2(g)] and sector ring [Fig. 1.2(h)] also comes under the category of smaller shape as compared to rectangular geometry. Annular ring is symmetrical in shape like circular and due to the presence of inner and outer radii more fringing field is developed at both the edges as compared to circular shape resulting in higher bandwidth.

A comparison on effect of the shapes of microstrip patch antennas on various parameters is shown in table 1.1 and fig 1.3.

TABLE 1.1 COMPARISONS OF VARIOUS REGULARLY SHAPED MICROSTRIP ANTENNAS (ε_r =4.4, h =0.8 mm and f_0 =2.43 GHz)

S. No.	Configuration	Dimensions (in mm)	Bandwidth (in MHz)	Input Impedance (in Ω)	Directivity (in dB)
1	Square	L= 28.8	46 (1.89 %)	Real part= 50.438 Imaginary part= 0.336	3.8363
2	Ellipse	minor axis= 16.56 major axis= 17.1	47.6 (1.95 %)	Real part= 50.002 Imaginary part= 0.451	4.0114
3	Annular Ring	outer radius = 36.81 inner radius = 21.59	42.2 (1.73 %).	Real part= 48.09 Imaginary part= 2.76	0.3443
4	Triangle (equilateral)	L= 38.7	34.9 (1.43%)	Real part= 50.30 Imaginary part= 0.158	3.3706

It can be easily seen from the results mentioned in table 1.1 that when there is a need for compact size then square shaped patch antenna could be considered. On the other hand when we can compromise somewhat with the size then elliptical antenna could be a better option.

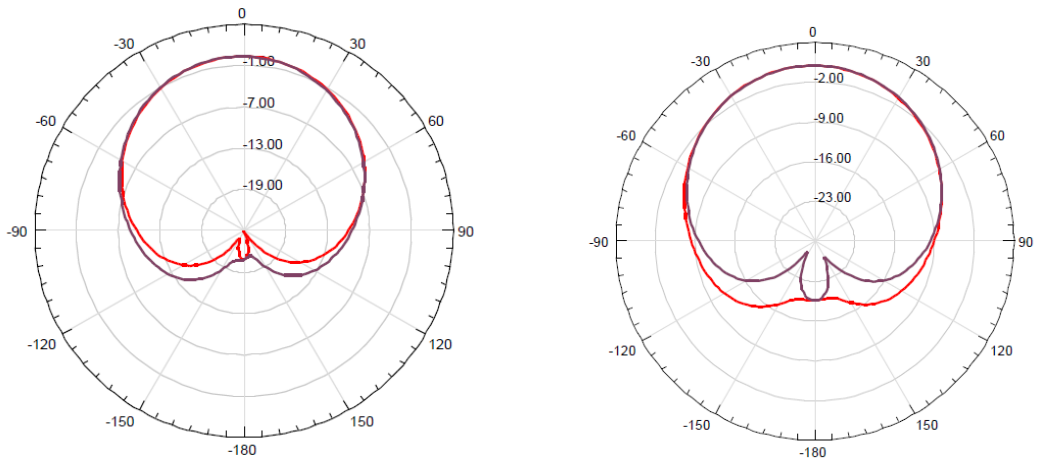

(a) (b)

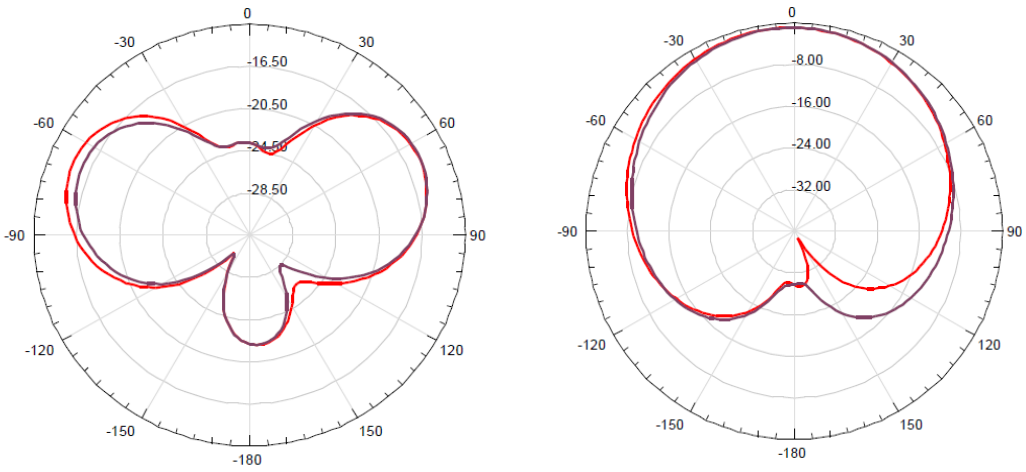

(c) (d)

Fig. 1.3 Radiation Pattern for (a) Square (b) Elliptical (c) Annular Ring (d) Triangular shaped Microstrip Patch Antennas [22]

As indicated in Fig. 1.3 that, for annular ring path antenna the radiation pattern has high side lobe level which is not desirable while other shapes has nearly similar radiation pattern [24]. This can be improved by increasing the size of the annular ring patch.

A semicircular patch has half the area of the circular and has a smaller bandwidth, but its gain is only slightly less. A triangular has a smaller bandwidth and gain but its area is also smaller. For obtaining circular polarization square patches and elliptical patches are preferred. In order to achieve low cross polarization symmetrical shapes are used and this caused circular and elliptical geometries to be used quite often [2]. Moreover the symmetry of the shape also gives higher accuracy for analyzing geometries using full wave analysis techniques during early days. But now with growth of computational electronics and availability of rigorous simulation tools any geometrical shape can be analyzed with much ease and good accuracy.

1.3 Advantages and disadvantages of microstrip antennas

Microstrip antennas offers quite a lot advantages in contrast to conventional antennas and therefore these antennas are utilized in numerous applications over a frequency ranging from approximately 100 MHz to about 50 GHz and even higher.

Microstrip patch antennas are becoming increasingly popular these days for the use in wireless systems due to their attractive features. These antennas can be easily accommodated in mobile handsets and small wireless devices. They have been successfully used in telemetry and satellite communication. Some of their principal merits over other antennas are [2]:

- Lighter weight and small in size.
- The antennas have low scattering cross section.
- Fabrication of feed structure and matching networks along with the antenna.
- Ease of compatibility with the host surface.
- Mass manufacturing is possible due to low fabrication cost and ease of fabrication
- Easy integration with MICs.
- Linear and circular polarization can be achieved with simple changes in the feed position.
- Dual and multi frequency antenna can be designed.
- Active devices such as filters, mixers, oscillators, amplifiers etc, can be easily integrated with antennas.

Despite many advantages of patch antennas, they do have some considerable drawbacks compared to conventional microwave antennas. The major disadvantages are [2][25]:

- Narrow bandwidth: (typically 1 - 2%).
- Surface waves radiation.
- Lower efficiency and gain than conventional microwave antennas.
- Unwanted radiations.
- Can be used for low power only.

Most of the demerits mentioned above are associated with conventional microstrip antenna and by using suitable design and feeding techniques many of them can be overcome.

1.4 Motivation

The exponential technology advancement in wireless communication and information world has generated the necessity for key improvement in antenna designs. The user community and service providers generally demand wireless devices with antennas that are economical, compact in size, can work efficiently for longer duration, mass manufacturing in large quantities and compatible with other components in the system. To fulfill theses requirements antenna designers and researches considered wide range of design structures. The monopole antenna has been the best choice for this due to simplicity in design and having all essential performance specifications which are compatible with modern technology. In cellular mobile networks embedded antennas with small size and wide operational bandwidth are mainly required. In wireless networking for Wi-Fi, WLAN and Wi-MAX there is a demand for high performance, low cost antenna which is conformal to host surface. It also requires that antenna size should be reduced without any significant impact on its bandwidth, gain and efficiency. Now a day's single antenna has to serve many devices and applications associated with it. The compact antenna with multiband and multi frequency operation which can also cover a broad spectrum has been in great demand.

1.5 Applications of microstrip antennas

Some prominent application areas where microstrip antennas have been used are:

- Satellite Communication
- Doppler Radars
- Telemetry
- Remote sensing
- Biomedical Radiator
- Phased Array Radars

Some more typical applications of printed circuits antennas are listed in table 1.2.

TABLE 1.2. APPLICATIONS USING PRINTED CIRCUIT ANTENNAS

Applications	Frequency Band
GPS 1200 GPS 1575	1227-1575 MHz 1565-1585 MHz
Radio Frequency identification(RFID)	865 - 868 MHz, 2.446 -2.454 GHz
Digital video Broadcasting -Handheld	470 MHz – 702 MHz
Cellular Phone	824-849 MHz 869-895 MHz
Personal Communication Systems	1.85-1.99 GHz 2.18-2.20 GHz
GSM	890-915 MHz 935-960 MHz
Direct Broadcast Satellite	11.7-12.5 GHz
Automatic Toll Collection	905 MHz 5-6 GHz
Collision Avoidance Radar	60 GHz, 77 GHz 94 GHz
Wide Area Computer Networks	60 GHz
Cellular Video	28 GHz
Digital communication system (DCS)	1.71-1.88 GHz
Universal Mobile telecommunication system (UMTS)	1920 MHz to 2170 MHz
Wi-MAX	Low band (2.49 to 2.69 GHz) Medium band (3.25 to 3.85 GHz) High band (5.25 to 5.85 GHz)
Wireless local Area Networks (WLAN)	2.45 to 2.484 GHz 5.15 to 5.825 GHz
ISM 2.4 ISM 5.2 ISM 5.8	2400-2484 MHz 5150-5350 MHz 5725-5825 MHz
Ultra wide band communication	3.1 -10.6 GHz

1.6 Scope and outline of the thesis

The major challenges in microstrip patch antenna are to achieve adequate bandwidth and compact size. These antennas in their original form resonate at a single resonance frequency corresponding to their dominant mode. For modern communication systems, antennas capable of resonating at two or more frequencies

simultaneously are preferred and hence development in these geometries is desired if they have to be applied in future communication systems.

The main aim of this thesis is to design and develop compact, multiband and broadband antennas which may find application in wireless communication systems. Extensive simulation and experimental work is carried out to validate the performance of designed structures. All patch antenna geometries discussed in this thesis are designed and simulated on glass epoxy FR4 substrate. The entire simulation analysis during the present work is carried out by applying electromagnetic simulation software CST and IE3D. After extensive optimizations in slot dimensions, slot location, patch dimension etc., prototype antennas are fabricated and tested with available resources.

This thesis is organized into six chapters which are as follows: After introduction presented in this chapter, the second chapter contains review of work carried out worldwide by different researchers in the field of microstrip antenna. A comprehensive literature survey is required to learn more about an antenna that requires nominal modification to ensemble the design requirements. In this chapter, more importance is given to those developments which took place during past few years. A brief description of radiation parameters, feeding techniques, antenna fabrication and measurement is also included in this chapter.

In third chapter of this thesis; the design and analysis of two geometries with defected ground for dual band operation is discussed. The modifications in geometries are carried so as to achieve compact structure with improved radiation performance. The first design considered is a modified pentagonal patch and in the first step a rectangular slot is etched in the ground plane and then simulated by optimizing the dimension of slot. In the next step, a pentagonal slot is cut in the patch and a rectangular strip is added in the ground plane. The performance of this antenna is again simulated by optimizing the length, width and location of strip and finally a prototype antenna is developed and tested. With these modifications in pentagonal patch geometry, antenna parameters like impedance bandwidth and gain are improved considerably. The simulated results are verified experimentally and proposed antenna geometry can be used for lower and upper band of Wi-Max and

WLAN. The second design in this chapter is compact modified square patch microstrip antenna with off-centered T-shaped ground plane. It is found that on introducing circular slot in the patch and truncating ground plane, the impedance bandwidth of antenna improves considerably. By introducing a protruding rectangular stub in the ground plane an additional mode operating at a higher frequency gets excited and the antenna resonates at two different frequencies. The position and dimensions of the stub in the ground plane is adjusted for antenna to resonate in the median band and upper band allocated for Wi-Max communication systems.

The fourth chapter includes two compact antenna geometries for broadband operation. In the first section of this chapter design and performance of a compact triangular patch antenna with slotted ground plane is analyzed and results are systematically presented. The combined effect of modifications in patch geometry and ground plane provided significantly improved impedance bandwidth along with gain enhancement in comparison to a conventional triangular patch antenna. Measured results are in good concurrence with the simulated results. This antenna is specifically designed looking Indian requirements for the lower band of UWB communication systems. At present, Indian wireless requirements are mainly limited within obtained bandwidth range. In the second section of this chapter modified circular patch antenna with reduced ground plane and an extensive analysis of this modified circular patch antenna is reported. The stepwise modifications in the circular patch antenna are done and radiation performance of patch antenna is analyzed after each step. The first step is truncation of ground plane to enhance the bandwidth without increasing the size of patch antenna. The second step is inserting elliptical slot with optimized dimensions in the patch for reducing the resonant frequency which results in minor reduction in gain value also. This achieved bandwidth is suitable for modern communication systems. The third step is etching two identical square slots along the y-axis for bandwidth enhancement and gain improvement. The antenna is fabricated using FR-4 substrate and experimental results are compared with simulation results, appropriate for various wideband communication systems particularly working in the C-band. It is also found through

parametric analysis that shape and dimension of the finite ground plane and slot in the patch are the key factors in enhancing the bandwidth of the proposed geometry.

The fifth chapter of thesis presents the design, development and analysis of stacked arrangement of rectangular and hexagonal patches. In veracity, a hexagonal patch antenna is a poor radiator having narrow bandwidth and low gain. An additional rectangular patch is introduced just over the hexagonal patch geometry. The patch lying on upper substrate is little larger in size than that of hexagonal patch and the upper structure does not have any metallic ground plane. The antenna geometry is further modified by applying a shorting pin in the driven element and by varying air gap between driven and parasitic elements. The air gap reduces the effective permittivity of substrate material that lowers the quality factor of cavity which in turn increases the bandwidth of antenna. By varying the dimensions of upper patch, air gap and shorting pin position the performance of this geometry is optimized to achieve best performance. It is established that the introduction of shorting pin not only improves the performance of antenna to a great extent in terms of bandwidth and gain but also antenna now exhibits circular polarization also.

The last chapter of this thesis deals with the conclusions drawn from the presented work and suggestions for future studies on microstrip antennas in different applications. A detailed bibliography describing recently reported work in related fields is included at the end of this thesis.

Chapter 2

Literature review and preliminaries

This chapter comprises of two parts. The first part provides brief description of bandwidth enhancement and size reduction techniques in microstrip antenna and a brief review of the past work in the antenna field and historical perspective of the printed antenna technology in the past few decades is also described. The relevant research works in this field is reviewed with emphasis given to compact, dual and broadband microstrip antennas.

The second part incorporates feeding techniques and definition of important radiation parameters in microstrip antenna along with brief description of analytical models of analysis for microstrip patch antennas. The overview of fabrication process and methods of measuring radiation performance of microstrip antenna is also provided.

2.1 Challenges in the research area

Increasing antenna bandwidth and size reduction are the main challenges in this research area. An antenna used for wireless communication systems should be proficient enough to cover a wide frequency bandwidth or multi frequency bands. The requirement of small size gives flexibility to them to be implanted effortlessly into devices for improving portability.

2.1.1 The techniques commonly used for reducing size of an antenna are:

(a) Using substrate with high dielectric constant

(b) Using meandered patch

(c) Punching vias and shorting pin through the substrate

(d) Use of diodes

(a) Using substrate with high dielectric constant

A compact structure can be obtained using substrate having dielectric constant on higher side, whereas by using low dielectric constant substrate the efficiency of antenna can be enhanced. The reason for low efficiency of antenna, as we increase

the dielectric constant of the substrate is due to occurrence of unwanted surface waves, these waves perturb the radiation in the desired direction which results in reduction in total efficiency of the antenna.

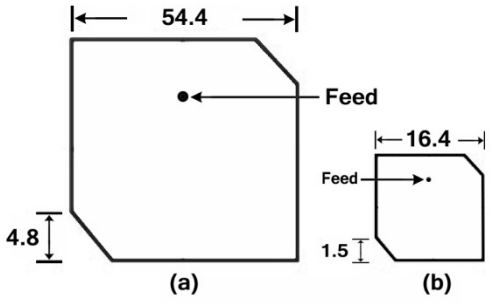

Fig. 2.1 Square microstrip antennas with Corner-truncated (a) Design with a microwave substrate (ε_r = 3.0, h= 1.524 mm); (b) Design with a ceramic substrate (ε_r = 28.2, h= 4.75 mm) [26]

A comparison of the required dimensions for two corner-truncated square microstrip antennas with different substrates for global positioning system (GPS) application is shown in figure 2.1. The first design uses a microwave substrate with relative permittivity ε_r=3.0 and thickness h=1.524 mm; the second design uses a high-permittivity or ceramic substrate with ε_r=28.2 and h=4.75 mm. From the patch areas of the two designs, it can be seen that the second design has a patch size about 10% of that of the first design. This result suggests that an antenna size reduction as large as about 90% can be obtained if the design with ε_r = 28.2 is used instead of the case with ε_r =3.0 for a fixed operating frequency [6][26].

(b) Using meandered patch

Compact operation of microstrip antennas can be obtained by meandering the radiating patch [27-28]. This kind of patch-meandering technique is achieved mainly by loading several meandering slits at the non radiating edges. By meandering the rectangular patch with slits as shown in figure 2.2, at the non-radiating edges of the patch, the resonant frequencies, of the two operating modes can be significantly lowered, with the radiation characteristics slightly affected. As specified in the table 2.1 the antenna with no meandered slits is operating at higher resonant frequencies (1915 MHz and 3620 MHz) while antenna loaded with meandered slits have lower resonant frequencies (1096 MHz and 2590 MHz). This clearly indicates that a large

antenna size reduction can be obtained, as compared to the slot-loaded patch without slits.

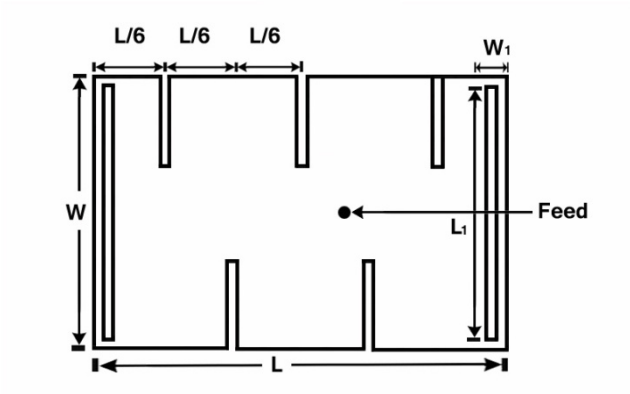

Fig. 2.2 Geometry of meandered rectangular microstrip antenna with slots [28]

TABLE 2.1 VARIATION OF BANDWIDTH WITH NO. OF SLITS

Slit length (mm)	Lower band resonant frequency, BW (in MHz)	Higher band resonant, BW (in MHz)
0	1915,1.78	3620,1.19
4	1811,1.60	3620,1.16
8	1553,1.48	3318,1.12
12	1196,1.34	2730,1.37
13	1096,1.46	2590,1.24

(c) Punching vias and shoring pin through the substrate

With the shorting-pin-loading technique, the antenna size reduction is mainly due to the shifting of the null-voltage point at the center of the rectangular patch (excited at the TM_{01} mode) and the circular patch (operated at the TM_{11} mode) to their respective patch edges, which makes the shorted patches resonate at a much lower frequency. Thus, at a given operating frequency, the required patch dimensions can be significantly reduced.

An equilateral triangular patch antenna with shorting pin was reported in [29]. It was shown in figure 2.3, without shorting-pin loading, the triangular microstrip patch resonates at 1.93 GHz and with shorting-pin loading, the resonant frequency of the triangular patch is slightly less. The length of triangular pin shorted antenna was L=15.3 mm, and; for a conventional antenna the length was L=59.9 mm. This means

a reduction of about 74% of the linear dimension of the antenna, or the size of the compact antenna is only about 7% of that of the conventional microstrip antenna.

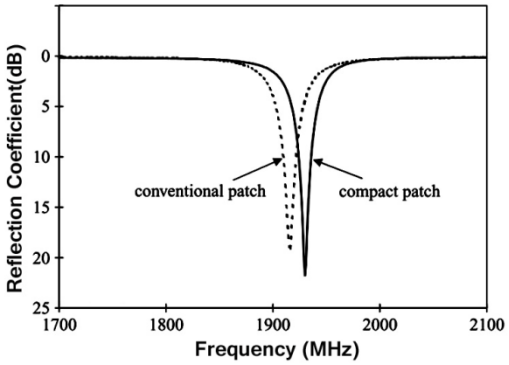

Fig. 2.3 Measured return loss of shorted and conventional triangular microstrip antennas [30]

A U-slot patch antenna with a shorting pin was investigated in [30]. Unlike the regular patch antenna, the U-slot patch antenna is a wideband antenna. The results show that, after the U-slot patch area is reduced by a shorting pin, the bandwidth of the resulting antenna remains above 10%, thus satisfying the requirement of most wireless communication applications.

(d) Use of diodes

The use of varactor diodes also contributes in reducing size of the antenna by means of changing the resonant frequency. A circular patch having radius of 20 mm with varactor diode was reported in [31]. The variation of reflection coefficient (S_{11}) with frequency is shown in figure 2.4. It was clearly visible in the figure that at the bias voltage of 4V the operating frequency was reduced to 2.2 GHz as compared to resonant frequency of 2.8 GHz (without diode). Varactor diode actually contains a capacitance which can be altered by varying their voltage and it helps in reducing the operating frequency without compromising with the size of antenna geometry. The only problem with this method is that if varactor diode and coaxial probe are in close proximity it develops unwanted coupling, whereas increasing the distance between them will disturb the impedance matching [32].

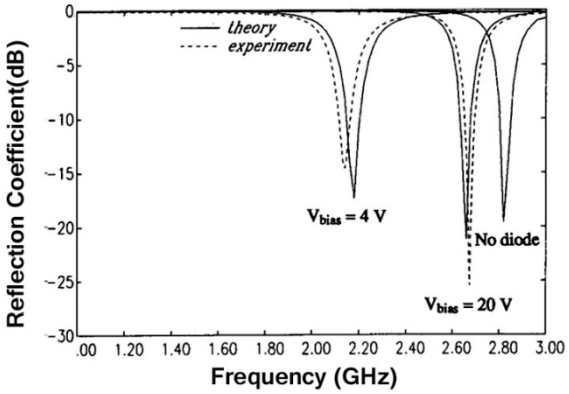

Fig. 2.4 Measured and calculated reflection coefficient of the antenna [31]

A compact design of reconfigurable square patch antenna was described in [33]. The patch has length of 40 mm and loaded with a hexagonal slot having extended slot arms. A hexagonal slot placed at its centre reduces the fundamental resonant frequency of the patch from 1.885 GHz to 1.74 GHz, giving enhanced size reduction. Dual frequency operation is achieved by embedding a protruding slot arm, which divides the fundamental resonant frequency into two distinct resonant modes, with orthogonal polarization planes. Thus the central hexagonal slot with the two slot arms significantly increases the effective lengths of the two excited resonant modes, and the excited patch surface current densities are disturbed in such a way that these two modes can be excited for dual frequency operation with a single feed. A high tuning range of 34.43% (1.037–1.394 GHz) and 9.27% (1.359–1.485 GHz) was achieved for the two operating frequencies respectively, when the bias voltage is varied from 0 to −30 V. The antenna provides size reduction up to 80.11% and 65.69% for the two operating frequencies compared to conventional rectangular patches.

Antenna miniaturization and reconfiguration using Ferroelectric (FE) thin film varactor technology was investigated [34]. A quarter wavelength notch antenna with a Barium Strontium Titanate thin film provides size reduction of approximately 56% with respect to the initial antenna size and simulation results provide agility of 13%.

2.1.2 The commonly used techniques for obtaining broad bandwidth in antennas are:

(a) Implanting slots at appropriate location in the radiating patch

(b) Use of multiple closely spaced patches

(c) Use of stacked patches

(a) Implanting slots at appropriate location in the radiating patch

By implanting appropriate slots in patch, the current distribution disturbs and two or more resonant modes are excited and when the bandwidths of two or more modes are overlapping, the overall bandwidth of antenna improves considerably.

A new design of modified rectangular slotted antenna was demonstrated in [35]. Improvement in bandwidth was obtained by embedding pair of right angle slots and U shaped slots. The proposed geometry has nearly 2.2 times of bandwidth as compared to conventional rectangular microstrip antenna. The dimensions of slots were optimized for bandwidth enhancement with good radiating characteristics. The operating bandwidth of the unslotted rectangular patch antenna was about 25 MHz while proposed design has bandwidth of 53 MHz. The proposed antenna has gain of about 2.2–2.7 dBi within the operating bandwidth.

A modified geometry of circular patch antenna with concentric diamond cut slot was investigated [36]. On applying a diamond slot on patch geometry the path of patch current increases, which in turn improves the impedance bandwidth of antenna. In addition to this few additional modes also get excited resulting in bandwidth enhancement. The conventional circular patch resonates at 5.81 GHz and 7.14 GHz and while the proposed design is operating at four resonant frequencies (5.76 GHz, 6.23 GHz, 6.86 GHz and 7.67 GHz). The impedance bandwidth obtained for the proposed design is 0.87GHz or 13.58% which is nearly six times higher than that of conventional circular patch antenna with same radius. The insertion of slot at the appropriate position not only increases bandwidth but also leads to enhance of other radiation properties of antenna also like gain and radiation pattern.

(b) Use of multiple closely spaced patches

Another common technique for bandwidth enhancement is the use of multiple closely spaced patches. This can be achieved by placing coplanar multiple resonator elements close to each other. The key idea in this technique is that if the resonant frequency of the coplanar multiple patches are slightly diverse to that of the driven patch, there is enhancement in the overall bandwidth of the antenna. The operating frequency and bandwidth of the antenna can be controlled to some extent by varying dimensions of each patch and the gap between each patch [37].

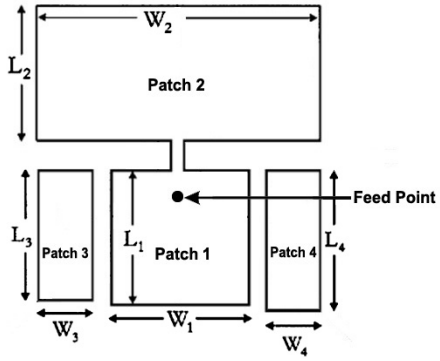

Fig. 2.5 Geometry of broadband microstrip antenna with directly coupled and parasitic patches [37]

The geometry of broadband microstrip antenna with directly coupled and parasitic patches is shown in figure 2.5. The design consists of four patches in which patch 1 is directly coupled to patch two and two parasitic patches are gap-coupled. This arrangement results in excitation of three additional modes at frequencies near the fundamental frequency of the excited patch and hence broad bandwidth is obtained. The bandwidth obtained for proposed design is as large as 365 MHz, which is about 12.7% with respect to the center frequency at 2879 MHz while the rectangular microstrip antenna patch 1 has antenna bandwidth of about 54 MHz or about 2% with respect to the center frequency of 2710 MHz without directly coupled and parasitic patches, the obtained antenna bandwidth for the proposed antenna is antenna 6.35 times that of the antenna with patch 1. This clearly indicates that by incorporating the techniques of directly coupling and gap coupling additional patches to a rectangular microstrip antenna, significant enhancement in bandwidth can be obtained.

(c) Use of stacked patches

The arrangement of patches in stacked configuration is another practice employed to improve the bandwidth of a microstrip antenna. The philosophy behind this technique is that only the bottom patch is fed and the top patches are electromagnetically coupled to the bottom patch (driven patch). If the resonance frequencies of these two patches are near to each other, then broad bandwidth is obtained.

Stacked configuration of square patch using tuning stubs for broadband performance with circular polarization was investigated [38]. In first step the conventional single layer square patch antenna with and without stub were considered. The impedance bandwidths of antenna with and without stubs were 2.7% and 4.3% respectively. In next step, square patch antenna was put in stacked arrangement with an edge truncated circular patch antenna as shown in Fig. 5. The square patch with stub was taken as driven patch and truncated circular patch having larger patch area than driven element as stacked patch. The proposed structure resonates at two closely spaced frequencies (2.41GHz and 2.59GHz) with an impedance bandwidth 16 % (0.54GHz). This value of impedance bandwidth was nearly five times higher than the impedance bandwidth value achieved from single layer structure. The location of feed point, amount of truncation of stacked circular patch and dimension and position of stubs are optimized to achieve circular polarization and improved gain.

Another design of stacked arrangement of edge truncated elliptical patch and conventional circular patch antennas was proposed [39]. The geometry was capable in providing improved impedance bandwidth with circularly polarized radiations. Initially the performance of a single layered edge truncated elliptical patch designed on glass epoxy FR-4 substrate was presented. The resonance frequencies of this antenna were 2.692 GHz and 2.802 GHz and impedance bandwidth with respect to central frequency 2.75 GHz is 180MHz or 6.54%. The antenna has gain of nearly 2dBi in the operating bandwidth. Looking at the limitations of single layered edge truncated elliptical patch antenna the geometry, stacked arrangement of two patches

was proposed. Both patches were designed on two independent glass epoxy FR-4 substrates separated by thin air gap.0 The two patches are placed one over other in such a way that their centers also lie one over other. The size of upper circular patch is marginally larger than lower edge truncated elliptical patch which is acting as driver patch. By optimizing the dimensions of the patch and air gap between the stacked patches the proposed arrangement of patches has two resonance frequencies 2.96 GHz, 3.16 GHz and 3.76 GHz with respect to central frequency 3.36GHz and impedance bandwidth of 27.9% (0.94 GHz) along with circularly polarization. This clearly reveals that stacked arrangement significantly improves the bandwidth of Microstrip antenna with improvement in gain and other parameter also.

Since normal microstrip antennas in their original shape may not be applied in these systems, extensive work to amend these geometries started and several amended geometries were proposed in past with improved performance.

2.2 Literature review

2.2.1 Dual Band Microstrip Antennas

A novel geometry of strip-sleeve monopole antenna operating at dual-frequency for laptop was discussed in [40]. The antenna operates in the frequency bands allocated to AMPS (824–894 MHz) and PCS (1.85–1.99 GHz) systems. The bandwidth of lower band was 201 MHz (782 MHz to 983 MHz) and upper band was 243 MHz (1.823 GHz to 2.066 GHz). Effects of several laptop parameters on the radiation pattern, input impedance and directivity were also given. This antenna has more omni directional pattern when side-mounted as compared to top mounted on the laptop.

A dual frequency microstrip line feed microstrip antenna resonating at 2.4 and 5.2 GHz band used for personal communication network and wireless local area network applications was presented in [41]. The measured impedance bandwidth obtained were 18.75% and 7.7% for lower and higher frequency. The highest gains attained were 4.23 dBi at 2.4 GHz and 3.58 dBi at 5.2 GHz. This antenna can be easily integrated with other devices for various applications.

A novel geometry of F-shaped dual-band antenna was presented [42]. The antenna structure has one vertical metallic line and two horizontal lines which are arranged in such a way to look like an F shape. The antenna resonates at two bands and has overall dimension of 80 mm ×45 mm. The lower band has bandwidth of 570 MHz (2.185–2.755 GHz) with uniform gain of almost 2 dBi in the operating band and upper band has bandwidth of 280 MHz (5.115–5.395 GHz) with gain nearly 2.5 dBi in the whole band. Both the bands can be utilized for WLAN applications.

A new geometry of octagonal-shaped planar antenna was reported in [43]. The structure has two ports which are fed electromagnetically with the use of two 50 Ω perpendicular Microstrip lines. The impedance bandwidth for Port 1 was 3.82% (1.7625 to 1.8313 GHz) with respect to central frequency of 1.8 GHz and that of Port 2 was 4.65% (2.3625 to 2.475 GHz.) with respect to central frequency of 2.4 GHz. Both the operating band could be utilized for mobile communication and bluetooth. The results of proposed geometry were compared with circular patch having similar operating band. It was demonstrated that size reduction of 29% was achieved with better isolation between two bands in contrast to circular patch.

A quarter-wave U-shaped patch antenna having unequal arms was proposed in [44]. The antenna has dual frequency and wideband characteristics and patch was placed over circular ground plane of diameter 200 mm. The proposed antenna was resonating at 900 and 1800 MHz bands with the substrate height of 11mm and offers impedance bandwidth of 13.3% and 20%.

A compact dual-band planar inverted F antenna for GSM/DCS was investigated [45]. The proposed antenna offers impedance bandwidth of 77 MHz (885 GHz to 962 MHz) which is useful for GSM (890–960 MHz) band and 207 MHz (1708 MHz to 1915 MHz) which is applicable to DCS band (1710–1880 MHz). The proposed design has two meandered metallic strips of slightly different lengths and one nearly-rectangular patch along with a shorting pin. For the GSM band, gain attains about 2.7 dBi, and for the DCS band, the peak antenna gain is about 2.1 dBi.

A novel patch antenna with dual-band for application in Global System for Mobile Communication (GSM)/Digital Communication System (DCS) was presented [46]. The antenna resonates at two different bands ranging from 880 MHz to 974 MHz and 1710 MHz to 1902 MHz by implanting a slit having T-shape in the patch. The measured impedance bandwidth of both the bands (10.1% and 10.6%) permits the geometry to be used for GSM and DCS systems. The antenna gain for GSM band was from 0.7 to 1.4 dBi and for DCS band was from 2.0 to 3.2 dBi. The compact size (120 mm×60 mm) of proposed antenna makes it suitable for mobile phones or PDA phones applications.

A novel geometry of dual-band triangular shaped using coplanar waveguide as a feed was proposed [47]. The measured impedance bandwidth at the lower band was nearly 240 MHz and that at the upper band was close to 2 GHz, which can be useful for the DCS 1800 and the upper band of WLAN. The antenna has gain ranging from 2.3 to 3.6 dBi and 3.9 to 5.6 dBi over the lower band resonating at 1.71 GHz and higher band resonating at 5.62 GHz, along with good radiation pattern.

A dual-band patch antenna with thick air substrate was proposed [48]. The antenna has bandwidth of 72 MHz (888–960 MHz) for lower band and 180 MHz (1710–1880 MHz) for upper band, so it can be used for GSM (890–960 MHz)/DCS (1710–1880 MHz) operation in a Personal Digital Assistant phone. The antenna's top patch consists of narrow strip and a subpatch. The bandwidth improvement was obtained by applying widened end portion to narrow strip for GSM and a tapered end portion to the subpatch for DCS operation. Good radiation characteristics of the proposed antenna have also been observed. The proposed geometry has compact size of 60 mm× 120 mm and was a good candidate for thin mobile phone applications. The effects on holding PDA phone by user's hand with proposed antenna on its performance were analyzed.

A compact design of multiband loop antenna for GSM, DCS, PCS and UMTS applications was investigated [49]. The antenna has a symmetric loop pattern and the loop pattern mainly comprises two symmetric meandered sections and a central widened section along the 1-mm wide loop strip. With the presence of the two

meandered sections, the loop antenna can achieve a compact size of 45 mm×50 mm. Effects of the major parameters on the antenna performances were systematically presented. The antenna's lower band has a bandwidth of 90 MHz (888–978 MHz), which covers GSM operation and upper band has a bandwidth of 500 MHz (1670–2170 MHz), which covers DCS/PCS/UMTS operation. The bandwidth was calculated for 3:1 VSWR (6-dB return loss). The antenna gain in the lower band was varying from 0.1 to 0.9 dBi and the radiation efficiency was 55%. For upper band gain varied from 1.3 to 3.0 dBi with radiation efficiency of about 80%.

A geometry of a compact dual band antenna mounted on the roof for automotive applications was presented in [50]. The antenna with flipper shape and its dimensions constrains (52 mm×52 mm) were selected as per current automotive market. The geometry allowed easy integration of a small GPS patch antenna without having any affect on bandwidth and radiation pattern. The proposed antenna efficiently covers the lower and upper band of 824–960 MHz and 1710–2170 MHz.

A dipole antenna with dual-band characteristics for WLAN application was proposed in [51]. The geometry was compact in size and consists of rectangular and two "L" shaped radiating elements. The antenna covers 2400–2500 MHz and 4900–5875 MHz frequency bands with good efficiency. The overall dimension of the antenna was limited to 51 mm×16 mm and also has wide band characteristic at frequency of 5 GHz.

A microstrip antenna with two U-shaped slots for dual wideband operation was proposed [52]. The design is useful for applications including AWS, GSM, Wi-MAX and WLAN bands and has overall size of 52 mm×71 mm. The geometry offers two wideband centered at 2.1GHz and 5.4 GHz. The radiation patterns have been measured and its variation as a function of frequency and angle was studied.

A compact elliptical patch antenna with gap coupled assembly for enhanced bandwidth was presented [53]. The geometry offers dual band and the two operating frequencies (3.414 and 3.645 GHz) were in lower frequency band of Wi-Max having operating bandwidth of 380 MHz whereas the third resonant frequency (5.547 GHz)

was lying in the upper band of Wi-Max application with nearly 120 MHz bandwidth.

A folded strip monopole antenna with a protruding stub in the ground plane for WLAN and RFID was presented [54]. The antenna has two resonant paths, one in the radiating element (folded strip) and the other in the protruding stub of the ground plane. The bandwidth at lower band was 810 MHz (at resonating frequency of 2.4 GHz) and 590 MHz (at resonating frequency of 5.81 GHz). The proposed antenna has simple and compact size (50 mm×35 mm), providing broadband impedance matching, consistent radiation pattern and appropriate gain characteristics in the WLAN and RFID frequency regions.

This paper presents a dual-band planar antenna with a compact radiator for 2.4/5.2/5.8-GHz wireless local area network (WLAN) applications [55]. The antenna consists of an L-shaped and E-shaped radiating elements to generate two resonant modes for dual-band operation. Parametric study on the key dimensions is investigated using computer simulation. The effects of the feeding cable used in the measurement system and the housing and liquid crystal display of wireless devices on the return loss, radiation pattern, gain and efficiency are also investigated. The impedance bandwidths for the lower band were from 120 MHz (2.39 to 2.51 GHz) and for the higher band was 1.1 GHz (5 to 6.1 GHz), with both bands satisfying the requirements of the WLAN standards.

A rhombus slot antenna for dual-band operation was reported [56]. The geometry was CPW fed and has rhombic ring feeding structure and rectangular bulge components for impedance matching. The antenna can provide two separate impedance bandwidths of 607 MHz (centered at 2.45 GHz) and 1451 MHz (centered at 5.5 GHz), which could be useful for WLAN band.

A compact and coplanar waveguide fed patch antenna for operating in dual band was investigated in [57]. By optimizing the location and size of the five slots including two straight slots, two L-shape slots and inverted-T-shape slot, the fabricated antenna exhibits measured bandwidth of 250 MHz (2.3–2.55 GHz) and

1.25 GHz (5.13–6.38 GHz) which makes it appropriate for the WAVE (wireless access in the vehicular environment) and WLAN (2.4/5.2/5.8 GHz) applications. The simulation results were verified experimentally and the proposed antenna has an average gain of 2.3 dBi(1.7 to 2.6 dBi) and 3.2 dBi (2.1 to 3.7 dBi) in the two resonating bands.

A new geometry of dual band antenna was presented in this work [58]. The patch consists of duo triangle shaped structure with coaxial feed. By optimizing the size and structure of the patch and position of feed dual bandwidth of 7.68% and 36.56% covering the range from 1.745-1.884 GHz and 2.229-3.226 GHz has been obtained.

A compact design of dual-band antenna for WLAN applications and Long Term Evolution (LTE) was investigated [59]. The overall size of antenna was 66 mm×41 mm and has operating bandwidth of 79 MHz in the first band having resonant frequency of 854.5 MHz and 80 MHz in the second band with resonant frequency of 2.44 GHz. The Sierpinski Gasket fractal shape modified by using particle swarm optimization (PSO) to obtain the desired requirement. There is good concurrence between the simulation and experimental results.

A design of dual band planar inverted fractal antenna was described [60]. The lower band has resonant frequency of 2.610 GHz and an operational bandwidth 0.235 GHz (9%) and the upper operating band has resonant frequency of 5.395 GHz, an operational bandwidth 0.575 GHz (10.6%). The radiation characteristics including radiation pattern and current distribution were studied with changes in fractal dimensions. The antenna was useful for Future Wireless Sensor Networks communication.

A novel design of folded antenna for mobile phone applications was reported [61]. The antenna operates in the frequency band of 870 to 1010 MHz and 1710 to 2490 MHz. The antenna can be utilized for mobile phone applications, namely, GSM, Digital Communication System, Personal Communication Services, UMTS and Bluetooth. The antenna geometry consists of two folded inverted-L shaped radiators

and one matching arm with overall size of 95 mm×50 mm. The variation of efficiency for its use in mobile phone, when gripped with human hand was also discussed.

A dual band microstrip antenna with defected ground strucuture was proposed for WLAN/(IMT)/(ISM)/(Wi-MAX)/Bluetooth applications [62]. The design had multistrip geometry with a cross-shaped stripline feeding mechanism having two horizontal strips and one vertical strip. The measured impedance bandwidth of 10% ranging from (2.3-2.54 GHz) and of 11% from (5.26- 5.85 GHz) was attained from antenna with moderate gain and good radiation characteristics.

A dual-band bow-tie-shaped CPW-fed slot antenna design for wireless WLAN was proposed [63]. The geometry has two conducting strips, signal strip and bow-tie-shaped slots with compact size of 60 mm×45 mm. The operating bandwidth of the proposed antenna is 0.31 GHz (2.26–2.57 GHz) in the lower band and 1.75 GHz (4.81–6.56 GHz) in the upper band. The gains at the resonant frequencies are 2.55 dBi and 3.65 dBi.

Analysis of F-shape antenna was reported for dual band operation was reported in this work [64].The bandwidth of the F-shape antenna at lower band was 464 MHz at resonating frequency of 2.25 GHz whereas at upper band was 354 MHz at resonating frequency of 5.27 GHz. The results are verified by theoretical analysis using circuit theory concept based on modal expansion cavity model. Various radiation parameters such as input impedance, VSWR, return loss were calculated for different values of dielectric constant, height and length.

The comparison of few structures described in the literature review of dual band antennas is shown in table 2.2.

TABLE 2.2. COMPARISON OF RECENTLY REPORTED DUAL BAND ANTENNAS

Reference	Antenna Size (in mm)	Frequency	Bandwidth	Gain (dBi)	Applications
[54]	50×35	2.4 GHz 5.81 GHz	810 MHz 590 GHz	3.7 3.57	WLAN and RFID
[55]	40×30	2.44 GHz 5.5 GHz	120 MHz 1.1 GHz	1.98	WLAN
[56]	50×50	2.45 GHz 5.5 GHz	607 MHz 1.45 GHz	1.9 4.5	WLAN
[58]	35.51×43.16	1.8 GHz 2.53 GHz	139 MHz 1.04 GHz	1.89 2.9	WIMAX
[62]	30×20	2.38 GHz 5.4 GHz	200 MHz 590 MHz	3 4	WLAN/IMT/ BLUETOOTH/WIMAX

The above table clearly reveals that in recent past several designs on dual band antenna have been proposed and as per the demand of today's wireless systems compact design with enhanced bandwidth covering the desired band are mainly required.

2.2.2 Broadband Microstrip Antennas

This paper presents alterations employed to the conventional aperture coupled patch antenna with stripline feed for bandwidth enhancement [65]. The measured results for two variations of slotted patches were discussed. The widest bandwidth of 18% (313 MHz) was achieved while the best matching was obtained for nearly 10% (203 MHz) impedance bandwidth where VSWR below 1.16:l was obtained.

The rectangular patch antenna with L shaped probe was presented in this paper [66]. It has an overall dimension of 100 mm×120 mm and the antenna accomplish 36% impedance bandwidth. Detailed parametric study for antenna was performed and experimental results were in good concurrence with simulation results. A two-element array design was also demonstrated for suppression of cross polarization.

A new geometry of rectangular patch antenna with probe-fed was proposed in [67]. The patch has a size of 65 mm×105 mm and in this work an air gap with thickness equivalent to 8% of the wavelength of centre operating frequency, was used between ground plane and patch substrate. Two wide slits were introduced at the radiating

edge of the patch. The proposed geometry has a broad bandwidth of around 24% (403 MHz) with respect to centre frequency of 1644 MHz and good radiation characteristics.

A U slot patch antenna and an L probe fed patch antenna were designed to provide wide-bandwidth and also described several techniques including utilizing a microwave substrate material, the addition of a shorting wall, and the addition of a shorting pin that may be utilized to decrease the resonant length of these patch antennas while maintaining the same bandwidth [68].

An internal antenna design suitable for mobile handset was proposed [69]. The proposed antenna has broad bandwidth of 740 MHz (1620 to 2360 MHz) with gain nearly approaching to 2.3 dBi. The design finds application in DCS, PCS and IMT-2000 bands. The antenna has size of 40 mm×75 mm and can be easily housed in mobile phone. The behavior of antenna in terms of bandwidth and gain with only case and case, battery was also described.

In [70] two geometries have been described. The first geometry is E-shaped microstrip antenna with a pair of tapered slots having air gap of 2 cm. The geometry has dimensions of 130×150 mm and bandwidth was 19.9% (172 MHz). Using the even-mode symmetry of E-shaped geometry the second geometry of rectangular patch antenna with single slot was realized. The size of this geometry was 130×75 mm which is nearly half of the previous geometry and bandwidth was 14.6% (127 MHz).

A novel geometry of wideband flower-shaped semicircle-fed microstrip patch antenna was investigated in [71]. The broadband characteristics were achieved by introducing flower petals at the four sides of a rectangular patch.

A new method for bandwidth improvement was described in [72]. An electromagnetically coupled feeding mechanism was used and bandwidth obtained was 1200 MHz for the rectangular patch while for triangular patch it was 1300 MHz. The size of the patch is 65.8×51.8 mm for both the antenna design. The proposed geometries can be useful for DCS, PCS, WLAN, UMTS and IMT-2000 bands.

A small broadband antenna that was competent to work within the 3G frequency range was investigated [73]. The geometry was made by introducing diverse shapes of slot in the ground and employing substrate having high permittivity. The H shape slot offers bandwidth of 290 MHz in the frequency band of 1.81GHz to 2.1GHz. The U shape provides impedance bandwidth of 220 MHz (1.89 to 2.11GHz.) with respect to the centre frequency of 2.0 GHz. Third design consists of slotted ground and a T shaped feed-line, the bandwidth obtained from this design is about 1 GHz (1.5 GHz to 2.5GHz) and finds applications in the PCS1900 and UMTS frequency bands.

In this paper, a novel design of thin dielectric slab with periodic circular patch mounted on the circular patch with annular ring patch for WLAN router was presented [74]. The proposed geometry has bandwidth of 23.6% (5.7–7.1GHz) and a gain of 5.91 dB with radiation pattern omni directional in nature. The parametric analysis of antenna dimensional parameters was also done.

A new design of right triangular patch antenna enclosing two parallel slits with 1 mm air gap was proposed [75]. The antenna operates at dual frequency (4.48 and 5.7 GHz) and offers bandwidth of 29% (1.495 GHz) with improved radiation parameters. The gains at the resonant frequencies are 3.63 dBi and 3.72 dBi.

A proximity-coupled microstrip antenna having narrow metallic cavity was proposed in this paper [76]. The narrow cavity increased the effective coupling and the bandwidth was improved. The measured impedance bandwidth close to 40% was obtained from fabricated antenna. The geometry also has good front to back ratio radiation.

A modified rectangular microstrip antenna with V-slots and corner notches for broadband operation was presented [77]. The geometry has bandwidth of 51% (3.75 GHz to 6.33 GHz) with overall dimension of 60×60 mm. The simulated and measured radiation parameters are presented and discussed. The proposed antenna is suitable for IEEE 802.11.a (5.15–5.35 GHz, 5.725–5.825 GHz), WiMAX (5.25–5.85

GHz), HiperLAN2 (5.47–5.725 GHz) and HiSWaNa (5.15–5.25 GHz) wireless application bands.

A broadband antenna with compact size of 95×60 mm was proposed and studied [78]. The structure has two symmetric slot-monopole-hybrid (SMH) elements. Each SMH element combines an L-shaped slot directly fed by a 50 Ω microstrip feeding line and an inverted-L parasitic monopole. It has an impedance bandwidth of nearly 460 MHz (1.85–2.31 GHz). It may finds application in, PCS (1850–1990 MHz), PHS (1880–1930 MHz), DECT (1880–1900 MHz), and UMTS (1920–2170 MHz) bands. The diversity nature of the antenna was also examined by calculating the envelope correlation coefficient.

A modified circular patch antenna having off centered y slot was reported in this communication [79]. The proposed geometry offers enhanced bandwidth of 210 MHz as compared to conventional circular microstrip patch antenna(nearly 56 MHz). The location and dimensions of the slot was optimized to obtain best results. There was marginal improvement in the gain of antenna also. The radiation patterns of the fabricated antenna were also symmetric in nature in the entire bandwidth.

A compact modified rectangular microstrip antenna with triangular slot was presented in this paper [80]. Introduction of triangular slot reduced the resonant frequency and a small triangular patch was added within the area of the triangular slot to enhance the gain and bandwidth of the antenna. The antenna size was decreased by almost 46% compared to a conventional geometry having 160 MHz bandwidth, 5.37 dBi gain along with 3 dB beamwidth of 137^0. The design can be useful to the median band of Wi-Max applications.

A small size broadband antenna for mobile phone applications was investigated in [81]. The overall dimension of antenna was 45mm × 85 mm and it consists of a gap-coupled feed, shorted line and a suspended line with a parasitic element. It has measured impedance bandwidth of 1.02 GHz (1.78–2.8 GHz) which covers of PCS, UMTS and Wi-MAX bands.

A monopole antenna with overall dimension 90×40 mm for WiFi/WiMAX applications was reported [82]. The antenna structure consists of two crescent shaped radiators fed by using a microstrip line which improves impedance matching and low mutual coupling. The antenna provides impedance bandwidth of 54.5% (over 2.4–4.2 GHz), and mutual coupling of 17 dB. By employing neutralization lines, the MIMO antenna criteria can be improved significantly. The proposed antenna also offers an average gain of 2.8 dBi in the operating frequency range.

In this work the patch and the ground plane are circular in nature [83]. The circular patch is shorted concentrically with a set of conductive vias. The antenna is fed at the center by a coaxial probe with an SMA connector which is placed below the ground plane. The antenna is analyzed using a cavity model. The antenna has a simple structure with a low profile of 0.024 wavelengths, and yields a wide impedance bandwidth of 18% (400 MHz) and a maximum gain of 6 dBi.

The comparison of few structures described in the literature review of broadband antennas is shown in table 2.3.

TABLE 2.3 COMPARISON OF RECENTLY REPORTED BROADBAND ANTENNAS

Reference	Antenna Size (in mm)	Frequency	Bandwidth	Gain (dBi)	Applications
[77]	60×60	5.29 GHz 6.13 GHz	51% (2.58 GHz)	5	IEEE 802.11.a, WiMAX, HiperLAN2 and HiSWaNa
[78]	95×60	1.9 GHz 2.25 GHz	22.2% 460 MHz	-	PCS, PHS, DECT and UMTS
[82]	90×40	2.45 GHz 3 GHz 3.5 GHz	54.5% (2.4- 4.2 GHz)	2.8	Wi-Fi/WiMAX
[83]	Diameter = 96	2.15 GHz 2.35 GHz	18% 400 MHz	6	S Band

2.2.3 Stacked Microstrip Antennas

The stacked arrangement of two rectangular microstrip antenna separated by foam spacer was presented in this paper [84]. Both the patches are designed on CuClad substrate (ε_r=2.33).The antenna was feed using microstrip line etched on alumina substrate (ε_r=9.8) having narrow rectangular aperture in the ground plane. The antenna offers a bandwidth of 18% between 8-10 GHz and can be used for phased array structures.

Two novel shorted patch antennas for mobile handsets were investigated [85]. The geometries consist of a stacked shorted patch antenna and single layer shorted patch antenna. The finite difference time domain method was applied for obtaining radiation pattern and impedance for two special cases i.e. on a handset and on a handset and close to heterogeneous heat circuit. The influence of putting a hand behind handset on antenna properties and specific absorption rate was also determined. The impedance bandwidth obtained for stacked configuration was 9.4% whereas for single layer was 8.2%. The proposed antennas reduced specific absorption rate in the head by nearly 70% with reference to the monopole. Moreover, it was also investigated that presence of hand brings down the efficiency by almost 10%.

A multi-frequency patch antenna consisting of a driven patch and four parasitic elements located below the driven patch was investigated in [86]. The driven patch was fed by a probe through an etched capacitor. The etched capacitor improved impedance matching by canceling the inductive effect of the probe. The parasitic elements were made by brass and to avoid the contact with feed a hole was inserted in all parasitic elements. Penta band behavior was obtained with 5 % bandwidth for first and last band and 2% bandwidth for middle bands.

A simple method for stacked microstrip antenna for improving the purity of circular polarization and enhancing axial ratio bandwidth was reported in [87]. In this technique a new C-type feeding method was used. The impedance bandwidth is from 4.83 GHz to 5.96 GHz and axial ratio bandwidth is from 5.24 GHz to 6.0 GHz. The total thickness of the antenna is nearly 7.8mm and by optimizing the location of

feed and the foam height between main and parasitic patches the desired results were obtained.

A broadband inverted E-H shaped microstrip patch antenna is proposed and experimentally investigated [88]. The antenna employs novel E-H shaped patch with L-probe feed technique. The designed antenna has a dimension of 80 mm×50 mm, leading to broad bandwidth covering from 1.76 GHz to 2.38 GHz. Stable radiation patterns across the operating bandwidth are observed. The parametric studies have addressed the effects of the width and length of slots of the patch and height of the air gap on the performance of the antenna.

Small size wideband microstrip patch antenna with slot in ground plane and stacked patch fed through microstrip line was presented [89]. By inserting slot on ground plane and stacked patch supported by wall, the bandwidth can improve up to 25% without significant change in the frequency. The bandwidth before adding the slot and the stacked patch was 3.72%, whereas after adding the slot and the stacked patch the bandwidth increased up to 25% ranging from 2.45 to 3.3 GHz. The radiation pattern has acceptable response at both E-plane and H-plane.

Stacked-patch antenna with magneto-dielectric layers was investigated in this paper [90]. In this paper, the use of will be extended to the application of designs. A fabrication technique for such substrates was described based on very thin ferromagnetic films on top of polymer layers. The geometry provides bandwidth of nearly 20% and significant miniaturization of antenna size.

A microstrip patch antenna having a stacked periodic structure with circular polarization was proposed and investigated [91]. By using SPS as a superstrate gain, impedance and axial ratio bandwidths are significantly enhanced. The proposed geometry attained bandwidth of 10.1% (2.328–2.576 MHz) and average gain of 8 dBi over the entire range of bandwidth. The cross-polarization discrimination of 20 dB was also observed within the overlapped bandwidth along with front-to-back ratio of more than 30 dB.

A wideband stacked circular patch antenna with circular polarization for Global Navigation Satellite System applications was presented in this paper [92]. The bandwidth was enhanced by using four capacitively coupled feeds. The antenna has operating bandwidth of 600 MHz (1.1 GHz to 1.7 GHz). The antenna properties like reflection coefficient, axial ratio, radiation pattern and gain have been measured from fabricated antenna and they were found to be in good match with simulation outcomes.

This work proposes a double layer antenna for enhanced bandwidth and circular polarization [93]. It offers an impedance bandwidth of 640 MHz (2.33 to 2.97 GHz) in the S Band. The geometry finds application in the ultra-broadband transceiver antenna in the S-band microwave communications. After the design of antenna structure and adjustment of size, the proposed antenna can achieve both the left and right-hand circular polarizations.

A compact design of broadband microstrip stacked patch antenna with circular polarization was reported [94]. The proposed geometry has two stacked patches fed with an S-shaped impedance-matching network (IMN), which is connected by a probe. The impedance bandwidth is larger than 15.1% and geometry can be used for mobile 2.45-GHz passive radio frequency identification (RFID).

A stacked arrangement of rectangular ring microstrip antenna and rectangular microstrip antenna with a shorting plate was investigated for tri-band operation [95]. The antenna was excited by an L-probe feed. The VSWR, axial ratio, radiation pattern and gain were simulated and compared with measured results. It covers applications including GPS, ETS (electric toll collection system) in Intelligent Transport System and VICS (vehicle information and communication systems). The bandwidths in the GPS, ETC and VICS bands are 11.5 MHz, 165 MHz and 43 MHz and gains are nearly 5 dBi, 3 dBi and 3dBi.

The comparison of few structures described in the literature review of stacked antennas is shown in table 2.4.

TABLE 2.4 COMPARISON OF RECENTLY REPORTED STACKED ANTENNAS

Reference	Driven Patch Dimension (in mm)	Stacked Patch Dimension (in mm)	Resonant Frequency (GHz)	Bandwidth	Gain (dBi)	Circular Polarization
[88]	-	80×50	1.91 GHz 2.21 GHz	30% (620 MHz)	9	No
[89]	33×10.25 12×12 84×6 84×4	28×47.73	2.6 GHz 3.1 GHz	25% (850 MHz)	-	No
[93]	41×41	32×32	2.45 GHz 2.89 GHz	24% (640 MHz)	-	Yes
[94]	16.5×16.5	36.3×36.3	2.45 GHz	15.1% (250 MHz)	6.32	Yes

2.3 Preliminaries

This section includes the antenna characteristics, description of feeding techniques of microstrip patch antenna, numerical techniques for analysis of microstrip patch antenna, simulation tools, fabrication process of antenna and its measurements methods.

2.3.1 Antenna Characteristics

The antenna performance is evaluated using by various radiation parameters. A frequently asked question is that the physical picture of every antenna is same then what is the need of analyzing each antenna separately. The answer is simple. Different antennas have different current and different charge distribution, which results in different approaches of analysis for each geometry. It is not convenient to apply same mathematical model to every antenna geometry, therefore we need to focus on some mathematical techniques which will be applied on different antenna geometry to analyze their performance. The design parameters like return loss, VSWR, input impedance and performance testing parameters like gain, bandwidth, efficiency, polarization and directional properties like directivity, radiation pattern, beamwidth of an antenna are fundamental to understand the antenna behavior and how it may be used in a RF communication system. The mentioned antenna properties are the function of frequency and we have measured many of these characteristics during present course of work. A brief depiction of these antenna characteristics is given here [96]:

(a) Reflection Coefficient or Return Loss

Return loss or reflection coefficient parameter is used to evaluate, how effectively the power is delivered to the antenna from transmission line. Let the power supplied or incident on the antenna is P_{in} and the amount of power which gets reflected or scattered from antenna is P_{ref}, the reflection occurs due to impedance mismatch between antenna and transmission line carrying the power. The ratio P_{in} / P_{ref} determines the level of mismatch between the incident and reflected power. This ratio should be as high as possible for effective delivery of power to the antenna.

The reflection coefficient is calculate in dB and expressed as

$$RL\,(in\,dB) = 10\,\log\left[\frac{P_{in}}{P_{ref}}\right] \quad . \tag{2.1}$$

The power can also be defined as field strength or voltage, then equation (2.2) can be written as

$$RL\,(in\,dB) = 10\,\log\left|\frac{1}{\rho^2}\right| . \tag{2.2}$$

where ρ is the reflection coefficient in complex form in antenna.

The return loss can be also expressed in terms of VSWR (Voltage standing wave ratio) as

$$RL\,(in\,dB) = 20\,\log\left[\frac{VSWR+1}{VSWR-1}\right] , \tag{2.3}$$

$$= (40\,\log_{10} e)\; ar\tanh\left|\frac{1}{VSWR}\right| \quad . \tag{2.4}$$

Another convenient way to express the return loss is through input impedance of the feed network Z_f and input impedance of antenna under consideration *i.e.*

$$RL(f) = -20\,\log\left[\frac{Z_f - Z_{in}(f)}{Z_f + Z_{in}(f)}\right], \tag{2.5}$$

where Z_f is the input impedance of the feed network to be used with antenna. Normally we apply a 50Ω coaxial cable for feeding a microstrip patch antenna.

(b) Voltage Standing Wave Ratio

For efficient operation of antenna, maximum power transmission between antenna and space should take place. Maximum transfer of power can only take place when the impedance of a transmitter (Z_f) is in good match with the impedance of antenna (Z_{in}). By any reason if there is mismatch between the two then some amount of power will be reflected back and this is the main source of the creation of standing waves, which can be described using Voltage Standing Wave Ratio (VSWR). It is the ratio of the maximum to the minimum RF voltage along the transmission line. VSWR can be used to measure the performance of an antenna when connected to a transmission line. The value of VSWR ranges between 1 to infinite. In mathematical form VSWR can be defined as.

$$VSWR = \frac{V_{\max}}{V_{\min}} = \frac{1+|\Gamma|}{1-|\Gamma|}, \tag{2.6}$$

where $$\Gamma = \left[\frac{Z_f - Z_{in}(f)}{Z_f + Z_{in}(f)}\right]. \tag{2.7}$$

When the input impedance of antenna is purely resistive and reactance is nearly zero and the resistance value is equal to the characteristic impedance of the transmission line than the perfect matching will occur and there will be no reflected wave. Under this condition the VSWR will attain value equal to one. However, if there is mismatching between the transmission line and antenna then some amount of power will be reflected and the value of VSWR will be more than one. If VSWR is close to 1.5, it is estimated that nearly 4% of the power will be reflected. At a value of around 2.0, almost 11% of power will be reflected. Hence, up to 2.0 value of VSWR is considered as good and above this not good enough for consideration.

(c) Input Impedance

Input impedance is one of the important parameter in antenna properties, it gives information about quality of impedance matching between transmission line and antenna. For efficient transfer of power between the transmission line and antenna, there should be excellent matching between input impedance of antenna and characteristic impedance of the transmission line. If mismatching occurs between the two, reflection will occur at the junction and the reflected wave will move in the backward direction towards the source. This result in loss of power and the radiation

parameters of the antenna are adversely affected. The mathematical relation of input impedance is given by

$$Z_{in} = R + jX = \frac{V}{I} = \frac{E_{av}h}{I}, \tag{2.8}$$

where I is the total current and E_{av} is the average electric field at feed. In ideal conditions, at resonance frequency Z_{in}= R. However, in practical case, the reactance has some small value even at the resonance frequency owing to the contribution from other modes which are non-resonant.

(d) Bandwidth

Bandwidth can be represented as difference among two frequencies within which the performance of an antenna is acceptable. The bandwidth of the microstrip antenna is expressed as the useful frequency range within which matching between antenna and feed arrangement occurs up to a well defined limit. In other words, the bands of frequencies within which antenna will have satisfactory performance i.e. it's one or more parameters such as input impedance, gain, pattern, have values confined in the specified limits. In general impedance bandwidth is given due importance in antenna parameters. On the other hand, other type of bandwidth also exists like VSWR bandwidth, axial ratio bandwidth, directivity bandwidth, polarization bandwidth, and efficiency bandwidth.

i) Impedance bandwidth/Return loss bandwidth -

The bandwidth of a wideband antenna could be explained as the ratio of the upper to lower frequencies for adequate operation. The bandwidth or impedance bandwidth of an antenna can be expressed as the percentage of the frequency difference (f_H - f_L) over the center frequency f_c corresponding to 10 dB return loss. In this thesis, throughout impedance bandwidth is mentioned. According to these definitions, bandwidth of antenna can be written as:

$$BW_{Broadband} = \frac{f_H}{f_L}, \tag{2.9}$$

$$BW_{Broadband}(in\%) = \left[\frac{f_H - f_L}{f_C}\right] \times 100. \tag{2.10}$$

ii) VSWR bandwidth -

The VSWR bandwidth for an antenna is typically defined as the permissible standing wave ratio (SWR) value within the given frequency band. To measure bandwidth, up to 2:1 ratio can be allowed. VSWR bandwidth can be defined in terms of quality factor (Q) as:

$$Band\ width\ (\%) = \frac{SWR - 1}{Q\sqrt{SWR}}. \tag{2.11}$$

iii) Directivity or Gain bandwidth -

It is the range of frequencies in which the directivity or gain of an antenna is maintained at certain level.

iv) Efficiency Bandwidth -

It is the range of frequencies in which the radiation/total efficiency will not be below a predefined value, depending on the application of antenna.

v) Axial ratio bandwidth -

This can be define as the range of frequencies in which the axial ratio is less than or equal to 3 dB. It accounts for the circular polarization.

vi) Polarization bandwidth -

This can be expressed as the frequency band in which the polarization remains same.

(e) Radiation pattern

The radiations of the antenna can be represented graphically in three dimensions using radiation pattern. Radiation pattern can be described as the power received or radiated by an antenna as a function of radial distance and angular position from the antenna. The radiation performance of antenna is typically evaluated in far-field region and verified in E-plane (vertical) plane and H-plane (horizontal) planes) which are perpendicular to each other.

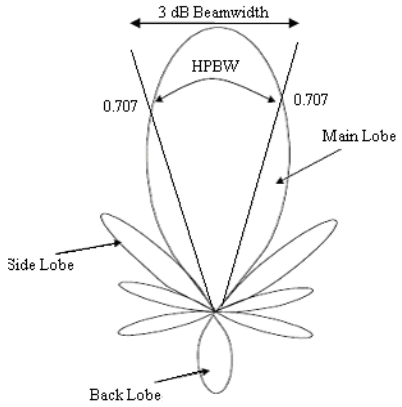

Fig. 2.6. Radiation pattern

The radiation pattern usually has a main lobe along with some minor lobes (which includes side lobes and back lobes) as shown in figure 2.5. The main lobe represents the direction in which maximum radiation is occurring. The minor lobes are unwanted because they cause radiation in undesired direction. The pattern can be expressed in Cartesian or polar form. It describes how the antenna focuses or directs the energy it radiates or receives. Antenna pattern are normally represented on a scale of relative power in dB with 360^0 angular pattern in a polar plot.

(f) Directivity

The directivity for an antenna is described as the ratio of the radiation intensity in a given direction from the antenna to the radiation intensity averaged over all directions. The average radiation intensity is equal to the total power radiated by the antenna divided by 4π.

Radiation intensity in a given direction is defined as the power radiated from an antenna per unit solid angle. The radiation intensity is a far-field parameter. It can be obtained by simply multiplying the radiation density by the square of the distance [96].The antennas having low permittivity substrate offer good directivity due to larger physical appearance in contrast to high permittivity substrate. The directivity is also proportional to the height of the dielectric substrate layer as the volume increase with increase in height of the substrate.

If U is the radiation intensity of antenna under consideration, $U_{\max}$ is the maximum radiation intensity and P_{rad} is the total radiated power, the directive gain (G_0) and directivity (D_g) of antenna will be expressed through:

$$G_0 = \frac{4\pi U}{P_{rad}}. \tag{2.12}$$

$$D_g = \frac{4\pi U\big|_{\max}}{P_{rad}}. \tag{2.13}$$

Directivity of an antenna is dimensionless quantity but it can also be expressed in decibels (*dB*). The directivity of antenna cannot be lower than unity.

(g) Gain

The gain is defined as the radiation intensity of an antenna in a given direction divided by the radiation intensity of antenna which radiates equal power in all the directions. Usually, the direction in which maximum radiation will occur is used for calculation of the gain. The calculation of gain is always relative i.e the antenna for which gain is to be measured versus a standard antenna.

(h) Radiation Efficiency

The radiation efficiency can be defined as ratio of the power antenna radiates divided by the power inputted from the source to the antenna. It can be also described as the ratio of the maximum gain divided by the directivity. The antenna with good radiation efficiency will radiate the majority of the power fed at the input terminals while in case of antenna with poor efficiency the majority of the input power will be consumed in the form of losses within the antenna. This efficiency can be expressed mathematically in terms of radiated power (P_r) and input power (P_i) as

$$\eta = \frac{\mathrm{P}_{\mathrm{radiated}}}{\mathrm{P}_{\mathrm{input}}}. \tag{2.14}$$

Microstrip patch antenna is less efficient for high permittivity substrate since more power is gone to the surface wave.

(i) Axial Ratio (AR)

The axial ratio is a measure to evaluate the purity of circular polarization and can be represented in dB. The value of axial ratio is obtained by the ratio of the major axis

of polarization divided by minor axis. Ideally the value of axial ratio should be 0 dB for circular polarization. However in practical use, if antenna has axial ratio value up to 3 dB it may be considered as circularly polarized.

(j) Polarization in antennas

Polarization for an antenna refers to direction of the electric field vector of electromagnetic energy radiated from antenna with respect to the earth's surface. It gives the information about the relative magnitude and time varying direction of the electric field of the transmitted wave. The antennas having low frequency are generally vertically polarized whereas antennas with high frequency are horizontally polarized. There are three types of polarization basically Linear, elliptical and circular. In linear polarization the electric filed has single component and it is varying linearly with respect to reference point. The circular polarization consists of two electric filed components which have equal amplitude and 90 degree out of phase. In elliptical polarization the magnitude and angle of the two field components may be different.

i) E -plane – for antennas with linear polarization, it is a plane which contains the electric field and the maximum radiation direction.

ii) H -plane - for antennas with linear polarization, it is a plane which contains the magnetic field and the maximum radiation direction

iii) Co-polarization – it is a kind of polarization in which antenna is designed to radiate or the polarization in which the radiation is desired.

iv) Cross-polarization - it is a polarization which is perpendicular to co-polarization or the polarization in which unwanted radiation will occur.

2.3.2 Feeding techniques

The feed structure directs the electromagnetic energy in the form of signal from the source to the section under the patch. A fraction of the signal goes beyond the boundaries of the patch and causes radiations into space. There are numerous techniques to feed the radiating patch. These include probe feed, microstripline feed, aperture coupled feed and proximity coupled feed. These can be also categorized into direct (probe and microstripline) and non-contact (aperture and proximity-coupled) techniques. In practice, the probe and microstripline feed are commonly used feeding method and in this thesis coaxial feed and microstripline feed

technique have been used. A brief description of each of these feeding methods is given here.

(a) Microstrip line feed or edge-feed

It is among the most popular method of feeding due to its simplicity of fabrication as shown in Fig. 2.7. The equivalent circuit for microstrip line feed patch is shown in Fig. 2.7 (b).Here the traditional RLC tank circuit represents the patch antenna and the stand-alone inductor represents the feed network [98]. The feed mainly consists of a conductor strip which seems like an extension of the patch. The feed structure and patch are of generally same material and etched on the same board. Due to this feature, this technique can be even applicable for antenna arrays and fractal geometries. Feed structure contribution to the radiation has been investigated in [99] and it was found that the position and size of the feed in the patch can be optimized to obtain desired outcomes from the antenna. The only limitation associated with this method is that it excites surface waves and unwanted radiation from feed with thicker substrate and this leads to degradation of antenna performance in terms of bandwidth.

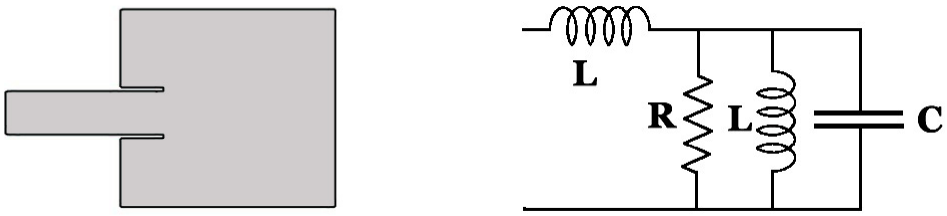

(a) Microstripline feed (b) Equivalent Circuit

Fig. 2.7. Microsripline feed and its equivalent circuit

(b) Coaxial or Probe feed technique

This is one of the oldest methods of feeding which came into existence in 1970s. It was proposed and demonstrated in the mid 1970s by Munson. The feed mechanism consists of a coaxial cable with inner conductor, which is drilled from the ground via substrate and extended upto the patch and the outer conductor remained connected to the ground as shown in Fig. 2.8. The location of the feed and radius of the inner conductor can be optimized to obtain good radiation performance from antenna. It also provides excellent impedance matching and can be applied to

any antenna configuration. The only disadvantage in using this technique is that due to drilling of hole there may be possibility of backward radiation. The coaxial feed, using Huygen's principle, can be modeled by a cylindrical band of electric current flowing on the center conductor from the bottom to the top along with the annular ribbons of magnetic current in the ground plane. A number of other approaches for the analysis of probe fed microstrip antenna are described [100-103]. The antenna impedance can be transformed to a desired value by introducing electromagnetic coupling between the patch and the probe. The equivalent circuit of a probe fed microstrip patch antenna is shown in Fig. 2.8(b). The feed is modeled by an equivalent inductance. The inductance becomes larger as the length of central conductor is increased.

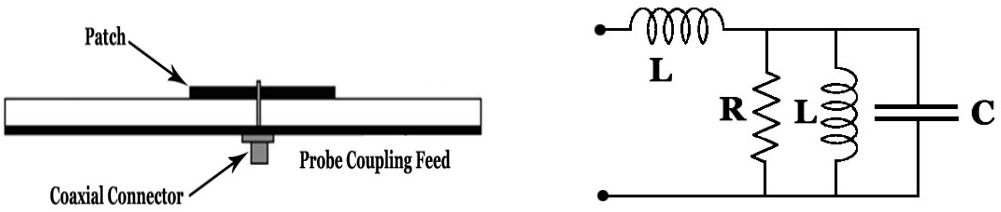

(a) Coaxial feed (b) Equivalent circuit

Fig. 2.8. Coaxial feed and its equivalent circuit

To overcome the limitations of the direct contact feeding methods, non-contacting feed methods were introduced. The aperture coupled feeding and proximity coupled feeding methods do not have direct contact with radiating patch so they comes under the non-contacting type feeding. These techniques have few advantages in contrast with direct feeding methods. Some of the merits related to non-contacting feeding techniques are:

- The performance of antenna is not much affected by feed as there is no direct contact amid feed structure and element responsible for radiation.
- The surface wave excitation is quite low
- The etching holes or slots is not required
- Provides better response stacked configurations and antenna arrays.
- Higher order modes can be suppressed easily.
- The performance of antenna is not degraded when used at high frequency.

(c) Aperture coupled feed technique

In aperture coupled feeding mechanism, the electromagnetic energy in the form of signal from the feed line is coupled to the patch using a rectangular slot which acts as an aperture, as shown in Fig. 2.9. Two different substrates are used in this method and ground plane is sandwiched in between. The feed line is mounted on the lower substrate and slot or aperture is created in the ground plane. When a signal or energy is applied to the feedline it is coupled to the patch situated on the upper substrate through the aperture in the ground plane. In practice, the dielectric constant of upper substrate is kept lower than the lower substrate. The reason for keeping permittivity of the upper substrate smaller is because it creates fringing fields which are loosely bounded and helps in improving radiation. The advantage of using high dielectric constant for lower substrate is that it suppresses spurious radiation efficiently [3]. The ground plane placed between the two substrate not only provides isolation but also helps in reducing unwanted radiation and improving polarization purity. The equivalent circuit of an aperture-coupled microstrip patch is shown in Fig. 2.9(b) [97] [104]. In this case, the patch is a load for the slot and then this combination is terminated with the open circuit stub (capacitance). This feed can be also designed to improve bandwidth by adjusting the shape and length of the coupling slot, width of the feedline and stub length. The aperture-coupled feed arrangement also provides more flexibility to researchers working in the field of antenna with availability of several parameters that can be varied to control the antenna properties. The analysis of this feed technique using mathematical model has been illustrated in [105-108].

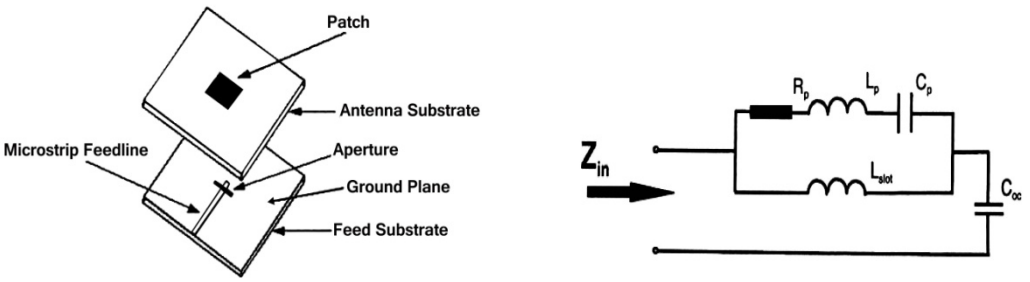

(a) Aperture coupled feed (b) equivalent circuit

Fig. 2.9. Aperture coupled feed arrangement and equivalent circuit [97]

The fabrication of this feeding technique is difficult and requires lot of accuracy as it involves multiple layers and misalignment of aperture will have adverse affect on antenna characteristics.

(d) Proximity coupled feed technique

Another form of non contact fed patches is the proximity-coupled patch [109]. The proximity-coupled feeding structure consists of two substrate layer, quiet similar to aperture coupled feeding but there is no ground in between the two layers as shown in Fig. 2.10. The capacitive nature of this non-contact excitation technique is presented in the equivalent circuit shown in Fig. 2.10(b). This type of feed method is also referred as electromagnetic coupling method. This is because the power from feedline to the patch is coupled electromagnetically. The key feature of this feed method is that it removes spurious feed radiation to large extent and gives very large bandwidth, as the thickness of the microstrip patch antenna is increased.

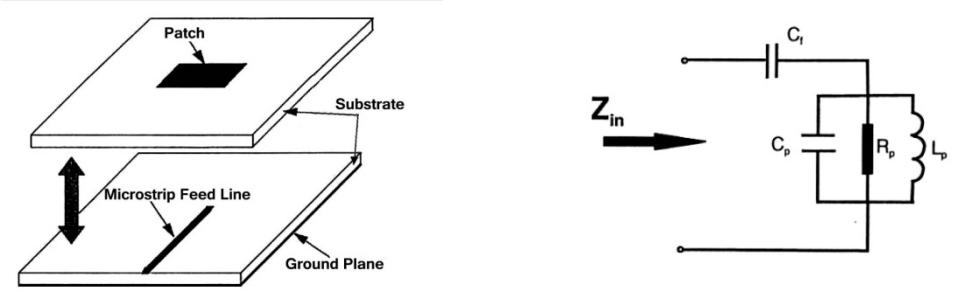

(a) Proximity coupled feed (b) Equivalent circuit

Fig. 2.10. Proximity coupled feeding mechanism and equivalent circuit [97]

Using this technique, antenna designers have choice of several parameters for optimization, to enhance the radiation performance. The length of feedline can be varied for obtaining good impedance matching. The major drawback of this feed scheme is that it is complicated to fabricate and requires proper alignment between the substrate layers. The analysis of this feed is reported in [110-111].

2.3.3 Numerical Techniques of analysis for microstrip patch antennas

Numerical methods are extremely significant in electromagnetics. In reality, only a small number of simple problems in electromagnetics can be answered analytically since there is no numerical technique that works better than any other technique for

all antenna problems. Each method has its advantages and limitations. One method may be ideally suited for a particular problem and may not be very well suited for other problems. Before selecting a numerical method for a specific problem, it is essential to consider the relative merits and limitations of different methods. Analysis is done for acquiring thorough knowledge about the philosophy and fundamentals that gives insight for designing new structures and for alterations of an available structure. The aim of antenna analysis is to foresee the antenna properties like bandwidth, radiation patterns, polarization, radiation efficiency, gain etc. Even though microstrip patch antennas are comparatively simple configuration, their analysis is rather complex. The analysis of patch antenna is complicated due to different shaped patches, integration of active devices with patch, substrate in homogeneity, large variety of feed methods, inhomogeneous boundary conditions, and narrow frequency band. Thus, a balance must be maintained among the complicatedness of method and accuracy of solution on the account of compromising few antenna properties.

In this section, various analytical and numerical approaches for the analysis of microstrip patch antennas are discussed in brief. Antenna analysis is important for several reasons like:

(i) The cost can be bring down by avoiding hit and trial methods

(ii) By carrying out antenna analysis, we can ascertain advantages and limitation of microstrip patch antenna.

(iii) An intensive analysis of any patch antenna geometry may provide information for designing new antenna geometries and possibilities of modifications in existing designs.

A tremendous amount of research has gone into developing analysis approaches and models. A model may be considered as an efficient model if it provides features [112]:

- Its results must be accurate enough for intended purposes
- It must be able to determine all properties of antenna under consideration.
- It must be easy to use, while maintaining the projected accurateness in results.
- It must lend itself to interpretation in terms of known physical phenomenon.

There are numerous methods of analysis for patch antennas. Cavity model, transmission line model and multi-port model are known as analytical techniques which are simple in application though less accurate. These models use simplifying assumptions but well suited for understanding physical phenomenon. A major drawback of these analytical models is that for thicker substrate the calculation of input impedance and resonant frequency is not very accurate. Further they have inadequate competence to deal with issues such as mutual coupling, surface wave effects, arrays and different substrate configuration. Full-wave methods have received attention due to their rigor and higher accuracy at the expanse of numerical simplicity. These numerical techniques can provide analysis of microstrip antenna in which all effects such as, surface wave loss, space wave radiation and coupling, mutual coupling between the edges and fringing field don't have to be modeled but these features are integrated in the analysis technique through an accurate Green's function. These techniques are very accurate and powerful. A brief introduction of some of these analysis techniques and their salient features are included here:

(a) Transmission line model

The transmission line modeling method (TLM) is an approach to numerical modeling in which a continuous system is approximated by a network of transmission lines and this discrete network is then solved exactly. The origin of TLM date back to 1944 and the work of Kron and others who noticed the similarity between circuit concepts and Maxwell's equations [113]. The TLM method, as a practical tool for solving electromagnetic field problems was introduced in 1971 [114]. TLM is a discrete system in which the results tend to the solution of the continuous system as the discretization steps tends to zero. Practical simulations must necessarily employ a finite discretization and this introduces numerical dispersion, which varies with frequency and direction of propagation [115]. Time domain TLM is most appropriate when output is required over a wide frequency range where the geometry is too complex for other solution methods. Inhomogeneous materials, non linearities and time variations can all be easily included.

This simple model did not consider the effect of substrate on radiation and input impedance. Later some modifications were suggested for calculation of mutual conductance between the radiating edges by integrating the interference component of the radiation patterns of two magnetic current sources of the patch antenna [116-117]. In another suggested model, the input impedance of antenna was not a function of feed position along the y-direction. Hence this model was modified by considering additional transmission line along the y-direction and represented its effect in the form of a reactance [118]. This transmission line model was further improved by including mutual coupling between the radiating edges through a mutual admittance connected between the two ends of transmission line [119]. This improved model is still applicable for the rectangular and square patch antennas. The field changes along the patch width were still not considered in this model. This model may be used for microstripline and probe feed only. The analysis of non contacting type fed patch antenna is not possible with this model.

A generalized transmission line model (GTLM) was also proposed by converting transmission line sections in π-network equivalent [120-121]. The voltage at the current source of the equivalent circuit is obtained by simplifying the circuits using standard star to delta and delta to star transformations technique. The GTLM can be applied to any type of geometry in microstrip patch antenna and unlike transmission line model it is not limited to rectangular shape only. The GTLM differ from transmission line model in a manner that the patch can be considered as a transmission lines along orthogonal directions. GTLM was applied to a host of separable geometries but its application to an arbitrary patch shape is not possible. Later more variations were proposed in this model so that it may also be applied to arbitrary shape antenna. In their model, radiation loss, dielectric loss and copper loss were combined and assumed distributed over the transmission line [122].

(b) Cavity model technique

Microstrip patch antennas generate higher order modes and bear a good resemblance to cavities with dielectric layers. In the cavity model, microstrip antenna is considered as a resonant TM_{mn} cavity, which mainly consists of the area lying between radiating patch and ground. The top and bottom sides of antenna are

considered to be perfect electrical conductor and perfect magnetic conductor is considered around the edge. The thickness of the dielectric layer is assumed to be negligible, therefore the field along the height of the substrate is considered to be uniform in nature. The geometry is two-dimensional in nature and fields beneath the patch for regular shapes such as rectangular, circular, triangular, and sectoral shapes can be represented as a sum of different modes. By solving wave equations for TM_{mn} modes, fields in the antenna are calculated. Since fringing fields crosses the boundary of the patch the electrical dimensions are larger than physical size. The cavity model may be applied to microstrip antennas because these are narrow band resonator antennas and can be termed as lossy cavities [123].

The interior fields determined by cavity model were correct only to the first order because loading effect produced by exterior fields was not included to determine interior field. In this model, mutual coupling between the apertures was included in an implicit manner by considering power only which accounts for mutual conductance but not mutual susceptance [3]. Moreover it did not estimate the ratio of aperture fields correctly in microstrip antennas having more than one aperture. Therefore this model was not much suitable for array application. It was modified to include the effect of radiation and other losses on the input impedance either in the form of an artificially increased substrates loss tangent or by impedance boundary conditions at the radiating walls [124]. This model was generalized by converting given geometry into an equivalent geometry with magnetic walls at the peripheries [125]. The electric and magnetic fields under the patch were obtained by applying planar circuit approach [126]. The Q factor of the patch was calculated by applying cavity model but input impedance was obtained from the ratio of the voltage and current at the feed point. In this model, the electric field under the patch was determined by segmenting the given patch into a number of regular shapes for which Green's function was obtained.

The techniques discussed in the previous section make a number of simplifying assumptions. Therefore, they suffer from a number of limitations. Most of the limitations might be for overcoming in the full wave analysis. They offer the most accurate results and may be applied to arbitrary structures. The full-wave analysis

includes formulations that are electromagnetically rigorous as well as computationally extensive. The principal assumption of this technique is that the substrate and the ground plane are infinite in lateral dimensions. Some of the characteristics of the full wave technique include accuracy, completeness, computational cost and versatility [112].

(c) Spectral domain full wave analysis

The spectral domain full wave method was discussed in [127-128]. It uses exact Green's function for the mixed dielectric nature of the microstrip antenna. The boundary conditions at patch are fulfilled by using Green's function for making electric field integral equation. The matrix equation is obtained from integral equations by dividing it into the linear equations using method of moment. The matrix equation is solved to attain the current distribution on the patch. The current distribution along with Green function is used for getting near and far field properties of antenna.

(d) Mixed potential integral equation analysis

Mixed potential integral equation analysis (MPIE) approach is perhaps computationally more efficient than spectral domain technique. The mixed potential integral equation technique can be used to analyze arbitrary shaped microstrip structures [129-132]. The starting point for the MPIE is the solution of an integral equation arrived from the boundary conditions for the electric field at the patch metalization. Different types of potential Green's functions are used in MPIE to set up integral equation. Among several possible choices, Sommerfield choice of potential is the most popular approach for solving stratified media problems. In MPIE, the integral equation was solved in the space domain. For this, the spectral domain potential Green's function should be transformed to the space domain. By applying this approach, various types of patch shapes, feed types, stacked geometries, anisotropic substrates and array geometries were analyzed.

(e) Finite difference time domain analysis

This method was first proposed in [133]. The major difference between FDTD and other numerical techniques was that analytical preprocessing and modeling were

almost absent in this model hence analysis of complex antennas was easy. This approach can be used to include the effect of finite substrate size and ground plane, which are very important in designing many microstrip antenna particularly for handheld receivers. Interaction between the device and circuits at the field level can be incorporated using FDTD model. This is necessary for accurate analysis of microwave active circuits and antennas. FDTD has been one of the most popular technique for designing antenna geometries from a complex design which include antenna arrays and many more to even a single layer simple patch antennas. The antennas designed using FDTD are successfully employed in significant areas of communication field including radar systems, aeronautics, satellite communication, GPS Systems, mobile handsets etc. FDTD has the following advantages over other techniques:

(i) From the mathematical point of view it is a direct implementation of Maxwell's curl equation. Therefore analytical processing of Maxwell's equations is almost negligible.

(ii) It is capable of predicting broadband frequency response because the analysis is carried out in the time domain.

(iii) The algorithm remains simple even when dealing with inhomogeneous objects

(iv) It is capable of analyzing structures using different types of materials e.g. lossy dielectric, magnetized ferrites, anisotropic plasma etc.

(v) A real time animation is provided, which is very helpful for understanding.

(vi) Has good computation efficiency for solving even complex problems which consumes more time.

The FDTD method has been extensively used for calculating frequency domain characteristics such as voltage or current distribution, propagation constants, S parameters, driving point impedance and so on. If we look into available literature on simulation analysis of antenna structure, we will find that commercially available FIDELITY simulation software launched by Zeeland Software, Inc, CA is one of the common simulation software. This software is based on FDTD model while available simulation software XFDTD3D is based on full-wave FDTD model.

(f) Method of moments (MOM)

The method of moment is a powerful tool which can be utilized to solve electromagnetic theory problems. This technique was first introduced by R. F. Harrington in 1968 [134]. In this method the integral equation are converted into a matrix equation using orthogonal expansions and linear algebra. The method of moments works on two main concepts, i.e. superposition and Green's functions. It is extremely appropriate technique for planar devices. Spectral domain method of moments was applied for analysis of a cylindrical omni-directional microstrip antenna with thin beams for wireless communication [135]. A moment method was developed as per new analytical entire basis function to analyze slot loaded trapezoidal patch antennas for obtaining multi frequency operation [136]. A solution using method of moments was given for a slot/printed patch antenna mounted on a thin finite substrate [137]. A circular microstrip patch antennas using aperture coupled feed for finite phased array was analyzed using MOM [138]. The major drawback of this method is it is not well suited for complex structure and inhomogeneous surfaces, as it takes large computation time and results are less accurate.

(g) Finite element method (FEM)

The FEM method can be applied on irregular shaped designs and complex structures. It gives accurate results for structures using anisotropic materials inhomogeneous surfaces. The FEM works on the principle of solving equivalent potential or solving the field distribution. The variational approach which is equivalent to Galerkin's method was adopted to solve the Maxwell's equation in differential form and finally the equations obtained are solved by numerical method. This method follows a principle of dividing the structure into large number of elements of finite size, these elements may be of any suitable shaper. The field or potential distribution is calculated using basis function which forms a quadratic or linear equations [139].

Although the finite element method is simple in concept, it suffers several disadvantages. The approximated solution derivatives are less accurate, for curved boundaries, it is very intricate to apply boundary conditions, the complicated and

complex geometries can be represented with less accuracy and precision and it cannot apply the meshes for non rectangular and non-uniform shapes. The finite element method also has some merits over other techniques. Firstly, complex geometrical problem can be resolved by dividing it into simple elements, which are called finite elements. Secondly, for every finite element, approximation functions are calculated keeping in mind that any continuous function can be expressed by algebraic polynomials with linear combination. The finite element method in association with Fourier transforms was applied to calculate radar cross-section of a cavity which is two dimensional in nature; embedded in an infinite ground plane [140].

2.3.4 Electromagnetic simulation software for microstrip antennas

In recent time much activity in the analysis of electromagnetic behavior by computer simulation has been realized. Computer simulation of electromagnetic behavior is a vital part in the designing of current electronic devices. With exponential growth in the field of electronic technologies the devices working at higher frequencies and having smallest possible size are in great demand. The designing simulation tools have to be very fast, accurate and precise to fulfill this demand. The introduction of electromagnetic analysis tools has become an integral part of research and such development in the field of electronics has shortened the development times and reduced the cost of development. Electromagnetic simulation is a new technique for obtaining highly accurate analysis and design of complicated antennas, RF and microwave devices and any other electronic device. This can be attributed to accelerate the research and development of microwave devices due to the explosive growth of microwave communication systems as well as the need to examine the electromagnetic behavior of high speed electrical signal and deal appropriately with the leakage of electromagnetic waves. The dimensions and other calculated parameters are not sufficient to directly fabricate an antenna unless they are further simulated and tested. This is done to increase the efficiency of the design process as it reduces the number of costly manufacture-and-test cycles. The deviation of the actual results from the calculated values is due to many reasons-

- Low accuracy of the model used to calculate the parameters.
- Assumptions taken for modeling the antenna on a certain model may not be valid under practical conditions.
- Neglecting certain parameters in the theoretical calculations for expediency may affect the characteristics.
- Finally to account for unforeseen conditions that might occur practically for which the theoretical model may not be sufficient, but rigorous simulators take this into account.

The use of simulation tools for designing have reduced the cost of manufacturing as the fabrication will be done only after getting satisfactory results using simulation. Typical simulation software has following salient features-

- The simulation tool will give user flexibility to vary different parameters of the design for desired performance.
- User friendly – allows user to concentrate on the designing part instead of wasting time in learning the steps.

A brief detail about the EM packages one could use for simulation purpose is given below.

(a) IE3D simulation software

IE3D is an electromagnetic simulation tool for designing of planar circuits including antennas, filters, couplers, MMIC etc. IE3D has been used in also electromagnetic simulator. It is a technique for electromagnetic simulation to provide high accurateness in analysis and designing of complex RF and microwave and circuits and other electronic devices. The IE3D has turn out to be the most resourceful, easy to use, proficient and perfect simulation tool because it has following important features [141]:

(i) It is based on the numerical technique, method of moment and solves current on 3D metallic structure in multilayered dielectric environment.

(ii) The Maxwell's equations are solved in the integer form and effects of radiation, coupling, discontinuities are included in the solution.

(iii) Using this tool various parameters including VSWR, current distribution, directivity, near field radiation patterns Z, Y, S parameters etc are calculated

(iv) The IE3D is an enormously useful tool for designing of RF printed circuits, MMIC microstrip antennas, wire antennas, filters, IC interconnects and high speed digital circuits.

(b) CST Microwave Studio

CST Microwave Studio is an expert tool for the simulating circuits and devices operating at higher frequency. The CST has turned out to be the most acceptable, user friendly, powerful and highly accurate electromagnetic simulation tool because it has following characteristics [142]:

- It has transient solver and frequency domain solver which does analysis of loss free and lossy structures efficiently.
- It has frequency domain solver which is basically a general purpose solver.
- The structure can be seen and modeled as 3D model or in circuit form.
- It takes less computation as compared to other simulation software and provides accurate results in almost no time.
- There is also an option of merging results on a signal graph to show variation of design parameters.

(c) Ansoft HFSS

Ansoft HFSS (High Frequency Structure Simulator) is an integrated full-wave electromagnetic simulation and optimization package for the analysis and design of 3-dimensional microstrip antennas and high frequency printed circuits and digital circuits such as microwave and millimeter-wave integrated circuits (MMICs) and high speed printed circuit boards (PCBs). HFSS™ utilizes a 3D full-wave Finite Element Method (FEM) to compute the electrical behavior of high-frequency and high-speed components. With HFSS, engineers can extract parasitic parameters (S, Y, and Z) and visualize 3D near and far-zone electromagnetic fields [143].

(d) FEKO

FEKO is a comprehensive electromagnetic simulation software tool for the electromagnetic field analysis of 3D structures. It offers multiple state-of-the-art numerical methods for the solution of Maxwell's equations, enabling its users to solve a wide range of electromagnetic problems encountered in various industries.

FEKO is based on the Method of Moments (MoM) and was the first commercial EM simulation software to utilise the multi-level fast multipole method (MLFMM) for the solution of electrically large problems when it was released with Suite 4.2 in June 2004. FEKO added its first time domain technique with its finite difference time domain (FDTD) solver with Suite 7.0 in 2014.

In FEKO, the MoM is hybridized with the following solution techniques [144]:

- Finite Element Method (FEM)
- Physical Optics (PO)
- Ray-launching Geometric Optics (RL-GO)
- Uniform Theory of Diffraction (UTD)

This hybridization implies that these solution techniques can be applied to different parts of the same model to optimize the solution time and results.

(e) Advanced Design System (ADS)

Advanced Design System is the electronic design automation software for RF, microwave, and high speed digital applications. In a powerful and easy-to-use interface, ADS uses technologies, such as X-parameters and 3D EM simulators, for WiMAX, LTE, multi-gigabit per second data links, radar, & satellite applications, ADS provides full, standards-based design and verification with Wireless Libraries and circuit-system-EM co-simulation in an integrated platform [145].

Key features of ADS

- Complete, integrated set of fast, accurate and easy-to-use system, circuit & EM simulators
- Complete schematic capture and layout environment
- Direct, native access to 3D planar and full 3D EM field solvers
- Broadest RF and MW process design kit (PDK) coverage
- EDA and design flow integration with other companies
- Optimization Cockpit for real-time feedback and control
- X-parameter model generation from circuit schematic
- Up-to-date Wireless Libraries for design and verification of the emerging wireless standards

2.3.5 Fabrication process

The antenna design is first simulated on the simulation tools described in the previous section. Based on simulation results; a prototype is fabricated. The dimensions of antenna are of paramount importance in planar circuits operating at microwave frequencies. Therefore fabrication of antenna geometry is done using photolithography. The fabrication is done in mainly three steps. The first step is UV exposure followed by developing and etching procedure.

The UV exposure involves transferring the antenna design on a film and this is done by CAD or any other software. The design with actual dimensions is made in the software and then transferred to photo resist sheet. The developing procedure starts with washing away the exposed resist in such a manner that pattern will be fully developed. The last step of the fabrication is etching. Etching is done to remove copper from the patch and ground side (if required), wherever it is required. The removal of copper is done by using blades and tweezers.

2.3.6 Antenna measurement methods

This section explains the techniques used for the measurement of fabricated antenna under study. The return loss, resonance frequency and input impedance measurements are carried out by using available Vector Network Analyzer. The specific port of the analyzer should be calibrated for the specific band of frequency using open, short and matched load, prior to the measurement. The frequency at which the return loss value is minimum is taken as the resonant frequency of the antenna. The range of frequency for which the return loss value is less than or equal to -10dB scale is typically considered as the band width of the antenna, usually expressed as the percentage of bandwidth. The radiation patterns of antenna were measured by placing antenna structure inside an anechoic chamber. The anechoic chamber is a small room which consists of absorbing material on the walls, ceiling and floor to avoid any reflections. As it provides almost negligible electromagnetic interference the radiation properties of fabricated antenna is measured here. The absorbers fixed on the walls are highly lossy at microwave frequencies. They have tapered shapes to achieve good impedance matching for the microwave power impinges upon it. The chamber is made free from the surrounding EM interferences by covering all the walls and the roof with aluminum sheet. The antenna under test

(AUT) was mounted on a computer-controlled arrangement lying on a one-meter diameter circular wooden platform. The position of transmitting horn antenna was kept fixed. The separation between transmitting horn antenna and receiving test antennas was kept around two meters. With the help of a sweep generator, the desired frequency signal was applied and radiation patterns for patch antenna were measured by changing elevation angle θ from 0^o to 360^o. These patterns are viewed in E -plane ($\theta = 0^o$) and H -plane ($\theta = 90^o$).

Chapter 3

Compact microstrip patch antennas with defected ground for Wi-Max and WLAN applications

3.1 Introduction

A microstrip patch antenna belongs to that category of antennas that are planar in nature and proficient of fulfilling the requirements of modern communication systems. The use of microstrip patch antennas in wireless devices is very common now a days and the capability of modified patch antennas to operate in dual or multiband has prompted researchers to work extensively in this area. If we look into available literature on microstrip antennas we will find that extensive work on broadband and multi band patch antennas has been reported [3] [146]. Numerous applications such as wireless local area networks (WLANs), world-wide interoperability for microwave access (Wi-MAX), Bluetooth, Wi-Fi and cellular phones requires High performance, compact size and low cost and multiband antennas [96] [13]. Many techniques have been proposed in open literature for reducing size of antenna without compromising with the radiation performance, defective ground structure (DGS) is one of the technique which has drawn much attention of antenna designers. DGS is an engraved non-periodic or periodic defect in the ground plane of a microstrip antenna which perturbs the current distribution in the ground plane and this perturbance will modify the characteristics such as inductance and line capacitance. In other words, any defect engraved in the ground of the microstrip antenna leads to escalating effective inductance and capacitance. DGS provides an extra degree of freedom in antenna and due to this in recent years it has become one of the most promising areas of research [147-148].

In this chapter, we have reported two compact antenna designs for dual-band operation. The main objectives of this work are that the basic structures of rectangular and square antenna are modified in steps to achieve dual band antenna for application to cover any two bands of Wi-MAX (Low band (2.49 to 2.69 GHz), Medium band (3.25 to 3.85 GHz), High band (5.25 to 5.85 GHz)) and WLAN (2.45 to 2.484 GHz and 5.15 to 5.825 GHz) communication systems currently applicable

in India. The gain is aimed to be uniform and variation should be well within 1dBi in the entire desired bands with stable radiation patterns.

3.2 Work done in past on compact dual band microstrip antennas for wireless applications

A compact planar inverted-F antenna (PIFA) appropriate for GSM, PCS, DCS, UMTS and 5 GHz WLAN bands was proposed in [149]. The antenna has capacitive loads, shorted parasitic patches and slots. The measured bandwidths were 70 MHz (870–940 MHz) for GSM band, 476 MHz (1608–2084 MHz) which covers UMTS, PCS, DCS band and 1128 MHz (4863–5991 MHz) operating in the WLAN band with VSWR below 2.5 with good efficiency.

A novel design of compact dual band antenna for WLAN has been proposed in [150]. The design consists of double L slit and shorting wall and by optimizing the location and dimensions; the proposed geometry can resonate in both 2.4 GHz and 5 GHz bands. The antenna is operating in 2.4 GHz band with bandwidth of 120 MHz and in 5 GHz band with bandwidth of 1400 MHz. The experimental result confirms that this antenna is useful for WLAN application. A modified planar inverted F antenna (PIFA) with compact size, having parasitic patch for mobile handset was investigated [151]. It was small in size and measured impedance bandwidth covers 140 MHz (1.74–1.88 GHz) in the Korean personal communication service (KPCS) band and 90 MHz (2.4–2.49 GHz) in the bluetooth band. The influence of the battery and phone case on antenna performance was also studied.

A dual band microstrip patch antenna using metamaterial was proposed for Wi-MAX/WLAN applications [152]. The design consists of an L-shape slotted ground microstrip patch antenna with complementary split ring resonator etched on patch structure. The fabricated prototype shows measured impedance bandwidth of around 200 MHz for 3.5 GHz and 5.8 GHz band with reasonable gain in the operating bandwidth. A two element rectangular microstrip patch antenna with double L-slot for Wi-MAX and WLAN applications was proposed [153]. The geometry was fed using coplanar waveguide and using parametric analysis the return loss, radiation pattern, gain and VSWR were optimized within the operating frequency range. The

results obtained from simulations and measurements were in concurrence with each other. A dual band coplanar waveguide microstrip patch antenna for Wi-Fi and Wi-MAX applications was reported in [154]. The geometry has ground with circular slot at the centre, a narrow feeding strip and two pairs of planar inverted L strips were connected with the slotted ground. The antenna has measured bandwidth of 600 MHz and 1040 MHz and stable radiation pattern.

Minkowski fractal DGS-based truncated slit antenna was investigated for dual band applications [155]. The antenna has compact dimensions of 40 mm×40 mm and offers bandwidth of 80 MHz and 45 MHz for lower and upper band. The proposed design combines the truncated dual L-shaped slits cut on diagonal corners of radiating patch and fractal defect on the metallic ground plane. Overall size reduction of 72% is achieved with this DGS-based antenna. Good agreement was found between the measured and simulated results of the operating antenna.

In this chapter, we have reported two compact antenna designs for dual-band operation. The first design consists of modified pentagonal microstrip antenna with defected ground. A pentagonal slot is inserted in the pentagonal patch and slot loaded ground through optimized dimensions is used in the antenna to resonate it at dual frequency. The geometry operates at two resonant frequencies (2.5 GHz and 5.58 GHz) and offers impedance bandwidth of 864 MHz and 554 MHz in the two bands of interest. The proposed antenna covers the lower band and upper band allocated for Wi-Max and WLAN communication systems. In the second design a dual band microstrip patch antenna is proposed that employs a square patch with circular slot along with a T-shaped defective ground plane. The designed antenna having finite ground plane resonates at two frequencies lying in two bands allocated for application in median and upper bands for Wi-Max communication systems. This antenna offers the impedance bandwidth of 1.05 GHz (29.49%) and 1.06 GHz (19.62%) in the two bands. Designed antenna is low profile and has simple structure, therefore can be easily included with microwave circuits and will be useful for application in Wi- Max communication systems.

3.3 Analysis of conventional rectangular microstrip patch antenna

Basically rectangular patch antenna element consists of conductor of length '*a*' and width '*b*', which is designed on a dielectric substrate having relative permittivity ε_r, substrate thickness '*h*' with patch height '*t*' is supported by an ground plane at the bottom of the substrate. The length of the rectangular patch antenna would be ranging from $0.333\lambda < L < 0.5\ \lambda_o$ where λ_o represents wavelength in free space. The rectangular patch can be fed using microstripline feed or coaxial feed. For the present analysis, we have considered microstripline feed setup. When the patch is energized, a charge distribution is being setup between beneath the patch and the ground. After the excitation by feed, let at any instant of time; ground plane is negatively charged and beneath the patch is positively charged. A force of attraction is being established between the planes i.e. ground plane and beneath patch. The fringing fields are developed between ground and beneath patch causes patch to radiate. The electric field attains maximum value at edges and at the centre it is zero. For an input signal from source, in accordance with the instantaneous signal the minimum and maximum changes are constantly sustained. This phenomenon is shown in figure 3.1.

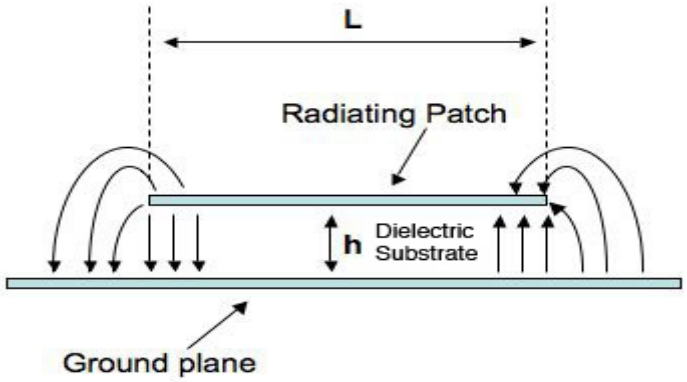

Fig. 3.1. Radiation mechanism of patch antenna

The rectangular patch antenna of 20×25 mm with ground dimension 40×40 mm is considered as the reference antenna with microstrip feedline as shown in fig. 3.2. The antenna design is simulated by using CST simulation software. The metal thickness is considered as 0.035mm, and the patch geometry is printed on glass epoxy FR4 (ε_r=4.4, substrate height "h" =1.59mm, loss tangent "tanδ" =0.025). The antenna is fed through a microstrip feedline having dimensions 4.5×7.5 mm.

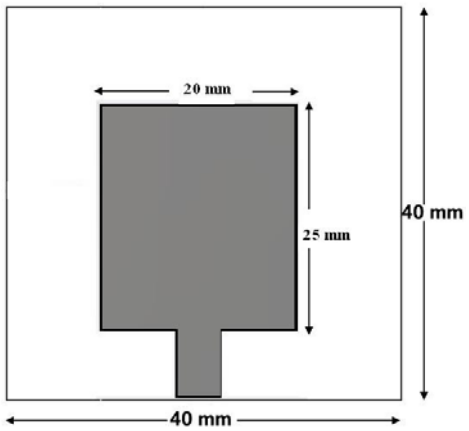

Fig. 3.2 Top view of simple rectangular geometry

A careful simulation analysis of this patch geometry indicates that rectangular patch antenna resonates at 7.48 and 8.04 GHz showing a good matching with feed network (return loss -53.47 dB and -17.43 dB) as shown in figure 3.3. The VSWR variation of antenna with frequency is shown in figure 3.4. The VSWR of this antenna corresponding to resonant frequencies is 1.004 and 1.31 which is very close to value 1.0 desired for excellent matching of antenna with feed network.

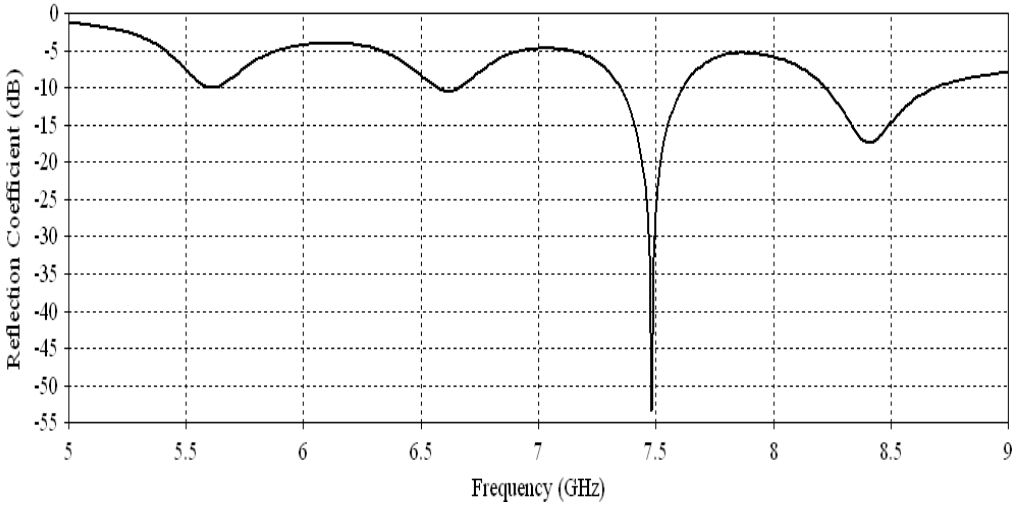

Fig. 3.3. Variation of reflection coefficient (S_{11}) with frequency for rectangular geometry

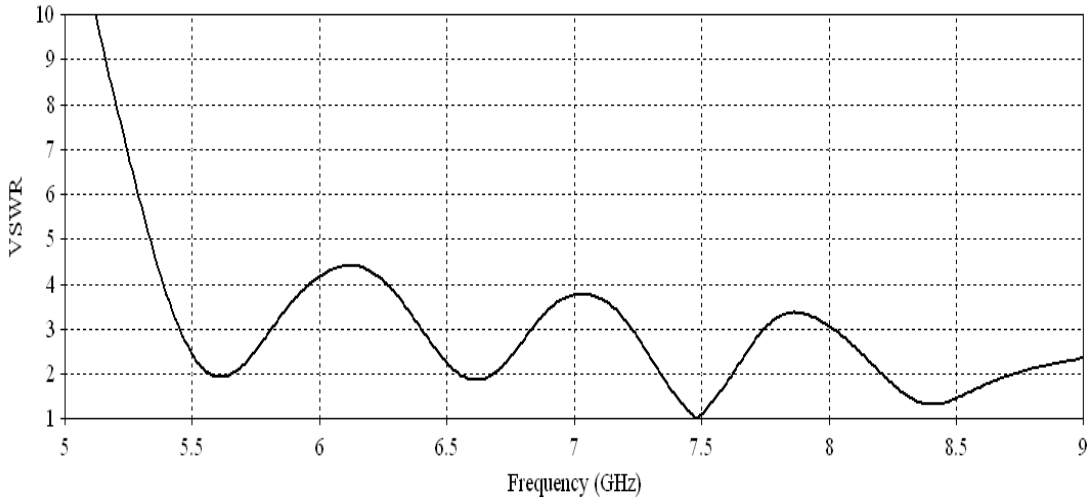

Fig. 3.4. Variation of VSWR with frequency for rectangular geometry

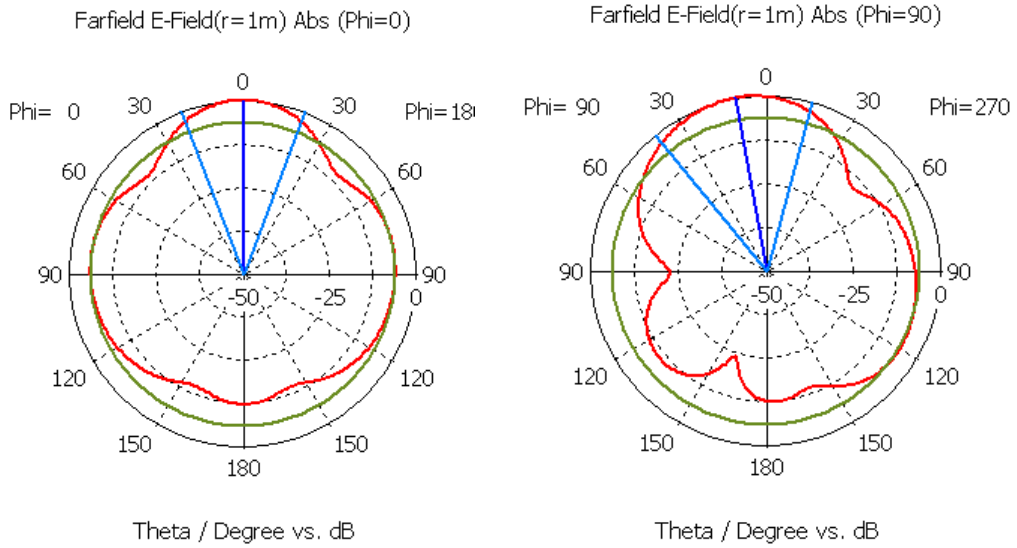

Fig. 3.5. E and H plane radiation pattern at 7.48 GHz

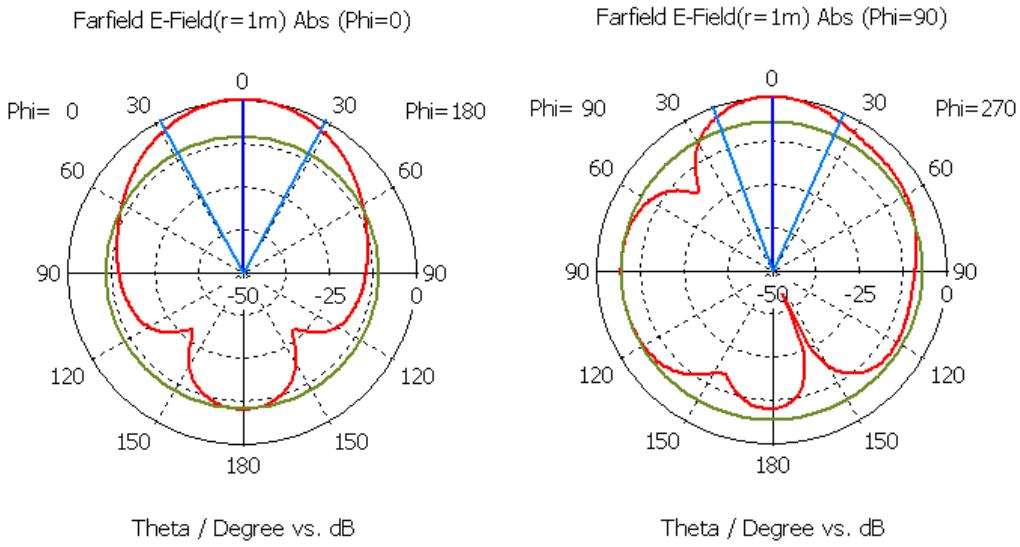

Fig. 3.6. E and H plane radiation pattern at 8.04 GHz

The E and H plane pattern at the resonant frequencies is shown in fig. 3.5 and 3.6 and it is realized that E-plane pattern at both resonant frequencies is directive in nature with 3 dB beamwidth of 40^0 at lower frequency and 60^0 at higher frequency. The H-plane pattern at lower frequency has maximum radiation tilted by 20^0 normal to patch geometry with 3 dB beamwidth of 40^0 while at higher frequency it is normal to patch geometry with 3 dB beamwidth of 45^0. Above results indicates that considered conventional rectangular patch antenna is resonating at a high frequency with narrow impedance bandwidth and needs improvement before it may be considered as a possible candidate for the application in modern communication systems. We therefore modified this antenna in steps to improve its overall performance. The performance of modified rectangular patch antenna is reported in the next section.

3.3.1 Performance of pentagonal patch antenna

In the previous section, we considered a conventional rectangular patch antenna and analyzed its radiation properties. We realized the limitations of this geometry and hence converted it into a pentagonal geometry after extensive optimizations. The performance of this antenna is first analyzed and later modified it further to achieve further improved performance. The pentagonal patch antenna with ground dimension 40×40 mm is considered as the reference antenna with microstrip feedline as depicted in fig. 3.7. The antenna is fed through a microstrip feedline having dimensions 2×10 mm.

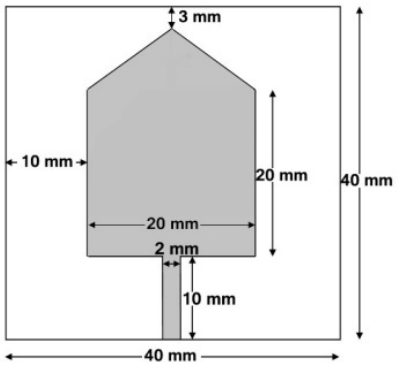

Fig. 3.7. Top view of pentagonal patch geometry

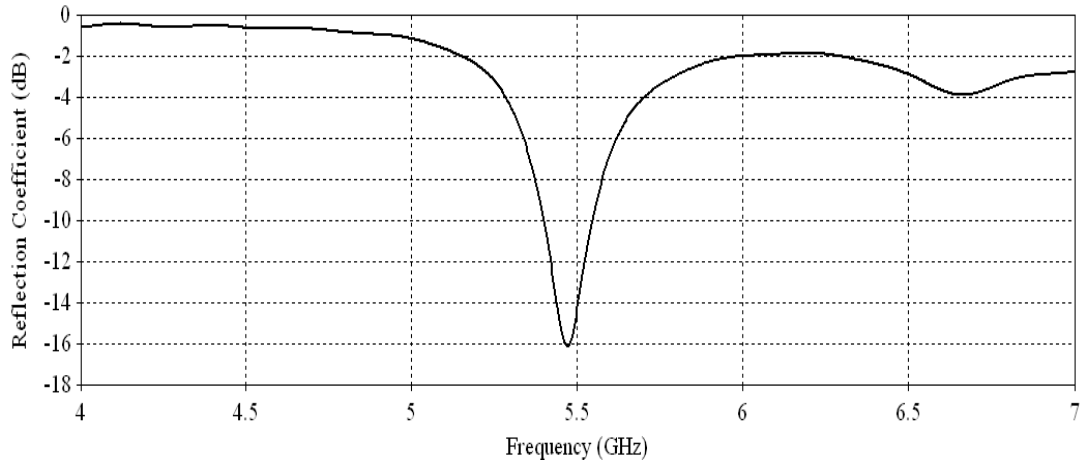

Fig. 3.8. Variation of reflection coefficient (S_{11}) with frequency for pentagonal geometry

The simulated variation of reflection coefficient (S_{11}) of this pentagonal geometry with respect to frequency is shown in fig. 3.8. Within the frequency range of 4 GHz to 7 GHz, this antenna resonates at a single frequency (f_r = 5.47 GHz) and the impedance bandwidth of this antenna is nearly 2.5%.

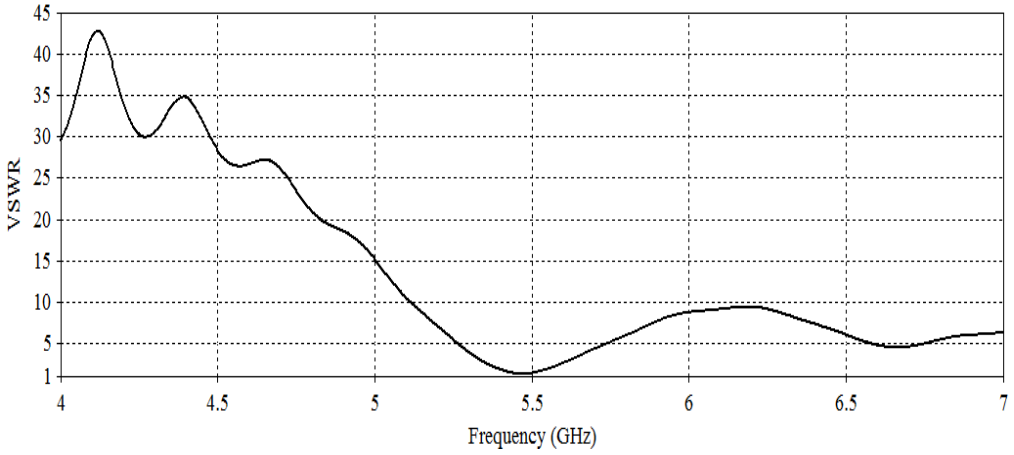

Fig. 3.9. Variation of VSWR with frequency for pentagonal geometry

The simulated VSWR value corresponding to the resonant frequency 5.47 GHz is 1.352 as can be seen from fig. 3.9. Although antenna is operating in the desired frequency range but it is presenting narrow bandwidth, this antenna in its present form is unsuitable for modern communication systems.

3.3.2 Pentagonal patch antenna geometry with rectangular slot in ground plane

In the last section we have carried out simulation analysis of pentagonal patch antenna. From the analysis we found that antenna in its simple form resonates at

single frequency, has narrow band. But current and future communication systems required for commercial and military applications need compact planar antennas operating at more than one frequency. This can be accomplished by etching slots in the ground plane at appropriate locations. We therefore modified the conventional geometry by applying rectangular slot in the ground plane as shown in fig. 3.10. Extensive parametric analysis is carried out with modified ground plane pentagonal patch antenna by varying dimensions of rectangular cut, length (Lg) and width (Wg).

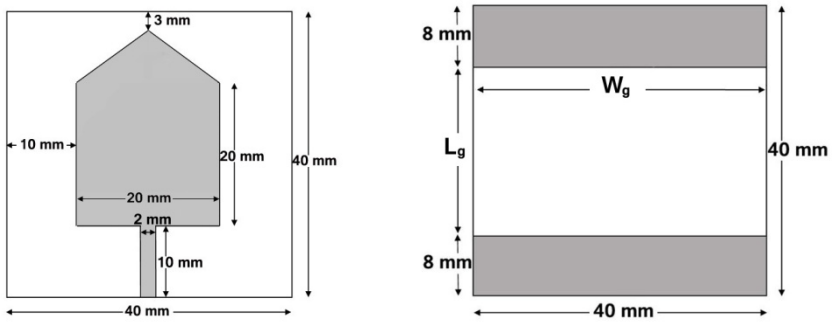

Fig. 3.10. (a) Top view of pentagonal geometry (b) Ground plane geometry with rectangular slot

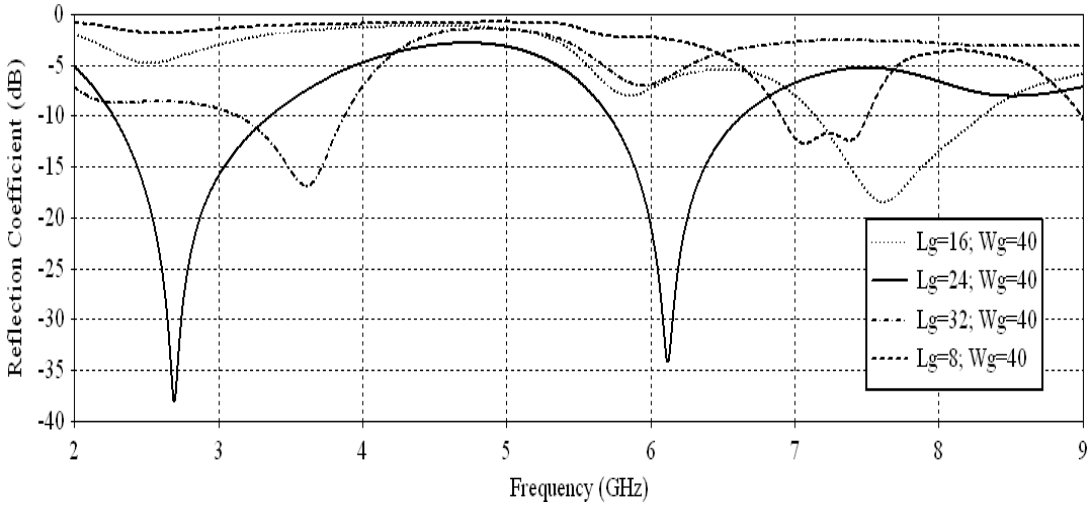

Fig. 3.11. Variation of reflection coefficient (S_{11}) with frequency for different ground slot dimensions

The variation of reflection coefficient for different ground slot dimensions with frequency is shown in fig. 3.11. The best analysis is obtained for ground slot (Lg=24 and Wg=40). At ground slot of 24 × 40 mm the antenna offers dual band, resonating at frequencies 2.69 GHz and 6.11 GHz as shown in figure 3.12. The lower band is ranging from 2.27 to 3.35 GHz and covers the entire lower Wi-Max and WLAN

band but upper band is ranging from 5.71 to 6.62 GHz and is not fitting in the median band of Wi-Max and upper band of WLAN. The variation of VSWR with frequency for pentagonal geometry with slot in ground (Lg=24 and Wg=40) is shown in fig. 3.13. The results show that VSWR for resonance frequencies are 1.01 and 1.04 respectively.

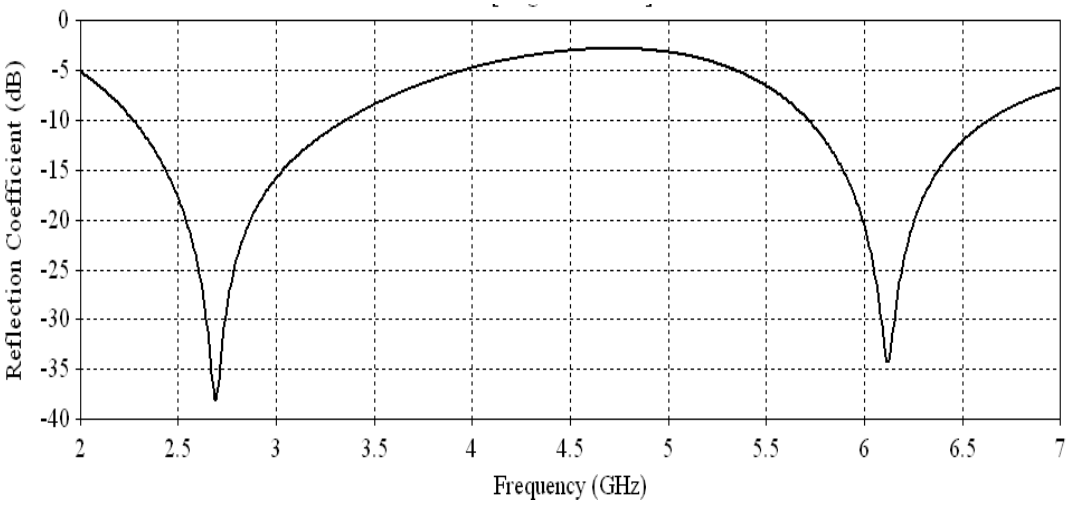

Fig. 3.12. Variation of reflection coefficient (S_{11}) with frequency for pentagonal geometry with ground slot

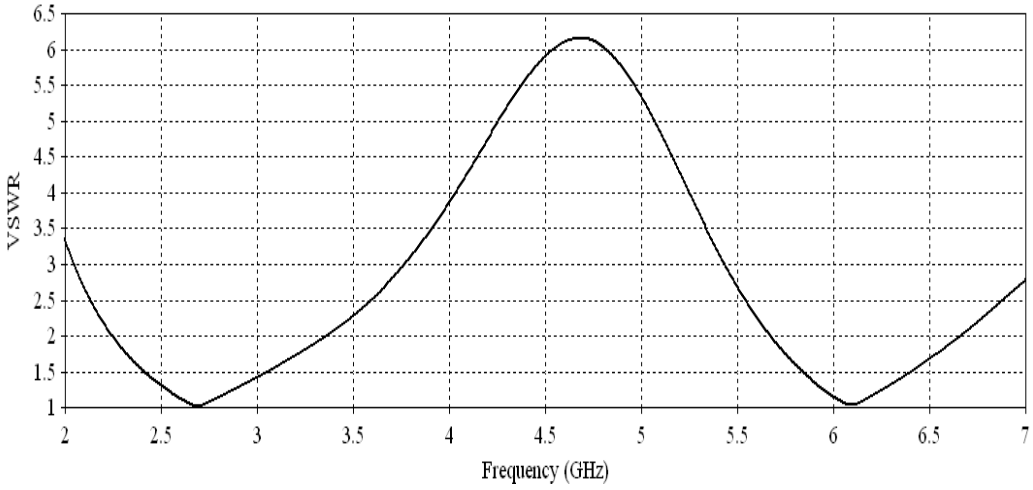

Fig. 3.13. Variation of VSWR with frequency for pentagonal geometry with ground slot

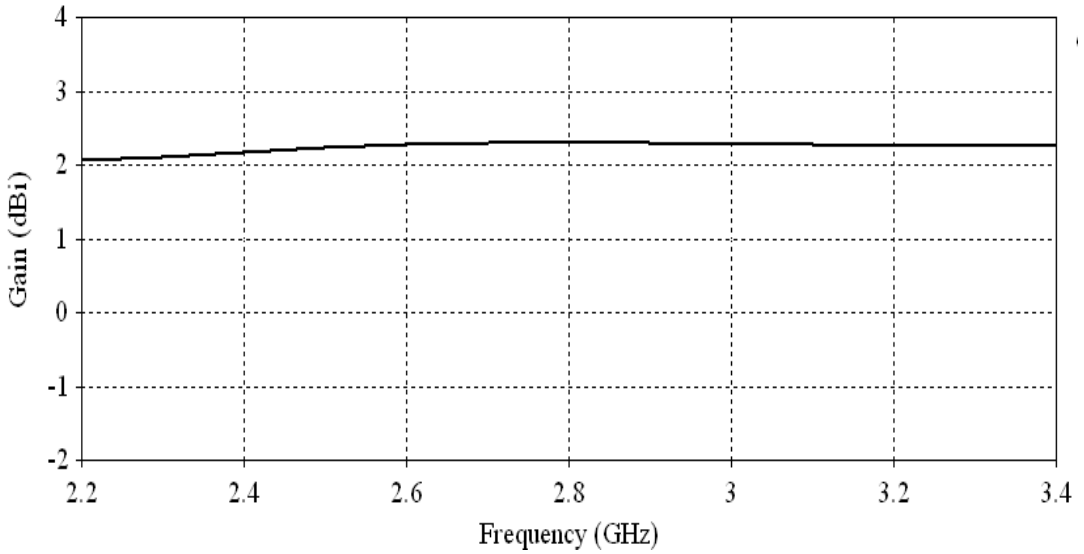

Fig. 3.14. Variation of gain as a function of frequency for lower band (2.69 GHz)

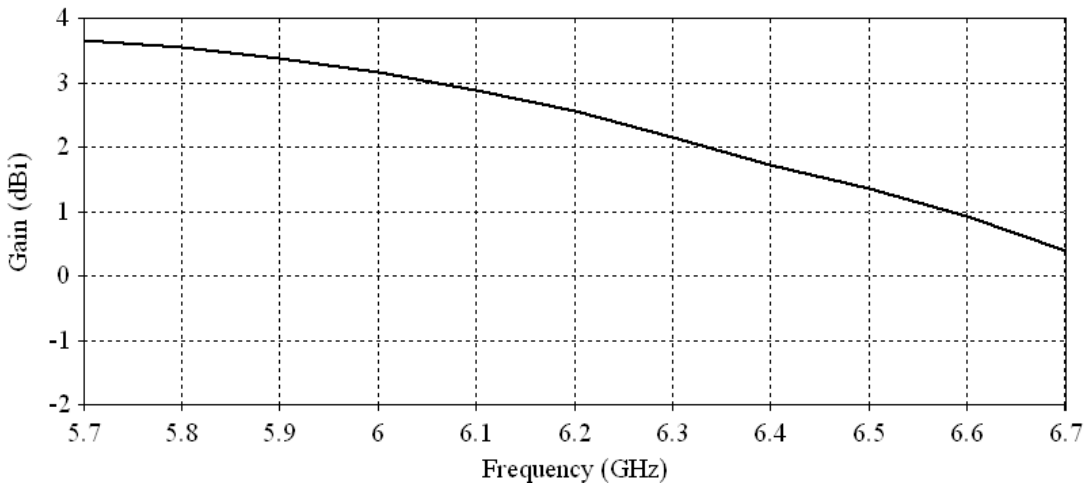

Fig. 3.15. Variation of gain as a function of frequency for upper band (6.11 GHz)

The simulated gain of this antenna at resonant frequencies is 2.3 dBi and 2.75 dBi as shown in fig. 3.14 and 3.15. The gain is found to be positive for the entire operating bands. As the antenna in current form is offering low gain and the upper band is not operating in the desired frequency band some modifications are required in the antenna geometry.

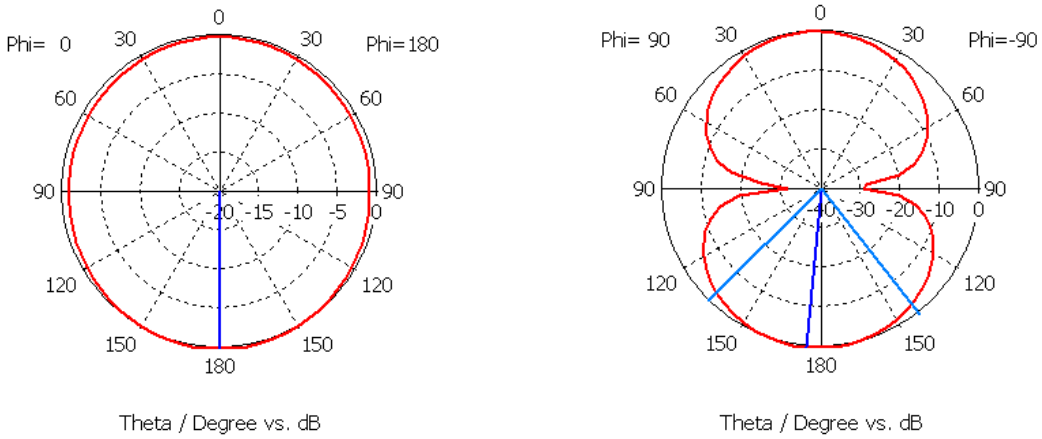

Fig. 3.16. E and H plane radiation pattern at 2.69 GHz

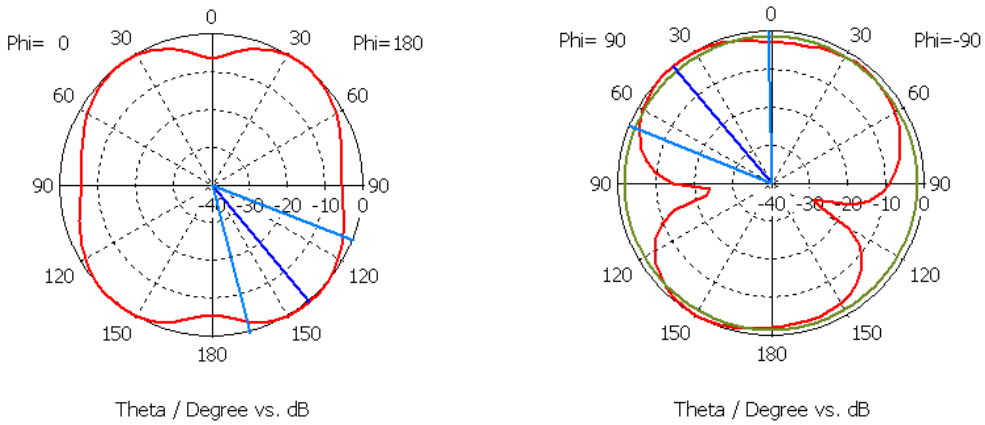

Fig. 3.17. E and H plane radiation pattern at 6.11 GHz

Fig. 3.16 and 3.17 shows the radiation patterns of the antenna in both the E-plane and H-plane at the respective resonant frequencies of 2.69 GHz and 6.11 GHz. The E-plane at higher resonant frequency is more directive than lower frequency. The direction of maximum radiation is normal to the patch for E-plane pattern at lower frequency and tilted by 30^0 at higher frequency. The H plane pattern has 3dB beam width of 75^o at lower frequency and 30^o at higher frequency.

3.3.3 Pentagonal patch antenna with defected ground

The next step of modification involves adding a strip in the ground plane as shown in fig. 3.18 and the variation of reflection coefficient with frequency for different dimensions of ground strip is shown in fig. 3.19

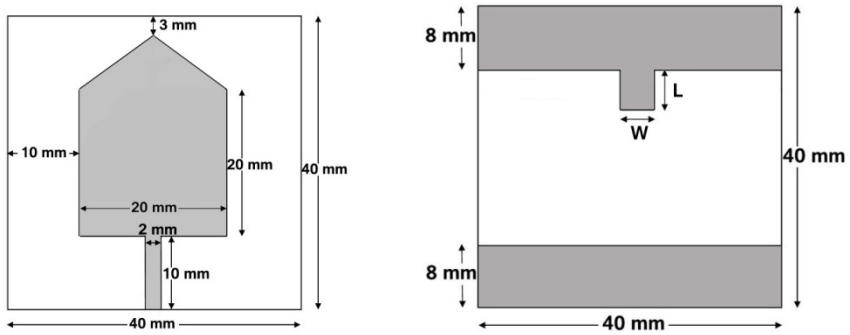

Fig. 3.18. (a) Top view of pentagonal geometry (b) Modified ground plane

It is observed that for strip dimension L=6 and W=5, the resonant frequency of upper band is reduced and the modified geometry is now resonating at 5.64 GHz and bandwidth is ranging from 5.35 to 5.93 GHz while not much changes are observed in the lower band which is resonating at 2.57 GHz and operating in the bandwidth from 2.18 to 3.11 GHz as shown in fig. 3.20.

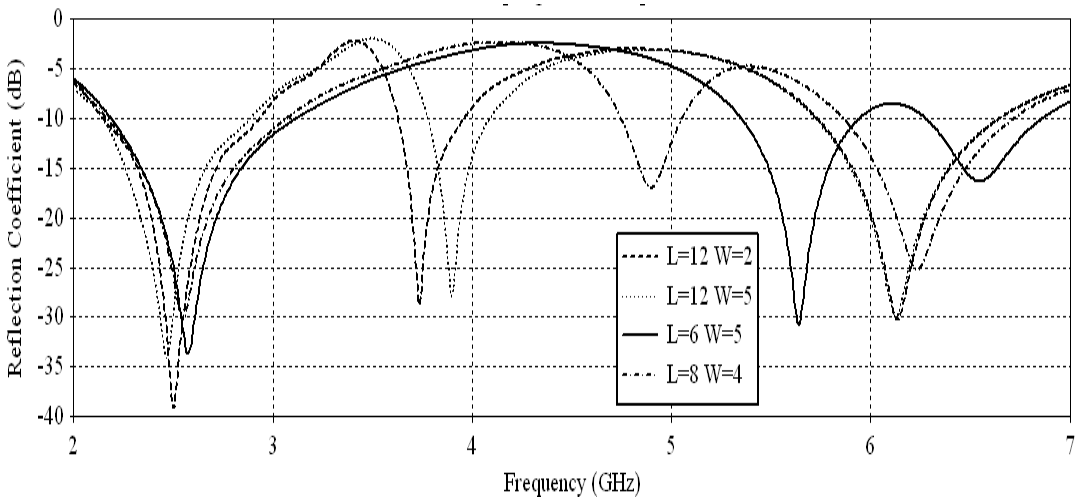

Fig. 3.19. Variation of reflection coefficient(S_{11}) with frequency for different ground strip dimensions

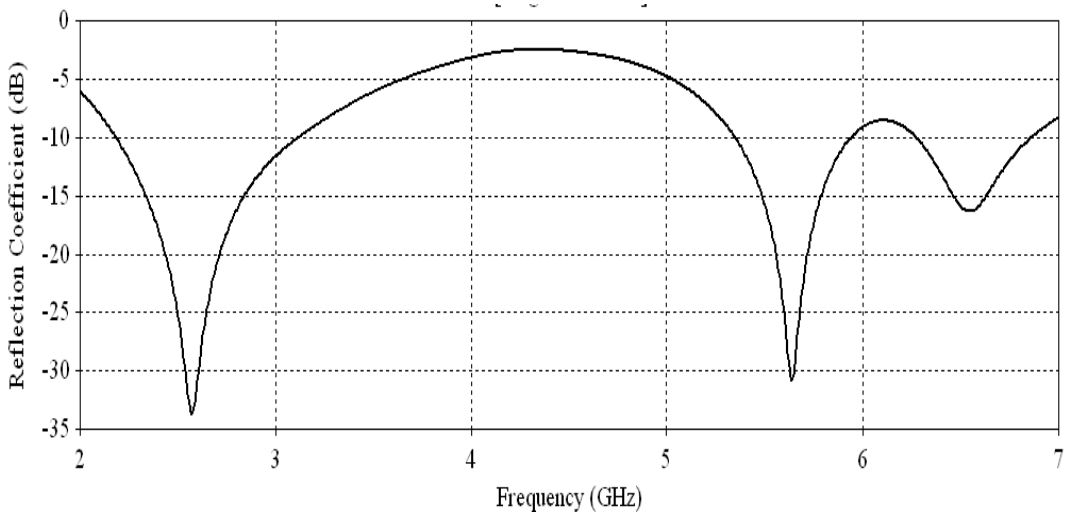

Fig. 3.20. Variation of reflection coefficient (S_{11}) with frequency for pentagonal geometry with modified ground

The VSWR in the frequency range of interest are well within acceptable value 2:1 and at two resonance frequencies of antenna are close to 1.0 which suggests an excellent impedance match between antenna and feed line as shown in figure 3.21.

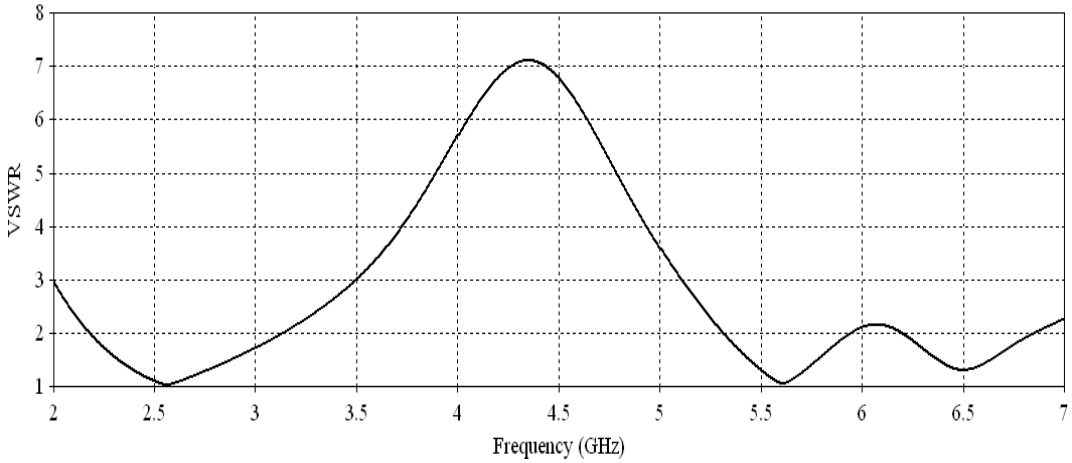

Fig. 3.21. Variation of VSWR with frequency for pentagonal geometry with modified ground

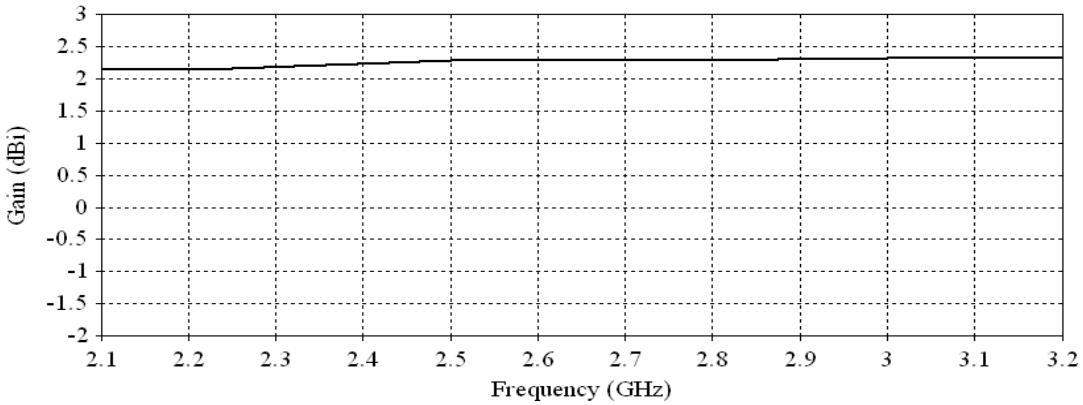

Fig. 3.22. Variation of gain as a function of frequency for lower band (2.57 GHz)

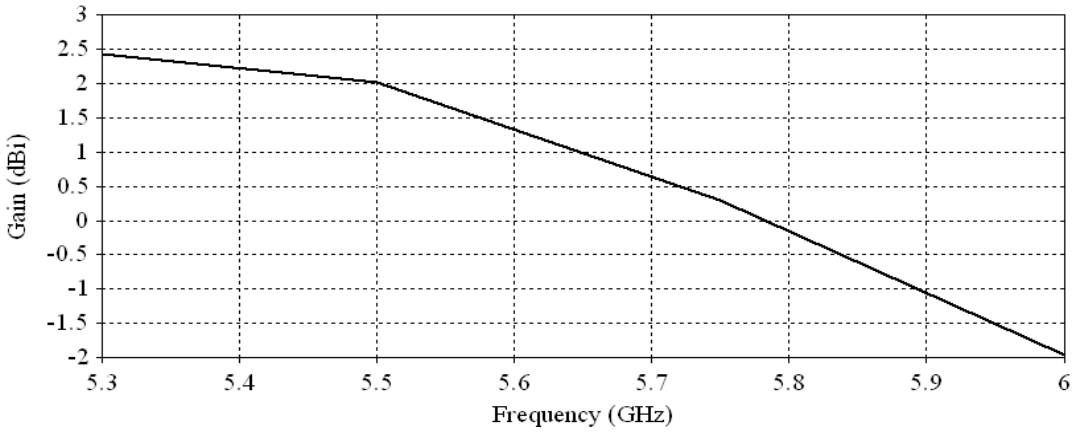

Fig. 3.23. Variation of gain as a function of frequency for upper band (5.64 GHz)

The gain of antenna is close to 2 dBi as given in figure 3.22, however the gain is decreasing in the upper band and reaches negative at higher frequency for upper band as shown in figure 3.23.

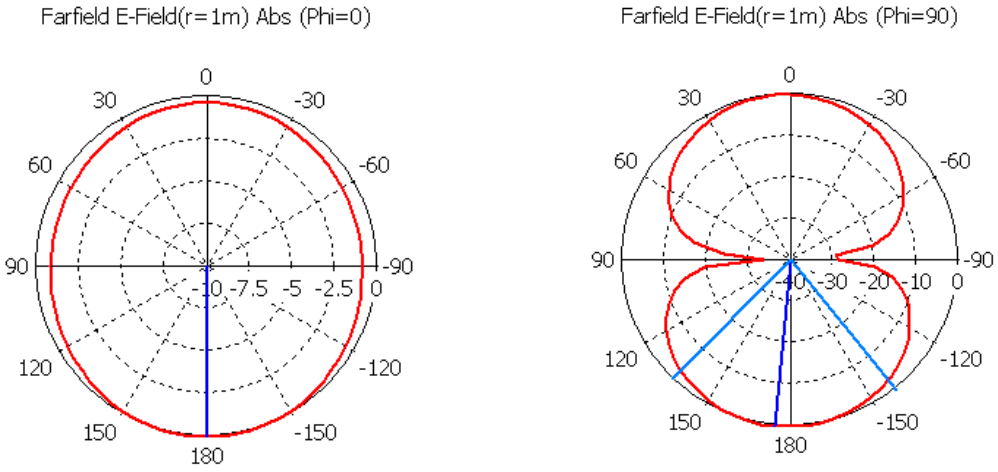

Fig. 3.24. E and H plane radiation pattern at 2.57 GHz

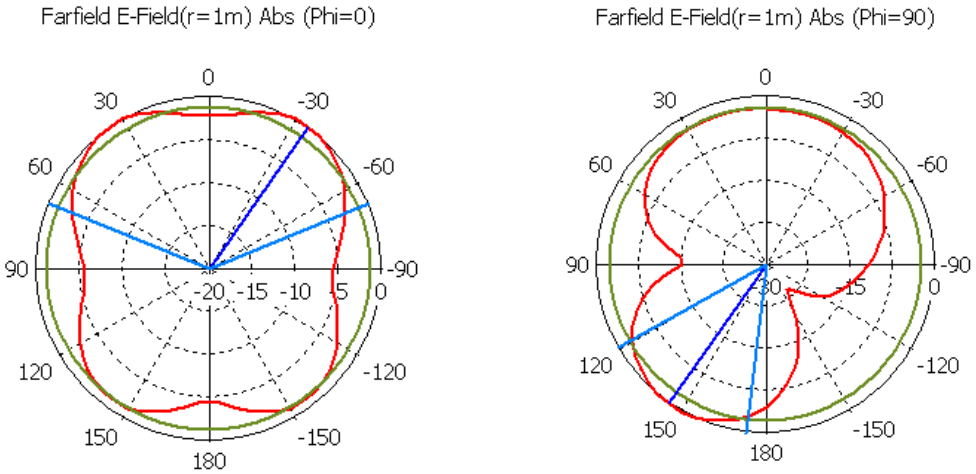

Fig. 3.25. E and H plane radiation pattern at 5.64 GHz

Fig. 3.24 and 3.25 presents the simulated two dimensional E and H plane radiation patterns of the antenna at the two simulated resonant frequencies of 2.57 GHz and 5.64 GHz. At lower resonance frequency, the E-plane pattern is omnidirectional and H-Plane patterns suggests almost equal radiations in front and back direction with 3dB beamwidth of 75^0. At higher frequency the E-plane pattern has maximum radiation tilted by 35^0 normal to patch geometry with 3dB beamwidth of 25^0 and H-plane pattern suggests that radiation in front directional is higher than that in back direction.

3.3.4 Modified pentagonal patch antenna with defected ground

Although the modified geometry is operating in the desired frequency bands of Wi-Max and WLAN applications but the gain is low and not positive for entire upper band. The patch design is now modified to obtain the desired results. The next step of modification is etching pentagonal slot in the patch and ground plane will be same as described in the previous section. The fabricated prototype of proposed antenna geometry is shown in figure 3.26.

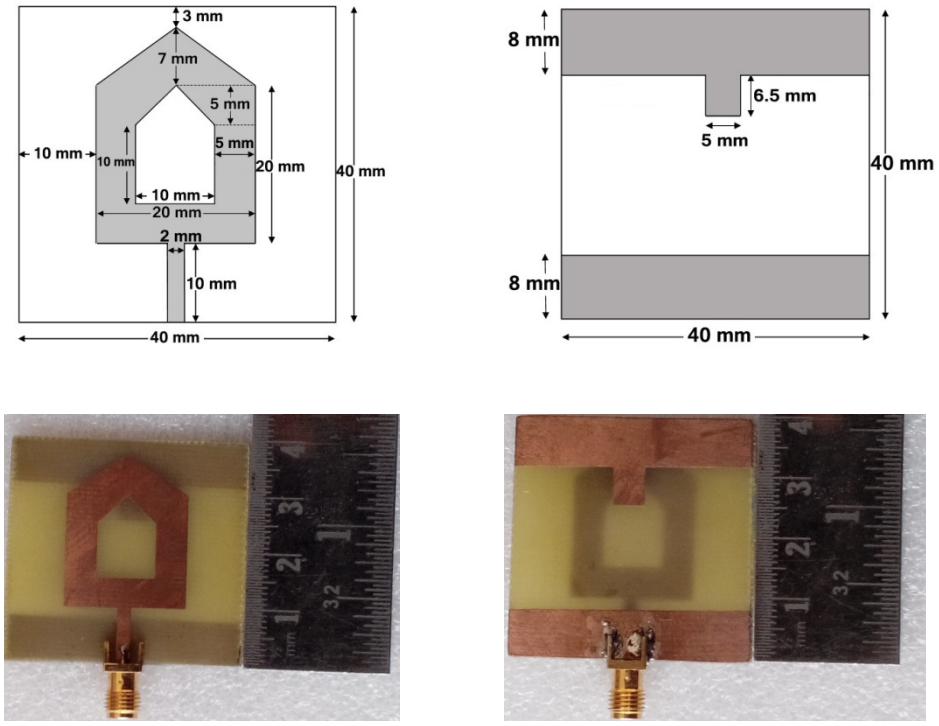

Fig. 3.26. (a) Top view of the proposed geometry (b) Back view of the proposed geometry (c) Top view designed geometry (d) Back view of designed geometry

3.3.5 Performance of modified pentagonal patch antenna with defected ground

(a) Reflection coefficient, VSWR and input impedance of proposed geometry

The design of an antenna starts with the selection of a proper feedline where the input impedance of antenna matches well with that of feed network. The feedline at which reflection coefficient at the desired resonant frequencies is close to -25 dB; is selected as final which is used at the time of fabrication. When antenna is fed at this location it gives good matching at both the frequencies and also shows broadband character as shown in figure 3.27. The simulated resonant frequencies of the proposed geometry are 2.5 GHz and 5.58 GHz while the measured resonant frequencies are 2.72 GHz and 5.75 GHz as shown in figure 3.28. The simulated VSWR at the resonant frequencies are close to unity (1.09 and 1.02) as shown in figure 3.29 while the measured VSWR at resonant frequencies are 1.03 and 1.19 which shows excellent matching with the microstrip feedline as depicted in figure 3.30. It may be observed that the simulated impedance bandwidth of antenna is 864 MHz (34.5%) and 544 MHz (9.74%) while measured impedance bandwidth is 742 MHz (27.2%) and 780 MHz (13.5%) Although the impedance bandwidth of both the bands is slightly reduced but now both the bands are operating in the lower and higher band of Wi-Max (2.495 to 2.695 GHz and 5.25 to 5.85 GHz) and WLAN (2.45 to 2.484 GHz and 5.15 to 5.825 GHz).

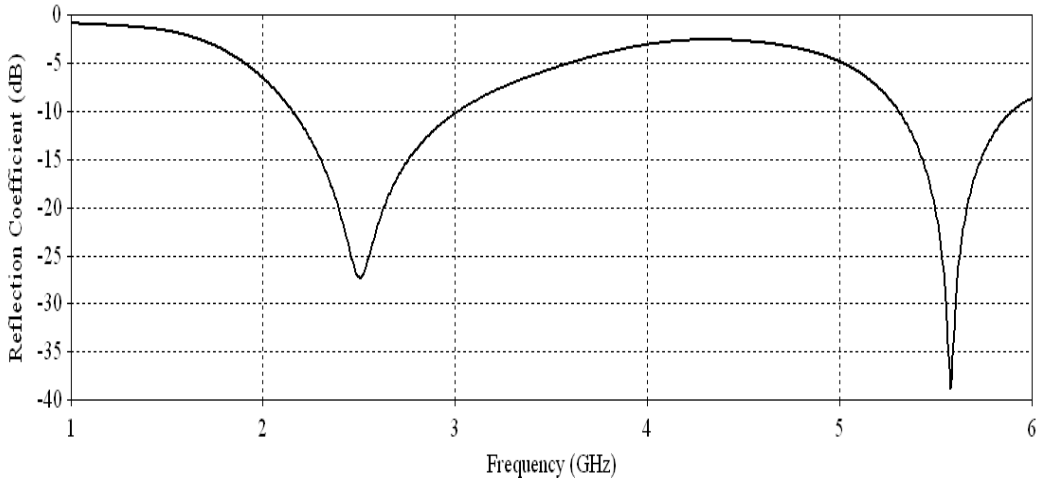

Fig. 3.27. Variation of reflection coefficient(S_{11}) with frequency for modified pentagonal patch with defected ground

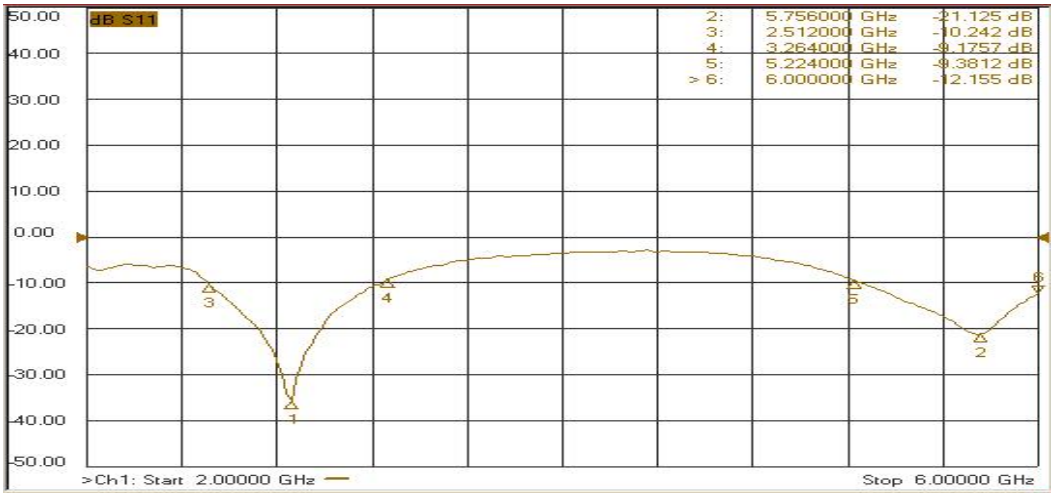

Fig. 3.28. Measured reflection coefficient (S_{11}) with frequency for modified pentagonal patch with defected ground

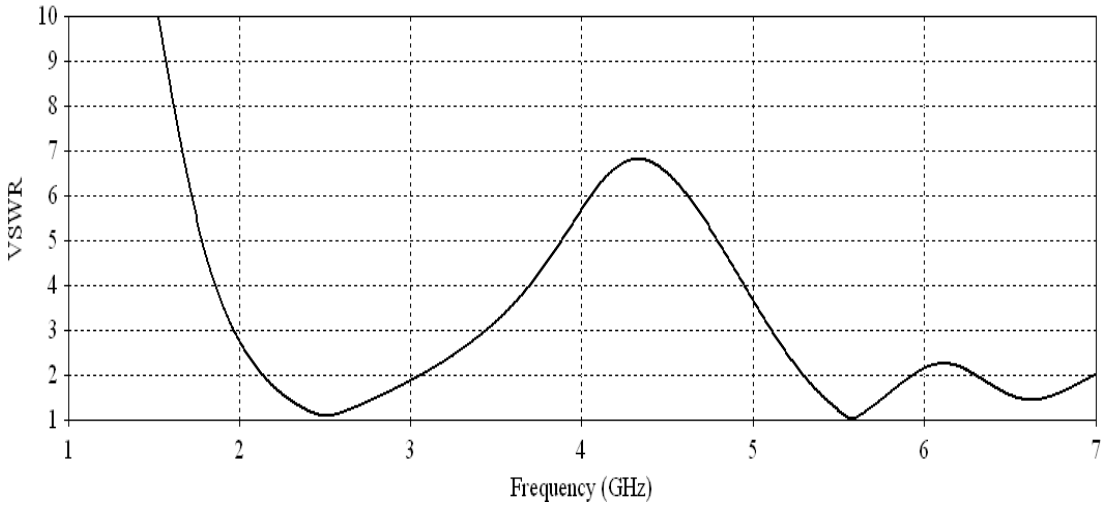

Fig. 3.29. Variation of VSWR with frequency for modified pentagonal patch with defected ground

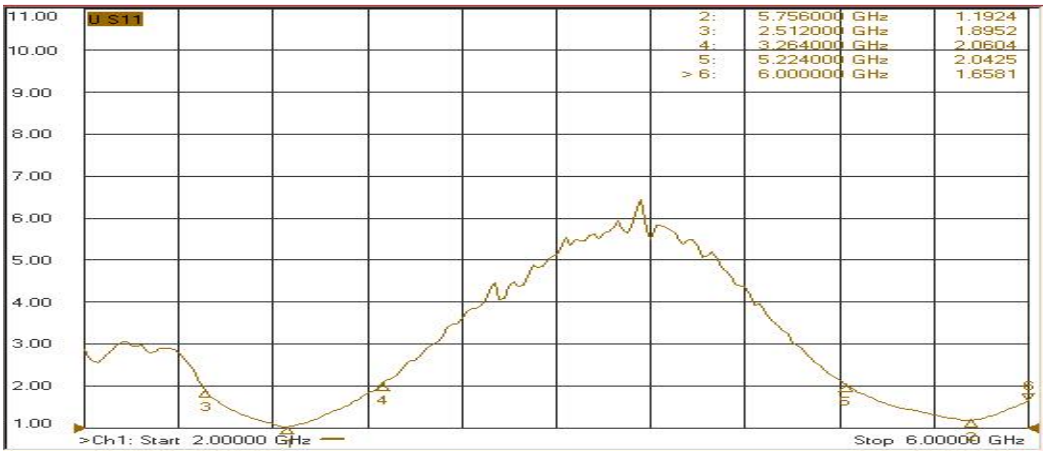

Fig. 3.30. Measured VSWR with frequency for modified pentagonal patch with defected ground

The measured input impedance variation with frequency is shown in figures 3.31. The measured input impedance related to resonant frequencies are (50.45–j1.38) ohm and (59.45+j1.92) ohm respectively which are nearly reaching to 50 ohm impedance of the microstrip feedline.

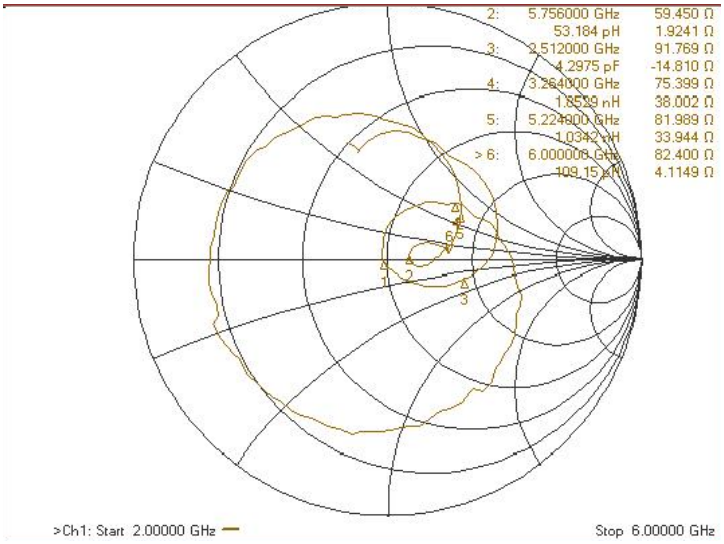

Fig. 3.31. Measured input impedance for modified pentagonal patch with defected ground

(b) Gain and Radiation Efficiency of proposed antenna

The variation in gain of proposed geometry as a function of frequency is shown in figure 3.32 and 3.33. The gain of antenna at both resonance frequencies is close to 3 dBi which is better than that of a conventional geometry. The variation in radiation efficiency is shown in figure 3.34 and 3.35 and is found to be uniform in nature.

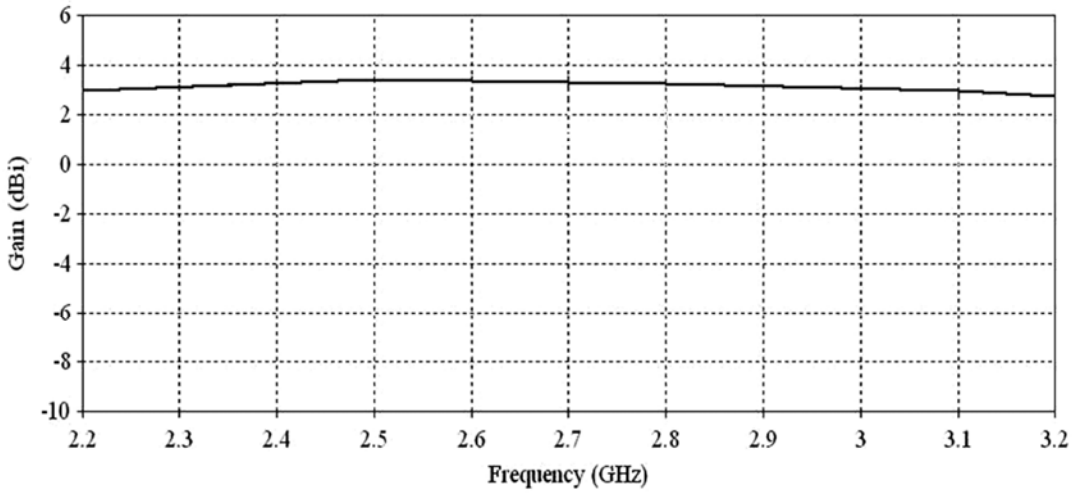

Fig. 3.32. Variation of gain as a function of frequency for lower band

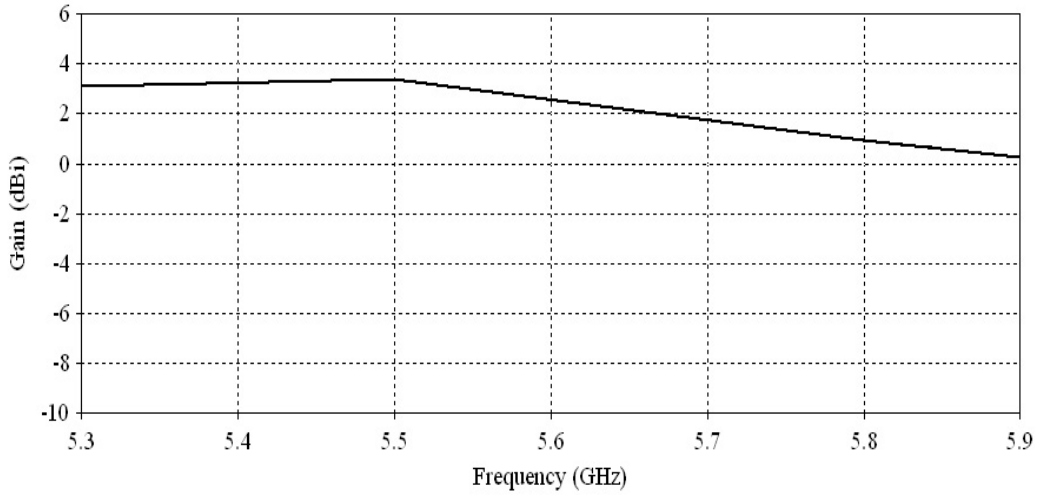

Fig. 3.33: Variation of gain as a function of frequency for upper band

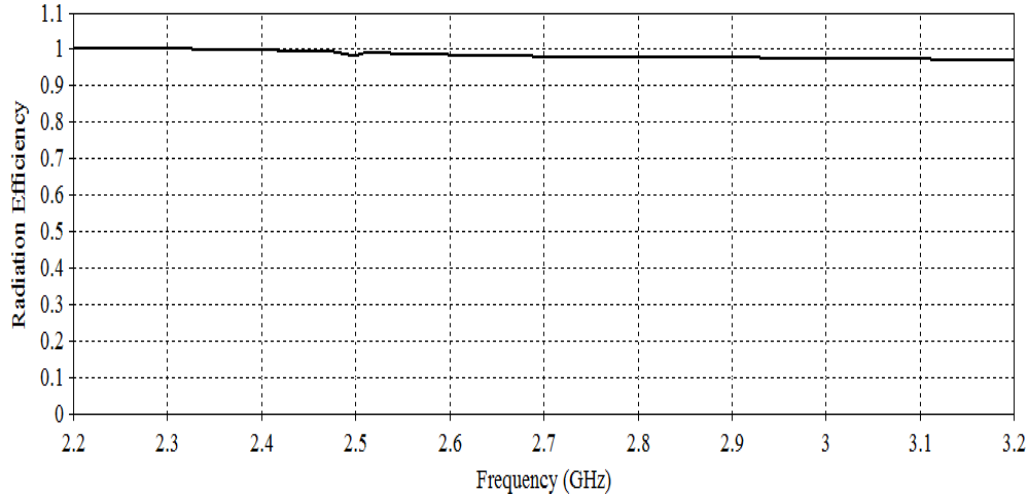

Fig. 3.34. Variation of radiation efficiency as a function of frequency for lower band

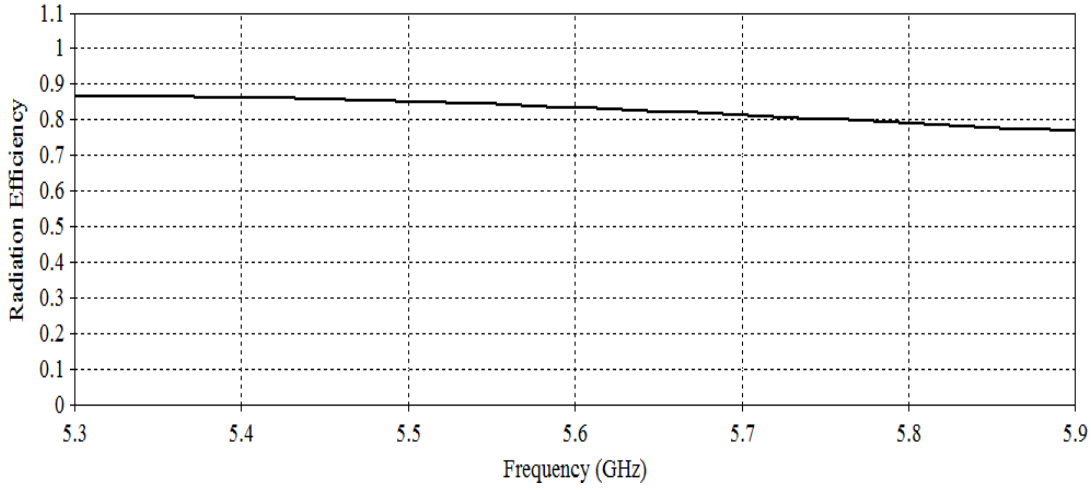

Fig. 3.35: Variation of radiation efficiency as a function of frequency for upper band

(c) Radiation patterns of proposed antenna

The simulated and measured E and H plane radiation patterns of proposed antenna at resonance frequencies are shown in figure 3.36 to 3.39. In fig. 3.36 the lower resonance frequency E-plane pattern is omnidirectional in nature while measured result depicted in fig. 3.38 shows directive nature of E pattern. However the H-plane pattern has equal radiations in front and back direction, normal to the patch geometry for simulated results while in measured results the pattern is inclined by 20^0 as mentioned in fig. 3.36 and 3.38.

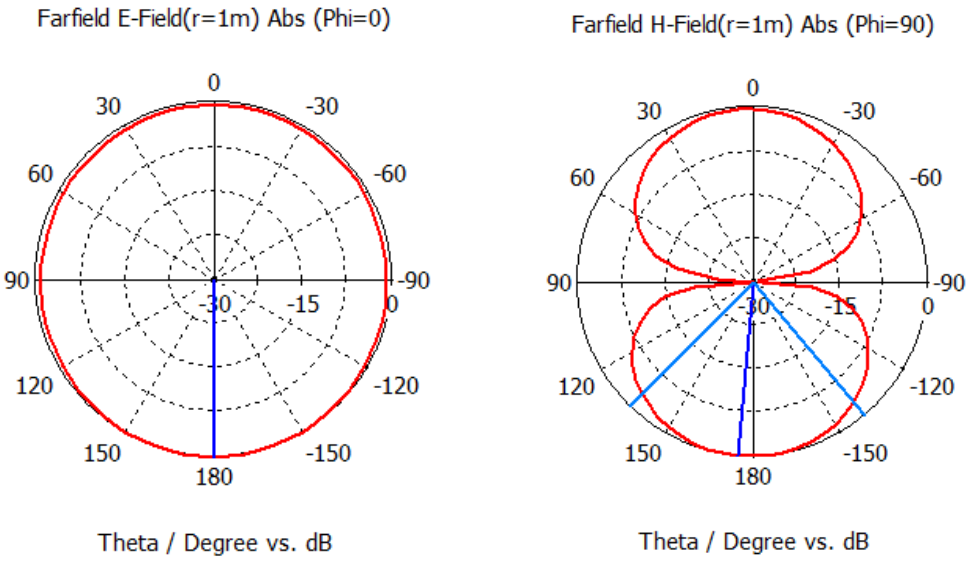

Fig. 3.36. Simulated E and H radiation patterns at 2.72 GHz

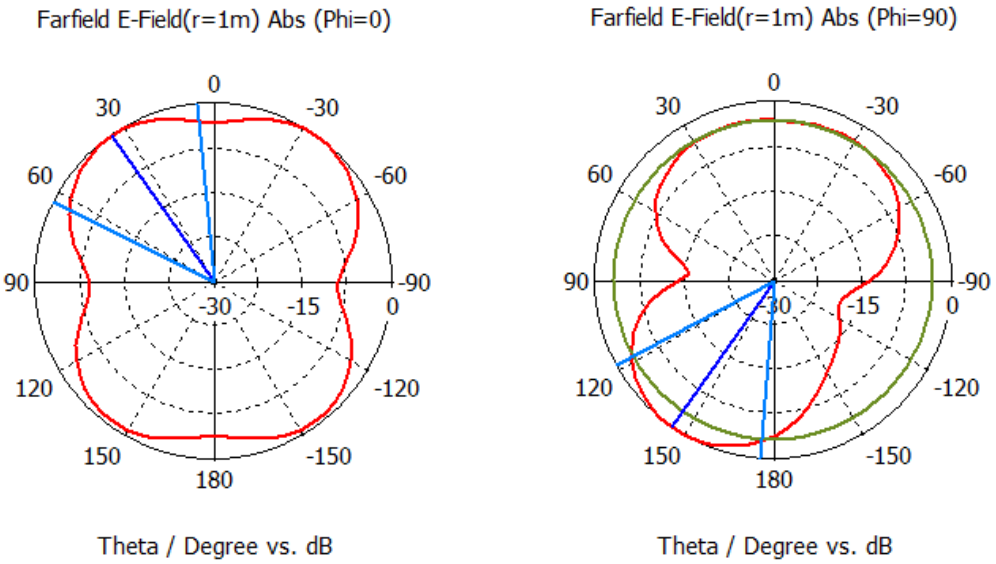

Fig. 3.37. Simulated E and H radiation patterns at 5.75 GHz

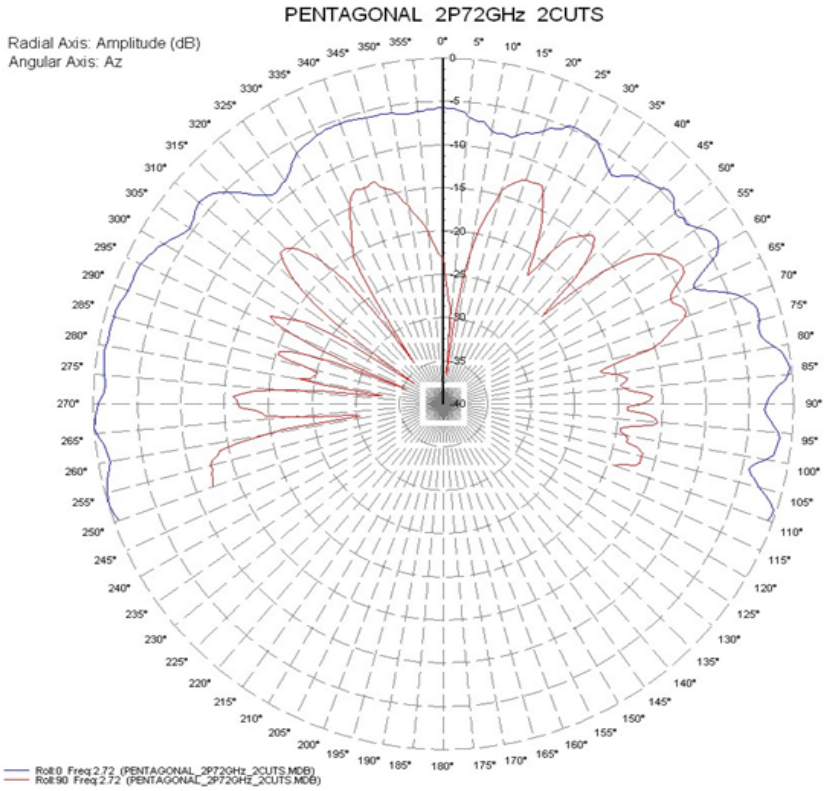

Fig. 3.38 Measured E and H plane radiation pattern of proposed geometry at 2.72 GHz

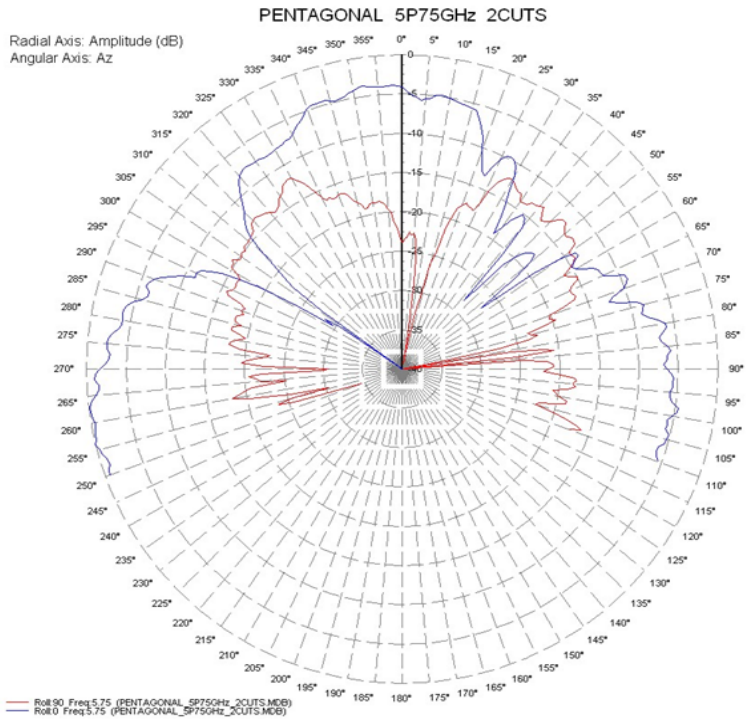

Fig. 3.39. Measured E and H plane radiation pattern of proposed geometry at 5.75 GHz

At upper resonance the simulated E-plane pattern shown in fig. 3.37 is more directive and has maximum radiation inclined by 15^0 normal to the patch with 3 dB beam width of 60^0 while measured E-plane pattern is normal to the patch geometry as indicated in fig. 3.39. The simulated H-plane pattern (fig. 3.37) has equal radiations in front and back direction while measured H plane pattern (fig. 3.39) is normal to the patch geometry.

(d) Current distribution of proposed antenna

To gain a better understanding of the behavior of the antenna, we examine the surface current distributions on the patch and the ground plane as shown in figures 3.40 and 3.41 for both resonance frequencies. Figure 3.40 shows the surface current density distribution in the patch and ground plane for lower resonant frequency. The currents are uniformly distributed over the patch and have slightly for more concentration along the edges. In the ground plane the currents has directions away from the protruding strip and mild current on the lower side of the ground.

For upper resonant frequency, the surface current distribution in the patch and the ground plane is depicted in figure 3.41. The current densities are stronger on the feed line and upper edge of the patch and for the ground plane the current is largely concentrated over the protruding strip, which shows that the upper resonance largely dependent on the protruding strip. The analysis of dual band geometry is described in the next section.

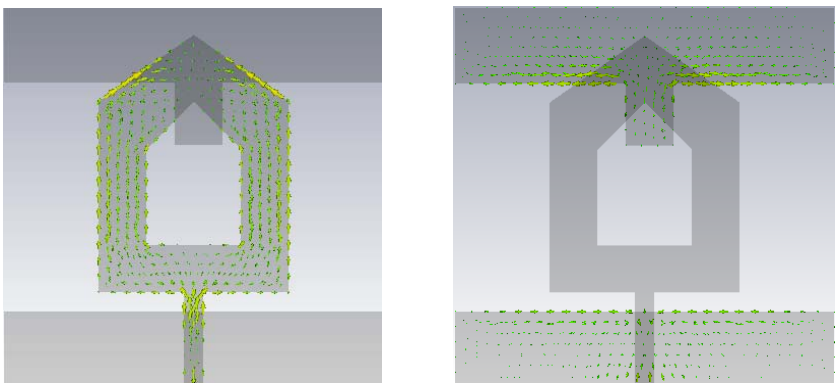

Fig. 3.40. Current distributions of the proposed antenna at patch and ground plane for 2.72 GHz

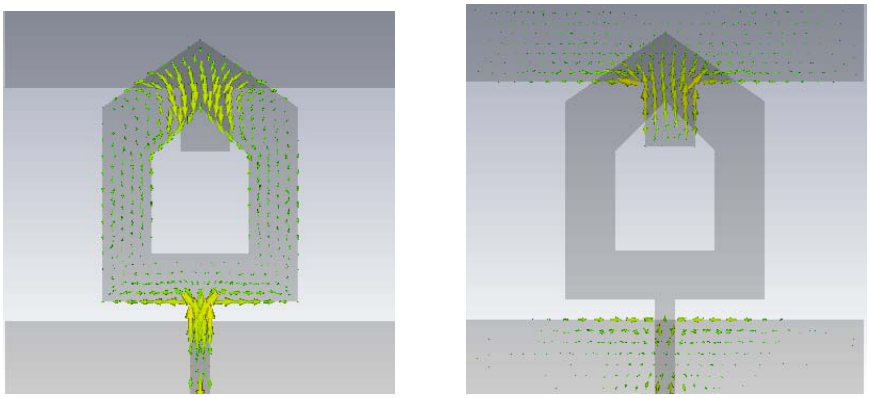

Fig. 3.41. Current distributions of the proposed antenna at patch and ground plane for 5.75 GHz

3.4 Analysis of conventional square patch antenna

Among the conventional patch geometries, microstrip antennas with rectangular, circular, square, and triangular shapes are widely investigated. In this section, we have also selected the square patch geometry and modified it to obtain improved performance. In the first step of proposed work, square microstrip patch antenna with arms length 20 mm each is considered that is fed through a line of length 10 mm and width 2mm as shown in figure 3.42. This antenna is designed on glass epoxy FR-4 substrate (substrate relative permittivity ε_r = 4.4, substrate thickness h = 1.59mm, loss tangent tanδ = 0.025) having finite ground plane of size 40×40 mm and is simulated using CST microwave studio. The simulated variation of reflection coefficient (S_{11}) of this square geometry with respect to frequency is shown in figure 3.43. Within the frequency range of 3 GHz to 9 GHz, this antenna resonates at dual frequencies (6.88 GHz and 7.74 GHz) and has very low bandwidth.

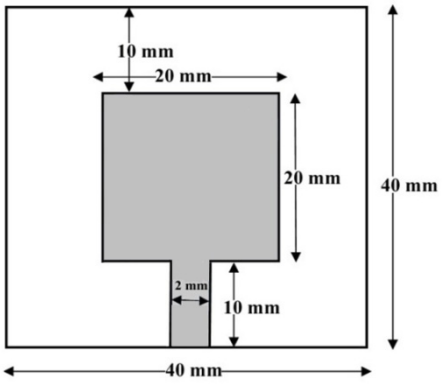

Fig. 3.42. Top view of square geometry

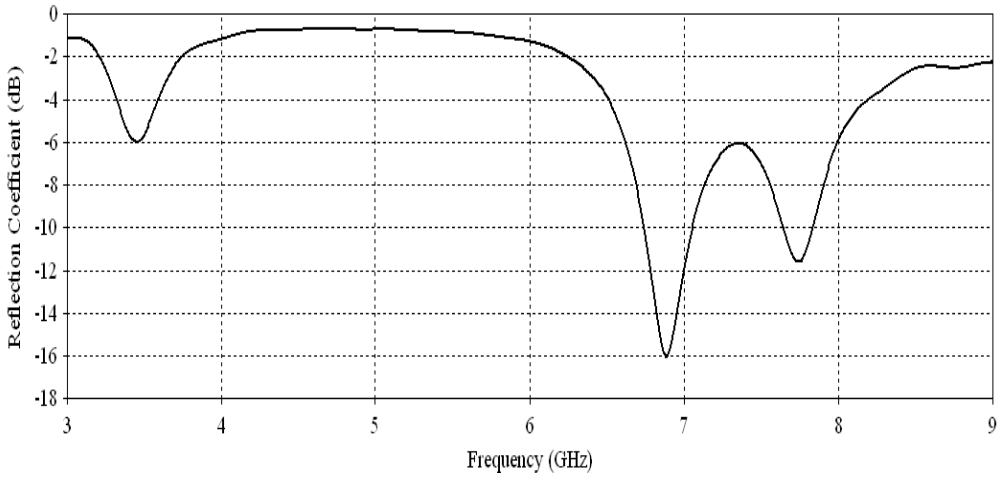

Fig. 3.43. Variation of reflection coefficient (S_{11}) with frequency for square geometry

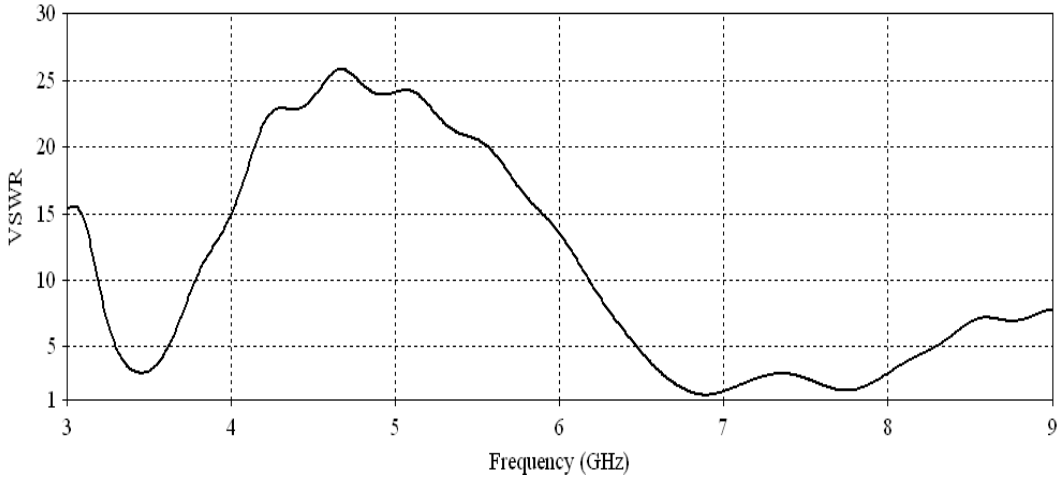

Fig. 3.44. Variation of VSWR with frequency for square geometry

The simulated VSWR values corresponding to the resonant frequencies are 1.37 for 6.88 GHz and 1.71 for 7.74 GHz as can be seen from figure 3.44.

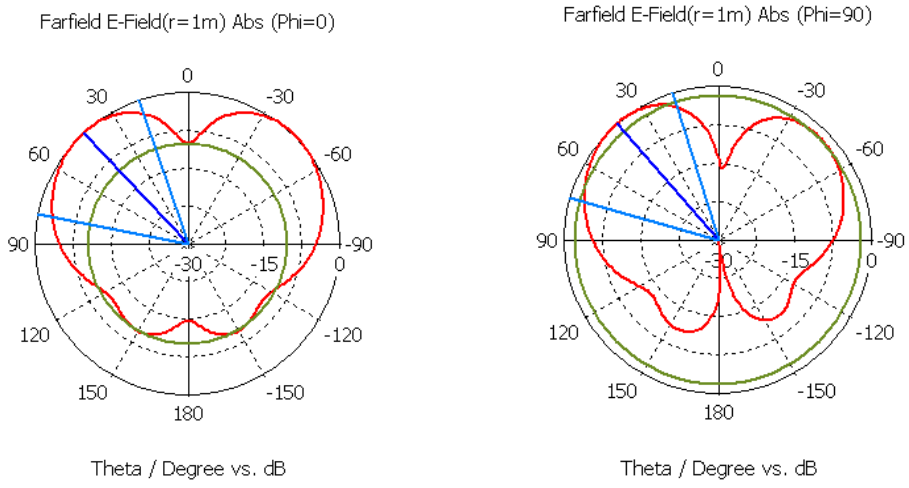

Fig. 3.45. E and H plane radiation pattern at 6.88 GHz

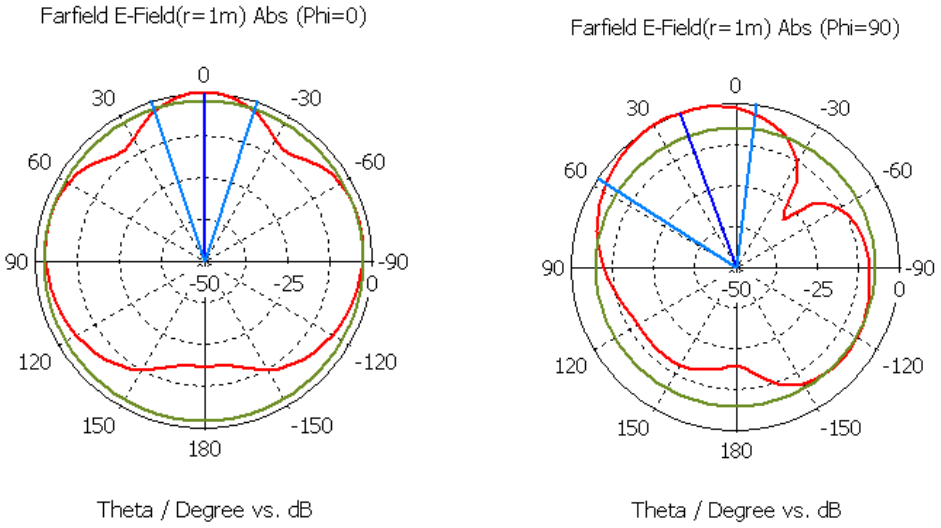

Fig. 3.46. E and H plane radiation pattern at 7.74 GHz

The radiation patterns are also depicted in figure 3.45 and 3.46 for both the resonant frequencies. The H-plane pattern is more directive in nature as 3dB beamwidth is close to 60^{o} for both the frequencies and the direction of maximum radiation is inclined by 30^{o} normal to the patch while E-plane patterns are somewhat omni-directional though both patterns resembles like patterns for dipole antenna. As antenna is operating at high frequency and presenting narrow bandwidth, the modifications needs to be done in the geometry.

3.4.1 Square patch antenna with reduced ground

The first step of modification involves truncating the ground plane to reduce its length as shown in figure 3.47. The effect of varying the ground dimension on reflection coefficient as a function of frequency is shown in figure 3.48. The ground plane of antenna is modified in steps and it is realized that on making ground size of 8×40 mm, antenna resonates at a single frequency (3.984 GHz) within the desired range (2 GHz to 6 GHz). The obtained bandwidth with respect to central frequency 3.984 GHz is 2.35 GHz as shown in figure 3.49.

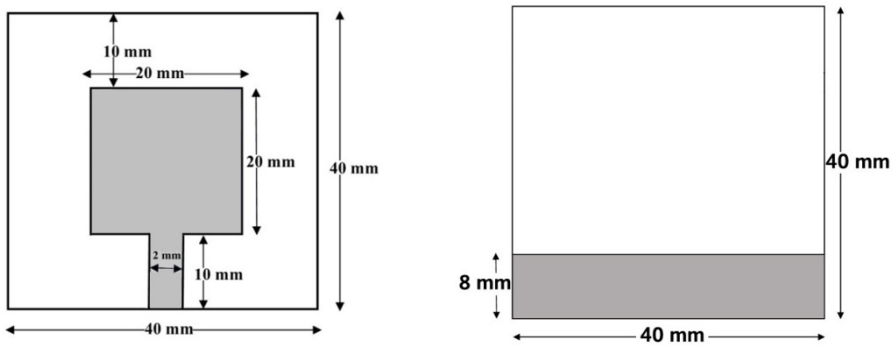

Fig. 3.47. Top and Bottom view of ground truncated geometry

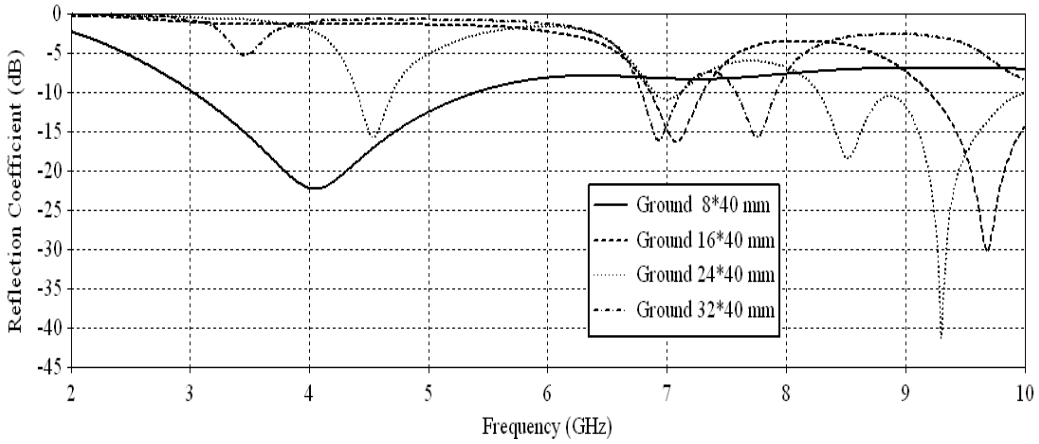

Fig. 3.48. Effect of varying ground dimensions on reflection coefficient as a function of frequency

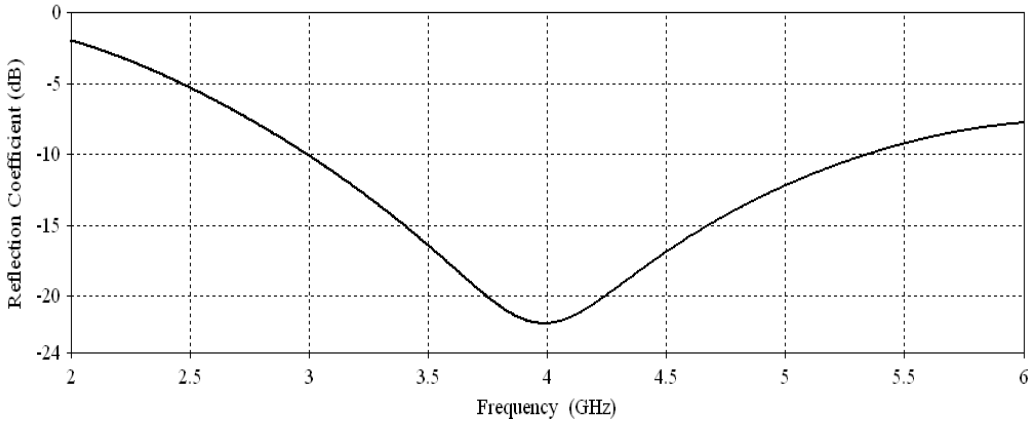

Fig. 3.49. Variation of reflection coefficient (S_{11}) with frequency for square geometry with ground truncation

This simulated VSWR for resonant frequency is 1.17 as observed from figure 3.50. The gain of the antenna as shown in figure 3.51 is almost flat and is 2.38 dBi at resonant frequency.

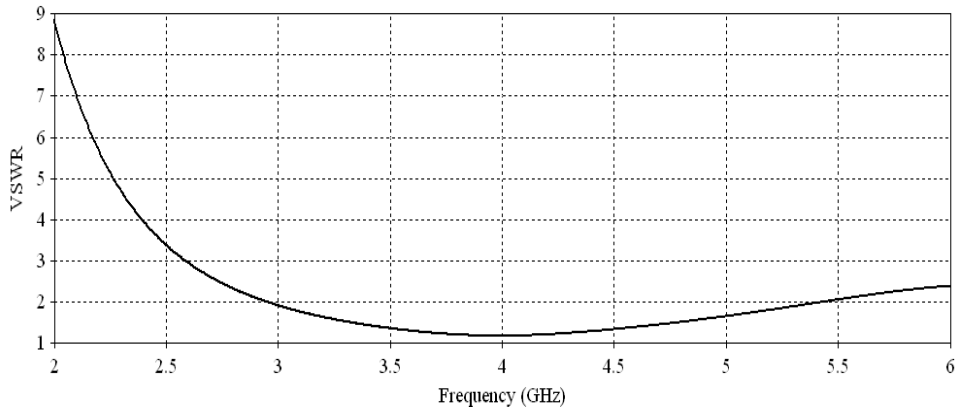

Fig. 3.50. Variation of VSWR with frequency for square geometry with ground truncation

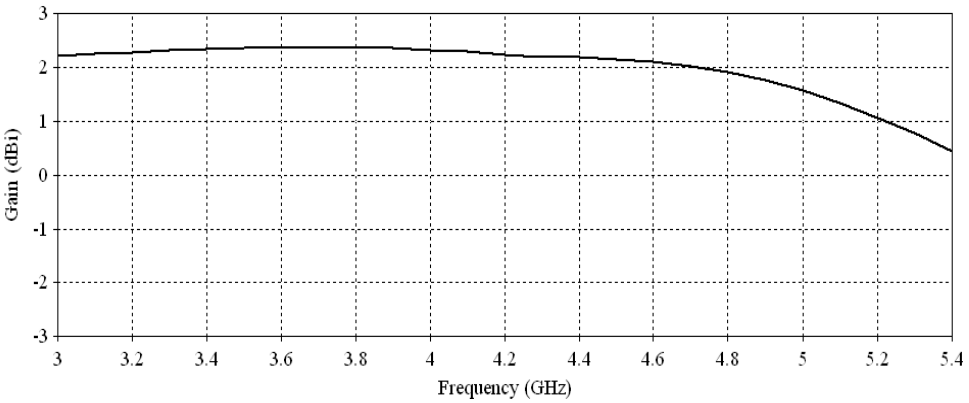

Fig. 3.51. Variation of gain as a function of frequency for square geometry with ground truncation

The radiation pattern at the resonant frequency is symmetric in nature with maximum radiation normal to the patch geometry as shown in figure 3.52.

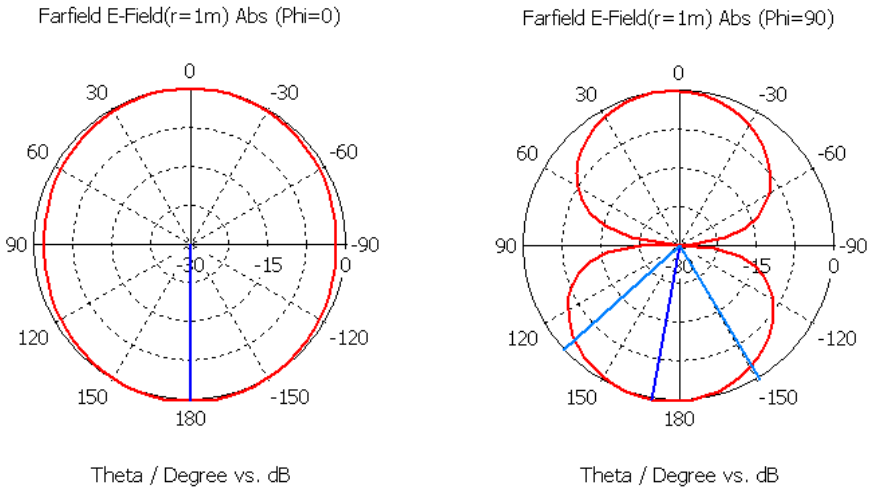

Fig. 3.52. E and H plane radiation pattern at 3.984 GHz

The square antenna geometry with partial ground is providing broadband response but the operating frequency range is covering only median band of Wi-Max, so the present geometry will be amended to make it suitable for dual band.

3.4.2 Square patch antenna with circular slot and reduced ground

In the next step of modification, a circular slot having radius '*r*' is applied in the patch and this radius is optimized to achieve best performance from antenna. The effect of varying circular slot radius '*r*' on reflection coefficient as a function of frequency is shown in figure 3.53.

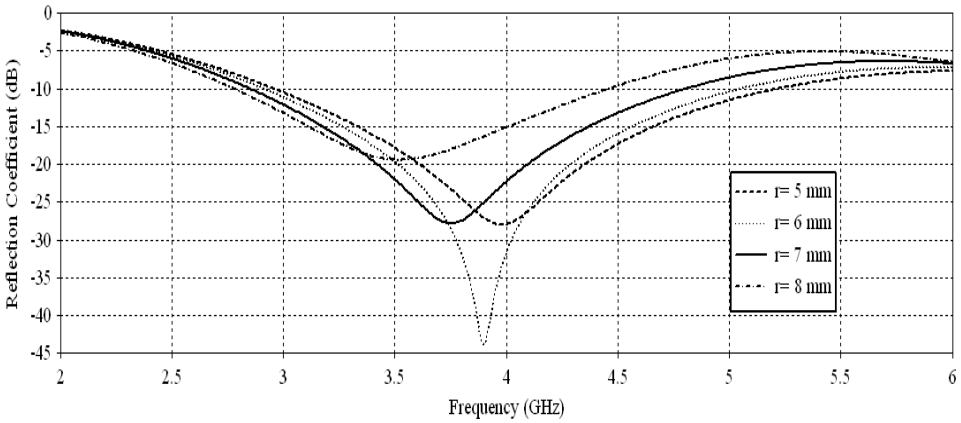

Fig. 3.53. Effect of varying circular slot radius in patch on reflection coefficient as a function of frequency

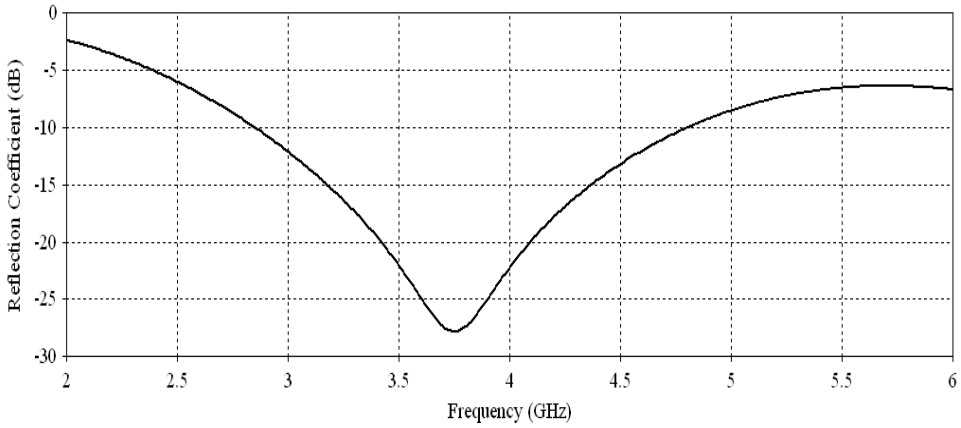

Fig. 3.54. Variation of reflection coefficient (S_{11}) with frequency for square patch with circular slot and reduced ground

It is realized that on making 'r' = 7mm, the design is still operating at single resonant frequency of 3.70 GHz. The achieved bandwidth with respect to central frequency 3.70 GHz is 1.94 GHz as shown in figure 3.54, and simulated VSWR at

resonant frequency is 1.06 from figure 3.55 also gain is improved a little as seen in figure 3.56 and obtained radiation patterns are symmetric in nature as shown in figure 3.57.

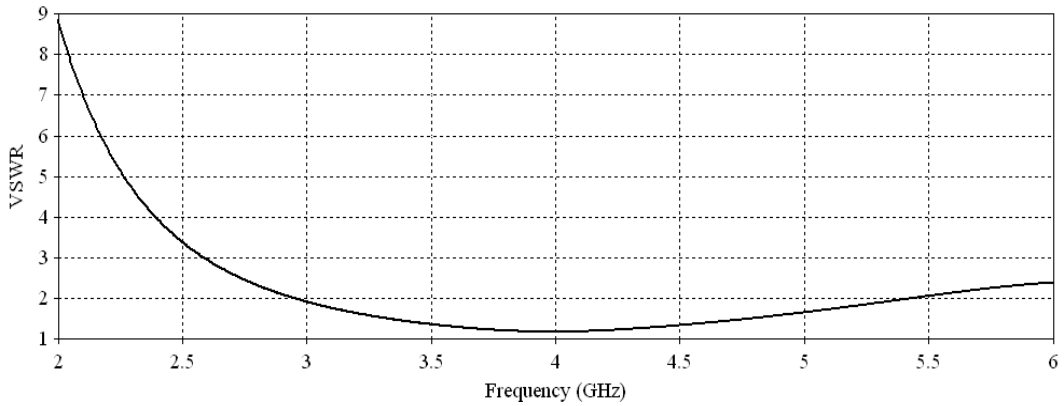

Fig. 3.55. Variation of VSWR with frequency for square patch with circular slot and reduced ground

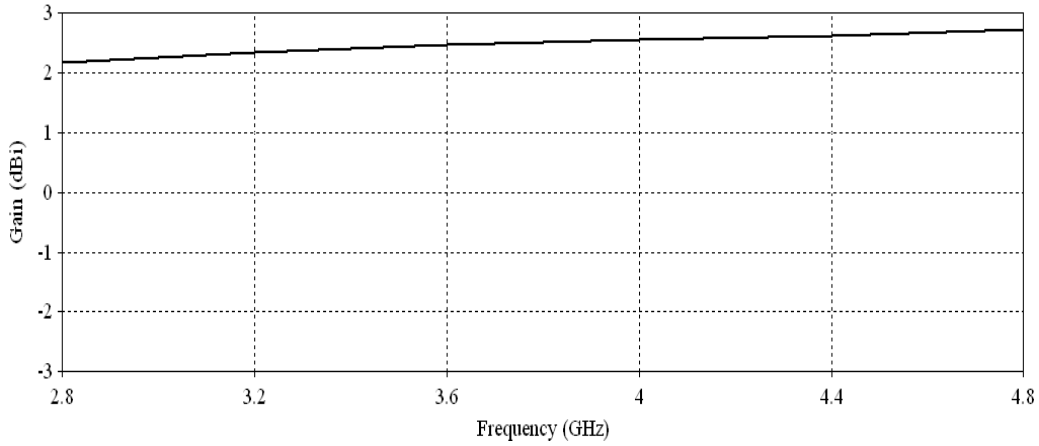

Fig. 3.56. Variation of gain as a function of frequency for square patch with circular slot and reduced ground

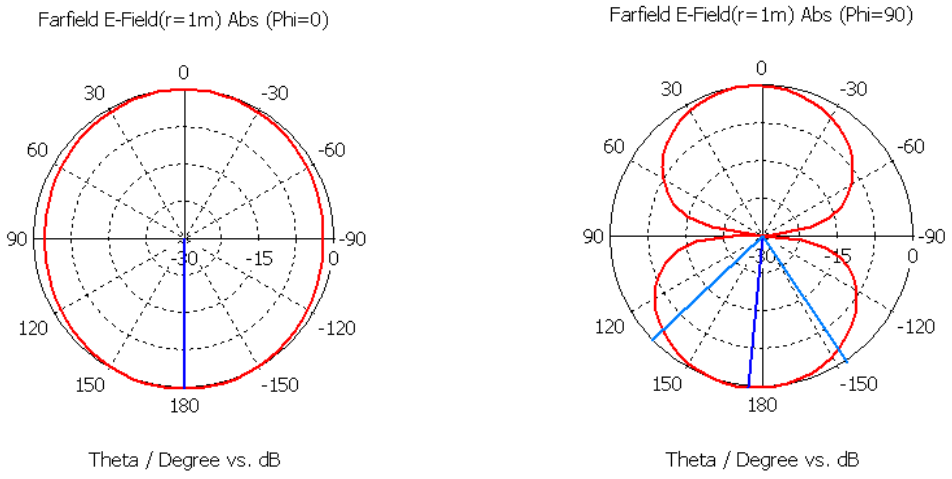

Fig. 3.57. E and H plane radiation pattern at 3.70 GHz

3.4.3 Modified square patch antenna with defected ground

The geometry described above is further modified by adding a strip of length L=3mm and width W=2mm in the ground plane as shown in figure 3.58. The effect of variation of strip length on reflection coefficient as a function of frequency is shown in figure 3.59 and effect of variation in strip position on reflection coefficient as a function of frequency is shown in figure 3.60.

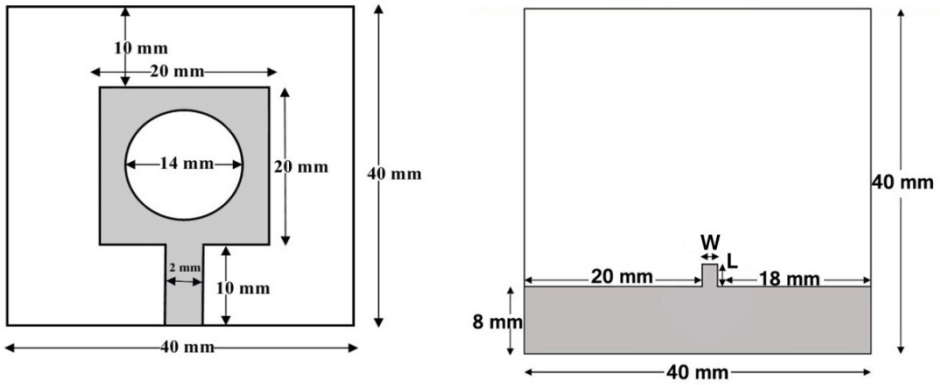

Fig. 3.58. (a) Top and back view of the modified square patch with defected ground

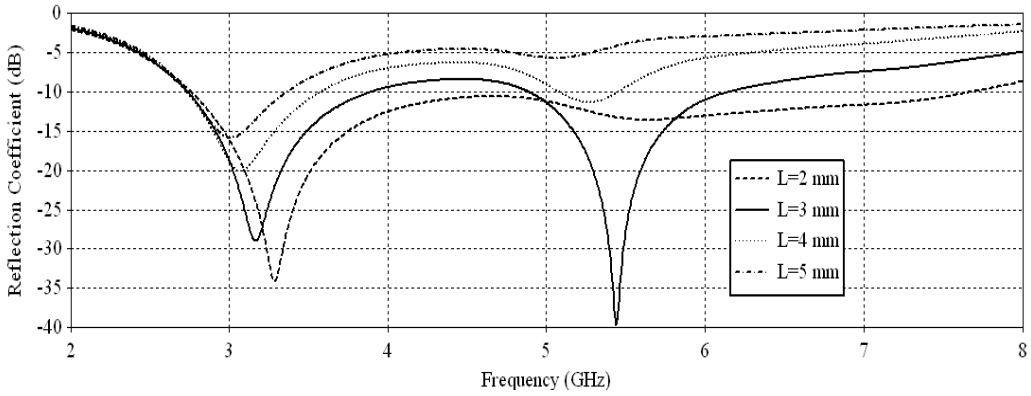

Fig. 3.59. Effect of varying strip length at ground on reflection coefficient as a function of frequency

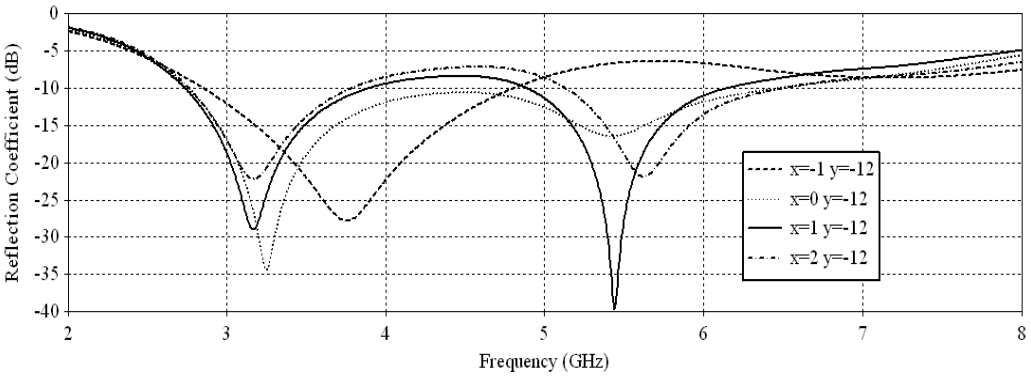

Fig. 3.60. Effect of varying strip position on reflection coefficient as a function of frequency

As observed from fig. 3.59 and 3.60 that on making L= 3 mm and W=2mm and adjusting the position of the strip, an additional mode operating at a higher frequency (5.43 GHz) gets excited. The geometry is now resonating at two frequencies in different bands and offering wide bandwidth in each band. The geometry is fabricated and the results are presented in the next section.

3.4.4 Performance of modified square patch antenna with defected ground plane

The prototype of the proposed antenna is fabricated as shown in figure 3.61 and tested in free space by using available facilities.

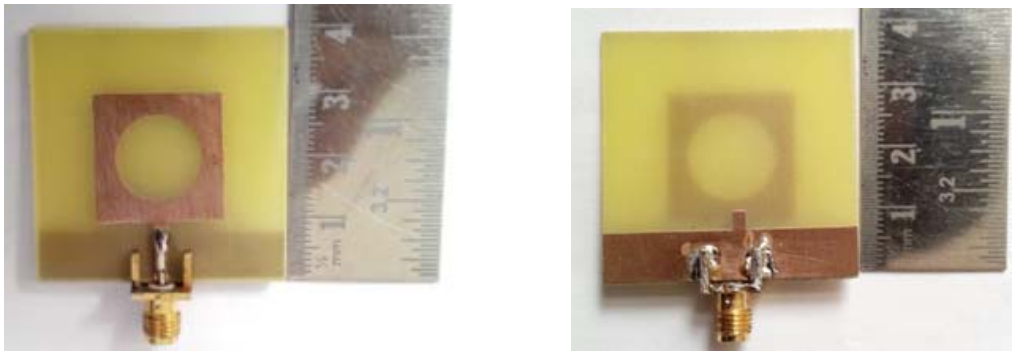

Fig. 3.61. (a) Top view designed geometry (b) Back view of designed geometry

The simulated resonant frequencies of proposed geometry are 3.19 GHz and 5.43 GHz shown in figure 3.62 while the measured resonant frequencies of this geometry as shown in figure 3.63 are 3.56 GHz and 5.40 GHz.

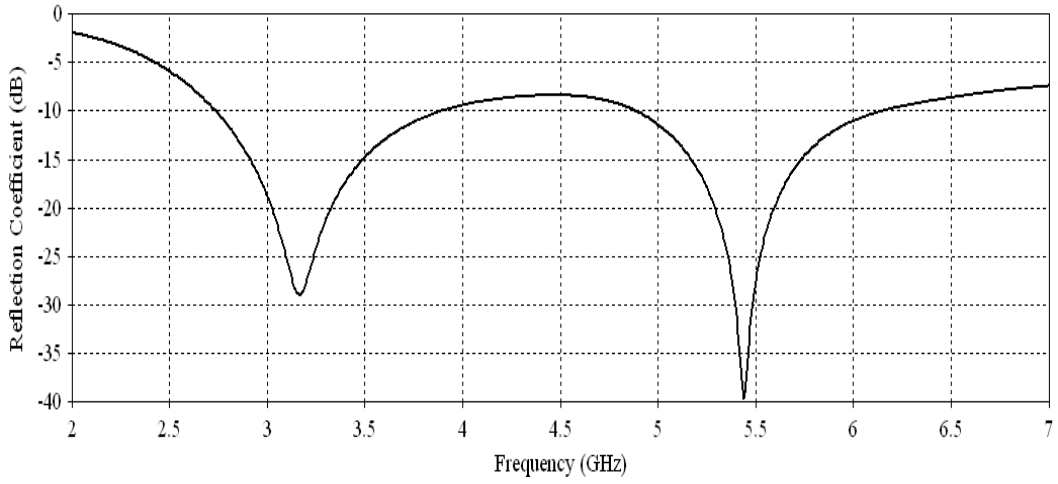

Fig. 3.62. Variation of simulated reflection coefficient (S_{11}) as a function of frequency for modified square patch antenna with defected ground

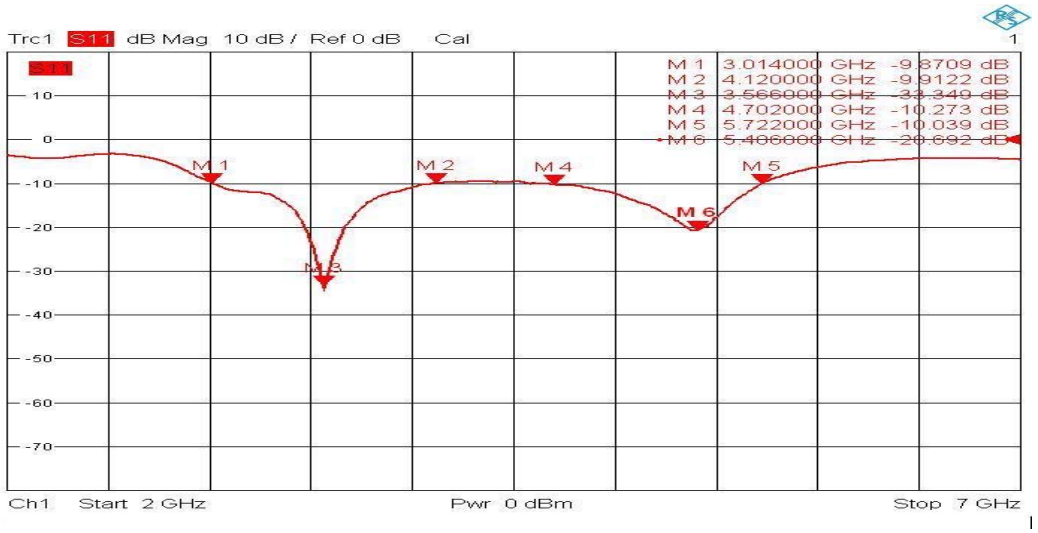

Fig. 3.63. Measured reflection coefficient with frequency for modified square patch antenna with defected ground

It may be observed that the measured impedance bandwidths of antenna are 1.05 GHz (29.49%) and 1.06 GHz (19.62%) with respect to respective central frequencies. The simulated VSWR at two resonating frequencies is 1.07 and 1.006 as shown in figure 3.64 while measured VSWR values at two resonating frequencies are approaching to unity (1.06 and 1.20 respectively) as shown in figure 3.65 which signify that antenna geometry has excellent match with the microstrip feed line.

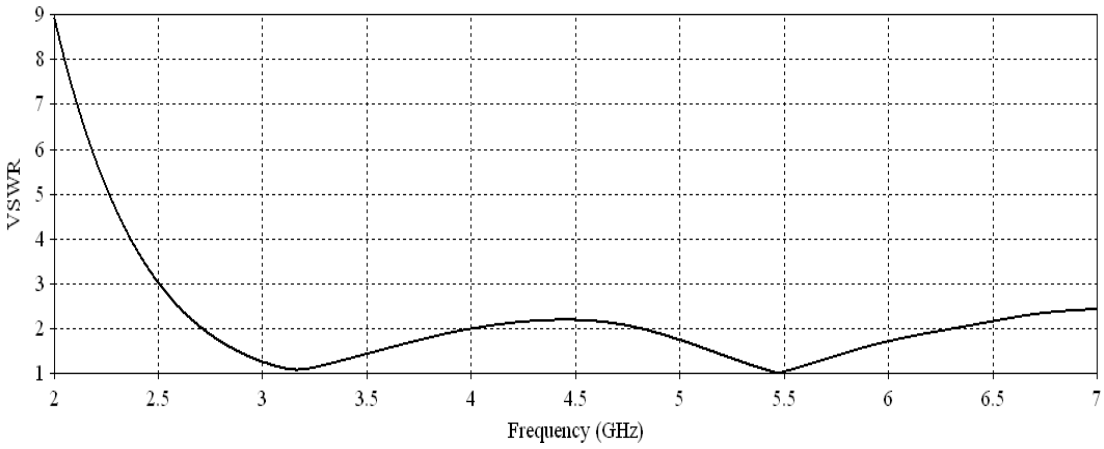

Fig. 3.64. Variation of VSWR with frequency for modified square patch antenna with defected ground

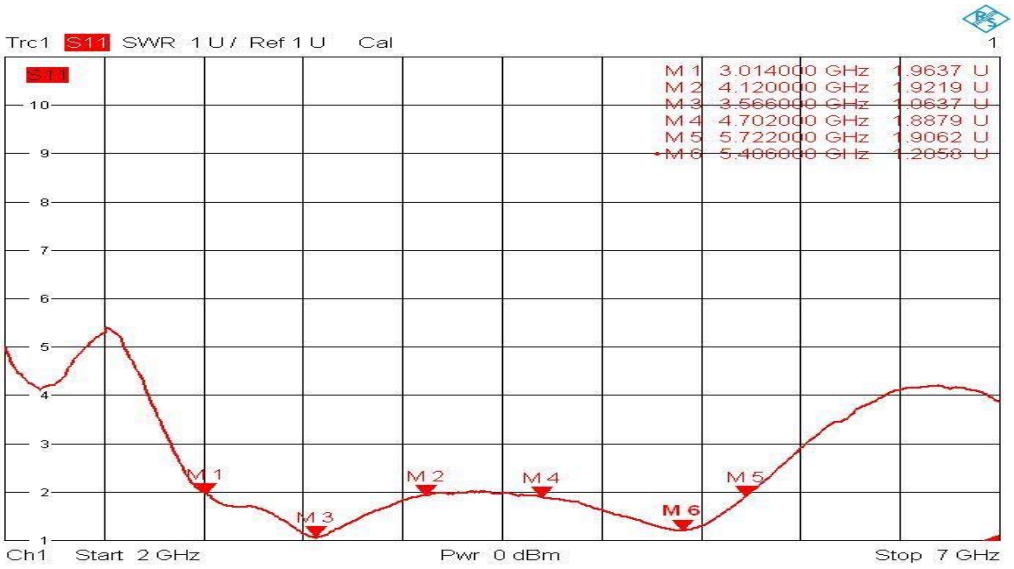

Fig. 3.65. Variation of measured VSWR with frequency for modified square patch antenna with defected ground

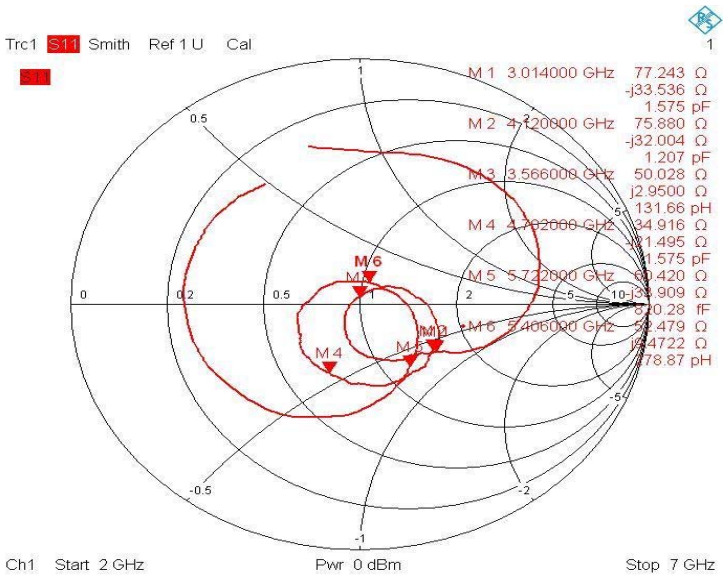

Fig. 3.66. Measured input impedance modified for square patch antenna with defected ground

The measured variation of input impedance of antenna with frequency for proposed geometry is shown in figure 3.66. The values of input impedances at two resonance frequencies are (50.02+ j2.95) ohm and (52.47+j9.47) ohm. This again confirms excellent matching between antenna and 50 ohm impedance of feed network.

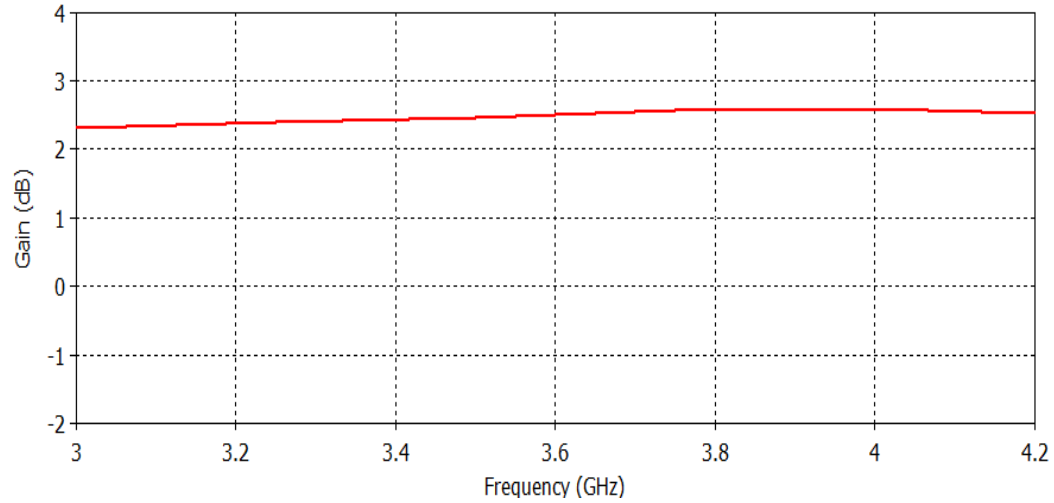

Fig. 3.67. Variation of gain as a function of frequency for lower band of modified square patch antenna with defected ground

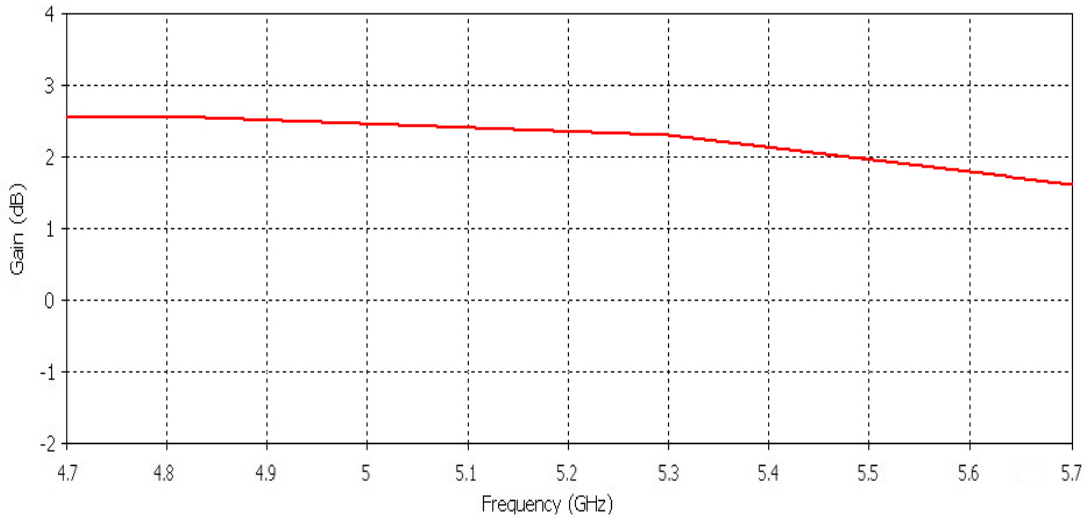

Fig. 3.68. Variation of gain as a function of frequency for upper band of modified square patch antenna with defected ground

The variation in gain of proposed geometry as a function of frequency is shown in figure 3.65 and 3.66. The gain response is almost flat in the lower band and higher band of antenna and is close to 2.5 dBi in the operating bandwidth.

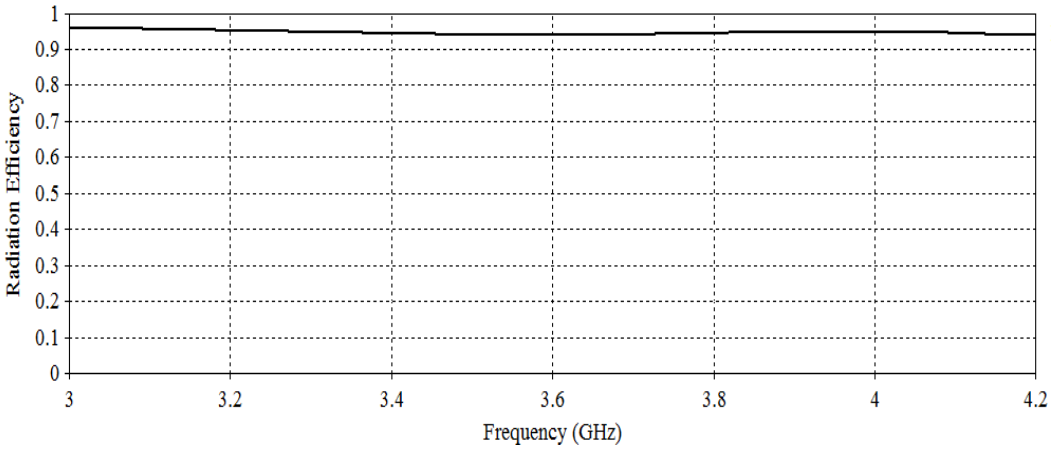

Fig. 3.69. Variation of gain as a function of frequency for lower band of modified square patch antenna with defected ground

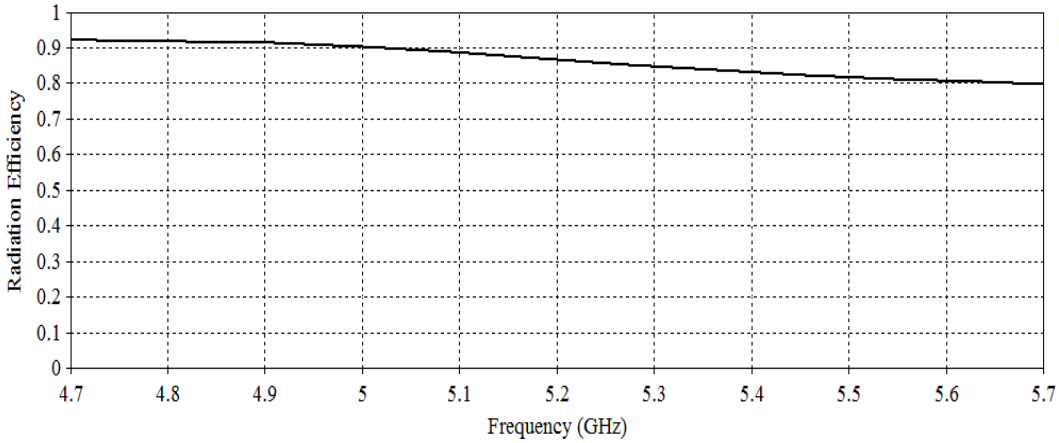

Fig. 3.70. Variation of gain as a function of frequency for upper band of modified square patch antenna with defected ground

The variation in radiation efficiency of proposed geometry as a function of frequency is shown in figure 3.69 and 3.70. The radiation efficiency is uniform in nature but the lower band has slightly higher radiation efficiency than upper band.

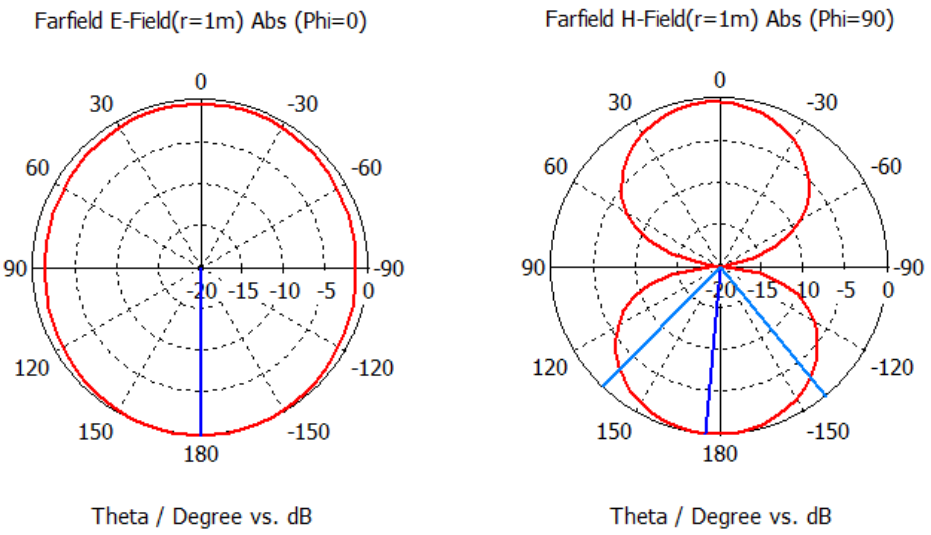

Fig. 3.71. Simulated E and H radiation patterns at 3.56 GHz

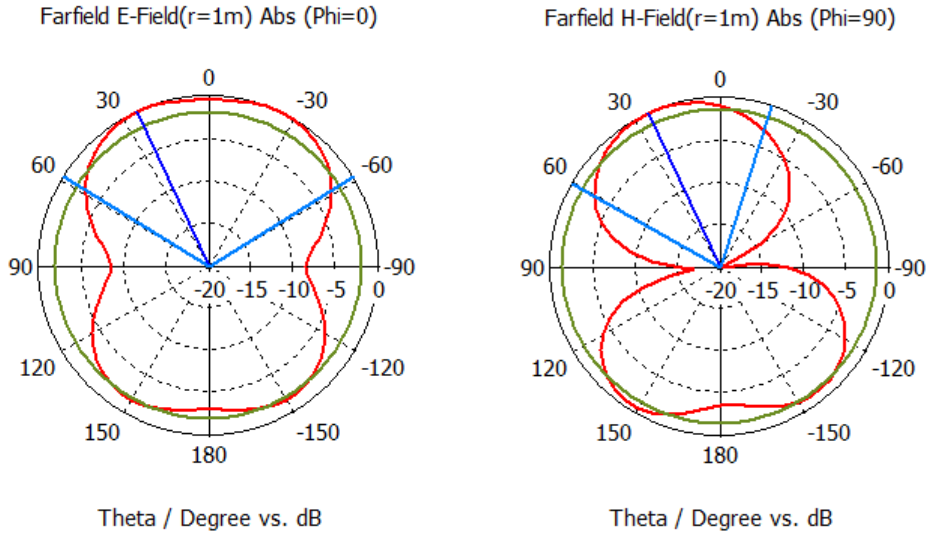

Fig. 3.72. Simulated E and H radiation patterns at 5.40 GHz

The simulated radiation patterns at two resonant frequencies are shown in fig. 3.71 and 3.72. The E-plane pattern at lower resonant frequency it is omnidirectional in nature while at higher resonant frequency it is more directive with 3 dB beamwidth of 100^{o}. The H-plane patterns are nearly similar for both the resonant frequencies with slight tilting of 15^{0} for higher frequency.

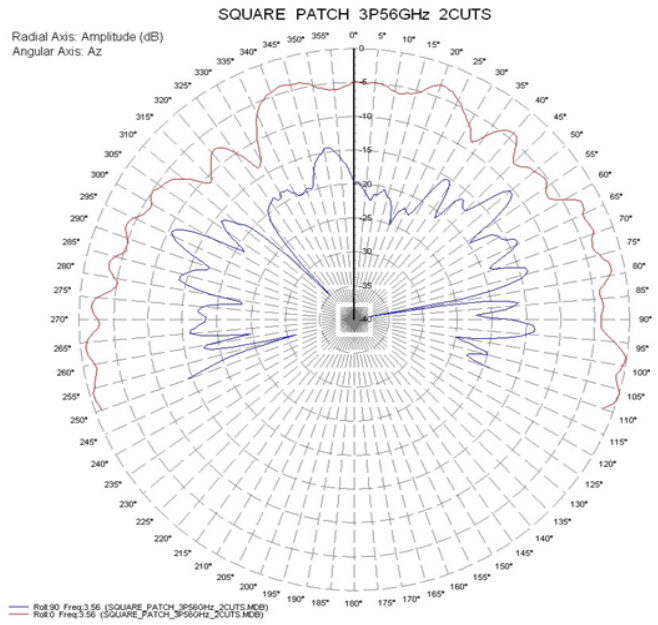

Fig. 3.73. Measured E and H plane radiation pattern at 3.56 GHz

The measured variations of two dimensional radiation patterns at two resonant frequencies are shown in figures 3.73 and 3.74 respectively. At lower resonance frequency the E-plane pattern has maximum radiation not normal to patch geometry but inclined at an angle of 95^0 and H-plane pattern has maximum radiation inclined at an angle of 50^0 normal to patch geometry.

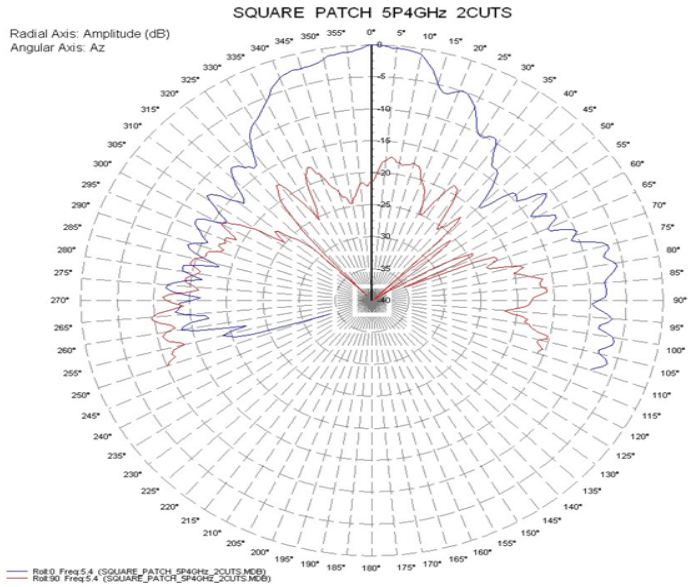

Fig. 3.74. Measured E and H plane radiation pattern at 5.40 GHz

At higher frequency E-plane pattern is directive in nature with 3 dB beamwidth of 40^o and direction of maximum radiation normal to patch geometry ($\theta = 0^o$) and the H plane pattern also has directive pattern with maximum radiation inclined at 30^0 normal to the patch geometry.

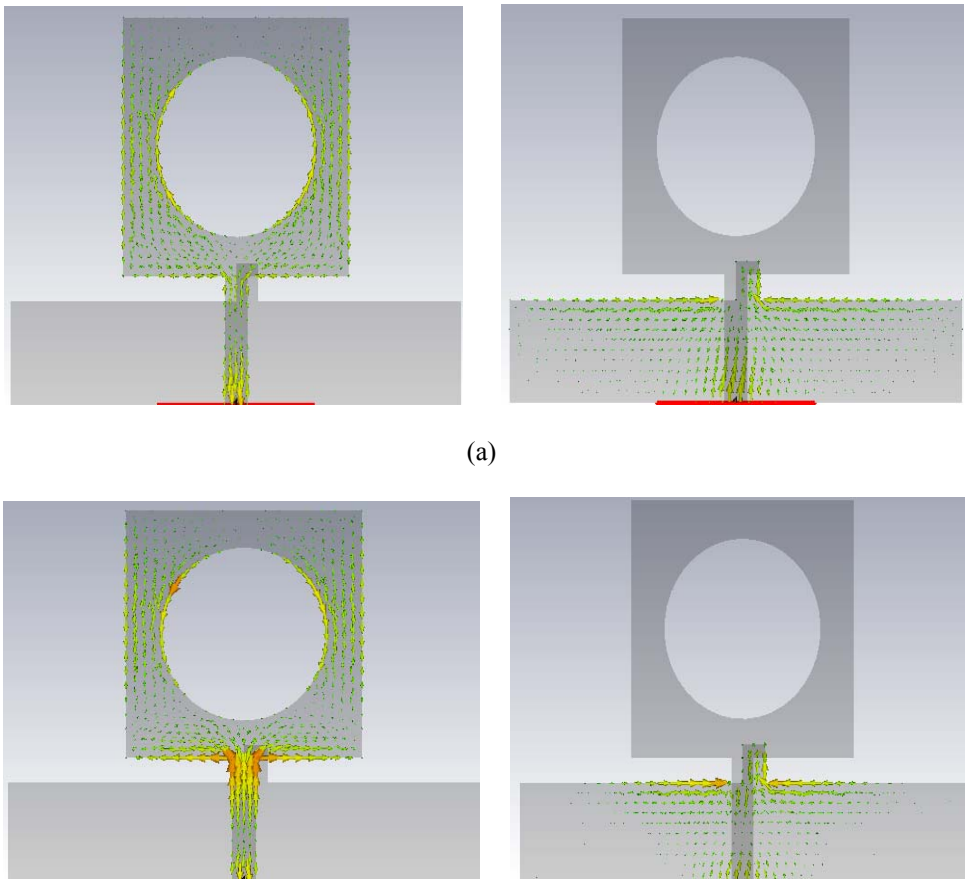

(a)

(b)

Fig. 3.75. Surface current distributions in patch and ground at resonant frequencies (a) 3.56 GHz and (b) 5.40 GHz.

The surface current distributions at the two resonant frequencies are graphically shown in figure 3.75. They further confirm the dual-band behavior of the proposed geometry. At 3.56 GHz, the simulated result in Fig. 3.75 (a) shows that the current was mainly on edges which contributed to resonance. While at 5.40 GHz, Fig. 3.75(b) shows that the current on the strip was quite large, contributing to resonance.

A comparison of existing antennas from the literature with proposed geometries is provided in the table 3.1

TABLE 3.1. COMPARISONS OF PROPOSED ANTENNAS WITH OTHER REPORTED ANTENNAS

Reference	Antenna Size (in mm)	Frequency	Bandwidth	Gain (dBi)	Applications
152	40×25	3.5 GHz 5.8 GHz	200 MHz 200 MHz	4.25 6.4	WIMAX/WLAN
154	40×30	3.67GHz 5.22GHz	600 MHz 1040 MHz	3.23 5.93	Wi-Fi/WIMAX
155	40×40	1.227 GHz 1.575 GHz	80 MHz 45 MHz	3.9 -0.5	GPS wireless receivers
Modified Pentagonal Geometry	40×40	2.72 GHz 5.75 GHz	742 MHz 780 MHz	3 3	WIMAX WLAN
Modified Square Geometry	40×40	3.56 GHz 5.40 GHz	1.05 GHz 1.06 GHz	2.5 2.5	WIMAX

3.5 Summary

In this chapter two antenna geometries for dual band operation are proposed. The first section describes a design consisting of modified pentagonal microstrip antenna with defected ground. A pentagonal slot is inserted in the pentagonal patch and a rectangular strip is added in the ground plane. The performance of this antenna is again simulated by optimizing the length, width and location of strip and finally a prototype antenna is developed and tested. The geometry operates at two resonant frequencies (2.5 GHz and 5.58 GHz) and offers impedance bandwidth of 864 MHz and 554 MHz in the two bands of interest. The proposed antenna covers the lower band and upper band allocated for Wi-Max and WLAN communication systems. In the second design a dual band microstrip patch antenna is proposed that employs a square patch with circular slot along with a T-shaped defective ground plane. It is found that on introducing circular slot in the patch and truncating ground plane, the impedance bandwidth of antenna improves considerably. By introducing a protruding rectangular stub in the ground plane an additional mode operating at a higher frequency gets excited and the antenna resonates at two different frequencies. This antenna offers the impedance bandwidth of 1.05 GHz (29.49%) and 1.06 GHz (19.62%) in the two bands. Designed antennas are compact and single layered, therefore could be useful for Wi- Max communication systems.

Chapter 4

Compact microstrip patch antennas with finite ground plane for broadband performance

4.1 Introduction

In the last few years, the microstrip antenna have been in tremendous use for applications such as radars, satellite, Radio frequency identifications (RFIDs), telemetry, aerospace etc. The microstrip antennas in their conventional form have certain limitations like narrow bandwidth, polarization impurity and large size for better performance. Primarily, the microstrip antennas are required to have high gain, compact size, broad bandwidth, flexibility, easy to be fabricated, etc. In particular, bandwidths, polarization, radiation patterns are considered the significant factors that influence the application of antennas in modern wireless communication systems. Microstrip antenna for applications such as mobile and other portable devices essentially be smaller in physical dimension so that they can be effortlessly implanted in devices and broadband in nature. The bandwidth enhancement in compact antennas has turn out to be an extremely critical design issue. The professionals from academic world and industry have been working in this direction for development of a variety of techniques to development small broadband antenna designs for different frequency bands. Recently, much progress has been made to broaden the bandwidths of microstrip antennas, to cover a wide frequency range for modern wireless communication [109][156-159]. Several ways to obtain wide bandwidth have been already mentioned in the literature like parasitic elements, aperture coupled, use of slots and active devices, etc[160-164].

In this chapter two compact antenna geometries for broadband operation are described. The main objectives of this work are that the basic structures of triangular and circular antenna are modified in steps with finite ground to achieve broadband operation applications in lower band of UWB (3.1 GHz to 4.85 GHz) and C Band (4 GHz to 8 GHz). The bandwidth is aimed to be more than 50% with uniform gain and other radiation characteristics.

4.2 Work done in past on broadband microstrip patch antenna

A novel E-shaped microstrip patch antenna with U-shaped slot was proposed to obtain an impedance bandwidth of about 33.8% in [165]. The introduction of washer not only further enhanced the bandwidth to 40% but also reduced the cross polarization. Antenna based on the Yagi–Uda dipole array provided 48% bandwidth, cross polarization of less than 15 dB, 12 dB front-to-back ratio and 3–5 dB gain was presented [166]. Finite-difference time-domain method was used in simulation and measured results are in good match with it. Due to its compact size and low mutual coupling characteristics it can be used for radar systems and millimeter-wave imaging arrays. A broadband microstrip antenna array of 20×20 mm for LMDS band and providing high gain was reported [167]. It has a rectangular patch antenna with parasitic patches and offers bandwidth of 15%. Recently, it was investigated that a half U-slot patch antenna and half E-shaped antenna maintain similar wide-band behavior while their physical sizes were decrease to half [168]. Other radiation parameters like radiation pattern and efficiency were also close to full size structures. An antenna having stepped patch with microstripline feed, dielectric resonator and an intermediate substrate was proposed. The antenna offers bandwidth of 50% around the center frequency of 10.16 GHz, and stable radiation patterns [169]. A novel ψ-shape microstrip patch antenna that provides wide-impedance bandwidth of 54% with good radiation performance was presented [170]. A foam substrate was used in addition to thin dielectric layer substrate for bandwidth enhancement.

There is a need of efficient wideband design with compact size. One of the techniques to achieve compact size is using finite ground plane. Since the antenna is usually used in small equipments or devices like mobile handset where conventional patch antennas are much larger to fit into. In previous studies it was found that the ground plane has strong influence on the radiation parameters of patch antenna [171-172]. Usually the requirement for a compact antenna is related with reducing ground plane to the extent that an antenna characteristic becomes strongly reliant on the ground plane shape and dimension. It is already investigated in past that the grounded dielectric excites a finite number of surface wave modes whose direction

of propagation is along the direction of air-dielectric interface [173]. The effects of change in finite ground plane dimensions on antenna impedance have been investigated and several techniques to enhance bandwidth and achieve dual polarization are reported [174-175]. The effect of different shapes of ground structure on polarization and cross polarization radiation was also investigated in past [176-177].

A monopole broadband antenna with stepped cut at the four corners was reported [178]. The proposed geometry has bandwidth from 900 MHz to 2.6 GHz and can be useful for GSM (900 MHz and 1.5 GHz), Wi-Fi (2.4 GHz) and LTE (2.6 GHz) applications. The methodology of the proposed antenna design has been presented in six stages. The simulated gain was varying from 2.6–4.7 dBi in the operating frequency range. The antenna prototype has been fabricated for all stages, and simulation results are experimentally verified with measurement.

A wideband antenna with total size 97 mm×60 mm, consisting of two symmetric elements for mobile communication was presented [179]. It provides impedance bandwidth of 1.14 GHz (1.61–2.75 GHz), and mutual coupling is lower than 15 dB. It covers the GSM1800, GSM1900, UMTS, LTE2300, LTE2500, and 2.4-GHz WLAN bands for the 2G/3G/4G mobile terminals. The radiation patterns for fabricated prototype were measured, and diversity performances also evaluated.

In this chapter two compact antenna geometries for broadband operation are presented. In the first section of this chapter design and performance of a compact triangular patch antenna with slotted ground plane is analyzed in steps and presented in systematic manner. A measured bandwidth of 60.3% in addition to enhanced radiation performance is obtained from fabricated prototype for possible application in lower band of UWB communication systems. In the second section of this chapter circular patch antenna is modified to achieve broadband performance. Initially we have analyzed the circular microstrip patch antenna and amendments are done in the geometry in stepwise manner. The final geometry with proposed modification provides bandwidth of 4.04-7.28 GHz (60.3%) which falls in the C-band region. The properties such as reflection coefficient, input impedance and VSWR are simulated

and experimentally measured. Parametric analysis of the design parameters of proposed geometries has been done and optimized for best results. The proposed antenna design is analyzed by simulation software CST microwave studio suit and tested in free space.

4.3 Analysis of conventional triangular patch antenna

The antenna geometry has finite ground plane and for its use in modern communication systems the dimension is limited to 30×30 mm as shown in figure 4.1. The initial design consists of, triangular microstrip patch antenna of height=10 mm and base= fed by a 50Ω microstrip line, which is printed on FR4 substrate, has a thickness of 1.59 mm and relative permittivity (ε_r) of 4.4, the geometry is simulated using finite element method based CST microwave studio.

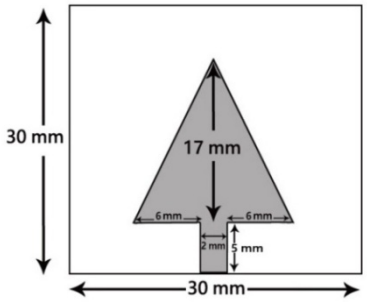

Fig. 4.1. Top view of triangular geometry

The reflection coefficient as a function of frequency for triangular patch antenna is shown in figure 4.2. The antenna is operating at single frequency of 8.77 GHz with very narrow bandwidth. The VSWR variation as a function of frequency provided by antenna is shown in fig. 4.3. For resonant frequency, the VSWR bears value lower than 2:1.

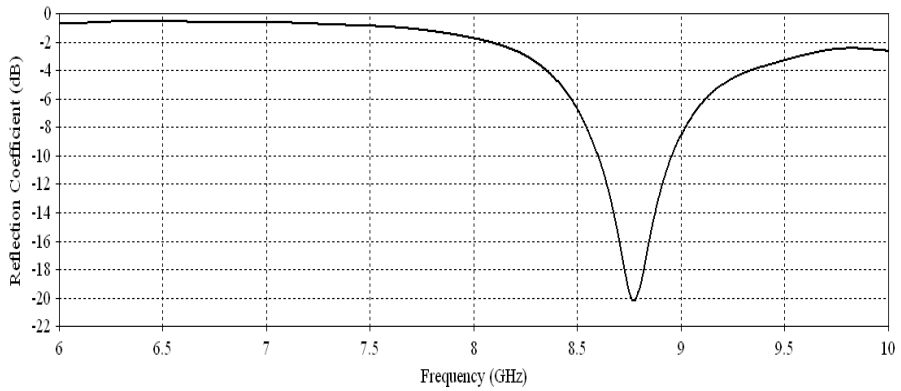

Fig. 4.2. Variation of reflection coefficient (S_{11}) as a function of frequency for triangular geometry

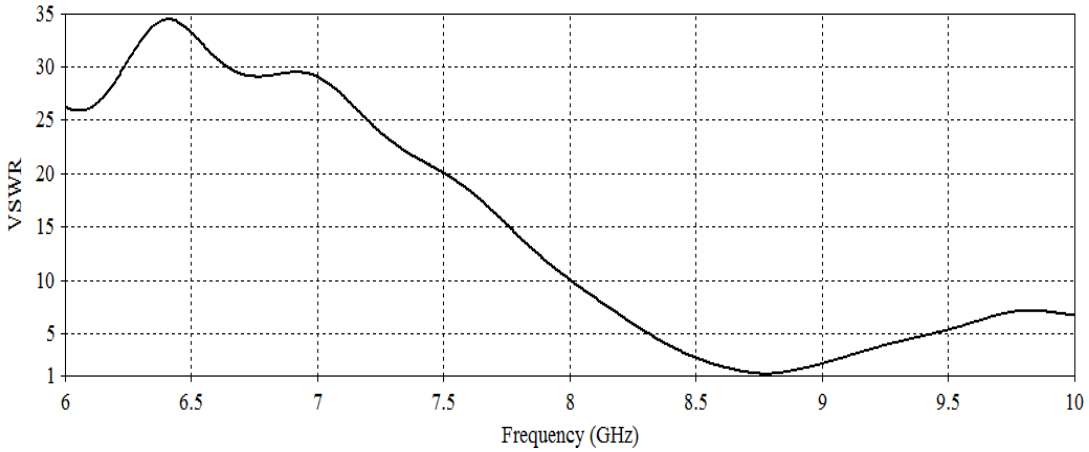

Fig. 4.3. Variation of VSWR as a function of frequency for triangular geometry

The simulated E and H plane elevation radiation pattern for resonant frequency is shown in figures 4.4. In E and H plane pattern the direction of maximum radiations is not normal to patch geometry but inclined at an angle 45^{o} from normal to patch geometry.

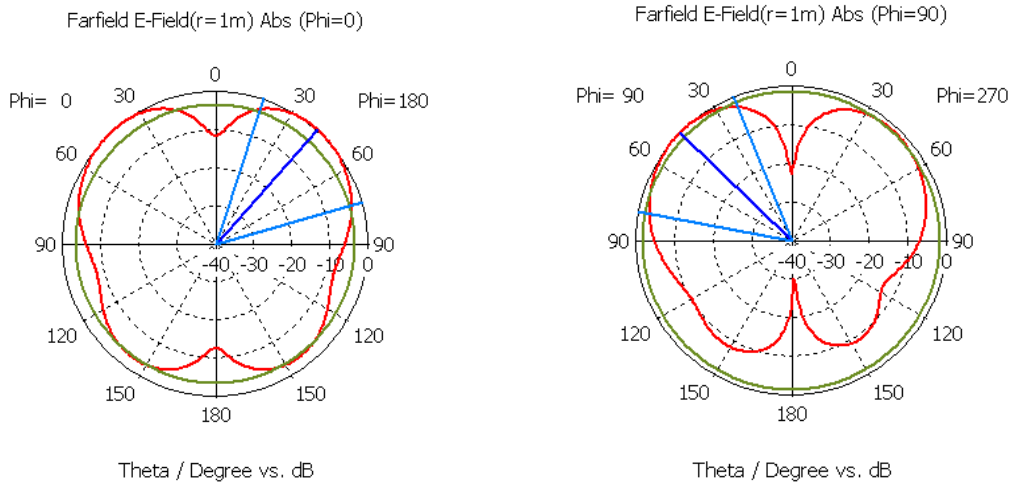

Fig. 4.4. E and H plane radiation pattern at 8.77 GHz

The antenna in present form has high resonant frequency and low bandwidth. In its present form this antenna is still not suitable for application in modern communication systems and some alteration needs to be done in the design.

4.3.1 Triangular patch antenna with slots in ground plane

The first step of modification involves etching slots in the ground plane as shown in figure 4.5. The effect of varying the slot shape and dimension on reflection coefficient as a function of frequency is shown in figure 4.6.

(a) Case 1 (b) Case 2 (c) Case 3

Fig. 4.5. Variation of shape and dimensions of the slot in the ground plane

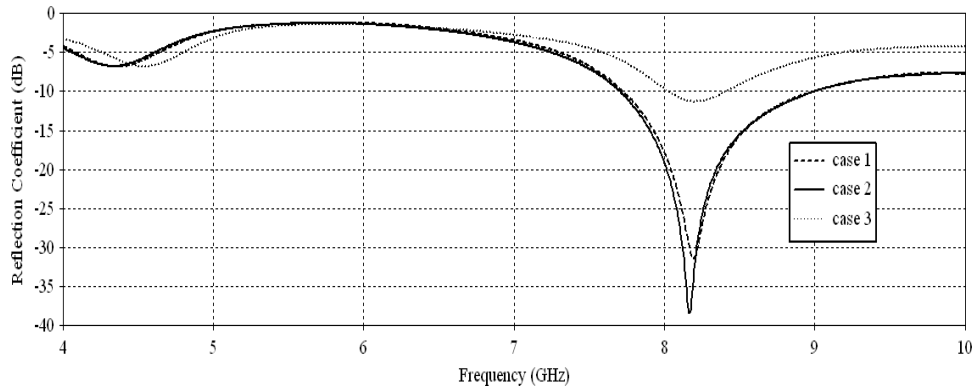

Fig. 4.6. Effect of varying slot dimensions on reflection coefficient as a function of frequency

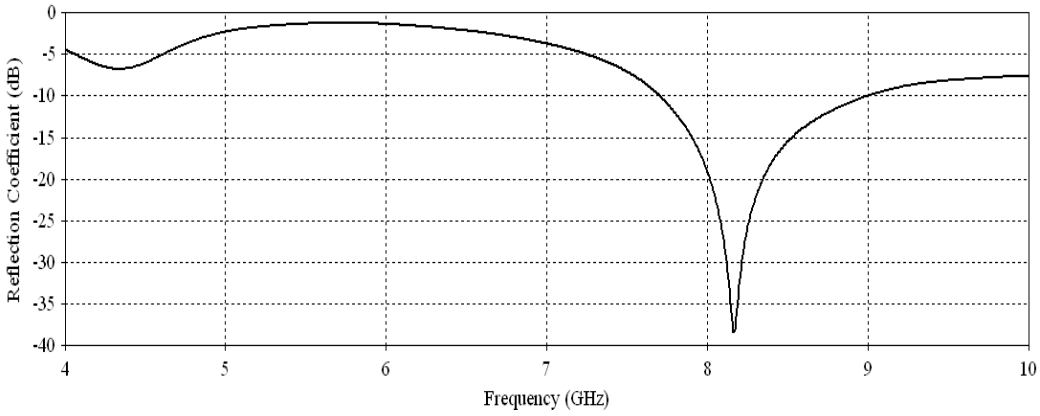

Fig. 4.7. Variation of reflection coefficient (S_{11}) as a function of frequency for triangular patch with slots in ground

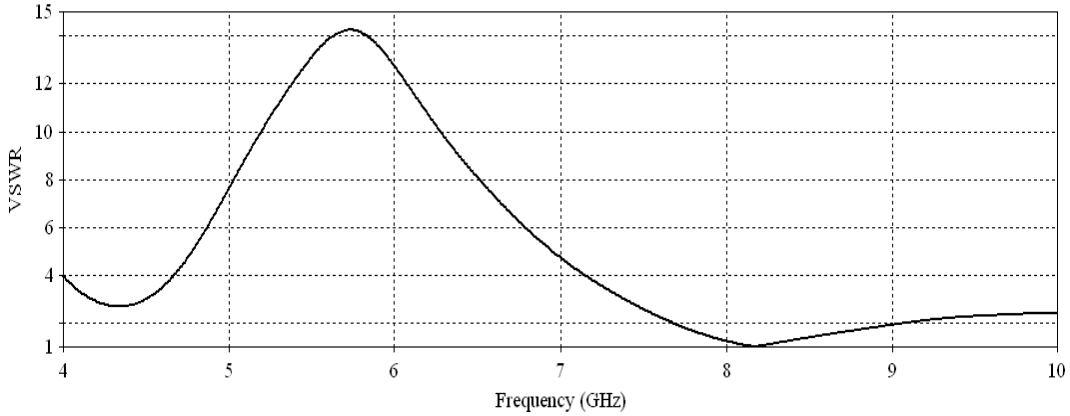

Fig. 4.8. Variation of VSWR as a function of frequency for triangular patch with slots in ground

It may be observed from results that case 2 has best radiation performance and in this case the antenna is resonating at frequency of 8.16 GHz at return loss of -38.39 dB and offers impedance bandwidth of 15.62% as shown in figure 4.7. The VSWR variation of considered structure with frequency is shown in figures 4.8. A very good matching between our designed antenna structure and the feed network is achieved. VSWR corresponding to resonant frequency is 1.02 which is close to desired value 1.0.

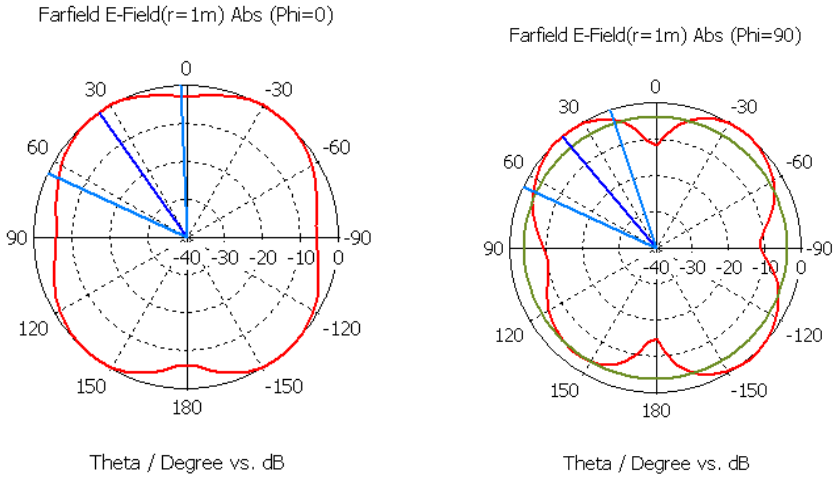

Fig. 4.9. E and H plane radiation pattern at 8.16 GHz

Figure 4.9 depicts the simulated E and H plane far- field radiation patterns of the triangular patch antenna with slots in the ground at resonant frequency. In E and H plane pattern the direction of maximum radiations is not normal to patch geometry but inclined at an angle 30^{o} from normal to patch geometry. The performance of

antenna reported in this section is improved to some extent. The patch and ground plane are further modified in next section to improve the performance.

4.3.2 Triangular patch antenna with asymmetric slot in ground plane

In the next step of work, the dimension of the patch antenna considered in previous section is reduced and the ground plane slot dimensions and shaped have been also optimized keeping the patch same, although extensive optimization of slot dimensions for various cases were done but only four best cases have been considered and variation of reflection coefficient with frequency for them is shown in figure 4.10.

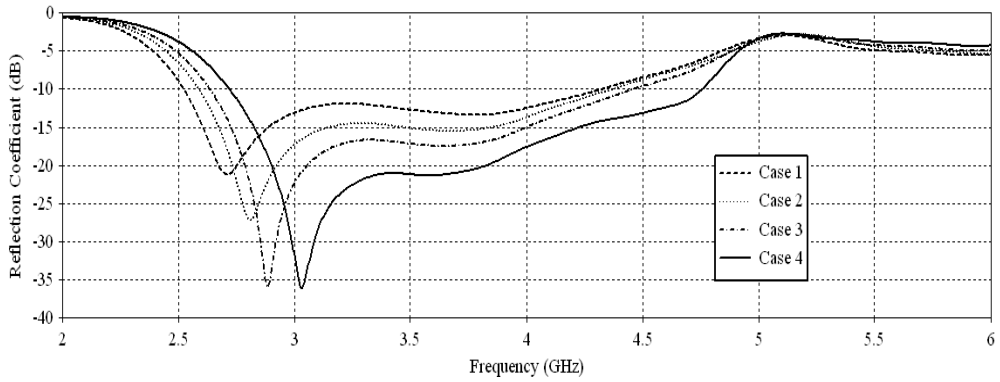

Fig. 4.10. Effect of varying ground slot dimensions on reflection coefficient as a function of frequency for four considered cases

The figure 4.10 clearly shows that case 4 has highest bandwidth among the all four cases and this is considered as the final geometry for fabrication. The final geometry with proposed modifications in ground is shown in figure 4.11

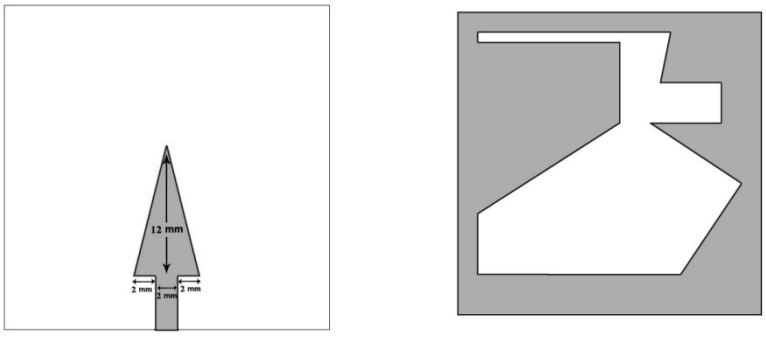

Fig. 4.11. Top and back view of the triangular patch with asymmetric slots in ground

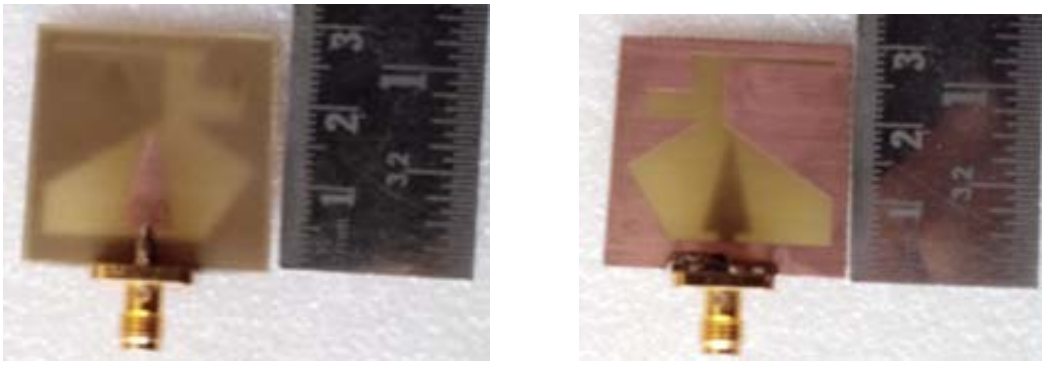

Fig. 4.12. Top and back view of the fabricated triangular patch with asymmetric slots in ground

The prototype of the proposed antenna is fabricated as shown in figure 4.12 and tested in free space by using available facilities. The variation of simulated and measured reflection coefficient with frequency for triangular patch antenna with asymmetric slots in ground is shown in figure 4.13 and 4.14 respectively.

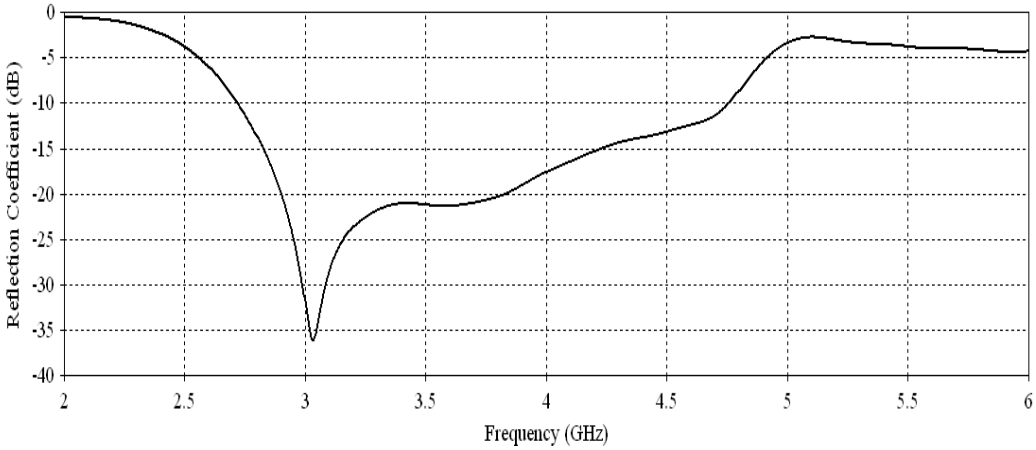

Fig. 4.13. Simulated reflection coefficient (S_{11}) as a function of frequency for triangular patch with asymmetric slots in ground

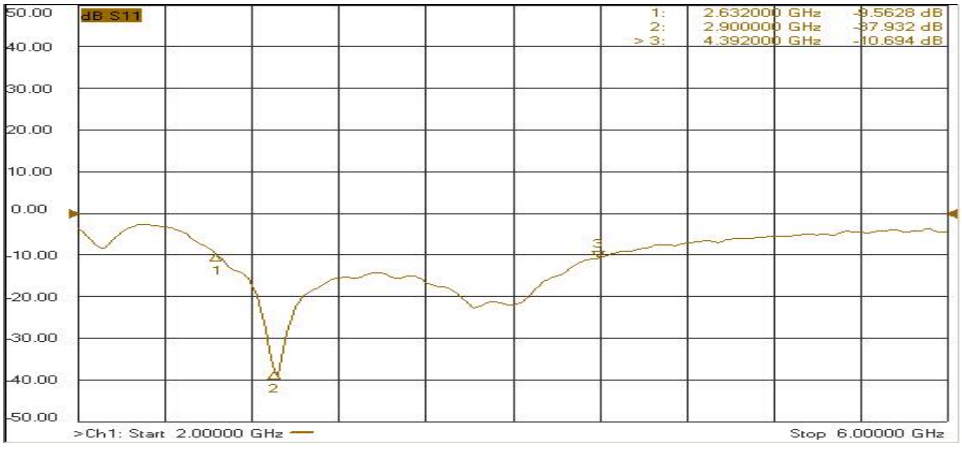

Fig. 4.14. Measured reflection coefficient (S_{11}) as a function of frequency for triangular patch with asymmetric slots in ground

The measured S_{11} variation of proposed antenna with frequency shows that proposed antenna now resonates at frequencies 2.90 GHz and presents an impedance bandwidth close to 60.3% with respect to central frequency of 2.90 GHz, while the simulated impedance bandwidth is close 67.06% with respect to central frequency 3.03 GHz. It is also observed from the measured result that the resonant frequency has shifted to little lower value. The simulated and measured variations of VSWR with frequency are shown are figure 4.15 and 4.16. In the obtained range of bandwidth the VSWR is less than desired 2:1 value which is an interesting feature of proposed antenna. This indicates that antenna is well match with the feed line in the entire frequency range of interest.

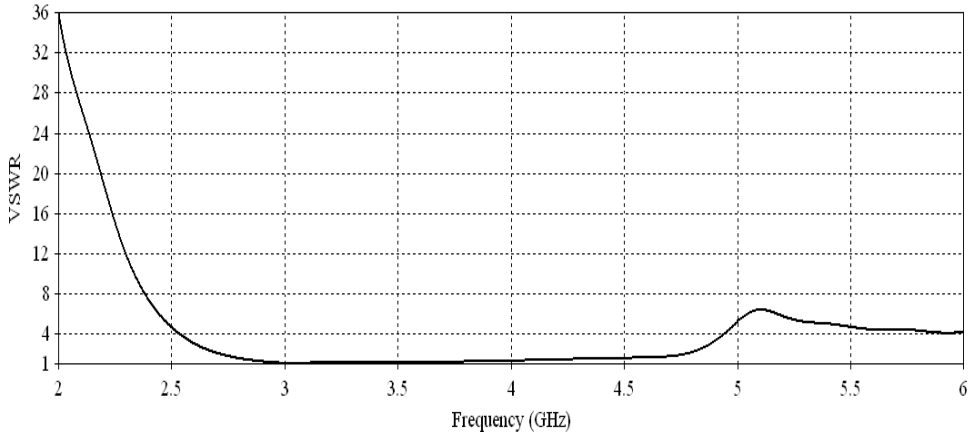

Fig. 4.15. Simulated VSWR as a function of frequency for triangular patch with asymmetric slots in ground

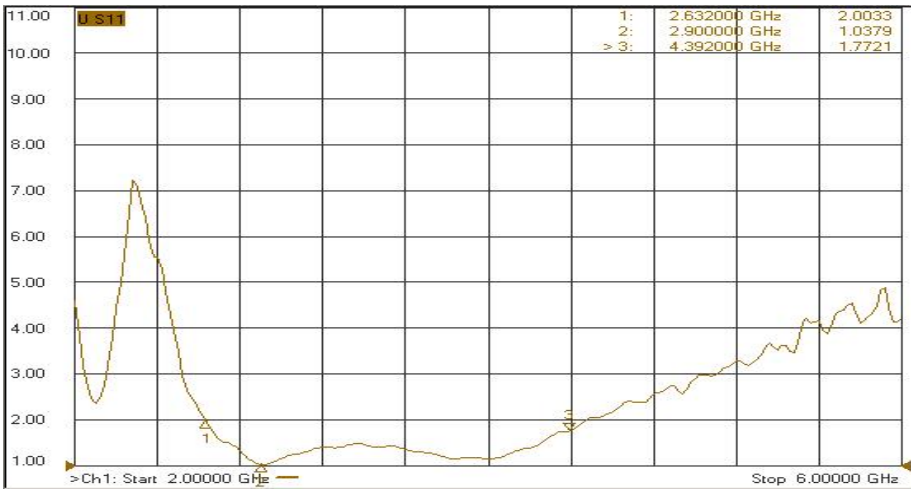

Fig. 4.16. Measured VSWR as a function of frequency for triangular patch with asymmetric slots in ground

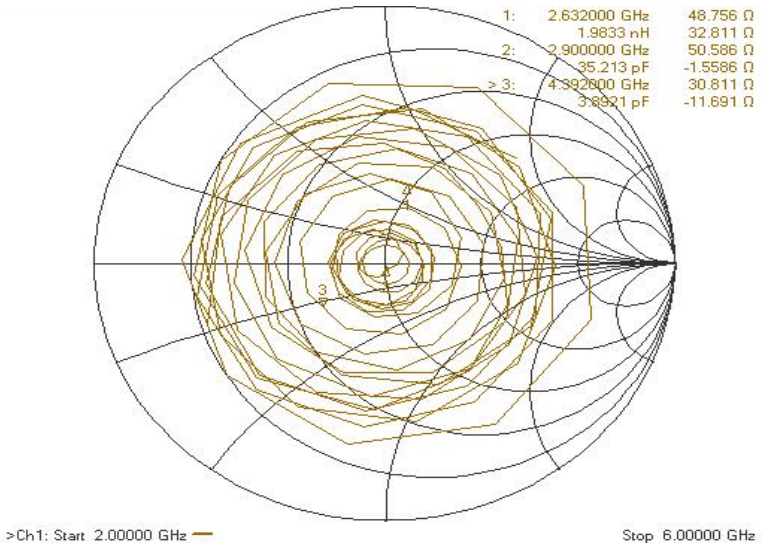

Fig. 4.17. Measured input impedance for triangular patch with asymmetric slots in ground

The input impedance at resonant frequency is (50.58 – j1.55) ohm as depicted in figure 4.17 which is close to 50 ohm impedance of the feed line considered for the present work.

The variation of gain of antenna as a function of frequency is shown in figure 4.18 which indicates that gain of antenna in operating frequency range is close to 3 dBi and almost flat in nature.

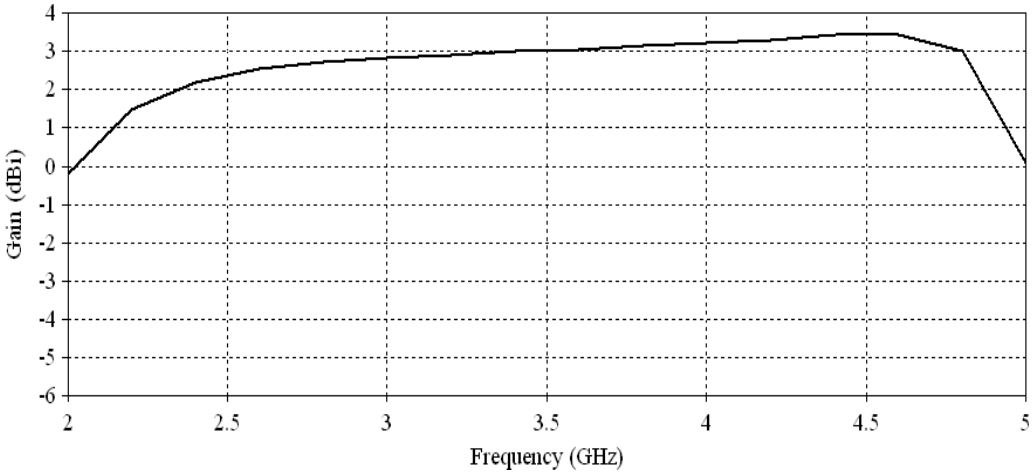

Fig. 4.18. Variation of gain with frequency for triangular patch with asymmetric slots in ground

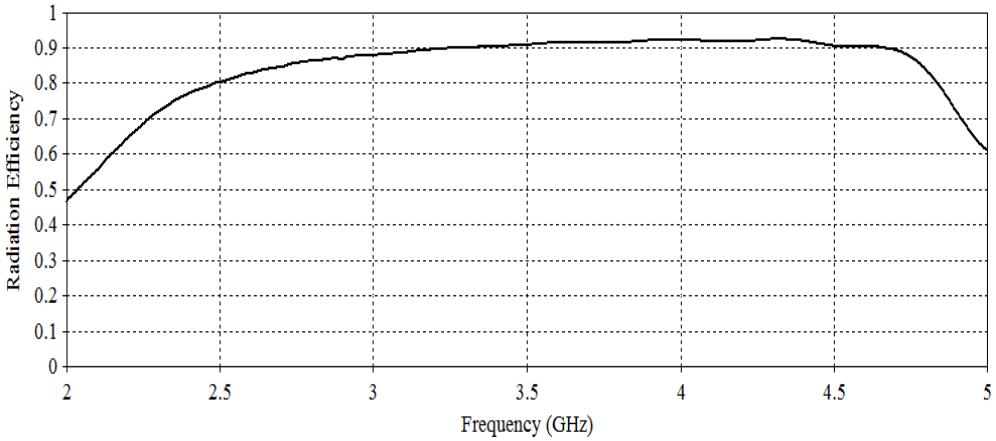

Fig. 4.19. Variation of radiation efficiency with frequency for triangular patch with asymmetric slots in ground

The variation of radiation efficiency of antenna as a function of frequency is shown in figure 4.19 which signifies that it typically varies in accordance with gain.

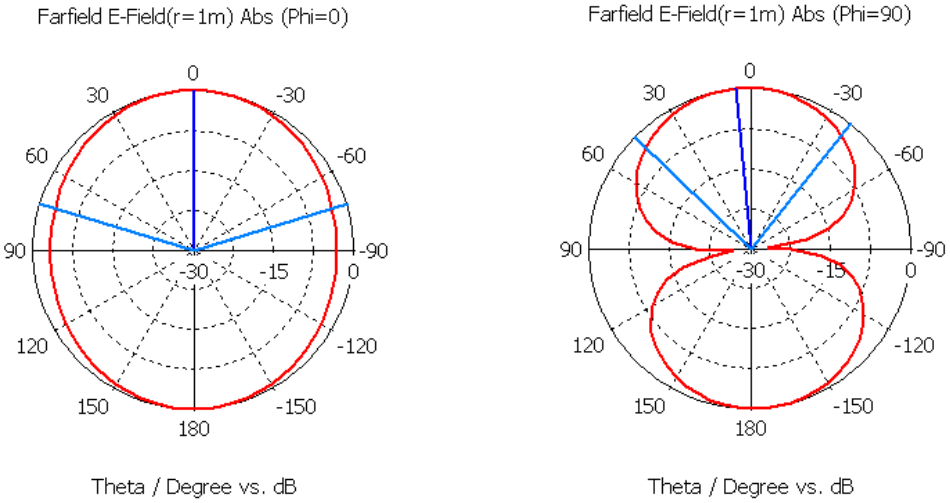

Fig. 4.20. Simulated E and H plane radiation pattern at 2.90 GHz

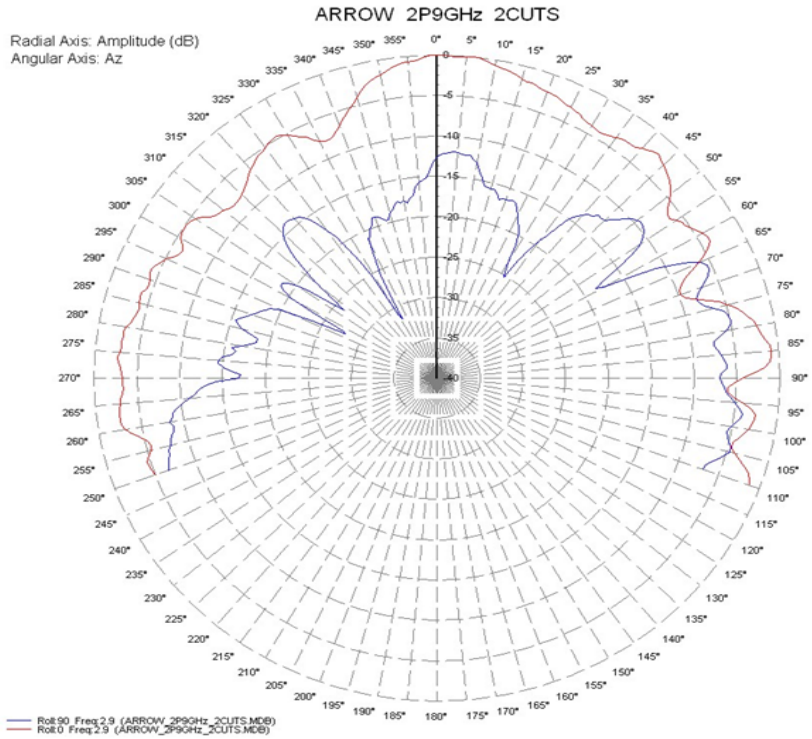

Fig. 4.21. Measured E and H plane radiation pattern at 2.90 GHz

The simulated and measured E and H plane far-field radiation patterns of antenna are obtained at 2.90 GHz as shown in figures 4.20 and 4.21 and found to be in good agreement with each other. These patterns show that in both the case direction of maximum radiation is normal to patch geometry ($\theta = 0^o$). The H-plane pattern is more directive in nature as 3dB beam is close to 60^o while E-plane patterns is omni-directional in nature.

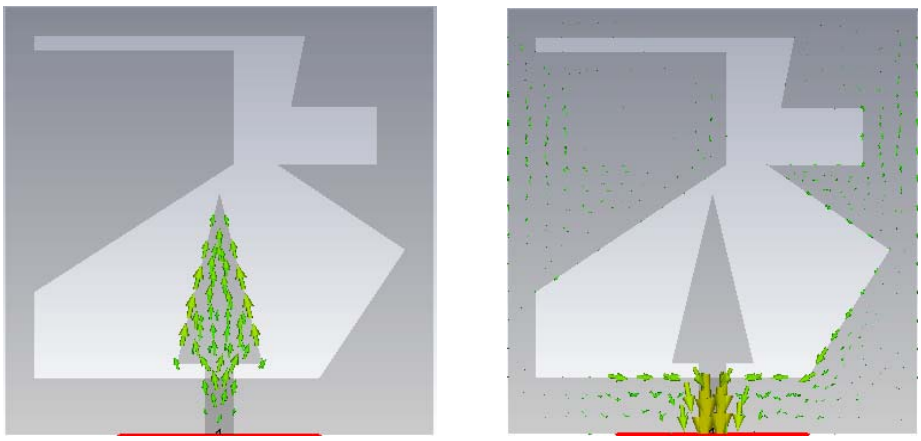

Fig. 4.22. The current distributions of the proposed antenna at patch and ground plane

The current distributions of the proposed antenna at patch and ground plane are illustrated in figure 4.22. The current uniformly distributes for the whole patch and there is very less amount of current in the ground plane which is concentrated over lower side, this distribution of current is responsible for wide bandwidth.

In the next section detailed analysis of another antenna geometry for broadband operation is described

4.4 Analysis of conventional circular patch antenna

In this section the performance of circular patch antenna with finite ground for its use in modern communication systems is investigated. The antenna geometry has dimension is limited to 30×30 mm as shown in figure 4.23. The initial design consists of, circular microstrip patch antenna of radius 10 mm fed by a 50Ω microstrip line, which is printed on FR4 substrate, has a thickness of 1.59 mm and relative permittivity (ε_r) of 4.4, the geometry is simulated using finite element method based CST microwave studio.

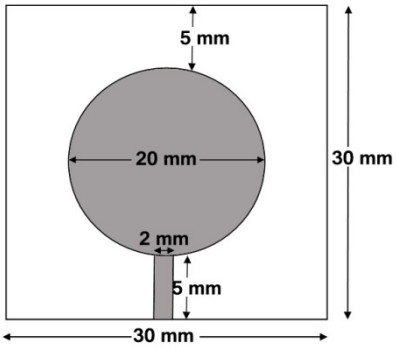

Fig. 4.23. Top view of circular geometry

The simulation results indicate that antenna that antenna is resonating at two frequencies 7.81 GHz and 9.43 GHz as shown in figure 4.24.

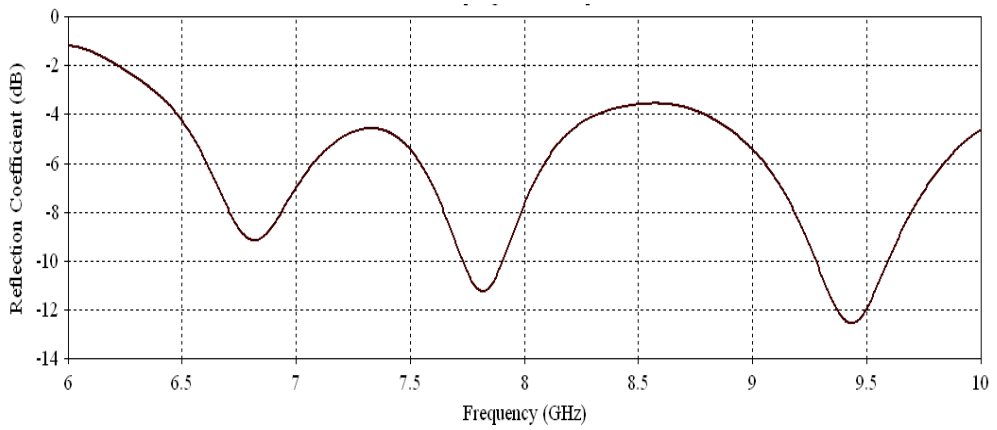

Fig. 4.24. Variation of reflection coefficient (S_{11}) as a function of frequency for circular geometry

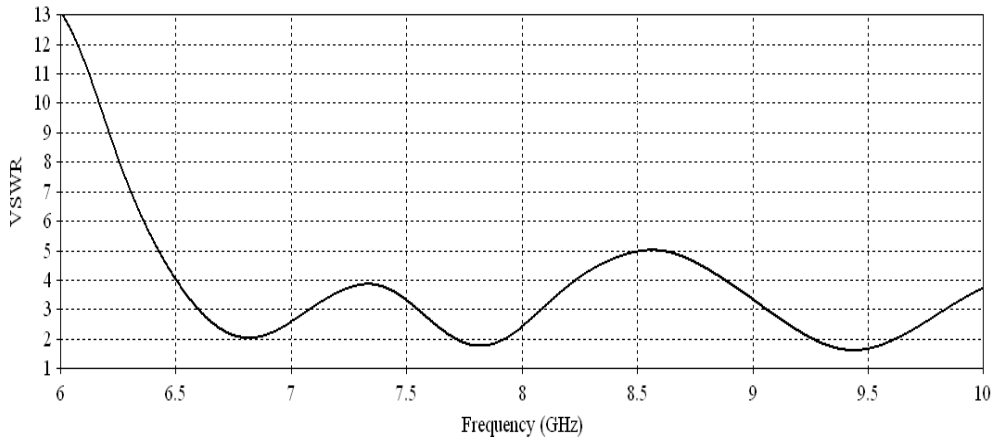

Fig. 4.25. Variation of VSWR as a function of frequency for circular geometry

The variations of VSWR of antenna with frequency indicate that VSWR values at resonance frequencies are 1.76 and 1.61 as shown in figure 4.25, which shows fair matching of this antenna with the feed network.

The simulated E and H plane elevation radiation patterns at two resonant frequencies are shown in figure 4.26 and 4.27 respectively. At lower frequency (7.81 GHz) in E and H plane pattern the direction of maximum radiations is not normal to patch geometry but inclined at an angle 40^o from normal to patch geometry. At higher frequency (9.43 GHz), the E-pane pattern is omnidirectional in nature while H-plane pattern is more directive and has direction of maximum radiations inclined at an angle 50^o from normal to patch geometry.

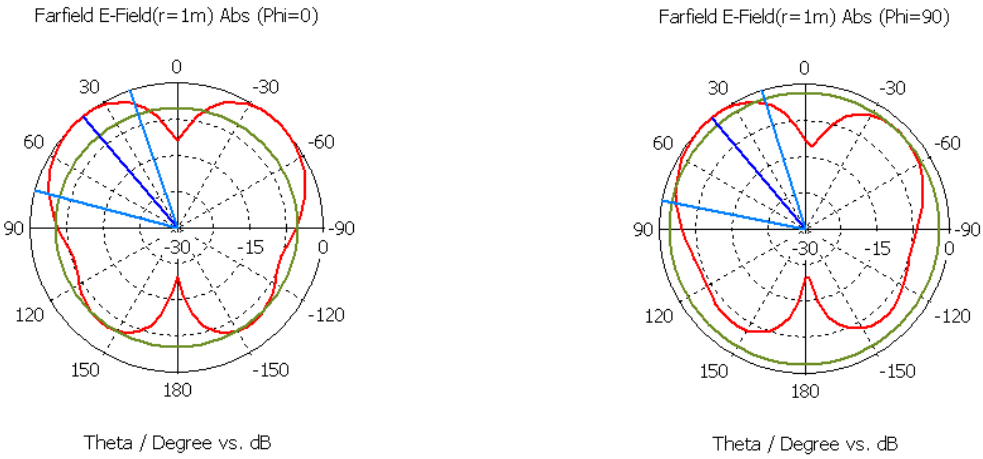

Fig. 4.26. E and H plane radiation pattern at 7.81 GHz

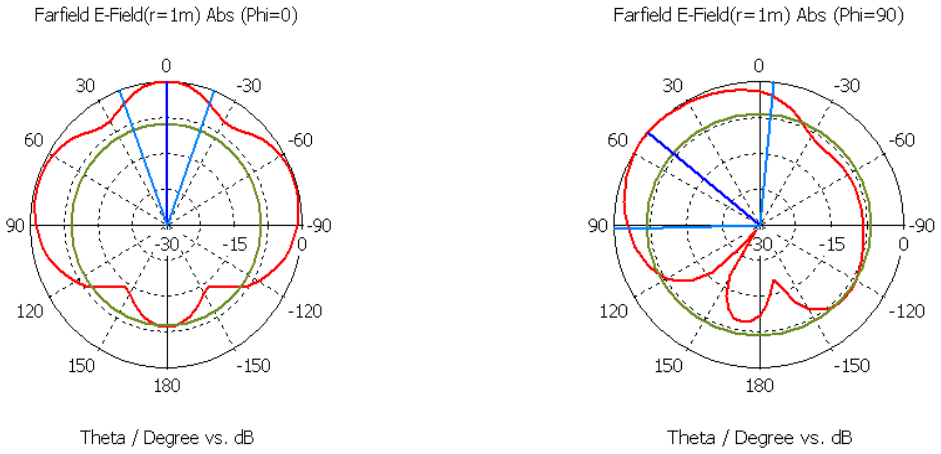

Fig. 4.27. E and H plane radiation pattern at 9.43 GHz

The antenna in present form has very high resonant frequency and low bandwidth so some modification needs to be done in the design.

4.4.1 Circular patch antenna with reduced ground plane

The first step of modification involves truncating the ground plane to reduce its length. The effect of varying the ground dimension on reflection coefficient as a function of frequency is shown in figure 4.28.

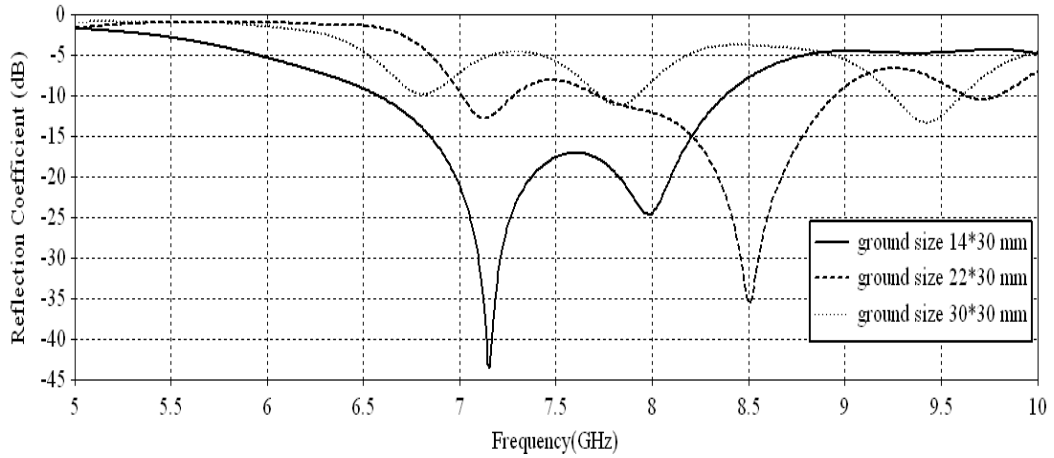

Fig. 4.28. Effect of varying ground dimensions on reflection coefficient as a function of frequency

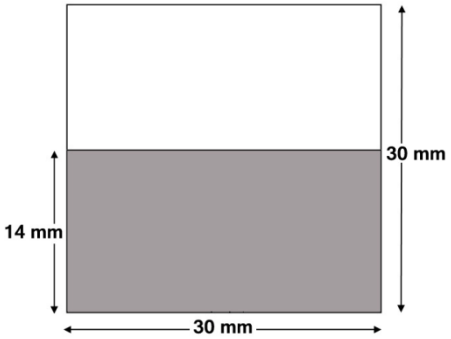

Fig. 4.29. The bottom view of the truncated ground plane

It may be observed that at ground size of 14×30 mm shown in figure 4.29 wideband is obtained and the antenna is resonating at dual frequency of 7.19 GHz and 7.98 GHz and offers a bandwidth of 1.79 GHz (6.58-8.37 GHz) as depicted in figure 4.30. On modifying the ground plane, the two modes prominently gets excited and resonance frequencies corresponding to these two modes are close enough hence the return loss curves for these two modes partly overlap each other to give broadband performance.

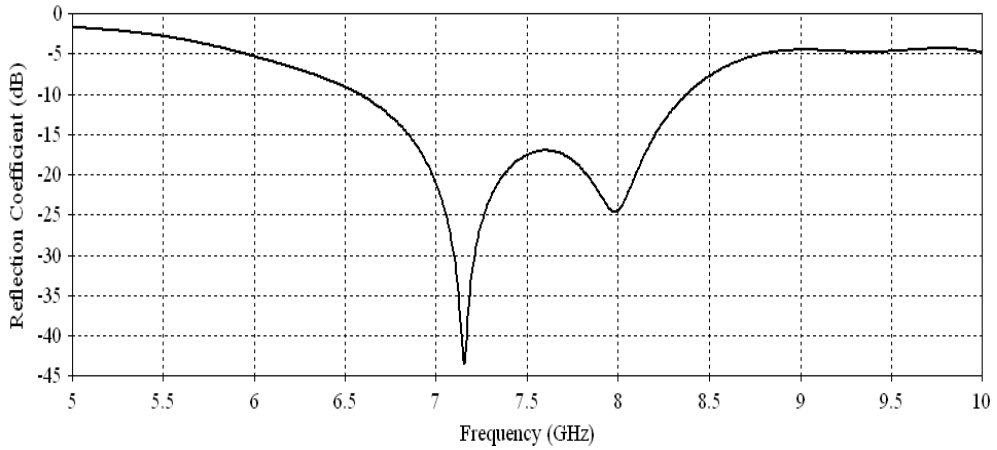

Fig. 4.30. Variation of reflection coefficient (S_{11}) as a function of frequency for circular patch with reduced ground

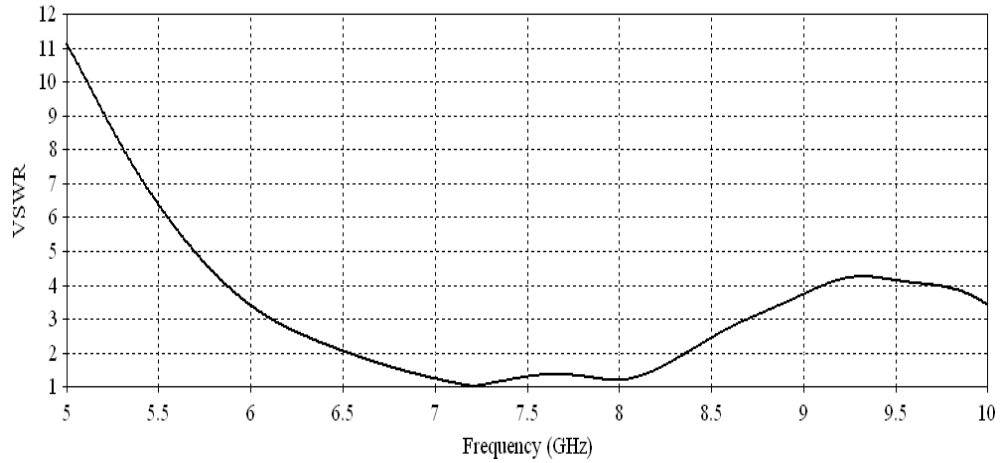

Fig. 4.31. Variation of VSWR as a function of frequency for circular patch with reduced ground

The variation of VSWR presented by antenna is shown in figure 4.31. It can be seen that the VSWR bears values lower than 2:1 at all the frequencies in the bandwidth range. From the figure; we can see that at two resonant frequencies, the VSWR values are 1.01 and 1.19. This result verifies excellent matching of this antenna geometry with the feed.

The variation of gain of modified antenna geometry with frequency is shown in figure 4.32. The gain of antenna at lower resonance frequency is 1.19 dBi and at higher resonance frequency it is 1.83 dBi.

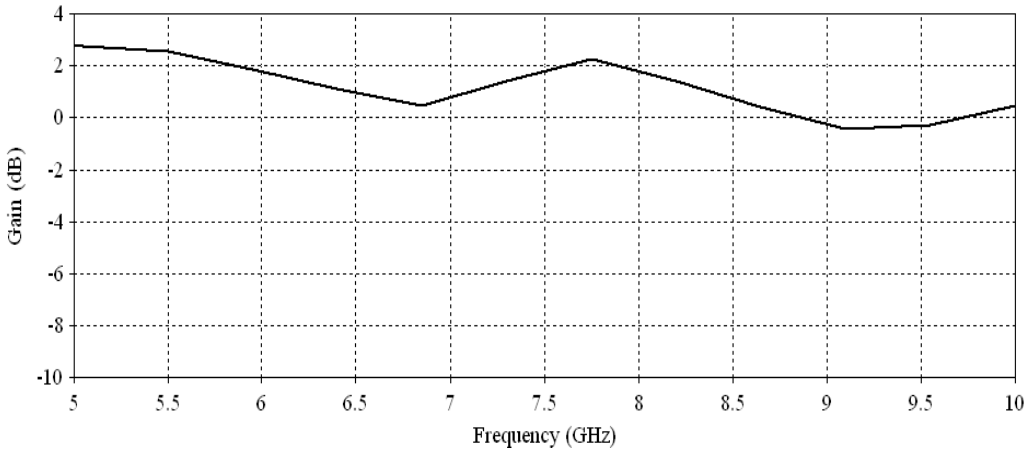

Fig. 4.32. Variation of gain as a function of frequency for circular patch with reduced ground

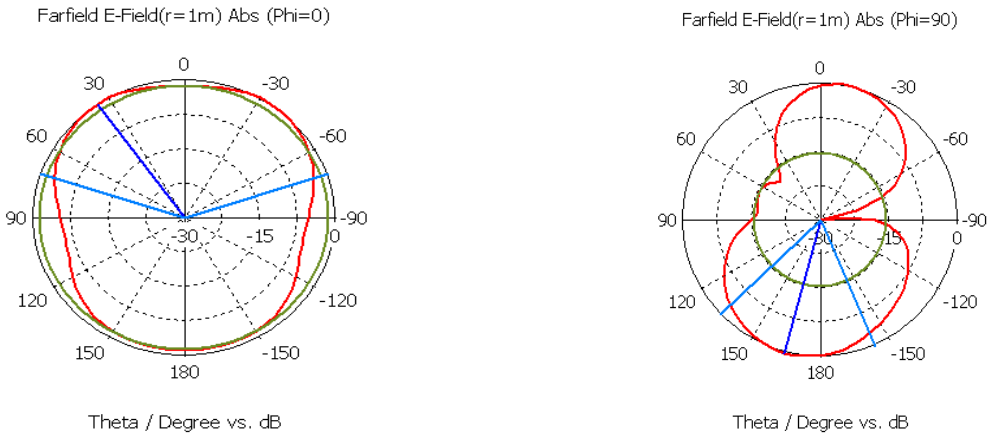

Fig. 4.33. E and H plane radiation pattern at 7.19 GHz

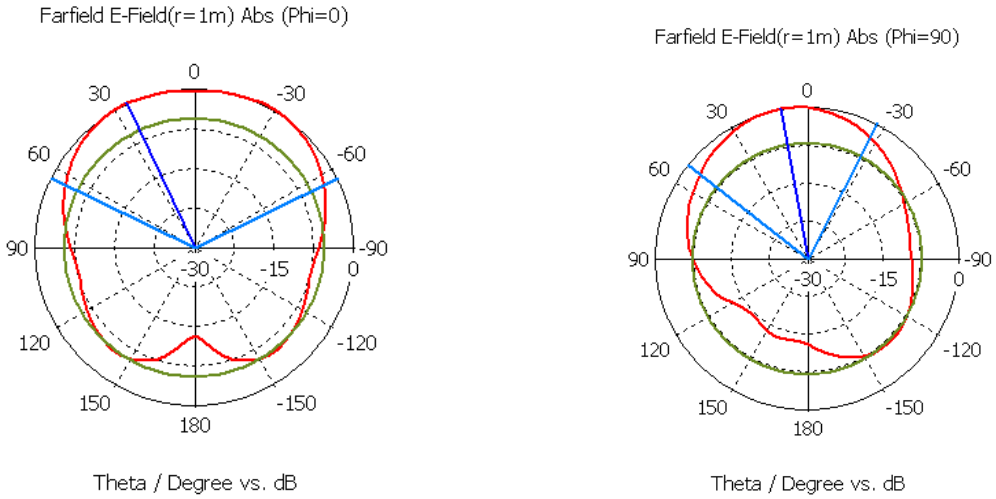

Fig. 4.34. E and H plane radiation pattern at 7.98 GHz

Figures 4.33 and 4.34 depict the E and H plane far-field radiation patterns of the proposed antenna geometry at resonance frequencies. The H-plane patterns are more directive in nature as 3dB beamwidth is close to 30^o for lower frequency and 70^o for higher frequency while E-plane patterns are omni-directional pattern though both patterns resembles like patterns for dipole antenna. In the next section patch geometry and ground plane is modified to achieve further improved performance.

4.4.2 Modified circular patch antenna with elliptical slot and reduced ground plane

The next step of modification involves etching an elliptical slot in the circular patch having semi-minor axis b=3 mm and semi major axis a=4 mm as shown in figure 4.35. The dimensions of the ground are retained identical to that of the patch considered in the previous section.

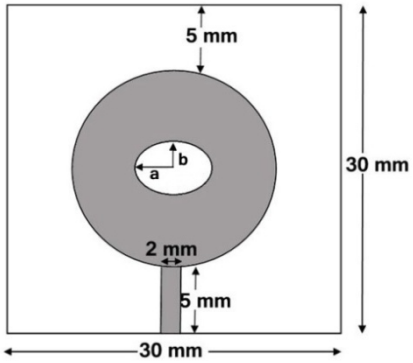

Fig. 4.35. Top view of modified circular patch with elliptical slot

The effects of varying the radius of major and minor axis elliptical slot on reflection coefficient as a function of frequency is shown in figure 4.36.

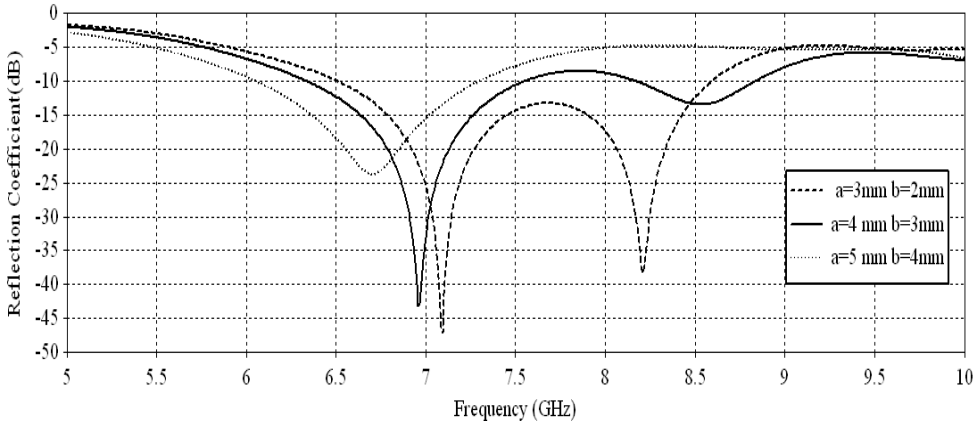

Fig. 4.36. Effect of varying elliptical slot minor axis and major axis radius in patch on reflection coefficient as a function of frequency

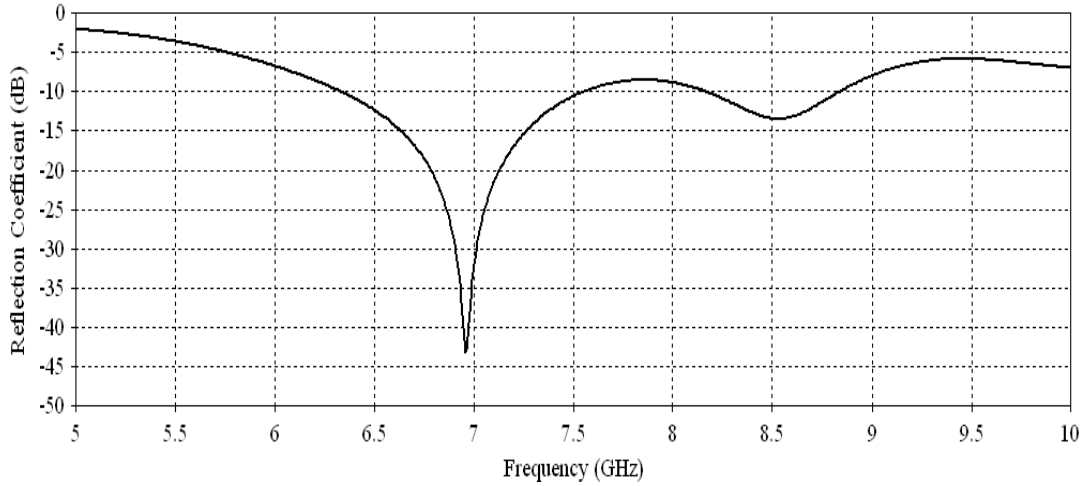

Fig. 4.37. Variation of reflection coefficient (S_{11}) as a function of frequency for circular patch antenna with elliptical slot

At a=4 mm and b=3mm the modified geometry is resonating at 6.958 GHz and 8.53 GHz, has impedance bandwidth of 1.21 GHz(6.33-7.54 GHz) as shown in figure 4.37, as compared to previous geometry resonant frequency is reduced and now the antenna is resonating in the required C-band but bandwidth is also reduced.

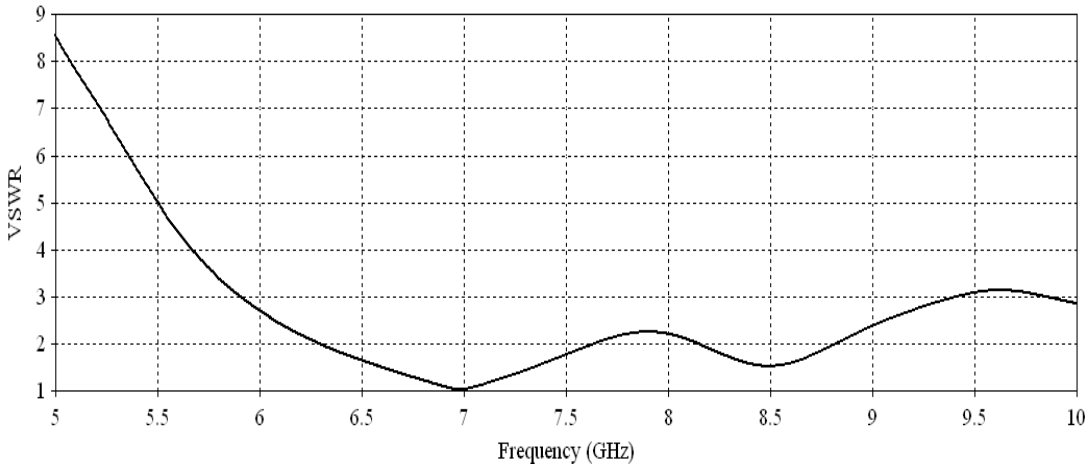

Fig. 4.38. Variation of VSWR as a function of frequency for circular patch antenna with elliptical slot

The VSWR at two resonant frequencies is 1.02 and 1.52 which represents good matching with the feedline as depicted in figure 4.38. The variation of gain with frequency for this modified geometry is shown in figure 4.39. At lower resonant frequency the gain is 1.05 dBi and at higher frequency it is 0.85 dBi.

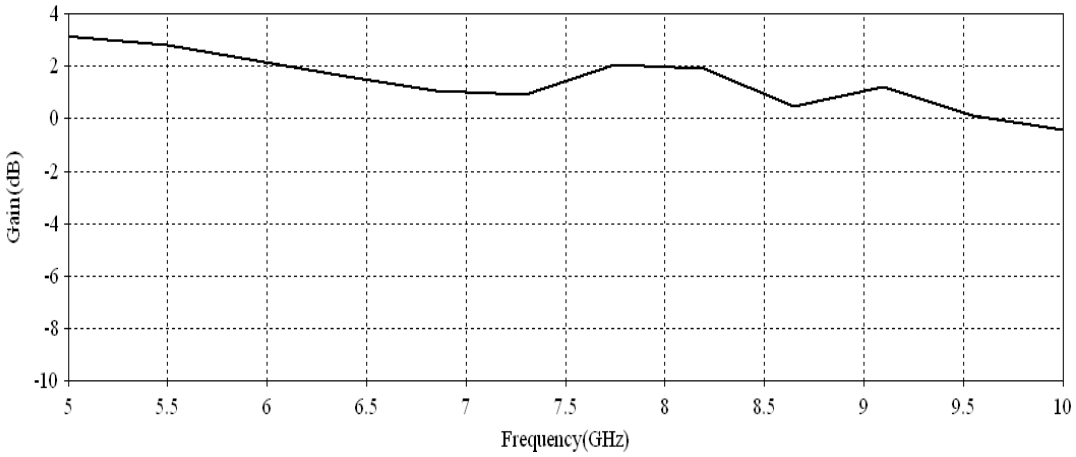

Fig. 4.39. Variation of gain as a function of frequency for circular patch antenna with elliptical slot

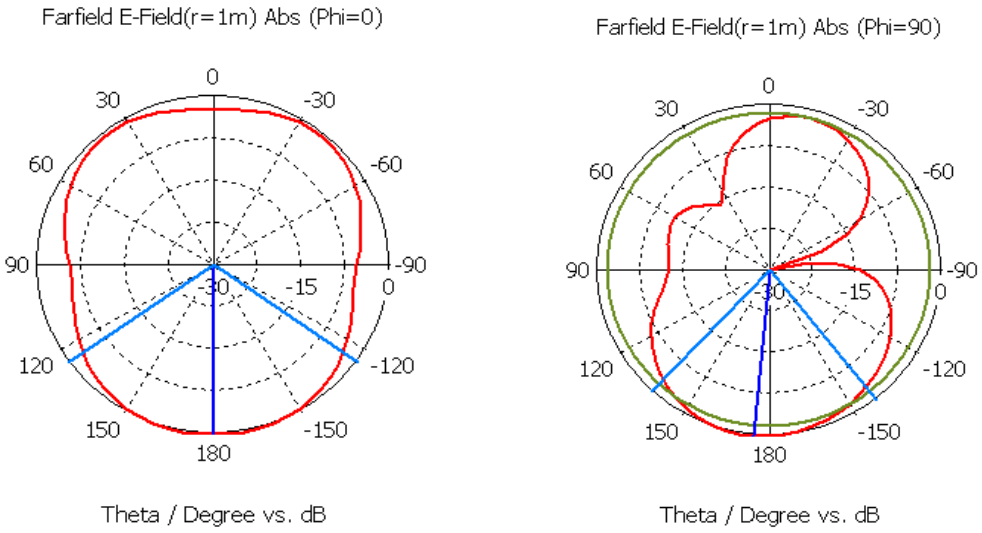

Fig. 4.40. E and H plane radiation pattern at 6.953 GHz

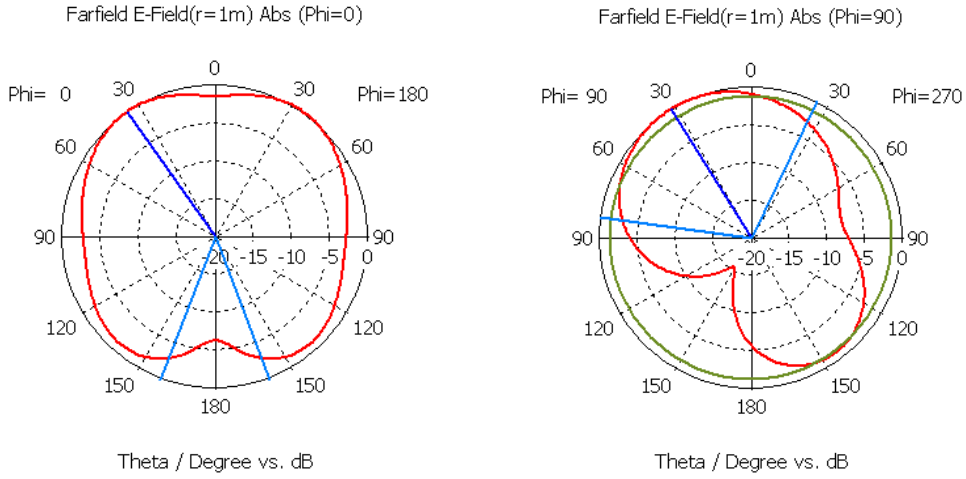

Fig. 4.41. E and H plane radiation pattern at 8.53 GHz

The E and H plane far-field radiation patterns of antenna are obtained at 6.935 GHz and 8.53 GHz are shown in figures 4.40 and 4.41 respectively. E plane patterns indicates that antenna is radiating large amount of power in the back direction ($\theta = 180^o$) and in forward direction ($\theta = 0^o$). In this way, this pattern may be considered as nearly omni-directional pattern in nature. At lower frequency H plane pattern shows more radiation of power in backward direction than forward direction and at higher frequency the H-plane pattern has maximum radiation tilted by 30^o normal to patch geometry.

4.4.3 Modified circular patch antenna with reduced ground plane

The antenna geometry reported in the previous section is further modified in steps by applying two identical slots of dimension 2×2 mm along the y axis at the patch. The size of the finite ground plane and slot location is also optimized to attain best performance. After extensive optimizations the ground was reduced to 4×30 mm and it exhibits wideband behavior. The fabricated prototype of proposed antenna geometry is shown in Fig. 4.42.

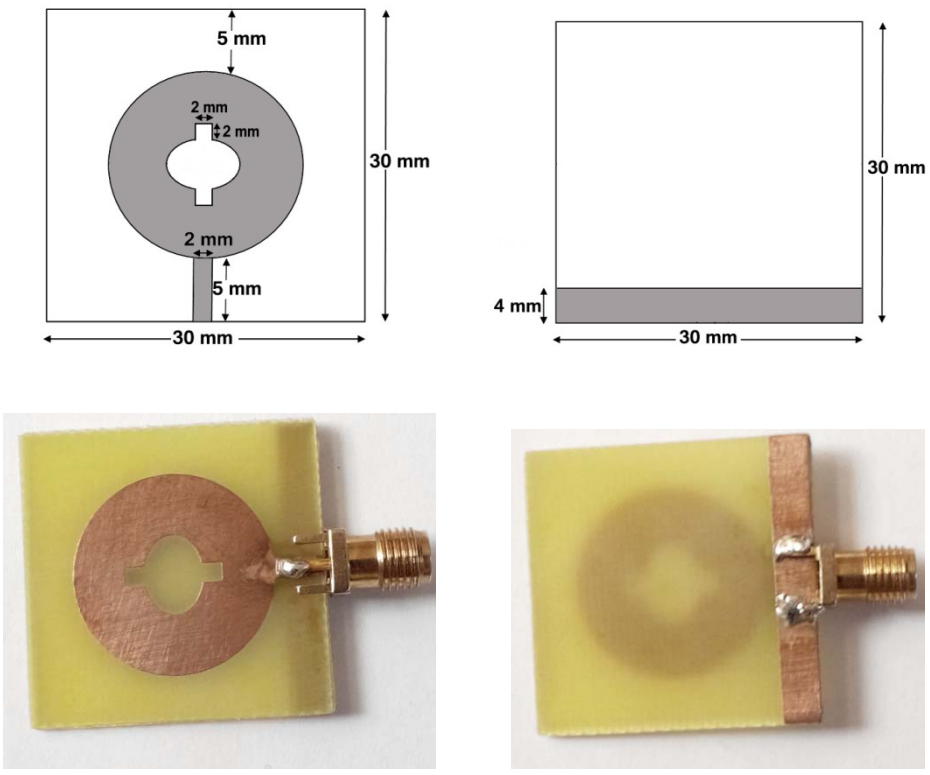

Fig. 4.42. (a) Top view of the proposed geometry (b) Back view of the proposed geometry (c) Top view designed geometry (d) Back view of designed geometry

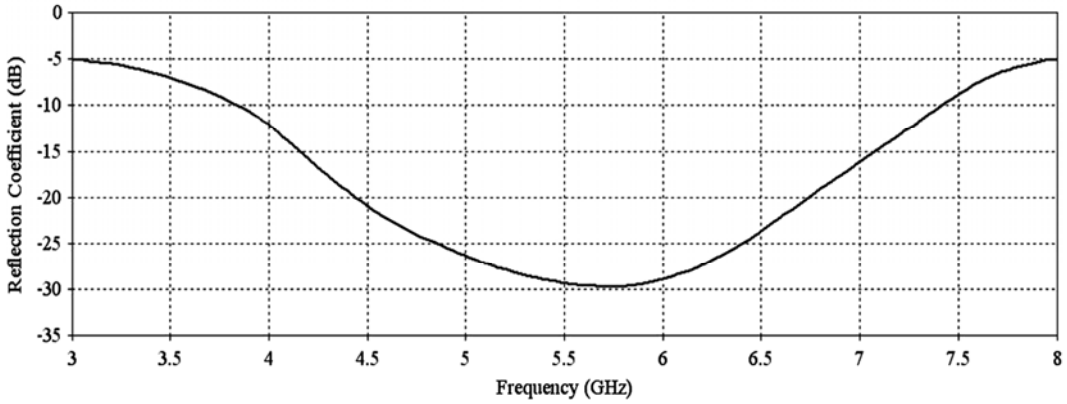

Fig. 4.43. Simulated reflection coefficient (S_{11}) as a function of frequency for modified circular patch with reduced ground

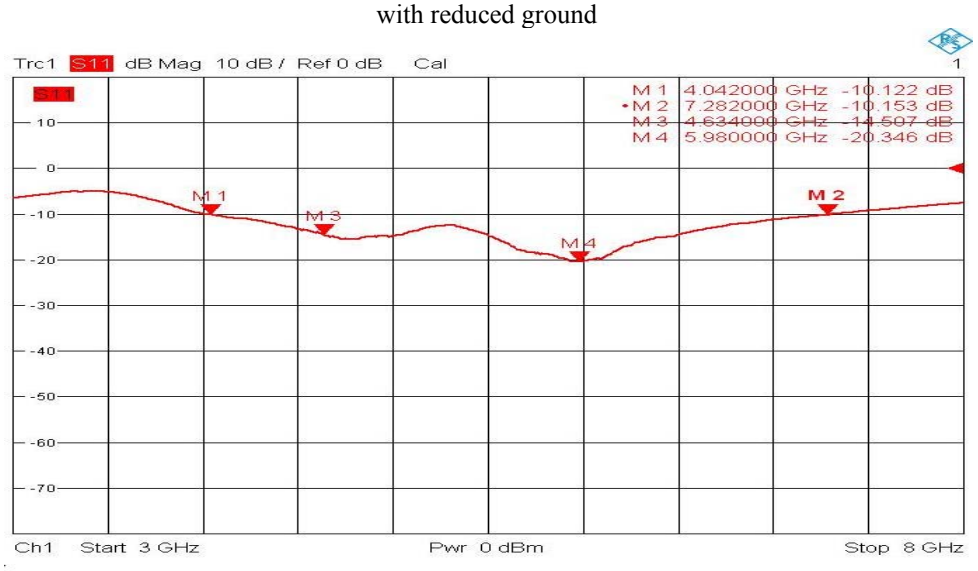

Fig. 4.44. Measured reflection coefficient with frequency for modified circular patch with reduced ground

The radiation parameters like refection coefficient (S_{11}) or return loss, VSWR and input impedance of the fabricated prototype is verified experimentally by testing it using vector network analyzer port operating in S_{11} mode. The particular port of the analyzer was standardized using the standard open, short and matched load for the frequency range of 3 to 8 GHz before starting the measurement. The measured resonant frequencies of this geometry are 4.75 GHz and 5.98 GHz as shown in figures 4.44. It may be observed that the simulated impedance bandwidth is 3.6 GHz (62.6%) at the central frequency of 5.75 GHz as shown in figure 4.43 and the measured impedance bandwidth of antenna has approached to 3.24 GHz (60.3%) corresponding to central frequency of 5.36 GHz.

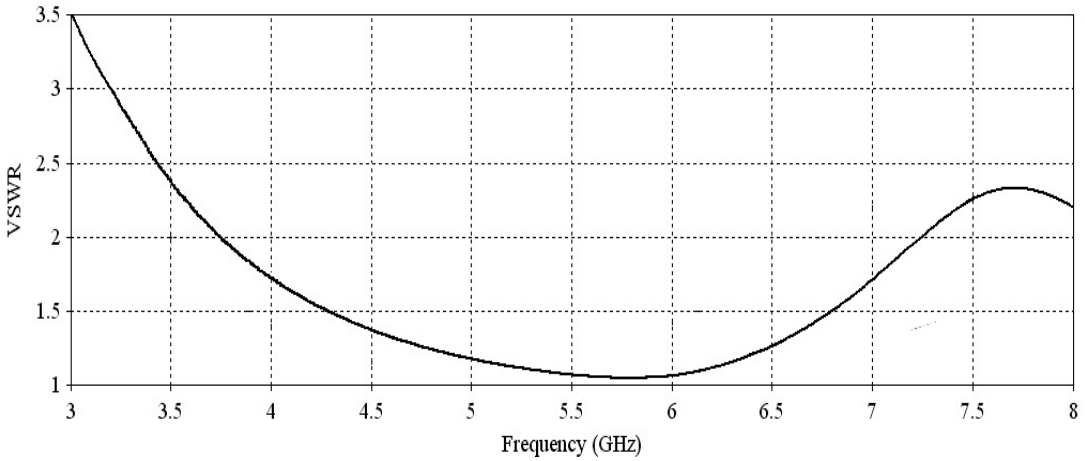

Fig. 4.45. Simulated VSWR as a function of frequency for modified circular patch with reduced ground

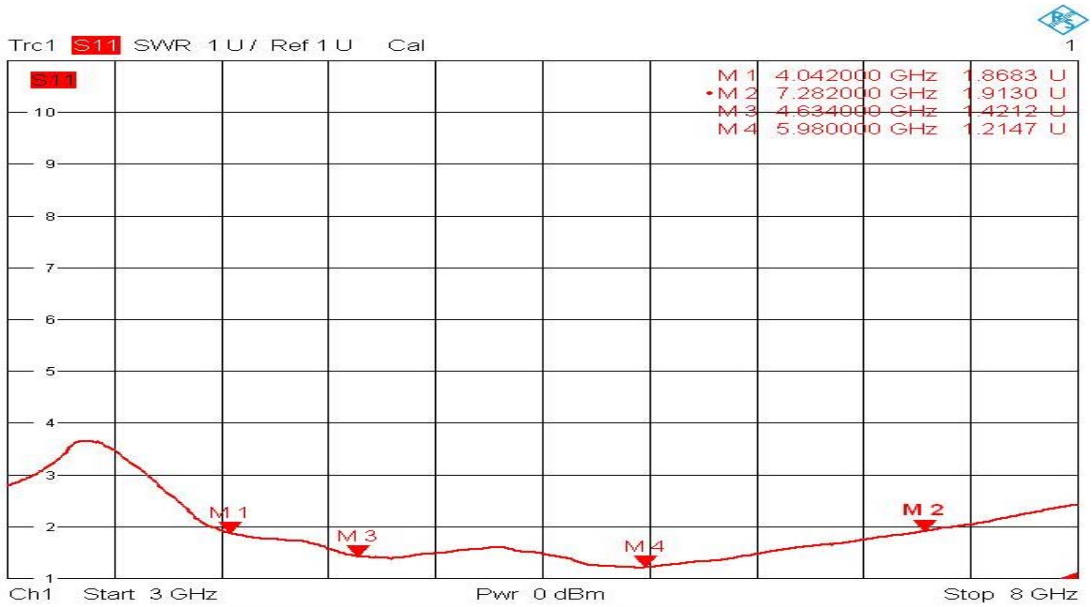

Fig. 4.46. Variation of measured VSWR with frequency for modified circular patch with reduced ground

The simulated VSWR value is 1.057 and the measured VSWR values at two resonating frequencies are ≤ 2 (1.32 and 1.21 respectively) as shown in figures 4.45 and 4.46, which suggest that antenna geometry has good matching with the microstrip feed line.

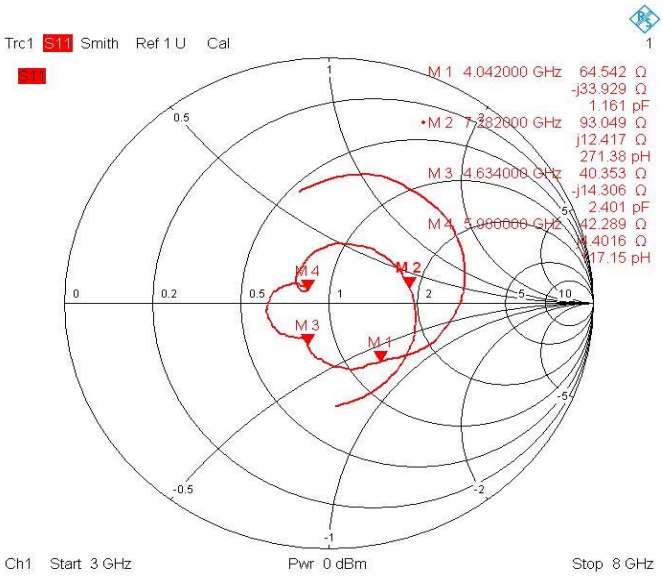

Fig. 4.47. Measured input impedance for modified circular patch with reduced ground

The measured input impedance related to two resonant frequencies are (42.35- j4.80) ohm and (42.28+j4.406) ohm respectively as shown in figures 4.47 which are nearly reaching to 50 ohm impedance of the microstrip feed line.

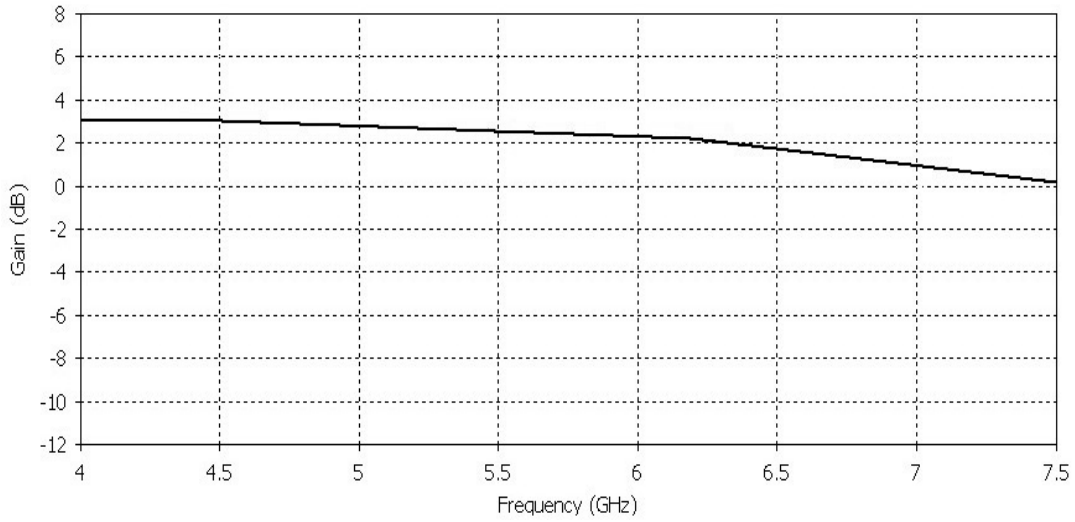

Fig. 4.48. Variation of gain as a function of frequency for modified circular patch with reduced ground

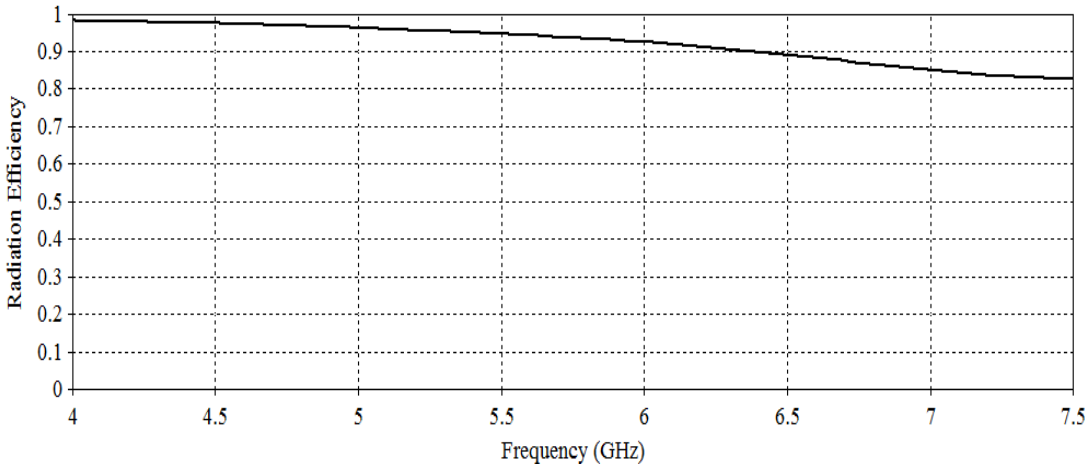

Fig. 4.49. Variation of radiation efficiency as a function of frequency for modified circular patch with reduced ground

The gain of the antenna as a function of frequency for the frequency range (4-7.5 GHz) is shown in figure 4.48. It indicates that gain is uniform in nature and nearly 3 dBi. The gain values are smaller than the desired one because bandwidth enhancement for this antenna was given preference over the gain and gain bandwidth product of antenna remains constant. The low value of gain is also due to high tangent loss of FR-4 substrate used.

The radiation efficiency as shown in figure 4.49 is stable and has been uniform in the entire operating bandwidth,

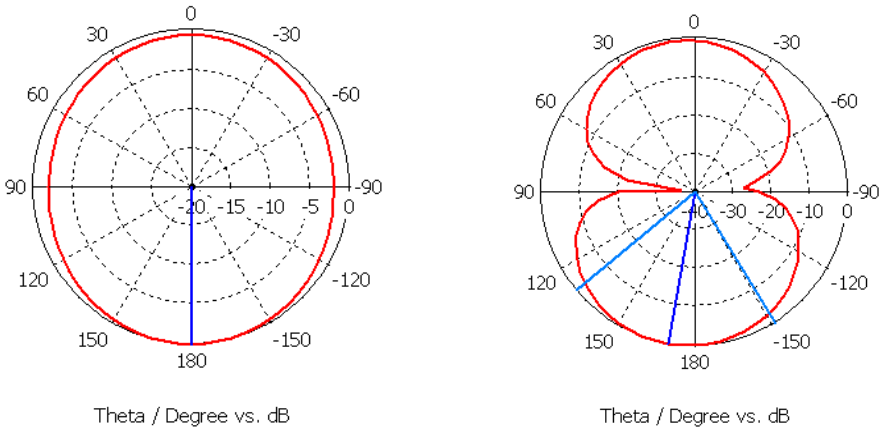

Fig. 4.50. Simulated E and H plane radiation pattern at 4.75 GHz

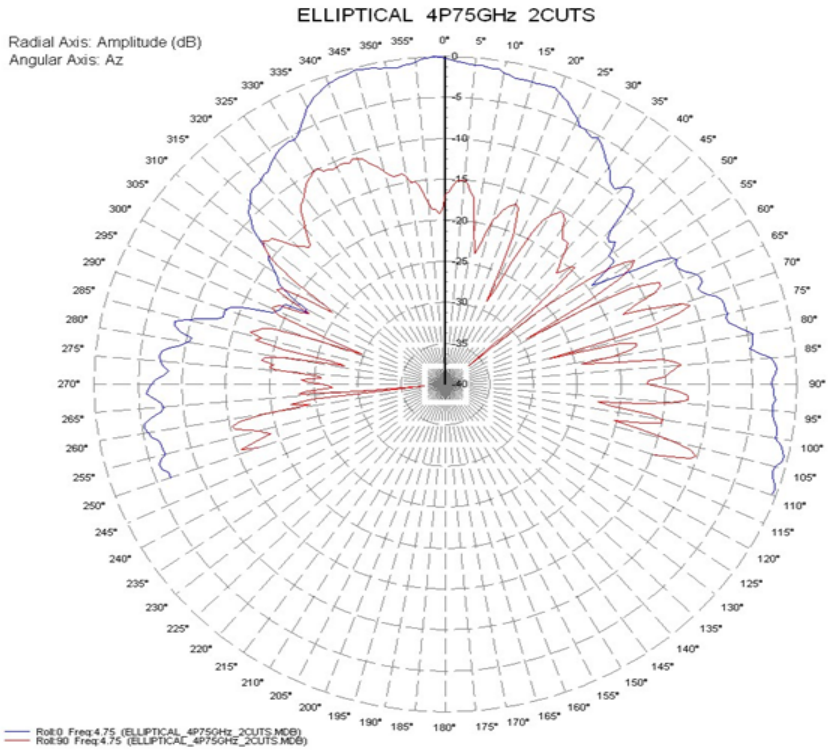

Fig. 4.51. Measured E and H plane radiation pattern at 4.75 GHz

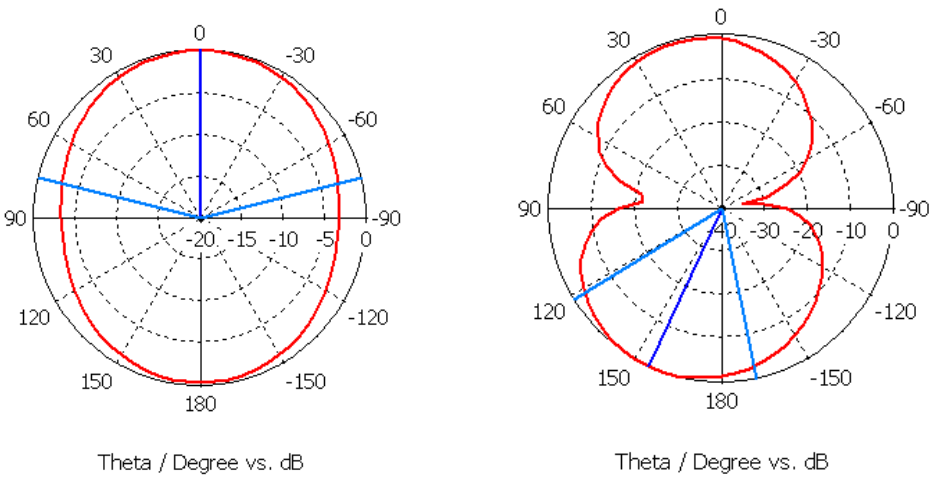

Fig. 4.52. Simulated E and H plane radiation pattern at 5.98 GHz

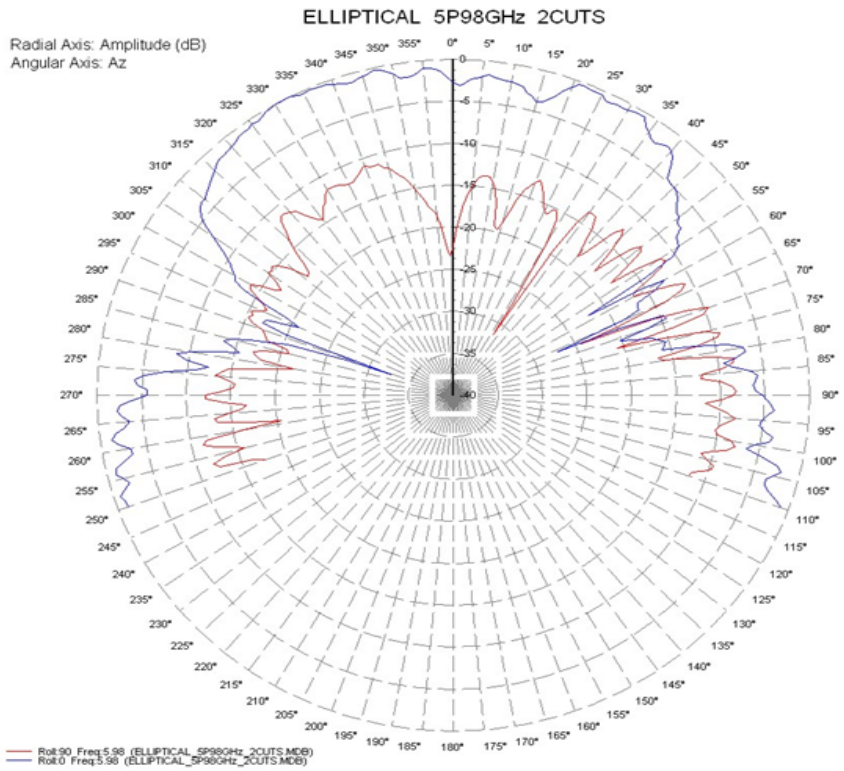

Fig. 4.53. Measured E and H plane radiation pattern at 5.98 GHz

The simulated and measured E and H-plane elevation radiation patterns of proposed geometry are obtained at two frequencies within frequency of interest and are shown in Figs. 4.50 to 4.53 respectively. The E-plane patterns are in good agreement with simulated results and have direction of maximum radiation normal to the patch geometry. At lower frequency the 3dB beamwidth of E-pane pattern is nearly 50^0 and for higher frequency it is close to 80^0. The H-plane patterns are more directive at both the resonance frequencies with direction of maximum radiation inclined by 30^0, perhaps due to fabrication error and presence of noise during measurement.

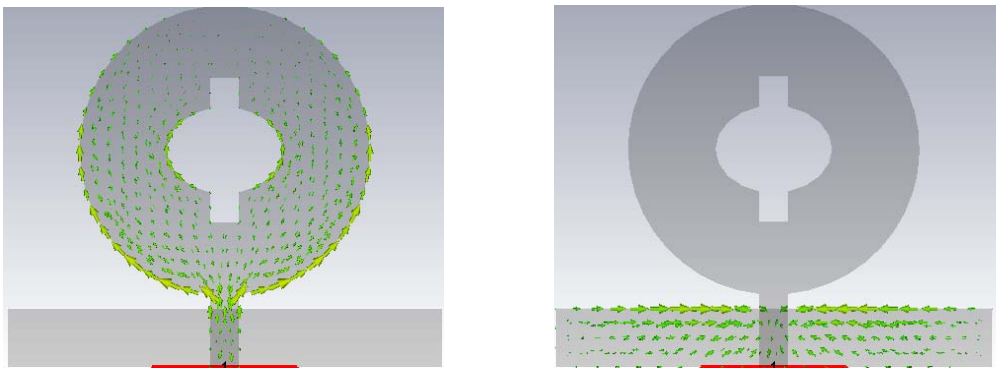

(a)

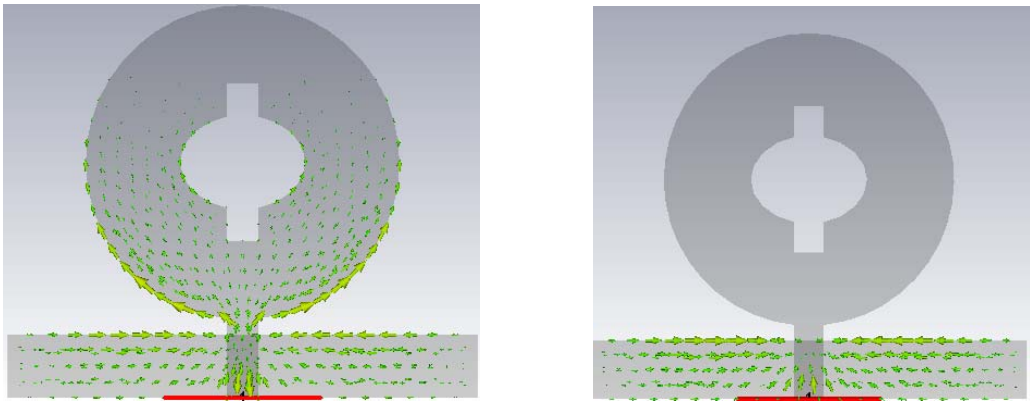

(b)

Fig. 4.54. Surface current distributions on the patch and the system ground plane at (a) 4.75 GHz (b) 5.98 GHz

Figure 4.54 shows the excited surface current distributions at 4.75 and 5.98 GHz on antenna and the ground plane. For the two excited resonant frequencies, the obtained surface current distributions are nearly similar as shown here.

A quantitative comparison of proposed geometries with the literature is provided in the table 4.1

TABLE 4.1. COMPARISONS OF PROPOSED ANTENNA WITH OTHER REPORTED ANTENNAS

Reference	Antenna Size (in mm)	Frequency	Bandwidth	Gain (dBi)	Applications
178	80×102	900 MHz 1.65 GHz 2.25 GHz	1.7 GHz	2.5 4.7 1.9	GSM, WiFi, LTE
179	97×60	1.8 GHz 2.5 GHz	53.02% 1.14 GHz	-	GSM1800, GSM1900, UMTS, LTE2300, LTE2500, and 2.4 GHz WLAN bands for the 2G/3G/4G mobile terminals
Triangular Geometry	30×30	2.9 GHz	1.76 GHz (60.6%)	3	Lower band of UWB
Modified Circular Geometry	30×30	4.75 GHz 5.98 GHz	3.24 GHz (60.3%)	3	C band

4.5 Summary

This chapter includes two compact antenna geometries for broadband operation. In the first section of this chapter design and performance of a compact triangular patch antenna with slotted ground plane is analyzed and results are systematically presented. The combined effect of modifications in patch geometry and ground plane provided significantly improved impedance bandwidth (60%) along with gain enhancement (~ 3dBi) in comparison to a conventional triangular patch antenna. This antenna is specifically designed looking Indian requirements for the lower band of UWB communication systems. At present, Indian wireless requirements are mainly limited within obtained bandwidth range. In the second section of this chapter modified circular patch antenna with reduced ground plane and an extensive analysis of this modified circular patch antenna is reported. The stepwise modifications in the circular patch antenna are done and radiation performance of patch antenna is analyzed after each step. A wide measured impedance bandwidth of order of 60.3% is achieved which is nearly fifteen times larger when compared with conventional (without) slot geometry. The designed antenna operates in the C-band in the frequency range 4-8 GHz giving a wide impedance bandwidth.

Chapter 5

Stacked arrangement of microstrip antennas for improved performance

5.1 Introduction

As we all know, that in this modern era, things are becoming smaller and everybody wants that the efficiency of things should be enough to use it anywhere. In this way microstrip patch antenna are developing day by day, but they are also bound due to their limitations. A more complex arrangement, comprising of two microstrip patches in a stacked arrangement, offering desired characteristics that are not generally achievable from the single-layer arrangement. These features include high gain and broad bandwidth [96]. The stacking of patches does not influence the surface area occupied by the element. So stacked element can be used in array configuration while maintaining the same element spacing. The radiation pattern and the phase centre of stacked element remains symmetrical over its operational band [2].

A wideband stacked patch antenna for UMTS, ISM and WLAN was proposed in [180]. The antenna is dual polarized and fed by two microstrip lines through a couple of crossed slots. The fabricated prototype confirms wide impedance bandwidth with good isolation. A wideband U-slot microstrip patch antenna in stacked configuration by means of circuit theory model was reported in [181]. The antenna demonstrated two resonance frequencies that are closed vicinity to provide wideband response. The frequency band of 186 MHz was achieved for the proposed antenna. An asymmetric U-slot patch antenna with low probe diameter for enhanced bandwidth was presented in [182]. It was shown that the measured bandwidth can be enhanced to 30% with an air gap of 8 mm and it can be further enhanced by increasing the airgap thickness but this leads to higher cross polarization level. A dual-frequency behavior of stacked microstrip patches has been reported in [183]. In this paper, fabricated prototype of stacked rectangular microstrip patches with dual frequency response were investigated. When the bottom patch was shorter than top

one, results showed that the upper resonance was obtained by the dimension of the bottom patch and the lower resonance was near to the resonance frequency of the isolated top patch. In opposite case, top patch dimensions significantly affects the upper resonance and isolated bottom patch resonant frequency was nearby the lower resonance. Other results also revealed that substrate dielectric anisotropy has more influence on the lower resonance in contrast with the upper resonance. In [184] a new way to attain broad bandwidth and broad beamwidth of microstrip antennas based on the stubs and gaps has been presented. The structure of the proposed antenna was based on a two-layer stacked Electromagnetically coupled microstrip antenna (ECMSA). The stubs and gaps were introduced on the radiating patch of the ECMSA to perturb the surface electric current for the sake of exciting multiple modes. The impedance bandwidth was up to 34.6% and the broad beamwidth pattern bandwidth was 13%.

In many applications, such as global positing system (GPS) and satellite communication and along with wide impedance bandwidth we require antennas having circularly polarized performance because circular polarization (CP) has the additional benefit of being not dependent on the orientation between the receiver and transmitter. CP operation is generally obtained by when two perpendicular linearly polarized waves with equal magnitude are 90^0 out of phase. There are two methods usually used to cause the CP in microstrip antennas; in the first method the geometry is made asymmetric for excitation of two degenerated mode perpendicular to each other and in phase quadrature using single feed arrangement. The second technique involves applying dual feed which consists of two perpendicular feeds having relative phase difference of 90° [3]. For using dual feed the necessary phase shift is provided by power splitter such as Wilkinson power divider. However, dual feed technique involves higher cost and complications in the antenna structure. Therefore, single feed approach is generally preferred for circular polarization.

The stacked arrangement of modified elliptical patch design and circular patch antennas was investigated in [39]. The elliptical patch is modified by truncating its edges. The proposed antenna provides circular polarization along with wide bandwidth. The dimension of lower modified elliptical patch was kept slightly

smaller than upper circular patch. The fabricated antenna on measurement gives 3.33% of axial ratio bandwidth and 940 MHz of impedance bandwidth. A dual-band circularly polarized stacked antenna was presented in [185]. Circular polarization was achieved by optimizing the dimensions of inserted slits and truncated corners of the hexagonal patches. The measured impedance bandwidths were 120 MHz (3.44 to 3.56 GHz) and 250 MHz (5.05 to 5.3 GHz) for lower and upper band, respectively. The antenna offered left hand circularly polarized axial ratio bandwidth of 24 MHz at 3.5 GHz (lower band) and right hand circularly polarized axial ratio bandwidth of 53 MHz at 5.18 GHz (upper band). Stacking can be also used to produce multiband patch antenna. In [186] a tri-band antenna in stacked configuration with circular polarization using single feed was reported. The proposed geometry is fed by probe feed and can be useful in receiver of global positioning systems. The symmetric I slot and slits were inserted in the multiple layer of stacked patches for desired performance. The bandwidth attained was 2.0%, 1.5%, and 1.7% at GPS L1, L2, and L5 bands, respectively. Additionally, broad beamwidth and minimum axial ratio of 0.51 dB was also obtained.

Stacked square patch with tuning stubs was proposed for broadband operation with circular polarization [187]. The driven patch was of square shape and stacked patch was truncated circular shape. The proposed geometry provides impedance bandwidth of 16%. The axial ratio at two frequencies 2.3GHz and 2.66GHz are 1.61dBi and 0.45dBi respectively which indicate circularly polarized nature of antenna. The antenna is designed on glass epoxy FR-4 substrate with overall thickness of structure 9.18mm.

A compact cross-shaped slotted microstrip patch antenna was proposed for circularly polarized (CP) performance [188]. A symmetric cross shaped slot, a square and a circular shaped slot was inserted beside the diagonal axes of the square patch for circular polarization and compactness. A comparison was done on the basis of three different slots. This leads to cross-shaped slot having higher operating frequency reduction for CP radiation in contrast with square and circular shaped slots. Arm width, rotation angle of the cross-shaped slot and ground plane of the antenna left an effect on the parameters of the antenna.

A stacked arrangement of rectangular ring microstrip antenna and rectangular microstrip antenna with a shorting plate for tri- band operation was reported [95]. It covers application including GPS, vehicle information and communications system and electric toll collection system in Intelligent Transport System. The antenna was excited by an L-probe feed. The VSWR, axial ratio, radiation pattern and gain were simulated and compared with measured results. Three geometries of hexagonal patch for bandwidth improvement and circularly polarized performance were investigated [189]. The measured impedance bandwidths obtained of the three antennas were 2%, 5.2% and 6.35%. The axial ratio bandwidth obtained was 4.73% for patch with slotted ground and 3.33% for the hexagonal patch antenna with parasitic element. A frequency selective surface was also proposed for gain enhancement and size reduction. Thus we can conclude that using stacked arrangement we can get both wide impedance bandwidth and circular polarization.

Circularly polarized stacked microstrip patch antenna with a small frequency ratio was presented [190]. The driven patch was having a pair of peripheral cuts in the circular patch with cross slot and truncated corner square ring was used as the stacked patch. The 3-dB axial ratio bandwidth is 1.4% for the upper band and 1.1% for the lower band. The measured results were in good agreement with the simulated. The antenna was having a dual-band frequency ratio of 1.05 and may utilized for circularly polarized wireless applications.

A stacked geometry of antenna for broadband operation with circular polarization is described here. The main objectives of this work is to demonstrate experimentally the use of stacked patches with shorting pin for significant improvement in the antenna radiation performance including enhancement in gain (5 dBi or more) and exploring possibility of pure circular polarization.

In this chapter, we will discuss compact probe fed stacked arrangement of hexagonal and rectangular microstrip antennas for circularly polarized broadband performance. The impedance bandwidth better than 1.398 GHz and axial ratio bandwidth close to 73 MHz were achieved with the proposed geometry. The simulated and measured results obtained are in good match with each other. The proposed antenna is simulated using commercial electromagnetic software IE3D based on Method of

Moment (MoM) and measured results are also presented for verification of simulated results.

5.2 Performance of conventional hexagonal patch antenna

Initially, we considered a single layer hexagonal patch antenna having length of each arm equal to 12 mm as shown in figure 5.1. The patch lies in XY plane with substrate height negligible as compared to free space wavelength with dielectric constant ε_r and relative permeability μ_r = 1, on an infinite ground plane. The magnetic field has basically x and y components. Because the height of the substrate is negligible, the field distribution along z-direction will be constant and at the edges; the normal component of the current of the microstrip antenna is nearly zero. This signifies that the antenna works in TM_{mn} modes [191]. With these suppositions, the structure is taken as a hexagonal resonator with magnetic sidewalls, top and bottom is bounded by electric walls. The considered simple hexagonal geometry is simulated by using IE3D simulation software, considering substrate relative permittivity ε_r = 4.4, loss tangent tanδ = 0.025 and substrate thickness h = 0.159 cm. The antenna has inset feed arrangement using SMA connector and associated 50 ohm feed line.

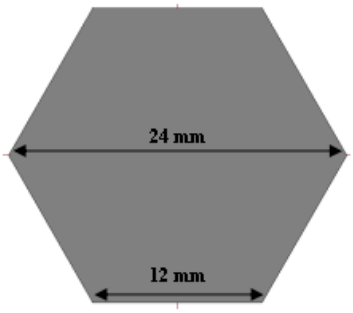

Fig. 5.1: Top view of simple hexagonal geometry

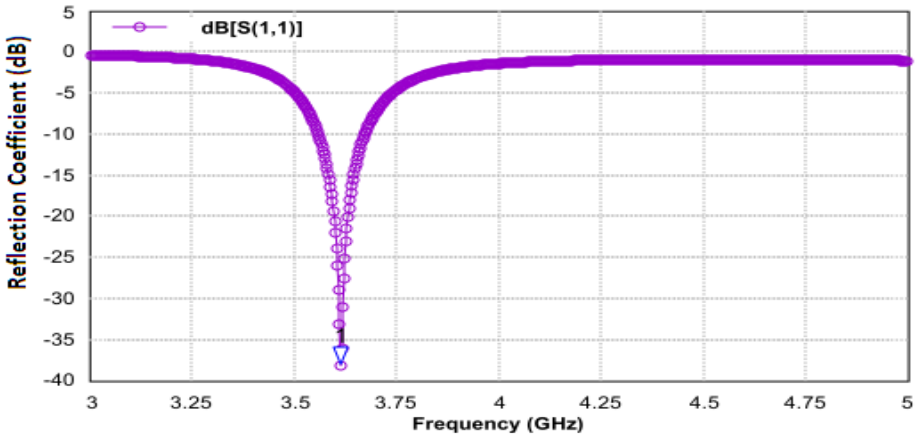

Fig. 5.2 (a): Simulated return loss of simple hexagonal geometry as a function of frequency

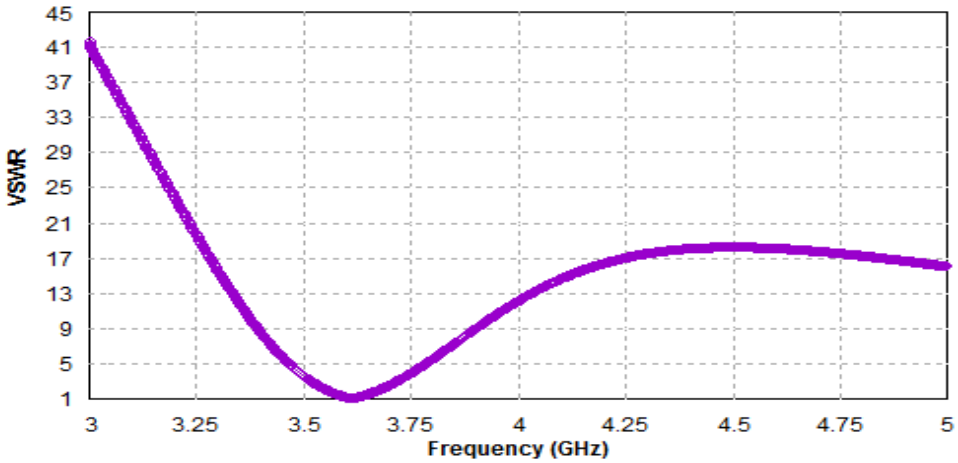

Fig. 5.2 (b): Simulated VSWR of simple hexagonal geometry as a function of frequency

The simulated variation of return loss of this simple hexagonal geometry as a function of frequency is shown in figure 5.2(a). In the considered range of frequencies (3 GHz – 5 GHz), this antenna resonates at a single frequency (f_r = 3.61 GHz). The simulated VSWR value corresponding to the resonant frequency 3.61 GHz is 1.352 while the impedance bandwidth (VSWR 2:1) of this antenna is nearly 3.5% as can be seen from figures 5.2(b). The simulated input impedance at the resonance frequency is close to (49.583 + j1.806) ohm as shown in figure 5.3.

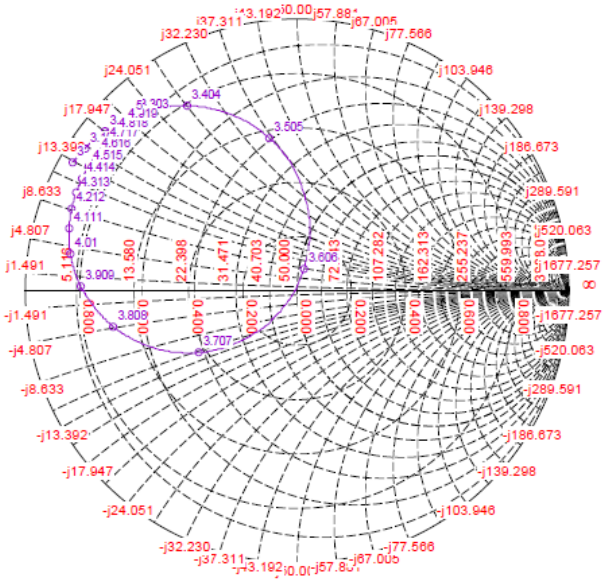

Figure 5.3: Variation of input impedance with frequency for hexagonal geometry

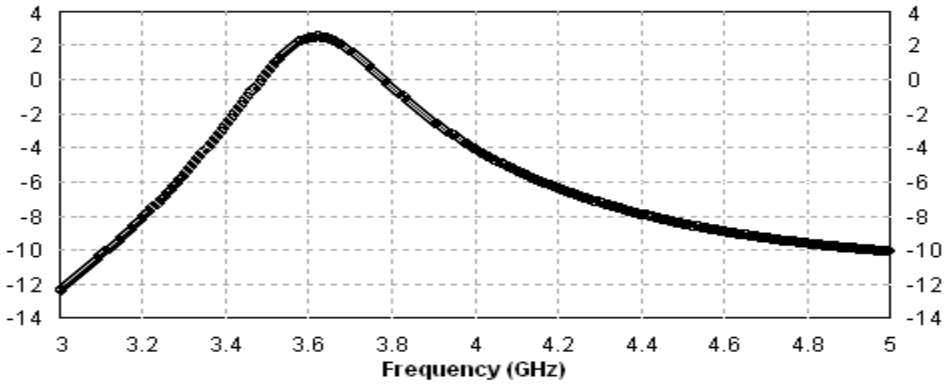

Figure 5.4: Variation of gain (dBi) with frequency for hexagonal geometry

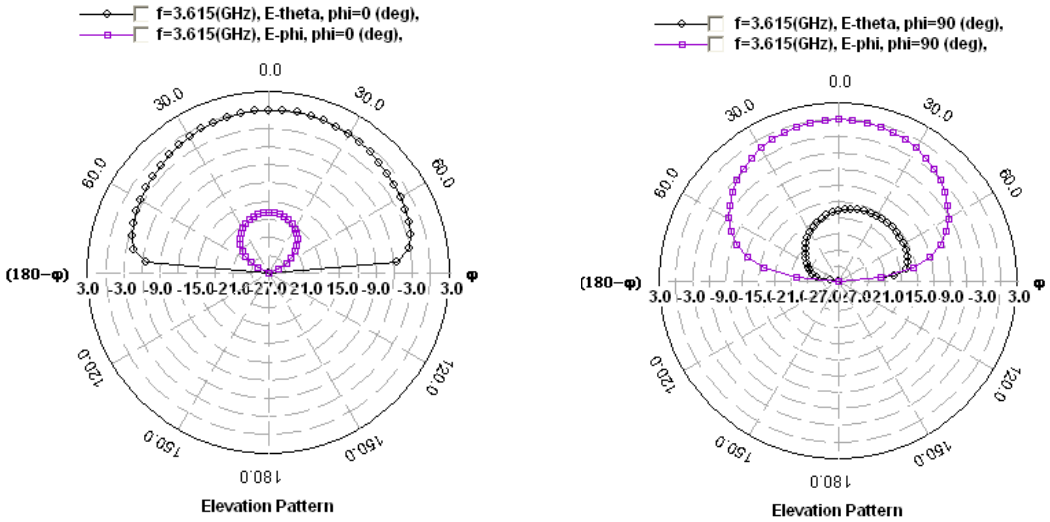

Figure 5.5: Simulated co and cross polar radiation pattern of simple hexagon at 3.61GHz a) E-plane b) H-plane

The gain of this antenna is also low (2.44 dBi) as indicated in figure 5.4. The E and H plane co and cross polar radiation pattern of antenna are shown in figure 5.5 which indicates that the radiation intensity is maximum normal to the patch geometry. It can be observed that in the range of 3 GHz to 5 GHz, antenna is resonating at a single frequency and its bandwidth is narrow and it is linearly polarized therefore needs improvement before it may be considered as a possible candidate for suitable application.

5.3 Stacked antenna structure

The stacked antenna structure is shown in figure 5.6. It consists of hexagonal and rectangular patches. An additional rectangular patch of dimension (length l' = 24 mm and width w = 21 mm is introduced just over the hexagonal patch geometry

through teflon screws. The patch lying on upper substrate is little larger in size than that of hexagonal patch and the upper structure does not have any metallic ground plane. These patches are formed on two glass epoxy FR4 substrates having substrate permittivity ε_r= 4.4, loss tangent tanδ= 0.025 and substrate thickness '*h*' = 0.159 cm. The size of upper patch is slightly greater than the size of lower patch which is optimized for obtaining wider bandwidth.

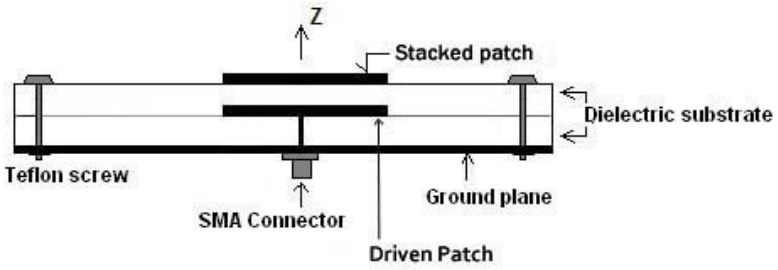

Figure 5.6: Top and side views of stacked antenna geometry without airgap

The probe feed is applied for excitation of lower patch of the antenna. The electromagnetic coupling among patches causes transformation of energy from the lower patch to the upper patch. The significant factor in improvement of the bandwidth of stacked patch antenna is due to overlapping of close resonant frequencies of lower and the upper patch.

5.4 Preliminary study

In this section, we will discuss step by step the preliminary analysis that we have performed out for designing antenna structure. This will help future designers to design more improved antenna geometries.

5.4.1 Dimension of parasitic patch

The inset feedline is applied on the lower hexagonal patch and in the first step of modification, separation between lower patch (driver element) and upper patch (parasitic patch) '*d*' is maintained equal to zero. In this way the upper patch is parasitically coupled to the lower patch or the driver element. By varying length and width of the upper rectangular patch the performance of antenna is optimized to achieve best performance. These optimizations were carried out by obtaining impedance bandwidth and directive gain values. The seven considered structures are

reported in table 5.1. The investigation for all seven cases was performed by using IE3D simulation software. Figs. 5.7 and 5.8 show the variations of reflection coefficient, and directive gain respectively as a function of frequency for all the seven cases.

TABLE 5.1: DIMENSIONS OF UPPER RADIATING PATCH

Sr. No.	Antenna Configuration	Upper Radiating Patch	
		Length (mm)	Width (mm)
1	Case 1	24	24
2	Case 2	24	23
3	Case 3	24	22
4	Case 4	24	21
5	Case 5	21	24
6	Case 6	22	24
7	Case 7	23	24

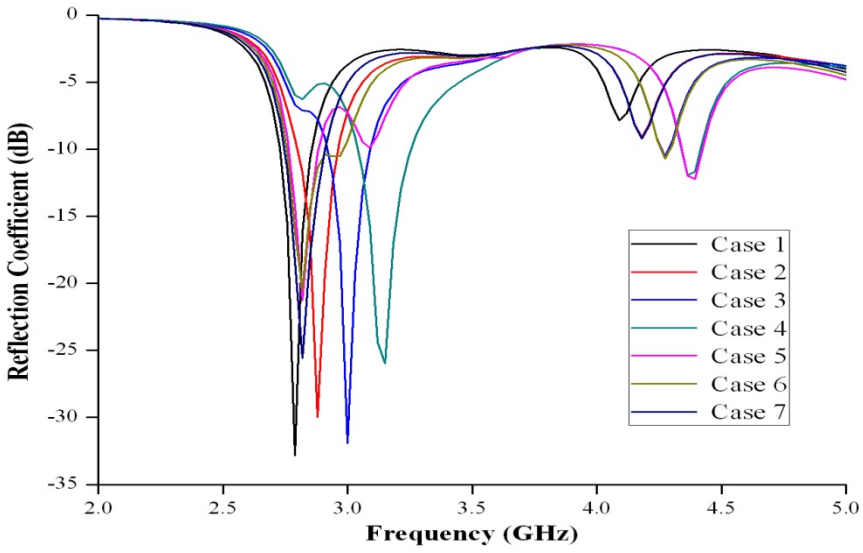

Fig. 5.7. Variations of reflection coefficient with frequency for seven considered configuration

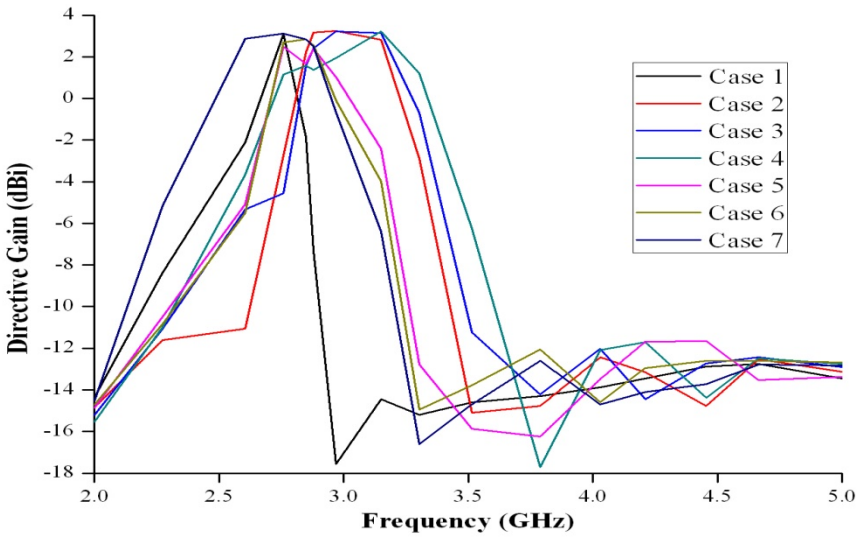

Figure 5.8. Variations of broadside directive gain with frequency for six considered configurations

From this investigation, we found that the case 4, (where the parasitic patch is slightly larger in length than the radiating patch) provide largest impedance bandwidth (7.66%). Furthermore it also gives the maximum directive gain of 3.25 dBi. Thus for further optimizations, we have selected the geometry considered under case 4. From this discussion we found that when parasitic patch is marginally larger than driven patch we get best performance.

The simulated return loss variation shown in figure 5.9 indicates that antenna now resonates at frequency 3.13 GHz. The resonance frequency of this modified antenna is marginally decreased in comparison to that of simple hexagonal geometry reported earlier (3.61GHz) perhaps due to increase of antenna thickness. As shown in figure 5.10, the simulated VSWR value corresponding to the resonant frequency is 1.08 which suggests good matching between antenna and feed arrangement.

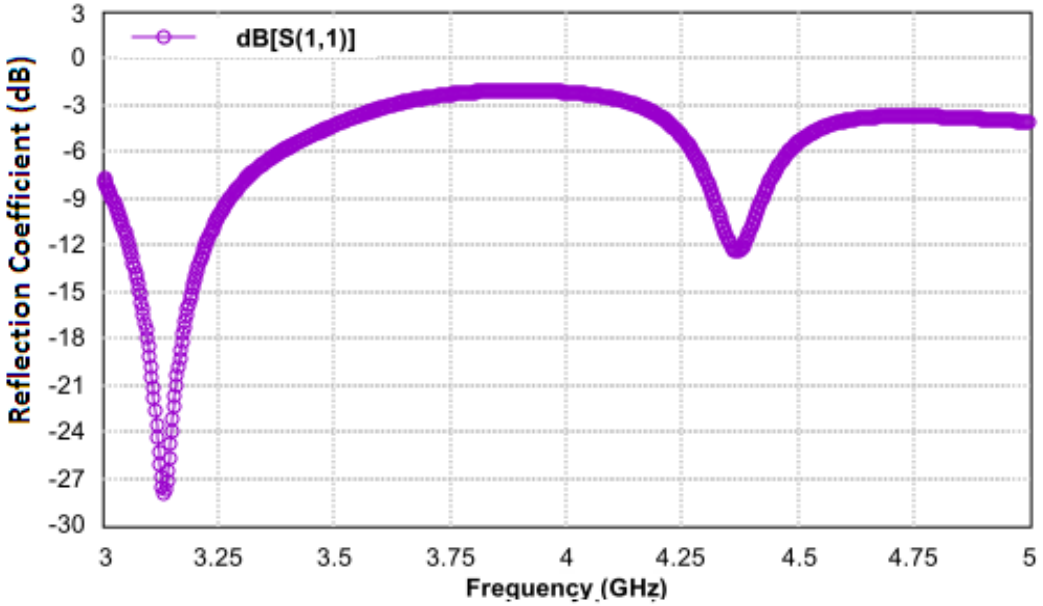

Fig. 5.9. Variation of reflection coefficient (S_{11}) of stacked geometry without air gap with respect to frequency

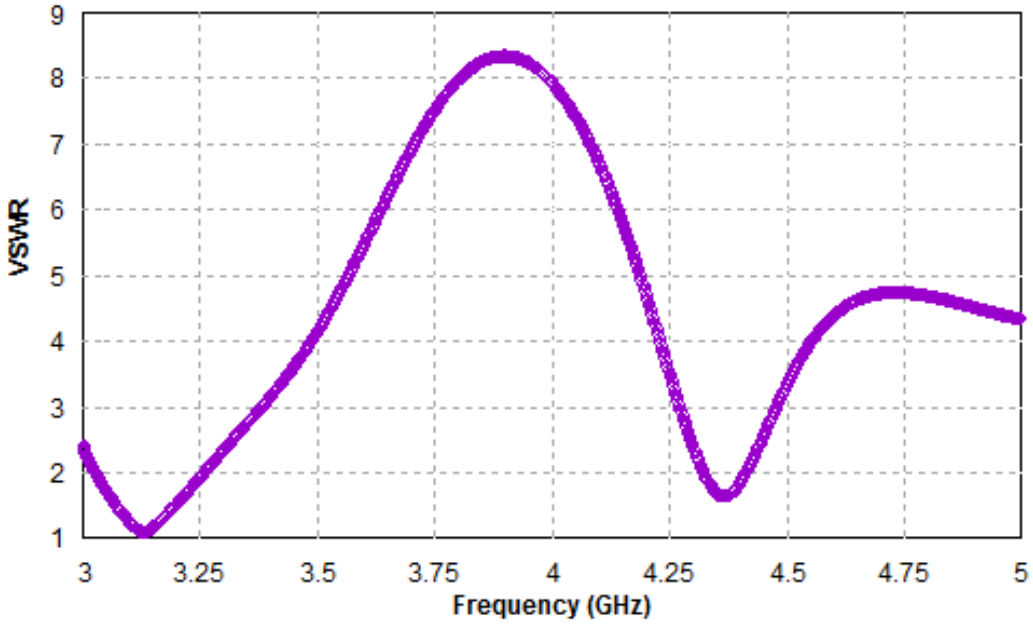

Fig. 5.10. VSWR of stacked geometry without air gap as a function of frequency

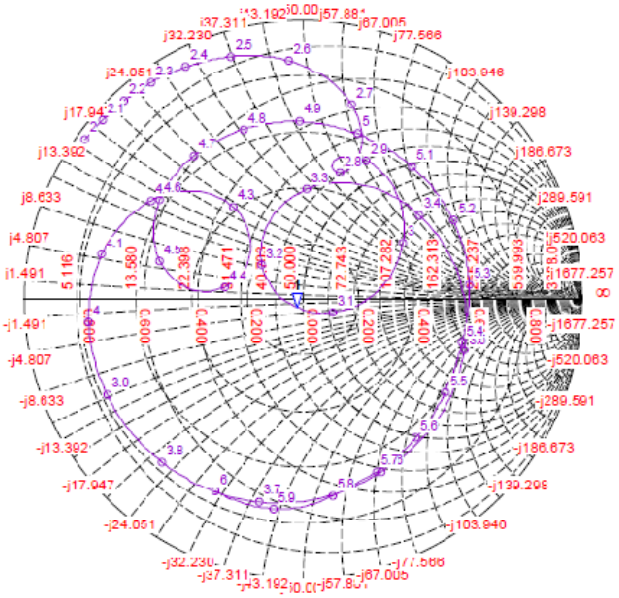

Fig. 5.11. Input impedance of geometry stacked geometry without air gap

The bandwidth of antenna is now increased to 7.66% which is twice more than that of earlier reported simple hexagonal patch geometry. The simulated gain of this antenna is close to 3.25 dBi while input impedance at the resonance frequency is close to (48.04-j3.36) ohm as shown in figure 5.11. These results again indicate that this modified patch geometries is still unsuitable for modern communication systems. Hence we separated the two substrate materials in steps. This separation in lower and upper substrates has reduced the effective permittivity and loss tangent of substrate material. The performance of this antenna is reported in next section.

5.4.2 Optimization of thickness of air gap

In the previous discussion; we have applied the parasitic and driven patches and patch dimensions are optimized. Now in this section, we will retain those patch parameters and we will vary the air gap to achieve best performance from antenna. The air gap is varied in the steps of 0.5mm and simulated parameters are reported in table 5.2.

TABLE: 5.2: VARIATION OF AIRGAP THICKNESS

Air gap	Resonant Frequency (GHz)	Impedance Bandwidth (%)	Gain (dBi)
0.5	4.86 6.0	5.06 13.55	1.694 0.386
1	4.32 4.94 6.06	7.9 6.57 15.26	3.42 1.87 0.39
1.5	4.25 5.6	9.62 25.4	5.88 0.71
2	4.21 5.66	10.11 23.58	5.59 1.09

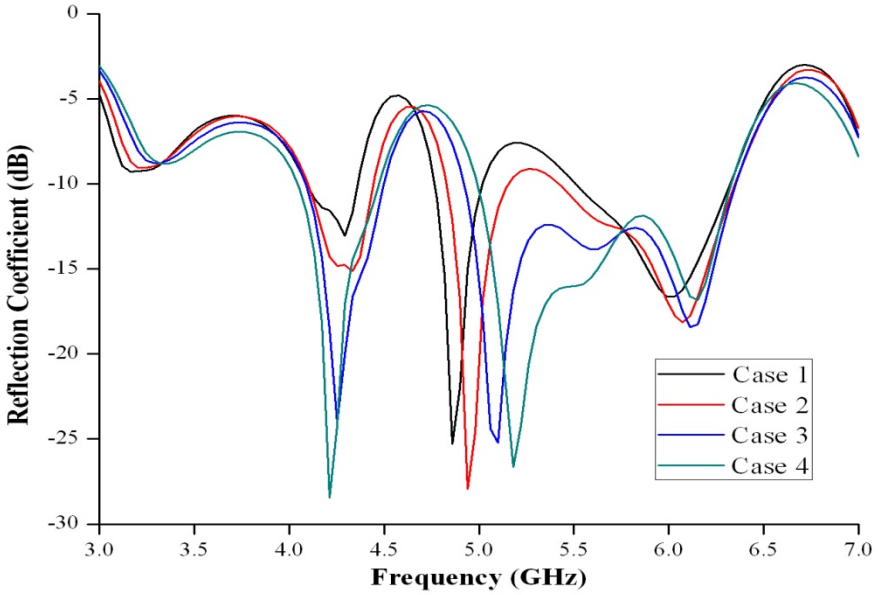

Fig. 5.12. Reflection coefficient versus frequency for different values of air gap in between driven and parasitic patches of stacked microstrip antenna configurations

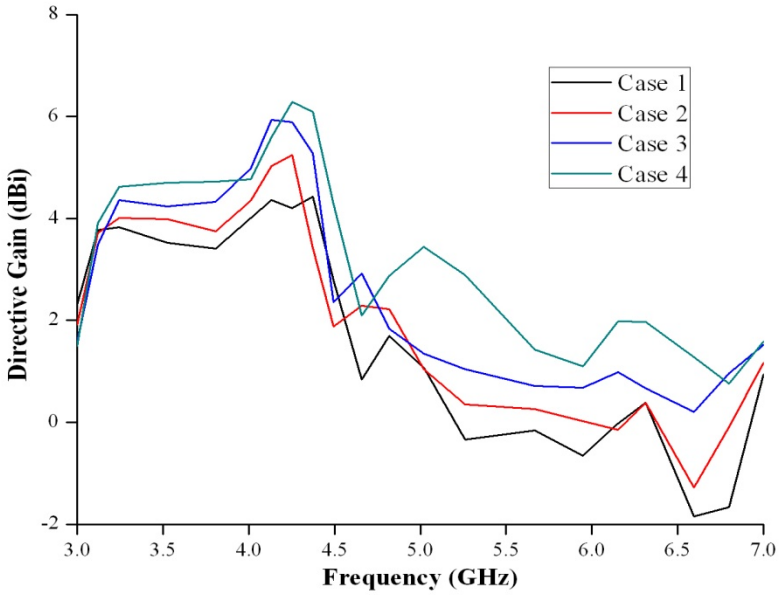

Fig. 5.13. Directive gain versus frequency for different values of air gap in between driven and parasitic patches of stacked microstrip antenna configurations

The variations of reflection coefficient and directive gain of antenna as a function of frequency are shown in figures 5.12 and 5.13. From the analysis; we found that when air gap is equal to 1.5 mm, we get maximum impedance band width (25.4%). On further increasing air gap, impedance bandwidth reduces.

5.4.3 Using pin short

Inserting pin short with feed is also a technique to enhance the bandwidth. Pin short technique is used to reduce the patch size. Pin short is used to create extra capacitance to reduce the inductive effect of the probe feed and this also increase the current path, which leads to improvement in the bandwidth [192-193]. The antenna geometry described in preceding section is further modified in steps by applying a shorting pin in the driven element and by varying air gap between driven and parasitic elements for best performance. The variation of shorting pin location and its effect on impedance bandwidth is reported in table 5.3.

TABLE: 5.3: VARIATION OF SHORTING PIN LOCATION

Sr. No.	Shorting pin location (mm)	Resonant Frequency(GHz)	Impedance Bandwidth (%)	Minimum Axial Ratio	Axial Ratio Bandwidth
1.	(-1, 9.5)	4.085	20.04	6 dB	--
2.	(-2, 9.5)	3.24 4.09	4.84 23.03	1.79 dB	64.7 MHz
3.	(-3, 9.5)	3.26 4.08	2.49 24.38	1.72 dB	46.6 MHz
4.	(-4, 9.5)	3.796	37.22	1.16 dB	58.44 MHz
5.	(-5, 9.5)	3.93	35.61	0.088 dB	73 MHz
6.	(-6, 9.5)	4.006	34.59	3.17 dB	--

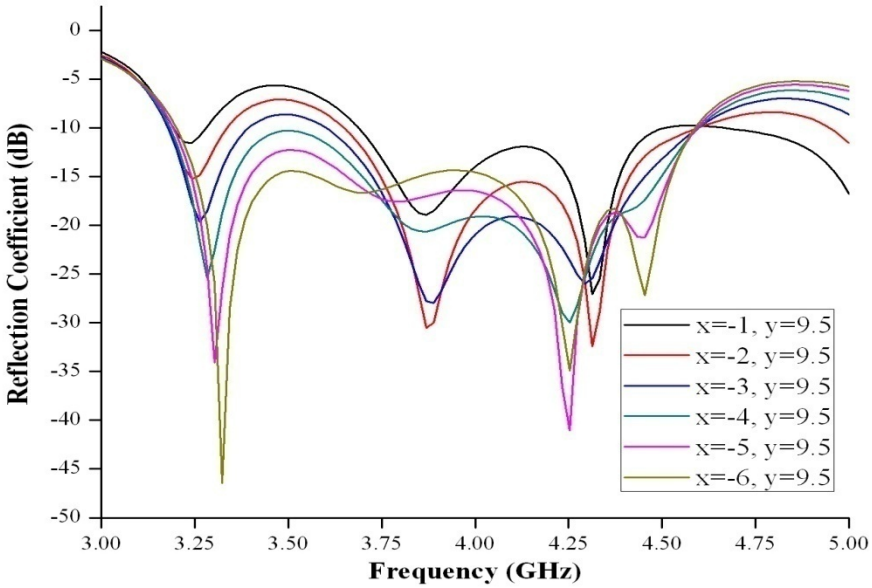

Fig. 5.14. Reflection coefficient versus frequency for different location of shorting pin in driven patch of stacked microstrip antenna configurations

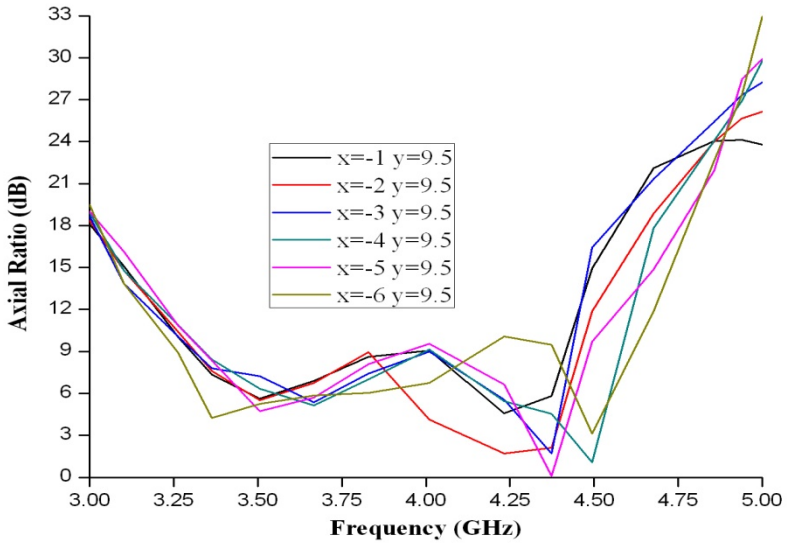

Fig. 5.15. Axial ratio versus frequency for different location of shorting pin in driven patch of stacked microstrip antenna configurations

The variations of reflection coefficient and axial ratio of the antenna as a function of frequency are shown in figures 5.14 and 5.15. From the analysis; we found that when shorting pin is located at (-5, 9.5), we get maximum impedance band width (35.61%) and axial ratio band width (73 MHz) and minimum axial ratio (0.088 dB). The variation of gain is almost constant with in the 10 dB impedance band width.

5.5 Stacked arrangement of hexagonal and rectangular microstrip patches for circularly polarized broadband performance

In this section, we applied a parasitic patch over the driven patch considered in previous section and an air gap is applied between the two dielectric layers with shorting pin. The patch dimensions of stacked patch, thickness of air gap and location of shorting pin are already optimized in previous sections and hence same values are retained for the present work. In this way, the overall thickness of antenna is less than 5 mm. The side view feeding arrangement on driven patch of stacked antenna arrangement is shown in Figure 5.16(a), also the designed geometry of parasitic patch and driven patch is shown in fig 5.16(b) and 5.16(c).

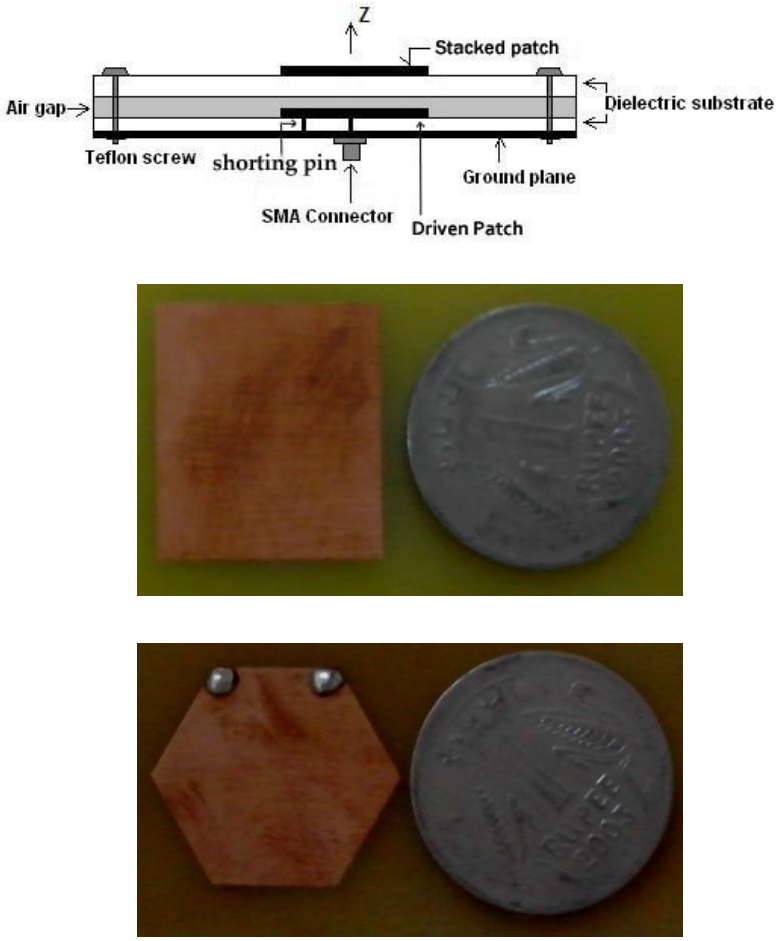

Fig. 5.16. (a) Side view of stacked antenna structure with shorting pin. (b) Top view of designed rectangular patch. (c) Top view of designed hexagonal patch with feed and shorting pin.

5.5.1 Experimental performance of fabricated arrangement of antennas

The performance of proposed probe-fed stacked arrangement of microstrip patch antenna was measured by using available experimental facilities and these measured parameters are compared with the simulated parameters obtained through IE3D simulator. The obtained results are systematically presented in this section.

(a) Reflection coefficient

The simulated and measured variation of reflection coefficient (S_{11}) for the stacked antenna as a function of frequency is shown in Figures 5.17 and 5.18 respectively. The measured variation of reflection coefficient (S_{11}) shows that antenna is resonating at two frequencies (3.41 GHz and 4.40 GHz) and presenting impedance bandwidth nearly 1.398 GHz or 31.72% with respect to central frequency of 3.94 GHz. The simulated variation of reflection coefficient (S_{11}) shows that antenna is

resonating at two frequencies (3.29 GHz and 4.24 GHz) and presenting impedance bandwidth nearly 1.53 GHz or 35.4 % with respect to central frequency.

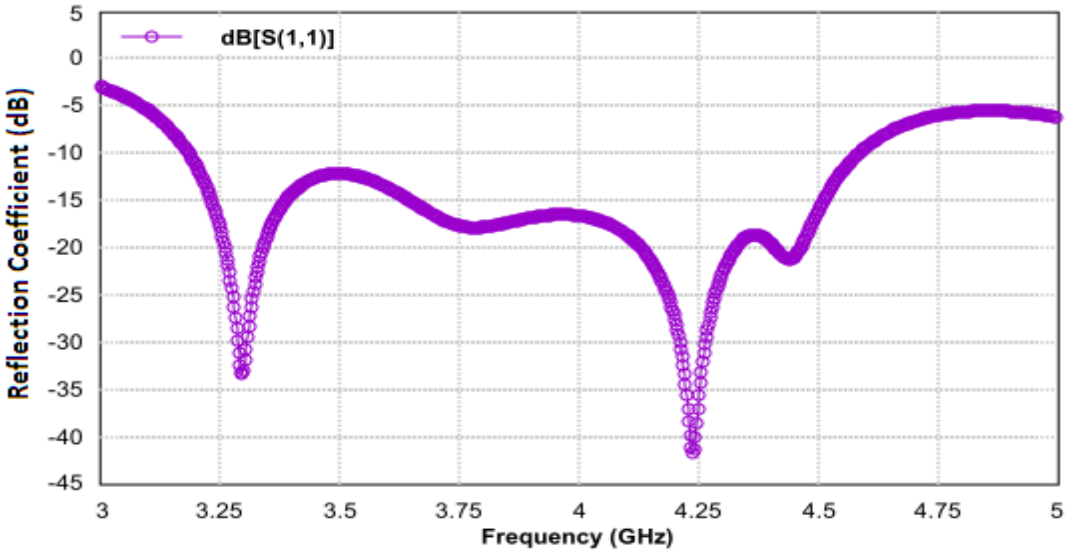

Fig. 5.17. Simulated reflection coefficient (S_{11}) of stacked geometry with air gap and shorting pin

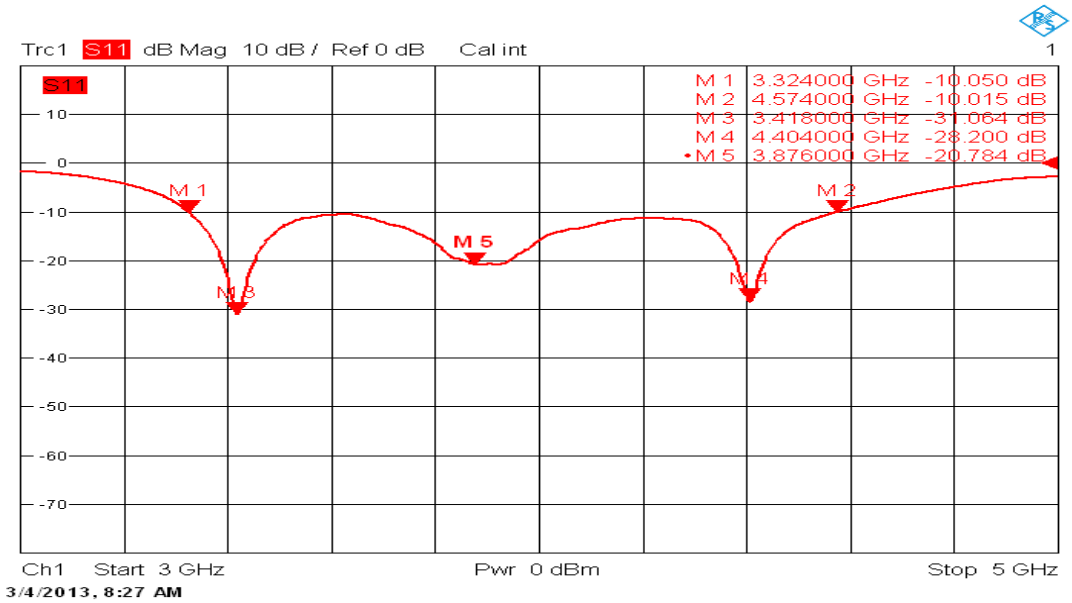

Fig. 5.18. Measured reflection coefficient (S_{11}) of stacked geometry with air gap and shorting pin

These results show good agreement between measured and simulated results. The reflection coefficient of the proposed geometry in the whole bandwidth is well below 10 dB which implies an excellent matching between the antenna and the feed structure in operating bandwidth band.

The simulated and measured VSWR variations of modified antenna with frequency are shown in figures 5.19 and 5.20 respectively. As desired, antenna presents good matching within the impedance bandwidth as the VSWR of antenna in entire bandwidth range is well below 2:1 value. The measured VSWR values at the two resonant frequencies are 1.05 and 1.08 which are comparable to the simulated results (1.05 and 1.101).

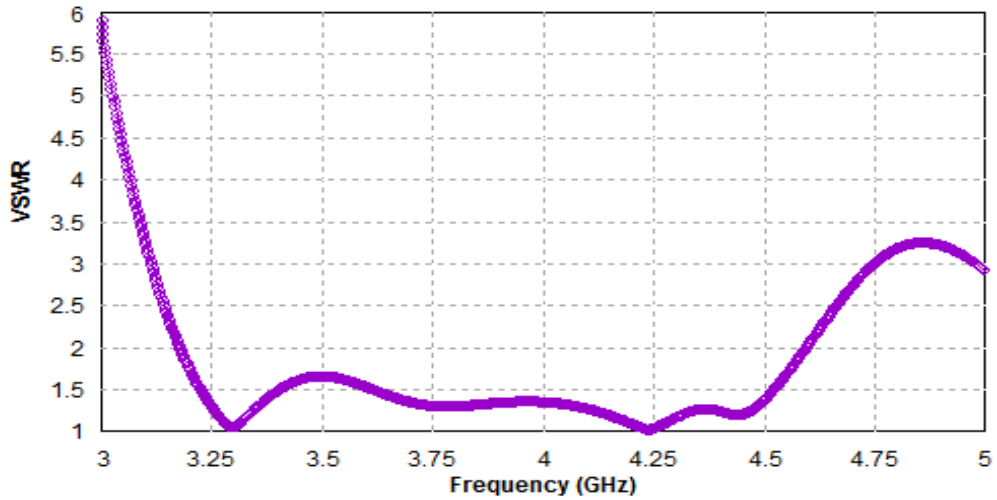

Fig. 5.19. Simulated Voltage Standing Wave Ratio (VSWR) of stacked geometry with air gap h_a = 1.59 mm and shorting pin

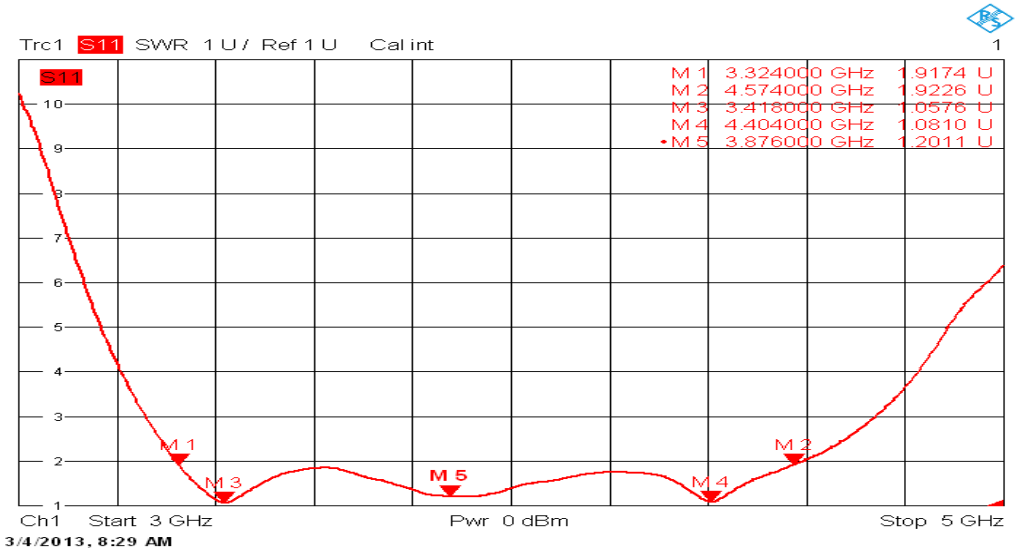

Fig. 5.20. Measured Voltage Standing Wave Ratio (VSWR) of stacked geometry with air gap h_a = 1.59 mm and shorting pin

(b) Input impedance and polarization

The simulated and measured input impedance variations of modified antenna with frequency are shown in figures 5.21 and 5.22 respectively. The measured input impedance related to two resonant frequencies are (52.36 - j1.61) ohm and (51.38 – j3.69) ohm respectively which are nearly reaching to 50 ohm impedance of the coaxial feed line. Possibility of circular polarization can also be observed from the smith chart, where a loop is formed. The loop area becomes very small, if the two degenerate modes which are essential for achieving circular polarization are very close to each. Larger is this loop area; larger will be axial ratio. The appearance of small loop in smith chart suggests that the excited mode in the conventional patch antenna is now split in two nearly degenerate orthogonal modes of equal amplitude but with 90^{o} phase difference which results into circular polarization. The possibility of circular polarization is confirmed by testing the axial ratio variation with frequency.

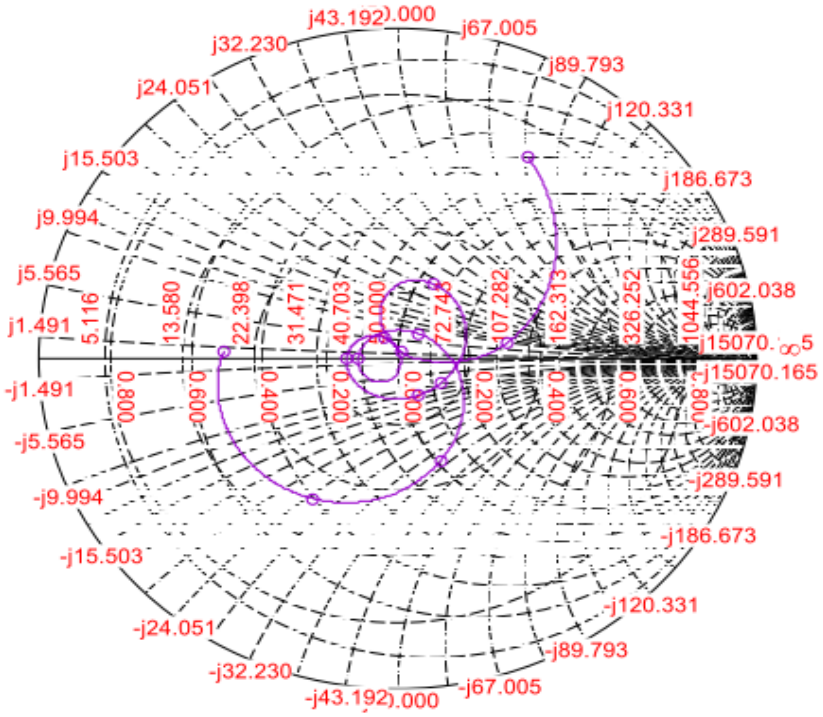

Fig. 5.21. Simulated input impedance of stacked antenna geometry with air gap and shorting pin

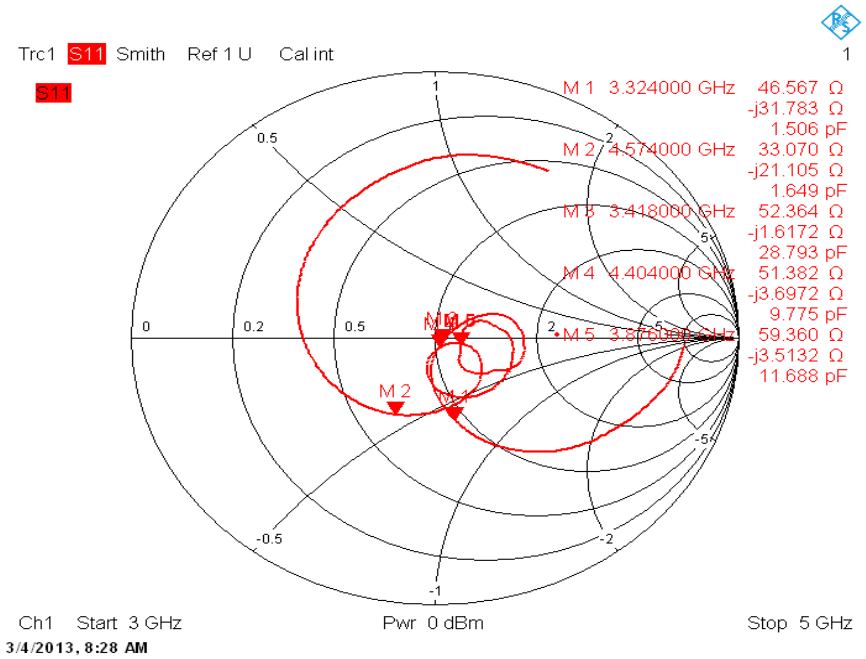

Fig. 5.22. Measured input impedance of stacked antenna geometry with air gap and shorting pin

The proposed stacked arrangement shows circularly polarized behavior over a range of frequency. By varying shorting pin location on the patch, axial ratio variation with frequency is achieved. The feed point is tuned till axial ratio reaches value close to 0 dB. The axial ratio versus frequency graph is shown in figure 5.23, which shows that axial ratio attains minimum value at resonance frequency of 4.352 GHz. The axial ratio is well within 3dB range in the whole range of axial bandwidth (from 4.311GHz to 4.384GHz). The axial ratio bandwidth is 73 MHz with respect to central frequency. For analyzing the type of polarization, simulated and measured E-plane right and left circularly polarized patterns of the stacked geometry at frequency 4.352 GHz is obtained as shown in figure 5.24 and 5.25. The simulated E-plane right circular pattern is nearly 34.3 dB down while in measured it is 15.5 dB down as compared to E-plane left circular pattern. This signifies that radiations at frequency 4.352GHz is left circularly polarized in nature.

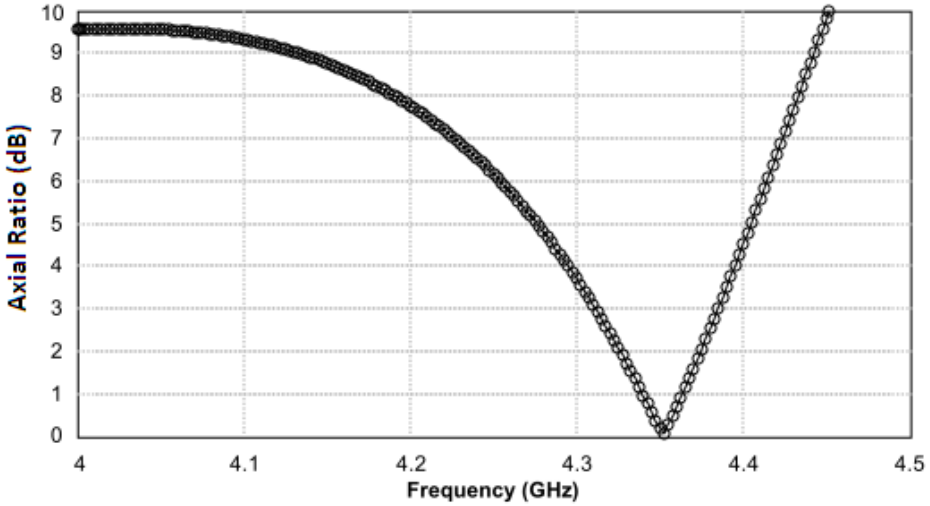

Fig. 5.23. Variation of axial ratio of stacked antenna geometry with air gap and shorting pin

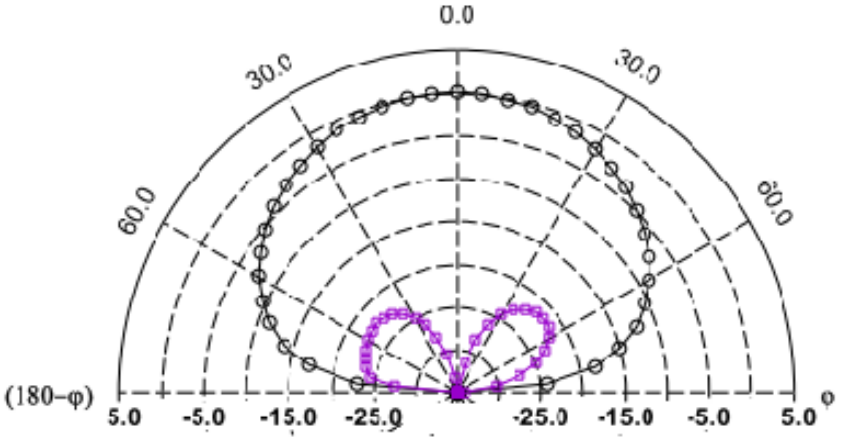

Fig. 5.24. E-plane left and right circular polarization patterns at 4.352 GHz

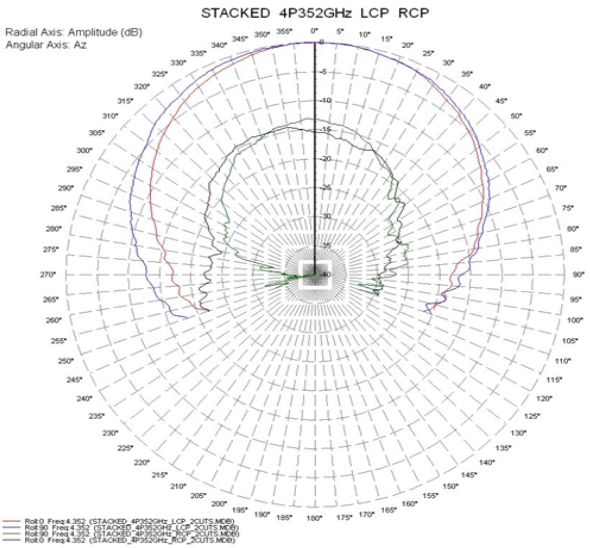

Fig. 5.25. E-plane left and right circular polarization patterns at 4.352 GHz

(c) Gain, Radiation efficiency and radiation patterns of antenna

The gain of the antenna with respect to frequency is shown in figure 5.26 that indicates that in the complete bandwidth; gain is uniform in nature and nearly 6 dBi. The variation in gain at the desired frequency range is well within 1 dBi.

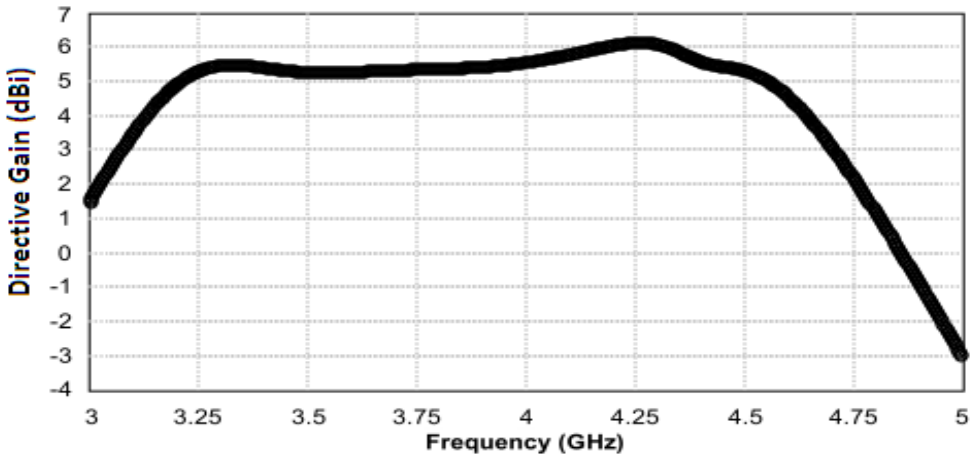

Fig. 5.26. Variation of gain with frequency of stacked antenna geometry with air gap and shorting pin

The radiation efficiency of proposed geometry is shown in figure 5.27 which is close to 55% for entire bandwidth.

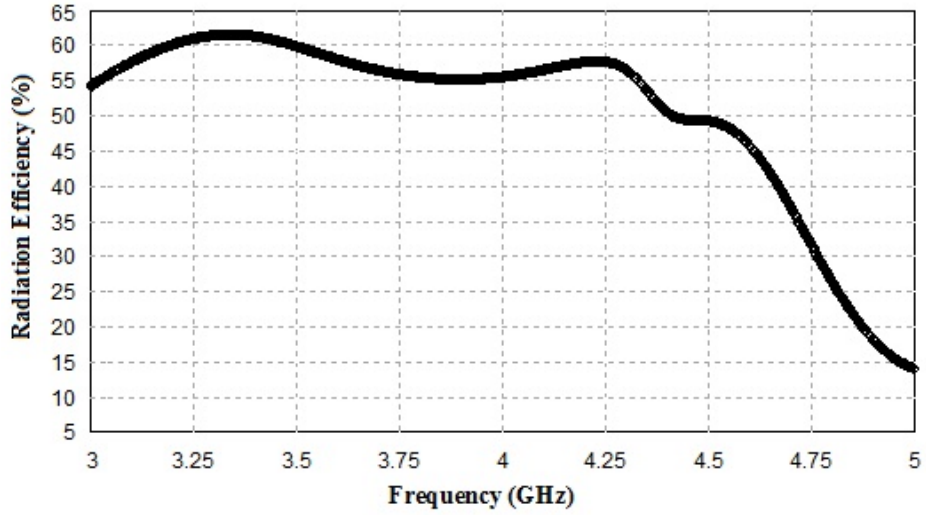

Fig. 5.27. Variation of Radiation Efficiency with frequency for proposed antenna

The simulated E and H plane elevation radiation patterns of antenna geometry with air gap (h_a = 1.59mm) at five different frequencies within the impedance bandwidth region have been shown in figures 5.28 (a) and (b). The measured E and H radiation patterns at two resonance frequencies of 3.41 GHz and 4.40 GHz are also shown in

figure 5.29 and 5.30. It may be seen that the radiation patterns at resonance frequencies are perpendicular to the patch and similar in shape.

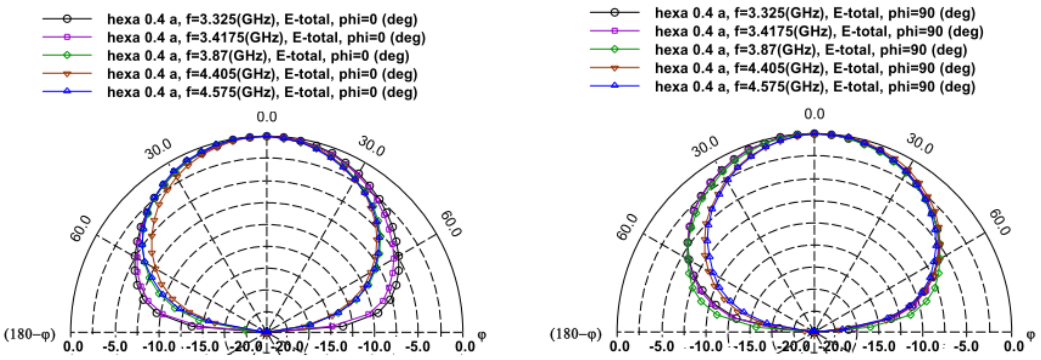

Fig. 5.28. Elevation gain pattern of antenna as a function of elevation angle and frequencies (a) Phi=0^0 and (b) Phi=90^0

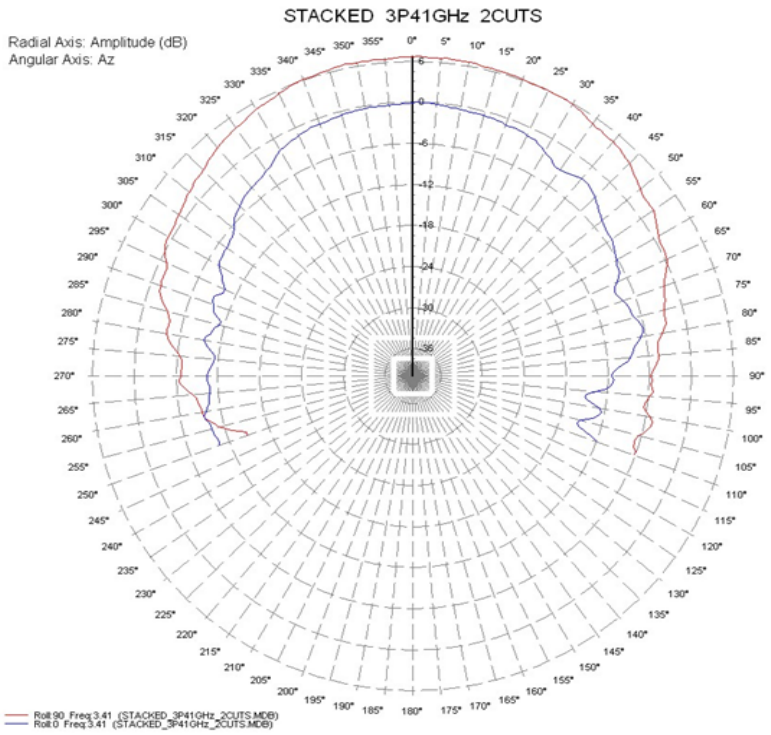

Fig. 5.29. Measured E and H radiation pattern at 3.41 GHz

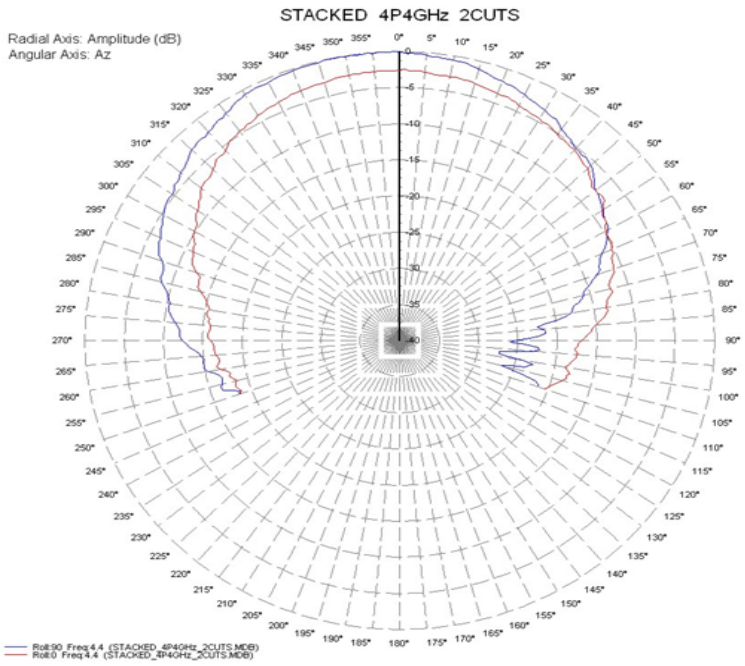

Fig. 5.30. Measured E and H radiation pattern at 4.40 GHz

A comparison between the radiation performances of different antenna geometries discussed in this chapter is given below:

TABLE 5.4: COMPARISON OF RADIATION PROPERTIES OF DIFFERENT ANTENNA GEOMETRIES

Antenna Geometry	Resonant frequency (GHz)		Impedance Bandwidth (%)		Gain (dBi)	
Conventional Hexagonal Patch antenna	3.61		3.5		2.44	
Stacked hexagonal and rectangular patch	3.13		7.66		3.25	
Stacked hexagonal and rectangular patches with shorting pin and airgap	Simulated	Measured	Simulated	Measured	Simulated	Measured
	3.29 4.24	3.41 4.40	35.4	31.72	5.19 5.72	5.7 4.3

A quantitative comparison of proposed geometry with the antennas reported in past is provided in the table 5.5.

TABLE 5.5: COMPARISON OF PROPOSED ANTENNA WITH OTHER REPORTED ANTENNAS

Reference	Driven Patch Dimension (in mm)	Stacked Patch Dimension (in mm)	Resonant Frequency (GHz)	BW	Gain (dBi)	Circular Polarization
39	Major axis=26 Minor axis=28.86	Diameter = 26	2.69 GHz 2.80 GHz	27.9% (940 MHz)	6	Yes
187	28×28	Diameter = 44	2.41GHz 2.59GHz	16% (540 MHz)	7.3	Yes
190	Diameter = 32	30×30	2.1 GHz 2.2 GHz	-	3	Yes
Stacked Geometry	L=24 W=20.5	24×21	3.41 GHz 4.40 GHz	31.72% (1.398 GHz)	5.7 4.3	Yes

5.6 Summary

In this chapter we have discussed three geometries single layer hexagonal patch, stacked arrangement of rectangular and hexagonal patches and stacked arrangement of hexagonal and rectangular microstrip patches with shorting pin for circularly polarized broadband performance. Single layer hexagonal patch antenna presents low impedance bandwidth and gain values. The radiations are linearly polarized in nature. On the other hand, stacked arrangement of rectangular patches provides significantly improved impedance bandwidth and gain. Finally stacked arrangement of hexagonal and rectangular microstrip patches is considered which not only provides further improved impedance bandwidth and gain but also axial ratio bandwidth.

Chapter 6

Conclusions and Future Work

6.1 Conclusions

In the past decade, microstrip antennas found significant applications in commercial as well as military appliances because of their low profile, small size and low manufacturing cost on mass production. Especially in the area of satellite mobile communications, Global Positioning Systems (*GPS*) and Modern Wireless Communication Systems based on techniques like Wireless Local Area Network (*WLAN*), Worldwide Interoperability for Microwave Access (*Wi-Max IEEE* 802.16) Communication Systems etc. applications in Deep Space Satellite Communication Systems, Handheld Mobile Sets, HiperLAN, Wireless Communication Systems based on techniques like Wireless Local Area Network (WLAN), Wireless Fidelity (Wi-Fi IEEE 802.11), Worldwide Interoperability for Microwave Access (WiMax IEEE 802.16), Bluetooth (IEEE 802.15.1), Zigbee (IEEE 802.15.4) and Ultra-Wide Band (UWB IEEE 802.11) Communication Systems etc. The utility of these antennas in a way have completely changed the scenario of new generation wireless communication technology. Bandwidth enhancement is generally insisted for several practical applications. Present day mobile communication systems need smaller physical antenna size in order to meet the specifications of mobile handset units which are getting smaller day by day. Thus two main areas viz. compact size and bandwidth enhancement are becoming critical design issues for practical applications of microstrip antennas and extensive amount of work has been reported to achieve compact and broadband microstrip antennas. the demand for microstrip antennas is most evident. In other areas, such as remote sensing, medical usage, automobile collision avoidance and aircraft systems, microstrip antennas also found important applications. Extensive research and development activities in the area of patch antennas are still underway to improve their performance. Efforts are mainly on to improve bandwidth, gain, directivity and efficiency as it is believed that these small size antennas will continue to benefit the human race for many future years.

In this thesis the main focus is given on designing of compact dual frequency and broadband microstrip patch antennas. Since the theoretical analysis of modified patch antenna geometry includes rigorous and crude mathematical approximations, the main emphasis is given to simulation and experimental work. The thesis reports the radiation characteristics of the following five geometries of microstrip antennas in free space:

i. Modified pentagonal patch antenna with defected ground plane for Wi-Max and WLAN applications.
ii. Modified square patch antenna with circular slot on defected ground for Wi-Max band.
iii. Triangular patch antenna with asymmetric slot in ground plane for broadband performance
iv. Modified circular patch antenna with finite ground plane for C- band applications.
v. Stacked arrangement of rectangular and hexagonal patches having wide impedance bandwidth and circularly polarized performance.

Before taking into consideration the antenna structures for present analysis, initially a detailed survey of recent existing literature with a view to facilitate the study was carried out. The conventional geometries are modified and extensive analysis of these modified geometries of microstrip antennas is carried out and their results are presented systematically.

No simulation result can be considered well versed for practical application of antenna in communication devices till its radiation characteristics are not verified experimentally. The selected antenna geometries are simulated with method of moment (MOM) based IE3D and CST Microwave studio simulation software, which are very strong in providing results with large accuracy. Antenna designs was simulated and optimized over and over again with variation in different geometrical parameters till satisfactory results are obtained. Based on this outcome, modified antenna geometries were locally fabricated on glass epoxy FR-4 substrate and designed antennas were mainly tested. Radiation patterns are measured in an anechoic chamber while input impedance, VSWR and return loss measurements are

done by using vector network analyzer. All the measured results are found in close match with simulated outcomes.

6.2 Scope for future work

Work on microstrip antennas has no limits. It requires only dedication, motivation and patience. The future work is proposed to have further improvement in the antenna performance. Extensive research work on microstrip antennas is going on in different parts of the world because these antennas are finding extensive application in handheld mobile sets, direct broadcasting systems (*DBS*), direct to home systems (*DTH*) and global positioning systems (*GPS*) and modern wireless systems. The utility of these antennas in a way have completely changed the scenario of communication technology.

To fulfill these requirements we have carried out study of various modified microstrip patch geometries having various types of slots in patch as well as modified patch boundaries. Since the mathematical modeling of these modified microstrip antennas includes a rigorous and complex mathematics. Most of the scientists find it easy to simulate these geometries using available EM simulation tool directly and verify the obtained results with measured results. Researchers having interest in mathematical modeling have enough scope of work in this direction. The antenna geometries with involved critical variations will need rigorous modeling due to involvement of boundary conditions. Most of the mathematical modeling is carried out by applying simple models like cavity model. With more involved models like method of moments, FDTD, finite integration method and finite element method etc. require more modeling and provide improved results in comparison to achieved with transmission line model and cavity model.

The solution of wave equations under the presence of these boundary conditions will also require development of software and hence scope of software development for designing of these patch antennas will also be required. This creates a vast scope for the researchers interested in computer programming. Since recent available softwares are very costly, this will be a useful effort for the research community. There are some discrepancies among simulated and measured results which are

caused by human errors that might occur during fabrication processes. Thus, further development is needed to further improve the fabrication processes. The fabrication process may involve laminator thermal transfer process, etching and soldering. Besides, a few of prototypes should be fabricated in order to get a good result in the measurement of the antenna as it is difficult to get a good result in just a fabrication process; experience and knowledge is needed. The importance of feed mechanism and choice of substrate cannot be ignored. The antenna performance to some extent is influenced by location and proper position of feed. In this thesis, only two types of feed have been used i.e. coaxial feed and microstriplne feed. In future, other types of feed methods can be applied to analyze the overall performance of the antenna along with optimization of other parameters.

In conclusion, this thesis has provided an insight into design and fabrication of novel compact dual band and broadband patch antennas useful for communication purposes. It will form a platform for researchers working in this field towards realizing the implementation of these geometries for current and future communication systems. In this way one can find enough scope of working on these highly versatile antennas.

References

[1] G.R.M. Garratt, "The Early History of Radio from Faraday to Marconi," *London Institution of Electrical Engineers*, 1994.

[2] Girish Kumar and K.P. Ray, *Broadband Microstrip antennas*, Norwood Artech House, 2003.

[3] R. Garg, P. Bhartia, I. Bahl and A. Ittipioon, *Microstrip antenna design handbook*, Artech House Inc., MA, England, 2001.

[4] C. G. Christodoulou and P. F. Wahid, *Fundamentals of Antennas: Concepts and Applications*, Bellingham, WA: SPIE Optical Engineering Press, 2001.

[5] Zhi Ning Chen and Michael Y. W. Chia, *Broadband Planar Antennas Design and Applications*, John Wiley & Sons Ltd, 2006.

[6] Kin-Lu Wong, *Compact and Broadband Microstrip Antennas*, John Wiley & Sons, Inc, 2002.

[7] N. Nasimuddin, *Microstrip Antennas*, InTech, 2011.

[8] G.A. Deshamps, "Microstrip Microwave Antennas," *Third USAF Symposium on Antennas*, 1953.

[9] W. Stutzman and G. Thiele, *Antenna Theory and Design*, New York, John Wiley & Sons, Inc., 1998.

[10] K. Fujimoto and J.R James, *Mobile Antenna Systems Handbook*, Artech House, 1994.

[11] Z. Aijaz and S. C. Shrivastava, "Effect of the Different Shapes: Aperture Coupled Microstrip Slot Antenna," *International Journal of Electronics Engineering*, pp. 103-105, 2010.

[12] I. J. Bahl and P. Bhartia, *Microstrip Antennas,* Dedham, MA: Artech House, 1980.

[13] J. R. James, and P. S. Hall, *Handbook of Microstrip Antennas,* Vol. 1, London: Peter Peregrinus Ltd., 1989.

[14] K. P. Ray and G. Kumar, ''Determination of the Resonant Frequency of Microstrip Antennas,'' *Microwave Optical Tech. Letters,* vol. 23, pp. 114–117, 1999.

[15] A. Benalla and K. C. Gupta, ‘‘Analysis of Two-Port Circular Microstrip Patch Antennas Using Multiport Network Model,’’ *Proc. ISAP,* pp. 9–12, 1989.

[16] F. Abboud, J. P. Damiano and A. Papiernik, ‘‘New Determination of Resonant Frequency of Circular Disc Microstrip Antenna: Application to Thick Substrate,’’ *Electronics Letters,* vol. 24, pp. 1104–1106, 1988.

[17] N. Kumprasert, and W. Kiranon, ‘‘Simple and Accurate Formula for the Resonant Frequency of the Circular Microstrip Disk Antenna,’’ *IEEE Trans. Antenna Propagation,* pp. 1331–1333, 1995.

[18] J. Q. Howell, ‘‘Microstrip Antenna,’’ *IEEE Trans. Antennas Propagation,* Vol. AP-23, pp. 90–93, 1975.

[19] I. Wolff, and N. Knoppik, ‘‘Rectangular and Circular Microstrip Disk Capacitors and Resonators,’’ *IEEE Trans. Microwave Theory Tech.,* pp. 857–864, 1974.

[20] A. G. Derneryd, ‘‘Microstrip Disc Antenna Covers Multiple Frequency,’’ *Microwave Journal,* pp. 77–79, 1978.

[21] J.G. Kretzschmar, “Wave Propagation in Hollow Conducting Elliptical Waveguides,” *IEEE Transactions on Microwave Theory and Techniques,* vol. 18, pp. 547-554, 1970.

[22] N. Kumprasert, “Theoretical Study of Dual-Resonant Frequency and Circular Polarization of Elliptical Microstrip Antennas,” *IEEE Antennas and Propagation Society International Symposium*, vol. 2, pp. 1015-1020, 2000.

[23] K. P. Ray and G. Kumar, ‘‘Multiport Network Model for Fundamental and Higher Order Modes of Semicircular Microstrip Antennas,’’ *Microwave Optical Tech. Letters,* vol. 28., pp. 237–241, 2001.

[24] S. Sharma, B. Bhushan, S. Gupta and P. Kaur, “Performance Comparison of Micro-strip Antennas with Different Shape of the Patch,” *International Journal of u- and e- Service, Science and Technology* vol. 6, pp. 13-22, 2013.

[25] R. E. Collin, *Foundations for Microwave Engineering*, 2nd ed., John Willey& Sons, 2007.

[26] C -Y Huang and M -H Lin, “Ceramic GPS Antenna for Remote Sensing,” *Proceedings IEEE International Symposium on Geoscience and Remote Sensing*, pp. 2182 – 2184, 2000.

[27] S. Dey and R. Mittra, “Compact microstrip patch antenna,” *Microwave Optical Tech. Letters* vol. 13, pp. 12–14, 1996.

[28] K. L. Wong, C. L. Tang and H. T. Chen, "A compact meandered circular microstrip antenna with a shorting pin," *Microwave Optical Tech. Letters* vol. 15, pp. 147–149, 1997.

[29] K. L. Wong and S. C. Pan, "Compact Triangular Microstrip Antenna," *Electronics Letters* vol. 33, pp. 433-434, 1997.

[30] A.K. Shackelford, K.F. Lee, K. M. Luk and R.C. Chair, "U-slot patch antenna with shorting pin," *Electronics Letters* vol. 37, pp. 729-730, 2001.

[31] J.T. Aberle, M. Chu and C.R. Birtcher, "Scattering and radiation properties of varactor-tuned microstrip antennas," *IEEE Antennas and Propagation Society International Symposium,* pp. 2229 – 2232, 1992.

[32] R. Waterhouse and N. Shuley, "Full characterisation of varactor-loaded, probefed, rectangular, microstrip patch antennas," *IEEE Proceedings on Microwaves Antennas and Propagation*, vol.141, pp. 367-373, 1994.

[33] S.V Shynu, G Augustin, C. K Aanandan, P. Mohanan and K. Vasudevan, "Design of Compact Reconfigurable Dual Frequency Microstrip Antennas Using Varactor Diodes," *Progress in Electromagnetics Research, PIER*, pp. 197-205, 2006.

[34] V H Nguyen, C Borderon, R Benzerga, C Delaveaud and A Sharaiha, "Miniaturized and Reconfigurable Notch Antennas Using a BST Thin Film Varactor," *International Symposium on Antennas and Propagation and USNC-URSI National Radio Science,* 2012.

[35] J. Y. Sze and K. L. Wong, "Slotted Rectangular Microstrip Antenna for Bandwidth Enhancement," *IEEE Transactions on Antennas and Propagation*, vol. 48, pp. 1149-1152, 2000.

[36] Garima, D. Bhatnagar, V.K. Saxena, J.S. Saini and L.M Joshi, "Design of broadband circular patch microstrip antenna with diamond shaped slot," *Indian Journal of Radio and Space Physics*, vol. 40, pp. 275-281, 2011.

[37] C. K. Wu and K. L. Wong, "Broadband microstrip antenna with directly coupled and gap-coupled parasitic patches," *Microwave Optical Technology Letters* vol. 22, pp. 348-349, 1999.

[38] V. Sharma, B. Sharma, V.K. Saxena, K.B. Sharma, M. M. Sharma and D. Bhatnagar, "Circularly polarized stacked square patch microstrip antenna with tuning stubs," *IEEE Conference Publication of Indian Antenna Week (IAW) Kolkata*, pp. 1-4, 2011.

[39] P. Sekra, S. Shekhawat, D. Bhatnagar, V. K. Saxena and J. S. Saini, “Stacked arrangement of edge truncated elliptical and conventional circular patches for circularly polarised broadband performance,” *Microwave and Optical Technology Letters*, vol. 53, pp. 947-952, 2011.

[40] M. Ali, M. Okoniewski, M. A. Stuchly and S. S. Stuchly, “Dual-frequency strip-sleeve monopole for laptop computer", *IEEE Trans. Antennas Propagat.*, vol. 47, pp. 317-323 1999.

[41] Y. H. Suh and K. Chang, “Low cost microstrip-fed dual frequency printed dipole antenna for wireless communications,” *Electron. Lett.*, vol. 36, pp. 1177 -1179, 2000.

[42] Shih-Huang Yeh and Kin-Lu Wong, “Integrated F-Shaped Monopole Antenna For 2.4/5.2 GHz Dual-Band Operation,” *Microwave and Optical Technology Letters*, vol. 34, pp. 24-26, 2002.

[43] B. Paul, S. Mridula, C. K. Aanandan and P. Mohanan “A new Microstrip patch antenna for mobile communication and bluetooth applications,” *Microwave and Optical Technology Letters*, vol. 33, no. 4, pp. 285 -286, 2002.

[44] Yong Xin Guo, Kwai-Man Luk, Kai-Fong Lee and Ricky Chair, “A quarterwave U-shaped patch antenna with two unequal arms for wideband and dualfrequency operation”, *IEEE Transactions on Antennas and Propagation*, vol. 50, no. 8, pp.1082-1087, 2002.

[45] Shih-Huang Yeh, Kin-Lu Wong, Tzung-Wern Chiou, and Shyh-Tirng Fang, “Dual-Band Planar Inverted F Antenna for GSM/DCS Mobile Phones,” *IEEE Transactions on Antennas and Propagation*, vol. 51, pp. 1124-1126, 2003.

[46] L. Wong, Y. C. Lin and T. C. Tseng, “Thin internal GSM/DCS patch antenna for a portable mobile terminal,” *IEEE Trans. Antennas Propag.*, vol. 54, pp.238 -242, 2006.

[47] Chao-Ming Wu, “Wideband dual frequency CPW-fed triangular monopole antenna for DCS/WLAN application”, *Int. J. Electron. Commun.*, vol. 61, pp. 563–567, 2007.

[48] L. Wong, Y. C. Lin and B. Chen, “Internal patch antenna with a thin air layer substrate for GSM/DCS operation in a PDA phone,” *IEEE Trans. Antennas Propag.*, vol. 55, pp. 1165 -1172, 2007.

[49] Chun-I Lin and Kin-Lu Wong, “Internal Multiband Loop Antenna for GSM/DCS/PCS/UMTS Operation in the small-size Mobile Device,” Microwave and Optical Technology Letters, vol. 50, pp. 1279-1285, 2008.

[50] Matteo Cerretelli, Vasco Tesi and Guido Bif Gentili, "Design of a shape constrained dual-band polygonal monopole for car roof mounting," *IEEE Transactions on Vehicular Technology*, vol. 57, no. 3, pp. 1398-1403, 2008.

[51] O. Tze-Meng And T. K. Geok, "A dual-band omni-directional Microstrip antenna," *Progress in Electromagnetics Research*, vol. 106, pp. 363–376, 2010.

[52] B. Vedaprabhu and K. J. Vinoy, "An integrated wideband multifunctional antenna using a microstrip patch with two U-slots," *Progress in Electromagnetics Research B*, vol. 22, pp. 221–235, 2010.

[53] Vijay Sharma,V. K. Saxena, J. S. Saini, D. Bhatnagar, K. B. Sharma and L.M. Joshi, "Broadband gap-coupled assembly of patches forming elliptical patch antenna," *Microwave and Optical Technology Letters*, vol. 53, no. 2, 2011.

[54] J. R. Panda and R. S. Kshetrimayum, "A Printed 2.4 GHz/5.8 GHz Dual-Band Monopole Antenna with a Protruding Stub in the Ground Plane For WLAN And RFID Applications," *Progress in Electromagnetics Research*, vol. 117, pp. 425–434, 2011.

[55] Xiao Lei Sun, Li Liu, S. W. Cheung and T. I. Yuk, "Dual-Band Antenna with Compact Radiator for 2.4/5.2/5.8 GHz WLAN Applications," *IEEE Transactions on Antennas and Propagation*, vol. 60, no. 12, pp. 5924-5931, 2012.

[56] Chun-Cheng Lin, En-Zo Yu, and Chih-Yu Huang, "Dual-Band Rhombus Slot Antenna Fed by CPW for WLAN Applications," *IEEE Antennas and Wireless Propagation Letters*, vol. 11, pp. 362-364, 2012.

[57] Wen-Chung Liu, Chao-Ming Wu and Nien-Chang Chu, "A compact low profile dual-band antenna for WLAN and WAVE applications," *Int. J.Electron. Commun.*, vol. 66, pp. 467– 471, 2012.

[58] Stuti Srivastava, Vinod Kumar Singh, Ashutosh Kumar Singh and Zakir Ali, "Duo Triangle Shaped Microstrip Patch Antenna Analysis for WiMAX lower band Application," *International Conference on Computational Intelligence: Modeling Techniques and Applications (CIMTA),* pp. 554-563, 2013.

[59] Federico Viani, "Dual-Band Sierpinski Pre-Fractal Antenna for 2.4 GHz-WLAN and 800 MHz-LTE Wireless Devices," *Progress in Electromagnetics Research C*, vol. 35, pp. 63–71, 2013.

[60] C. G. Kakoyiannis and P. Constantinou, "Compact, slotted, printed antennas for dual-band communication in future wireless sensor networks," *International Journal of Antennas and Propagation*, pp. 1-17, 2013.

[61] Qingxin Guo, Raj Mittra, Fang Lei, Zengrui Li and Jilong Ju, "A penta-band folded antenna for mobile phone application," *Microwave and Optical Technology Letters,* vol. 55, no. 1, pp. 34-40, 2013.

[62] J. Kaur, R. Khanna and M. Kartikeyan, "Novel dual-band multistrip monopole antenna with defected ground structure for WLAN/IMT/bluetooth and WIMAX applications," International Journal of Microwave and Wireless Technologies, pp. 93-100, 2014.

[63] Lin-Chuan Tsai, "A Dual-Band Bow-Tie-Shaped CPW-Fed Slot Antenna for WLAN Applications," *Progress in Electromagnetics Research C*, vol. 47, pp. 167–171, 2014.

[64] Ashish Singh, Mohammad Aneesh, Kumari Kamakshi, Anurag Mishra and J. A. Ansari, "Analysis of F-shape Microstrip line fed dual band Antenna for WLAN Applications," *Wireless Netw* pp. 133–140, 2014.

[65] R. C. Hall and J. R. Sanford, "Performance enhancements for aperture-coupled microstrip antennas," *IEEE APS Symp. Dig.*, pp. 1040 -1043, 1992.

[66] C. L. Mak, K. M. Luk, , K. F. Lee, and Y. L. Chow, "Experimental Study of a Microstrip Patch Antenna with an L-Shaped Probe," *IEEE Transactions on Antennas and Propagation*, vol. 48, pp. 777-783, 2000.

[67] Kin-Lu Wong and Wen-Hsiu Hsu, "A broad-band rectangular patch antenna with a pair of wide slits," *IEEE Transactions on Antennas and Propagation*, vol. 49, no. 9, pp. 1345-1347 2001.

[68] A. K. Shackelford, Kai-Fong Lee and K. M. Luk, "Design of small-size wide-bandwidth microstrip-patch antennas," *IEEE Antennas and Propagation Magazine*, vol. 45, no. 1, pp. 75-83, 2003.

[69] Y-S. Shin, S-O. Park, and M. Lee, "A Broadband Interior Antenna of Planar Monopole Type in Handsets," IEEE *Antennas and Wireless Propagation Letters*, vol. 4, pp. 9-12, 2005.

[70] A. A. Deshmukh and G. Kumar, "Compact broadband E-shaped Microstrip antennas" *Electronics Letters*, vol. 41, no. 18, pp. 989 – 990, 2005.

[71] B. L. Ooi and I. Ang, "Broadband semicircle-fed flower-shaped Microstrip patch antenna," *Electronics Letters*, vol. 41, no. 17, pp.939-940, 2005.

[72] K. Alameddine, S. A. Chahine, M. Rammal and Z. Osman, "Wideband patch antennas for mobile communications," *International Journal of Electronics Communication*, vol.60, pp. 596 – 598, 2006.

[73] R. A. Abd-Alhameed, N. T. Ali, C. H. See, B Gizas and P. S. Excell, "Design of broadband slotted ground plane microstrip antenna for 3G communication," *IEEE Electrotechnical Conference, Malaga*, pp. 340-343, 2006.

[74] C. Kim, J. Jang, Y. Jung, H. Lee, D. Cho, S. Park and M. S. Lee, "A wideband planar surface wave antenna for the WLAN router," *Int. J. Electron. Commun*., vo. 64, pp. 888–894, 2010.

[75] Vijay Sharma, V. K. Saxena, J. S. Saini, D. Bhatnagar, K. B. Sharma, D. Pal and L. M. Joshi, "Wideband dual-frequency right triangular Microstrip antenna with parallel narrow slits," *Microwave and Optical Technology Letters*, vol. 52, no. 5, 2010.

[76] Dan Sun and Lizhi You, "A broadband impedance matching method for proximity-coupled microstrip antenna," *IEEE Transactions on Antennas and Propagation*, vol. 58, no. 4, 2010.

[77] M. S. Nishamol, V. P. Sarin, D. Tony, C. K. Aanandan, P. Mohanan and K. Vasudevan, "A Broadband Microstrip Antenna For IEEE802.11.A/WIMAX/HIPERLAN2 Applications," *Progress in Electromagnetics Research Letters*, vol. 19, pp. 155–161, 2010.

[78] Gaojian Kang, Zhengwei Du, and Ke Gong, "Compact Broadband Printed Slot-Monopole-Hybrid Diversity Antenna for Mobile Terminals," IEEE *Antennas and Wireless Propagation Letters*, vol. 10, pp. 15-162, 2011.

[79] Sumita Shekhawat, Pratibha Sekra, V. K. Saxena, J. S. Saini, D. Bhatnagar, "Circular microstrip antenna with off-centered Y-slot," *International Journal of RF and Microwave Computer-Aided Engineering,* vol. 21, pp. 407-412, 2011.

[80] U. Chakraborty, S. Chatterjee, S. K. Chowdhury and P. P. Sarkar, "A compact microstrip patch antenna for wireless communication," *Progress in Electromagnetics Research C*, vol. 18, pp. 211–220, 2011.

[81] B. Yu, C.W Jung, H. Lee, M. J Park, B. Kim, H. Wi, Y. Choi, D. Kim, and B. Lee, "Closely Mounted Compact Wideband Diversity Antenna for Mobile Phone Applications," *International Journal of Antennas and Propagation*, pp. 1-6, 2012.

[82] Chan Hwang See, Raed A. Abd-Alhameed, Zuhairiah Z. Abidin, Neil J. McEwan and Peter S. Excell, "Wideband Printed MIMO/Diversity Monopole Antenna for WiFi/WiMAX Applications, " *IEEE Transactions on Antennas and Propagation*, vol. 60, no. 4, pp. 2028-2035, 2012.

[83] Juhua Liu, Quan Xue, Hang Wong, Hau Wah Lai and Yunliang Long, "Design and Analysis of a Low-Profile and Broadband Microstrip Monopolar Patch Antenna," *IEEE Transactions on Antennas and Propagation*, vol. 61, no. 1, pp. 11-18, 2013.

[84] A. Ittipiboon, B. Clarke and M. Cuhaci, "Slot-coupled stacked microstrip antennas," *IEEE Antennas and Propagation Symp. Dig.*, pp.1108 -1111, 1990.

[85] J. T Rowley and R.B Waterhouse, "Performance of shorted microstrip patch antennas for mobile communications handsets at 1800 MHz," *IEEE Transactions on Antennas and Propagation,* vol. 47, pp. 815 – 822, 1999.

[86] Jaume Anguera, Carles Puente, Carmen Borja and Jordi Soler, "Multi frequency microstrip patch antenna using multiple stacked elements," *IEEE Microwave and Wireless Components Letters*, vol. 13, no. 3, 2003.

[87] N. Nasimuddin, K. P. Esselle and A. K. Verma, "Wideband circularly polarized stacked microstrip antennas," *IEEE Antennas and Wireless Propagation Letters*, vol. 6, pp. 21-24, 2007.

[88] M. T. Islam, "Broadband E-H Shaped Microstrip Patch Antenna For Wireless Systems," *Progress In Electromagnetics Research, PIER 98,* pp. 163-173, 2009.

[89] H. F. AbuTarboush, H. S. Al-Raweshidy and R. Nilavalan, "Bandwidth Enhancement for Microstrip Patch Antenna Using Stacked Patch and Slot," *IEEE International Workshop on Antenna Technology, 2009(iWAT 2009)* pp. 1-4, 2009.

[90] F. Namin, T. G. Spence, D. H. Werner and E. Semouchkina, "Broadband, Miniaturized Stacked-Patch Antennas for L-Band Operation Based on Magneto-Dielectric Substrates," *IEEE Transactions on Antennas and Propagation*, vol. 58, no. 9, 2010.

[91] S. Chaimool, C. Rakluea, K. L. Chung and P. Akkaraekthalin, "Single-Feed Circularly Polarized Microstrip Patch Antenna Stacked With Periodic Structure," *Microwave and Optical Technology Letters*, vol. 54, pp. 50-54, 2012.

[92] Du Li, Pengfei Guo, Qing Dai and Yunqi Fu, "Broadband capacitively coupled stacked patch antenna for GNSS applications," *IEEE Antennas and Wireless Propagation Letters*, vol. 11, pp. 701-704, 2012.

[93] Li Yuan, Guo Jia and Zhang Lei, "Design of S-Band Circularly Polarized Double-Layer Microstrip Antenna," *Trans. Tianjin Univ.*, pp. 248-252, 2012.

[94] Tingqiang Wu, Hua Su, Liyun Gan, Huizhu Chen, Jingyao Huang and Huaiwu Zhang, "A Compact and Broadband Microstrip Stacked Patch Antenna With Circular Polarization for 2.45-GHz Mobile RFID Reader," *IEEE Antennas and Wireless Propagation Letters*, vol. 12, pp. 623-626, 2013.

[95] Takafumi Fujimoto and Daisuke Tanaka, "An L-probe fed stacked rectangular microstrip antenna combined with a ring antenna for triple band operation in ITS," *Progress in Electromagnetics Research C*, vol. 37, pp. 1-13, 2013.

[96] C. A. Balanis, *Antenna Theory: Analysis and Design*, 3rd ed., Wiley Publication, 2001.

[97] R. B. Waterhouse, *Microstrip Patch Antennas: A Designer's Guide*, 1st ed., Springer Science+Business Media New York, 2003

[98] M.D. Deshpande and M.C. Bailey, "Input Impedance of Microstrip Antennas," *IEEE Transactions on Antennas and Propagation,* vol. 30, pp. 645-650, 1982.

[99] S C Wu, N. G Alexopoulos and O. Fordham, "Feeding Structure Contributions to Radiation by Patch Antennas With Rectangular Boundaries," *IEEE Trans. on Antenna and Propagation*, pp. 1245-1249, 1992.

[100] W.F Richards, "Experimental and Theoritical Investigations of the inductances Associated with Microstrip antenna Feed," *Electromagnetics*, vol. 3, pp. 327-346, 1983.

[101] J.T Abrele and D. M Pozar, "Analysis of Infinite Arrays of probe fed Rectangular Microstrip antenna Using a Rigorous Feed Model, " *Proc. IEE*, pp. 110-119, 1989.

[102] J P Damiano and A Papiernik, "Survey of Analytical and Numerical Models for Probe-fed Microstrip Antennas," *IEEE Proc., Microwave Ant. Propagat.*, pp. 15-22, 1992.

[103] C. Wu, et al, "Accurate Characterization of Planar Printed Antennas Using Finite Difference Time Domain Method," *IEEE Trans. on Antennas and Propagation*, pp. 526-534, 1992.

[104] D. M. Pozar and D.H. Schaubert "The Analysis and Design of Microstrip antennas and Arrays", *IEEE press, NewYork,* 1996.

[105] D. M. Pozar, "A Microstrip Antenna Aperture Coupled to a Microstripline," *Electron. Letters*, pp. 49-50, 1985.

[106] G. Gronau and I Wolff, "Aperture Coupling of a Rectangular Microstrip Resonator," *Electron. Letters*, pp. 554-556, 1985.

[107] P. L Sullivan and D H Schaubert, "Analysis of an Aperture Coupled Microstrip Antenna," *IEEE Trans. on Antenna and Propagation*, pp. 977-984, 1986.

[108] M . Himdi et al, "Analysis of Aperture Coupled Microstrip Antenna Using Cavity Method, " *Electron. Letters,* pp. 391-392, 1989.

[109] D.M. Pozar and B. Kaufman "Increasing the Bandwidth of a Microstrip Antenna by Proximity Coupling", *Electronics Letters,* vol. 23, pp. 1070-1072, 1987.

[110] H.G Oltman and D.A Huebner, "Electromagnetically Coupled Microstrip Dipoles," IEEE *Trans. on Antenna and Propagation*, pp. 151-157, 1981.

[111] P B Katehi and N G Alexopoulos, "On the modeling of Electromagnetically Coupled Microstrip Antennas-The Printed Strip Dipole," *IEEE Trans. on Antenna and Propagation*, pp. 1179-1186, 1984.

[112] D. M Pozar, "Microstrip antennas," *Proceedings of IEEE*, vol. 80 issue 2, pp. 79-91, 1992.

[113] G. Kron, "Equivalent circuit of the field equations of Maxwell, " Proc. IRE, vol. 32, pp. 289-299, 1944.

[114] P. B Johns and R. L. Beurle, "Numerical Solution of the Two-Dimensional Scattering problems using a Transmission Lie Matrix," Proc. IEE, vol. 118, pp. 1203-1208, 1971.

[115] J. S. Neilson and W. J. R. Hoefer, "A complete dispersion analysis of the condensed node TLM Mesh," IEEE Trans. Magnetics, vol. 27, no. 5, pp. 3982-3985, 1991.

[116] A. G Derneryd, "Linear polarized microstrip antennas," *IEEE Transactions on Antenna Propagation*, vol. 24, pp. 846-851, 1976.

[117] A. G Derneryd, "A theoretical investigation of the rectangular microstrip antenna element," *IEEE Transactions on Antenna Propagation*, vol. 26, no. 4, pp. 532-535, 1978.

[118] E. Lier, "Improved formulas for input impedance of coax-fed microstrip patch antennas," *IEE Proceedings H (Microwave, Optics and Antennas)*, vol. 129, issue 4, pp. 161-164, 1982.

[119] H. Pues and A. Van De Capelle, "Accurate transmission-line model for the rectangular microstrip antenna," *IEE Proceedings H (Microwave, Optics and Antennas)*, vol. 131, issue 6, pp. 334-340, 1984.

[120] A. K Bhattacharya and R. Garg, "Generalized transmission line model for microstrip patches," *IEE Proceedings H (Microwave, Optics and Antennas)*, vol. 132, issue 2, pp. 93-98, 1985.

[121] A. K Bhattacharya, L. Shafai, and R. Garg, 'Microstrip antenna: A generalized transmission line," *Progress in Electromagnetic Research*, vol. 4, Elsevier, New York. pp. 45-84, 1991.

[122] G. Dubost and A. Zerguerras, "Transmission line model analysis of arbitrary shape symmetrical patch antenna coupled with a director," *Electronics Letters*, vol. 26, issue 13, pp. 952 – 954, 1990.

[123] Y. T. Lo, D. Solomon and W. F. Richards, "Theory and experiment on microstrip antennas," *IEEE Transactions on Antennas and Propagation*, vol. 27, no. 2, pp. 137-145, 1979.

[124] William F. Richards, Yuen T. L O, and Danel D. Harrison, "An improved theory for microstrip antennas and applications," *IEEE Transactions on Antennas and Propagation*, vol. ap-29, no.1, 1981.

[125] V. Palanisamy and R. Garg, "Analysis of arbitrarily shaped microstrip patch antennas using segmentation technique and cavity model," *IEEE Transactions on Antennas and Propagation*, vol. ap-34. no. 10, pp. 1208-1213, 1986.

[126] Takanori Okoshi and Tanroku Miyoshi, "The planar circuit-an approach to microwave integrated circuitry," *IEEE Transactions on Microwave Theory and Techniques*, vol. mtt-20, no. 4, 1972.

[127] Nirod K. Das and David M. Pozar, "A generalized spectral-domain green's function for multilayer dielectric substrates with application to multilayer transmission lines," *IEEE Transactions on Microwave Theory and Techniques*, vol. 35, no. 3, 1987.

[128] M. C. Bailey and M. D. Deshpande, "Integral equation formulation of microstrip antennas," *IEEE Trans. Antennas Propagat.*, vol. ap-30, pp. 651-656, 1982.

[129] J. R. Mosig and F. E. Gardiol, "A dynamical radiation model for microstrip structures," in *Advances in Electronics and Electron Physics*, vol. 59. London: Academic Press, pp. 139-239, 1982.

[130] J. R. Mosig and F. E. Gardiol, "Analytical and numerical techniques in the Green's function treatment of microstrip antennas and scatterers," *Proc. Inst. Elec. Eng.*, vol. 130, pp.175 -182 1983.

[131] J. R. Mosig and F. E. Gardiol "General integral equation formulation for microstrip antennas and scatterers," *Proc. Inst. Elec. Eng.*, vol. 132, pp. 424 -432 1985.

[132] J. R. Mosig, "Arbitrarily shaped microstrip structures and their analysis with a mixed potential integral equation," *IEEE Transactions on Microwave Theory and Techniques*, vol. 36, no. 2, 1988.

[133] K. S. Yee, "Numerical solution of initial boundary value problems involving maxwell's equations in isotropic media," *IEEE Trans. Antennas Propagat.*, vol. ap-14, pp.302 -207 1966.

[134] R F Harrington, "Matrix methods for field problems," *Proceedings of the IEEE* vol. 55 no.2, pp. 136-149, 1967.

[135] Naftali Herscovici, Zvonimir Sipus and Per-Simon Kildal, "The cylindrical omnidirectional patch antenna," *IEEE Transactions on Antennas and Propagation*, vol. 49, no. 12, pp. 1746-1753, 2001.

[136] Claudio Vegni and Filiberto Bilotti, "Parametric analysis of slot-loaded trapezoidal patch antennas," IEEE Transactions on Antennas and Propagation, vol. 50, no. 9, pp. 1291-1298, 2002.

[137] Sergey N. Makarov, Shashank D. Kulkarni, Andrew G. Marut and Leo C. Kempel, "Method of moments solution for a printed patch/slot antenna on a thin finite dielectric substrate using the volume integral equation," IEEE Transactions on Antennas and Propagation, vol. 54, no. 4, 2006.

[138] H. R. Hassani and M. Jahanbakht, "Method of moment analysis of finite phased array of aperture coupled circular microstrip patch antennas," Progress in Electromagnetics Research B, vol. 4, pp. 197–210, 2008.

[139] L.C. Godara, Handbook of Antennas in Wireless Communications, CRC Press, 2001.

[140] Tri Van and A. W. Wood, "Finite element analysis of electromagnetic scattering from a cavity," *IEEE Transactions on Antennas and Propagation*, vol. 51, no. 1, pp. 130-137, 2003.

[141] "IE3D: EM Simulator." [Online]. Available: http://www.rfglobalnet.com/doc.html.

[142] "CST Microwave Studio." [Online]. Available http:// www.cst.com /Content /Products/MWS/Overview.aspx

[143] "Ansoft HFSS." [Online]. Available: http://www.ansys.com/Products/Simulation+Technology/Electronics/Signal+Integrity/ANSYS+HFSS

[144] "FEKO." [Online]. Available: https://www.feko.info/product-detail/overview-of-feko.html

[145] "Advanced Design System (ADS)." [Online]. Available :http:// www.keysight.com /en /pc-1297113/

[146] D. M. Pozar, "Microstrip antennas," *Proc. IEEE*, vol. 80, pp. 79-91, 1989.

[147] L. H. Weng, Y. C. Guo, X. W. Shi and X. Q. Chen, "An overview on defected ground structure," *Progress in Electromagnetics Research B,* vol. 7, pp. 173–189, 2008.

[148] S. H. Zainud-Deen, M. E. Badr, E. El-Deen, K. H. Awadalla and H. A. Sharshar, "Microstrip antenna with defected ground plane structure as a sensor for landmines detection," *Progress in Electromagnetics Research B*, vol. 4, pp. 27–39, 2008.

[149] P. Ciais, R. Staraj, G. Kossiavas and C. Luxey, "Compact internal multiband antenna for mobile phone and WLAN standards," *Electronic Letters*, vol. 40, pp. 920–921, 2004.

[150] Tae-Hyun Kim and Dong-Chul Park, "Compact dual-band antenna with double L-slits for WLAN operations," *IEEE Antennas and WirelessPropagation Letters*, vol.4, pp. 249– 252, 2005.

[151] Y. J. Cho, S. H. Hwang, and S.O. Park, "A dual-band internal antenna with a parasitic patch for mobile handsets and the consideration of the handset case and battery," *IEEE Antennas Wireless Propagation Letters*, vol. 4, pp. 429–432, 2005.

[152] J. Malik and M. V. Kartikeyan, "Metamaterial inspired patch antenna with L-shape slot loaded ground plane for dual band (WiMAX/WLAN) applications," *Progress in Electromagnetics Research Letters*, vol. 31, 35-43, 2012.

[153] R. Jothi Chitra and V. Nagarajan, “Double L-slot microstrip patch antenna array for WiMAX and WLAN applications,” *Computers and ElectricalEngineering*, pp. 1026–1041, 2013.

[154] M. Samsuzzaman, T. Islam, N. H. A. Rahman, M. R. I. Faruque and J. S. Mandeep, “Coplanar waveguide fed compact wide circular-slotted antenna for Wi-Fi/WiMAX applications,” *International Journal of Antennas and Propagation,* 2014.

[155] B. Rama Sanjeeva Reddy and D. Vakula, “Compact Dual-Band Truncated Patch Antenna with Fractal Defected Ground Structure for Wireless Applications,” *International Journal of Microwave and Wireless Technologies*, pp. 1-8, 2014.

[156] J. F. Zurcher, “The SSFIP: A global concept for high performance broadband planar antennas,” *Electron. Lett.*, vol. 24, no. 23, pp. 1433–1435, 1988.

[157] F. Croq and D. M. Pozar, “Millimeter-wave design of wide-band aperture coupled stacked microstrip antennas,” *IEEE Trans. Antennas Propagat.*, vol. ap-39, pp. 1170–1176, 1991.

[158] G. Kossiavas and A. Papiernik, “A circular or linearly polarized broadband microstrip antenna operating in L-band,” *Microwave J.*, pp. 266–272, 1992.

[159] J.-F. Zurcher and F. Gardiol, *Broadband Patch Antennas*. Norwood, MA: Artech House, 1995.

[160] G. Kumar and K. C. Gupta, “Non-radiating edges and four-edges gapcoupled with multiple resonator, broadband microstrip antennas,” *IEEE Trans.Antennas Propagat.*, vol. 33, pp. 173–178, 1985.

[161] Park and R. Mittra, “Apertur-coupled small microstrip antenna,” *Electron. Lett.*, vol. 32, no. 19, pp. 1741–1741, 1996.

[162] S. D. Targonski, R. B. Waterhouse and Pozar, “Wideband aperture coupled stacked patch antenna using thick substrates,” *Electron. Lett.*, vol. 32, no. 21, pp. 1941–1942, 1996.

[163] M. Yamamoto and K. Itoh, “Slot-coupled, microstrip antenna with a triplate line feed where parallel-plate mode is suppressed,” *Electron. Lett.*, vol. 33, no. 6, pp. 441–442, 1997.

[164] Zhang-Fa Liu, Pang-Shyan Kooi, Le-Wei Li, Mook-Seng Leong and Tat-Soon Yeo, “A method for designing broad-band microstrip antennas in multilayered planar structures,” *IEEE Transactions on Antennas and Propagation*, vol. 47, no. 9, pp. 1416-1420, 1999.

[165] B. L. Ooi and Q. Shen, "A novel E-shaped broadband microstrip patch antenna," *Microwave and Optical Technology Letters*, vol. 27, no. 5, pp. 348-352, 2000.

[166] N. Kaneda, W. R. Deal, Y. Qian, R. Waterhouse and T. Itoh, "A broad-band planar quasi-yagi antenna," *IEEE Transactions on Antennas and Propagation*, vol. 50, no. 8, pp. 1158-1160, 2002.

[167] S. Oh, S. Seo, M. Yoon, C. Oh, E. Kim and Y. Kim, "A broadband microstrip antenna array for LMDS applications," *Microwave And Optical Technology Letters*, vol. 32, no. 1, pp. 35-37, 2002.

[168] R. Chair, Chi-Lun Mak, Kai-Fong Lee, Kwai-Man Luk and A. A. Kishk, "Miniature wide-band half U-slot and half E-shaped patch antennas," *IEEE Transactions on Antennas and Propagation*, vol. 53, no. 8, pp. 2645-2651, 2005.

[169] Yacouba Coulibaly, Tayeb A. Denidni and Halim Boutayeb, "Broadband microstrip-fed dielectric resonator antenna for X-band applications," *IEEE Antennas and Wireless Propagation Letters*, vol. 7, pp. 341-345, 2008.

[170] S. K. Sharma and L. Shafai, "Performance of a novel ψ-shape microstrip patch antenna with wide bandwidth," *IEEE Antennas and Wireless Propagation Letters*, vol. 8, pp. 468-471, 2009.

[171] S. Noghanian. L. Shafai, "Control of microstrip antenna radiation characteristics by ground plane size and shape," *IEE Proc.-Microw. Antennas Propag.*, vol. 145, no. 3, pp. 207-212, June 1998.

[172] E T. Hamedani, L. Shafai and G. Rafi, "The effects of substrate and ground plane size on the performance of finite rectangular Microstrip antennas," *IEEE Antenna and Propagation Society International Symposium and USNCNRSI National Radio Science Meeting*. pp. 778-781, June 13-16, 2002.

[173] A.K. Bhattacharyya, "Effects of ground plane truncation on the impedance of a patch antenna," *IEEE Proceedings-H*, vol. 138, no. 6, pp. 560-564, d1991.

[174] K. L. Wong and T. W. Chiou, "Finite ground plane effects on broad-band dual polarized patch antenna properties," *IEEE Transactions on Antennas and Propagation*, vol. 51, pp. 903–904, 2003.

[175] T. Namiki, Y. Murayama and K. Ito, "Improving radiation pattern distortion of a patch antenna having a finite ground plane," *IEEE Transactions on Antennas and Propagation*, vol.51, pp. 478-482, 2003.

[176] C. K. and D. Guha, “Nature of cross-polarized radiations from probe-fed circular microstrip antennas and their suppression using different geometries of defected ground structure (DGS),” *IEEE Transactions on Antennas and Propagation*, vol. 60, no. 1, pp. 92-101, 2012.

[177] X. X. Yang, B. C. Shao, F. Yang, A. Z. Elsherbeni and B. Gong, “A polarization reconfigurable patch antenna with loop slots on the ground plane,” *IEEE Antennas and Wireless Propagation Letters*, vol. 11, pp. 69-72, 2012.

[178] A. M. Kordaliv and and T. A. Rahman, “Broadband Modified Rectangular Micro-Strip Patch Antenna Using Stepped Cut at Four Corners Method,” *Progress In Electromagnetics Research*, vol. 137, pp. 599–619, 2013.

[179] Y. Wang and Z. Du, “A Printed Dual-Antenna System Operating in the GSM1800/GSM1900/UMTS/LTE2300/LTE2500/2.4-GHz WLAN Bands for Mobile Terminals,” *IEEE Antennas and Wireless Propagation Letters*, vol. 13, pp. pp. 233-236, 2014.

[180] A. A. Serra, P. Nepa, G. Manara, G. Tribellini, and S. Cioci, “A wide-band dual-polarized stacked patch antenna,” *IEEE Antennas and Wireless Propagation Letters*, vol. 6, pp. 141-143, 2007.

[181] J. A. Ansari and R. B. Ram, “Broadband stacked U-slot microstrip patch antenna,” *Progress in Electromagnetics Research Letters*, vol. 4, pp. 17–24, 2008.

[182] G.F. Khodaei, J. Nourinia, and C. Ghobadi, “A practical miniaturized U-slot patch antenna with enhanced bandwidth,” *Progress in Electromagnetic Research B*, vol. 3, pp. 47-62, 2008.

[183] T. Fortaki, L. Djouane, F, Chebara and A. Benghalia, “On the dual-frequency behavior of stacked microstrip patches,” *IEEE Antennas and Wireless propagation letters,* vol. 7, pp. 310-313, 2008.

[184] Z.-S. Duan, S.-B. Qu, Y. Wu and J.-Q. Zhang, “Wide bandwidth and broad beamwidth microstrip patch antenna,” *Electronics Letters,* vol. 45, no. 5, pp. 249-250, 2009.

[185] K. Qian and X. H. Tang, “Compact LTCC dual-band circularly polarized perturbed hexagonal microstrip antenna,” *IEEE Antennas and Wireless Propagation Letters*, vol. 10, pp. 1212-1215, 2011.

[186] O. P. Falade, , M. U. Rehman, Yue (Frank) Gao, X. Chen and C. G. Parini, “Single feed stacked patch circular polarized antenna for triple band GPS receivers,” *IEEE Transactions on Antennas and Propagation*, vol. 60, no. 10, pp. 4479-4484, 2012.

[187] V. Sharma, B. Sharma, V.K. Saxena, K.B. Sharma, M. M. Sharma and D. Bhatnagar, "Circularly polarized stacked square patch microstrip antenna with tuning stubs," *IEEE Conference Publication of Indian Antenna Week (IAW) Kolkata*, pp. 1 - 4 2011.

[188] Nasimuddin, Zhi Ning Chen and Xian-Ming Qing, "A compact circularly polarized cross- shaped slotted microstrip antenna" *IEEE Transactions on Antennas and Propagation*, vol. 60, no. 3, 2012.

[189] N. Kushwaha and R. Kumar, "Design of slotted ground hexagonal microstrip patch antenna and gain improvement with FSS screen," *Progressin Electromagnetics Research B,* vol. 51, pp. 177-199, 2013.

[190] S. Kumar, B. K. Kanaujia, M. K. Khandelwal and A. K. Gautam, "Stacked Dual-Band Circularly Polarized Microstrip Antenna with Small Frequency Ratio," *Microwave and Optical Technology Letters* vol. 56, pp. 1933-1937, 2014.

[191] K. R. Carver and J.W. Mink, "Microstrip antenna technology," *IEEE Transaction on Antenna and Propagation*, vol. 29, pp. 2–24, 1981.

[192] A. K. Singh and M. K. Meshram, "Slot loaded shorted patch antenna for dual band operation," *Microwave Opti. Technol. Lett.*, vol. 50, pp. 1010–1017, 2008.

[193] A. Mishra, P. Singh, N. P. Yadav and J. A. Ansari and B. R. Vishvakarma, *"*Compact shorted microstrip patch antenna for dual band operation," *Progress in Electromagnetics Research C*, vol. 9, pp. 171–182, 2009.

Publications

- Sanyog Rawat and K K Sharma, "Design and analysis of modified pentagonal patch antenna on defected ground for Wi-Max/WLAN applications," *2nd International Conference on Emerging Technologies: Micro to Nano (ETMN-2015)*, 2015.
- Sanyog Rawat and K K Sharma, "Stacked configuration of rectangular and hexagonal patches with shorting pin for circularly polarized wideband performance," *Central European Journal of Engineering, Springer*, vol. 4, pp. 20-26, 2014.
- Sanyog Rawat and K K Sharma, "Annular ring microstrip patch antenna with finite ground plane for ultra-wideband applications," *International Journal of Microwave and Wireless Technologies*, pp. 179-184, 2014.
- Sanyog Rawat and K K Sharma, "A compact broadband microstrip patch antenna with defected ground structure for C-band applications," *Central European Journal of Engineering, Springer,* pp. 287-292, 2014.
- Sanyog Rawat and K K Sharma, "Design of modified square patch antenna on defected ground for Wi-Max applications," *(Communicated)*.
- Sanyog Rawat and K K Sharma, "A novel geometry of wideband microstrip patch antenna with finite ground plane," *International Conference on Telecommunication and Networks (TEL-NET 2013),* pp. 433-437, 2013.
- Sanyog Rawat and K K Sharma, "Circularly polarized microstrip patch antenna with T shaped slot," *International Conference on Advancement in Information Technology (ICAIT – 2013)*, 2013.
- Sanyog Rawat and K K Sharma, "Circularly polarized slotted microstrip patch antenna with finite ground plane," *Computer Engineering and Applications Journal*, vol. 1, no. 2, pp. 97-105, 2012.

Author Biography

Sanyog Rawat received Bachelor of Engineering in Electronics and Communication Engineering from Visvesvaraya Technological University in 2002. He did Master of Technology in Microwave Engineering from Rajiv Gandhi Proudyogiki Vishwavidyalaya (RGPV), Bhopal in 2004. Presently he is working as Assistant Professor with Amity School of Technology, Amity Univesity Rajasthan, Jaipur. He has around eleven years of teaching experience at the graduate and postgraduate level in engineering. He has organized workshops, national and international conferences and published papers in national and international journals and conference proceedings. His field of interest is microwave devices and planar circuits.